Figure 59: Cumulative frequency curves for selected sandstones from the Sunset Highway and Sweet Home Creek members of the Hamlet formation. The curves were constructed including the >4.5∅ (clay and silt) size fraction.
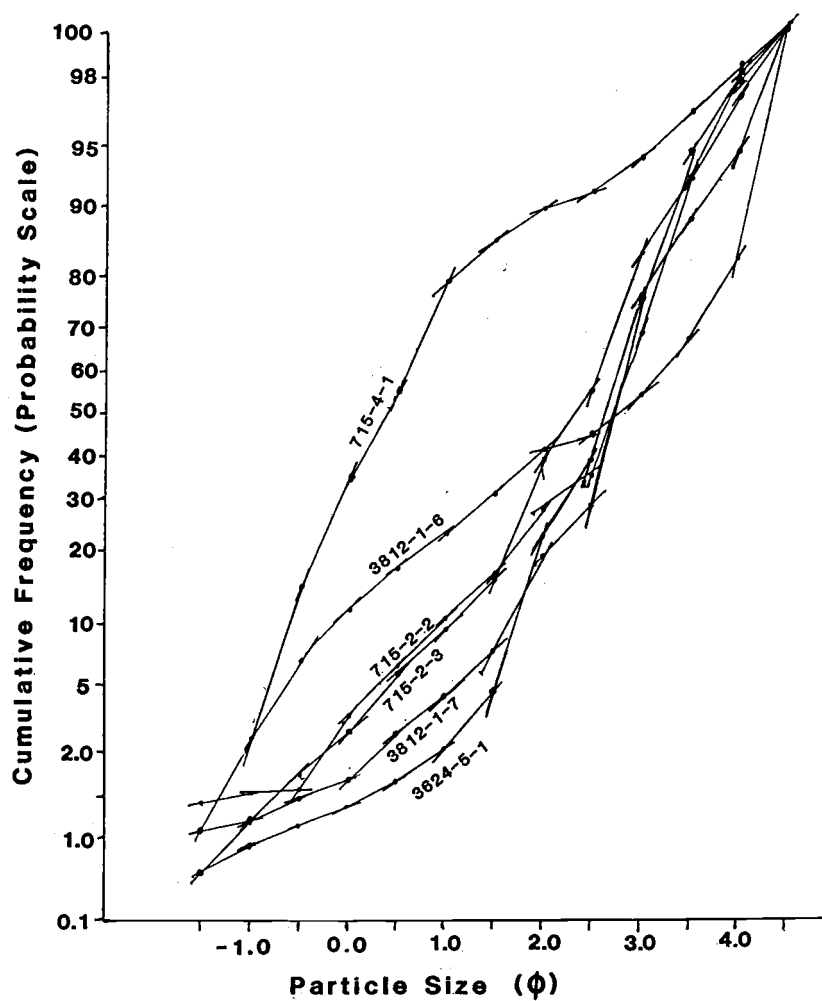
Figure 60. Cumulative frequency curves for selected arkosic and basaltic sandstones from the Sunset Highway member. The curves were constructed without the >4.5∅ (clay and silt) size fraction which is in part diagenetic.

both frequency curves (Appendix II). Petrographic and scanning electron microscopy studies of the samples reveal that the clay-sized fraction consists of both detrital and authigenic components, but that the detrital component is usually dominant. Therefore, it is felt that the clay-inclusive frequency distribution and statistical parameters best reflect the original grain size distribution of the samples.

The arkosic sandstone samples all have a fine sand mean grain size ($2.35\emptyset$–$2.75\emptyset$) and are moderately (4 of 5 samples) to poorly (1 of 5 samples) sorted. This suggests a moderate amount of reworking of the sediments before final deposition. The environmentally-sensitive inclusive graphic skewness values of the clay-inclusive arkosic sandstones range from 0.15 (fine-skewed) to -0.4 (strongly coarse skewed) with most samples (3 of 5) being coarse- or strongly coarse-skewed. This indicates that fine particle sizes (e.g. clay and silt) were generally winnowed by currents from Sunset Highway member sandstones. Graphic kurtosis values range from 0.82 (platykurtic) to 1.84 (very leptokurtic) with most samples being leptokurtic (3) or very leptokurtic (1). This peaked tendency occurs in the $3\emptyset$ and $3.5\emptyset$ sizes and suggests substantial current sorting of the of these sizes prior to deposition. One interesting feature of all Sunset Highway member sandstones is that the abundance of the $2.5\emptyset$ grain size is always less than the $2\emptyset$ and $3\emptyset$ grain sizes, accentuating the leptokurtic character of the sandstones.

Data generated by grain size analysis were plotted on a number of binary graphs to aid interpretation of the depositional environment of the Sunset Highway member. Friedman (1979) four plots to target a specific depositional environment. On a plot of mean versus standard deviation (Inland Dune versus River, not shown), four arkosic sandstones plot in the inland dune field and arkosic and one basaltic sandstone plot in the river field. On a plot of simple sorting versus simple skewness (River versus Beach), all Sunset Highway member samples plot in the "river field" of this diagram (fig. 61). All samples plot in the inland dune field of the other two graphs of beach vs. inland dune (fig. 62) and inland dune vs. nearshore dune (not shown), both of which plot inclusive graphic skewness against
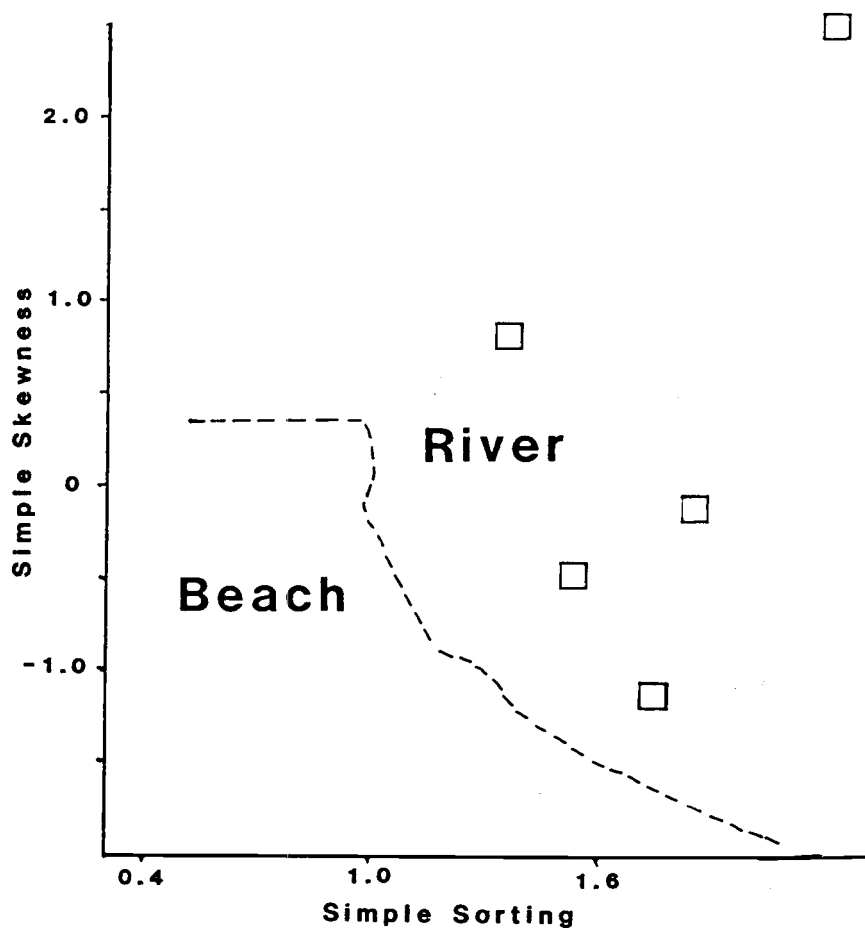
Figure 61: Sandstone samples from the Sunset Highway member plotted
on the simple skewness vs. simple sorting diagram of
Friedman (1979). All samples plot in the river field.
Sample 3812-1-6 plots well to the right of the simple
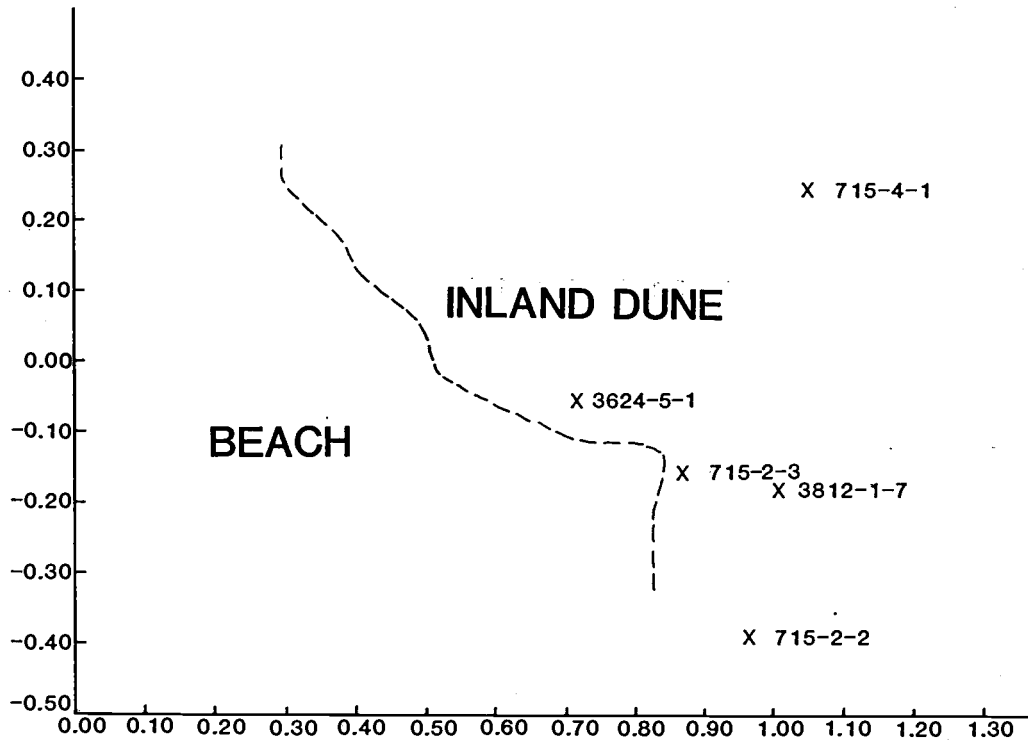sorting limit of the diagram.

Figure 62. Sunset Highway member sandstone samples plotted on the
inclusive graphic skewness versus inclusive graphic
standard deviation diagram of Friedman (1979). All
samples plot in the inland dune field.

inclusive graphic standard deviation. This suggests that the textural parameters of Sunset Highway are closest to those of inland dune sediments sampled by Friedman (1979). However, Sunset Highway member sandstones contain marine molluscan fossils and trace fossils and clearly were not deposited in a fluvial system or in an inland dune. The samples have simple skewness values comparable to Atlantic and Gulf of Mexico coast beach sediments but are more poorly sorted than these supposedly "typical beach sediments" analyzed by Friedman (1979). The inland dune sediments are primarily from flood plains and rivers on the craton. Sunset Highway member sediments were not deposited in such a system (e.g. major river delivering sediment to a developing forearc). Other factors which need to be accounted for include bioturbation and sediment mixing and the presence of diagenetic clays in Sunset Highway member sandstone. This indicates that the final depositional environment did not fully modify the grain size distribution of fluvial-sourced Sunset Highway member sandstones so that they mimic inland dune sediments analyzed by Friedman (1979).

Kulm and others (1975) distinguished beach sand from offshore sands of the modern Oregon coast on binary graphs of mean diameter ($\emptyset$) versus skewness and standard deviation (fig. 63). Sunset Highway member sandstones do not group with either the beach or offshore sands on these graphs, but do show greater affinity with the beach sands (fig. 63). In general, Sunset Highway member samples have slightly finer mean grain sizes than the beach sands and are more coarsely skewed that modern offshore sands. This may reflect textural parameters imparted to shelf sediments during Holocene transgression (e.g. mixing of relict sand and gravel with modern sands on the inner shelf and development of mixed sand and mud facies through bioturbation and mixing of overlying mud facies with underlying relict sand facies). In any case, Sunset Highway member sands have grain size parameters closer to modern beach sands analyzed by Kulm and others (1975).

When plotted on the CM diagram of Passega (1957) all arkosic sandstones plot in or near the boundary of the beach field (fig. 64). One sample plots in an area where the beach and turbidity current fields overlap, and one plots near the overlap of the beach and
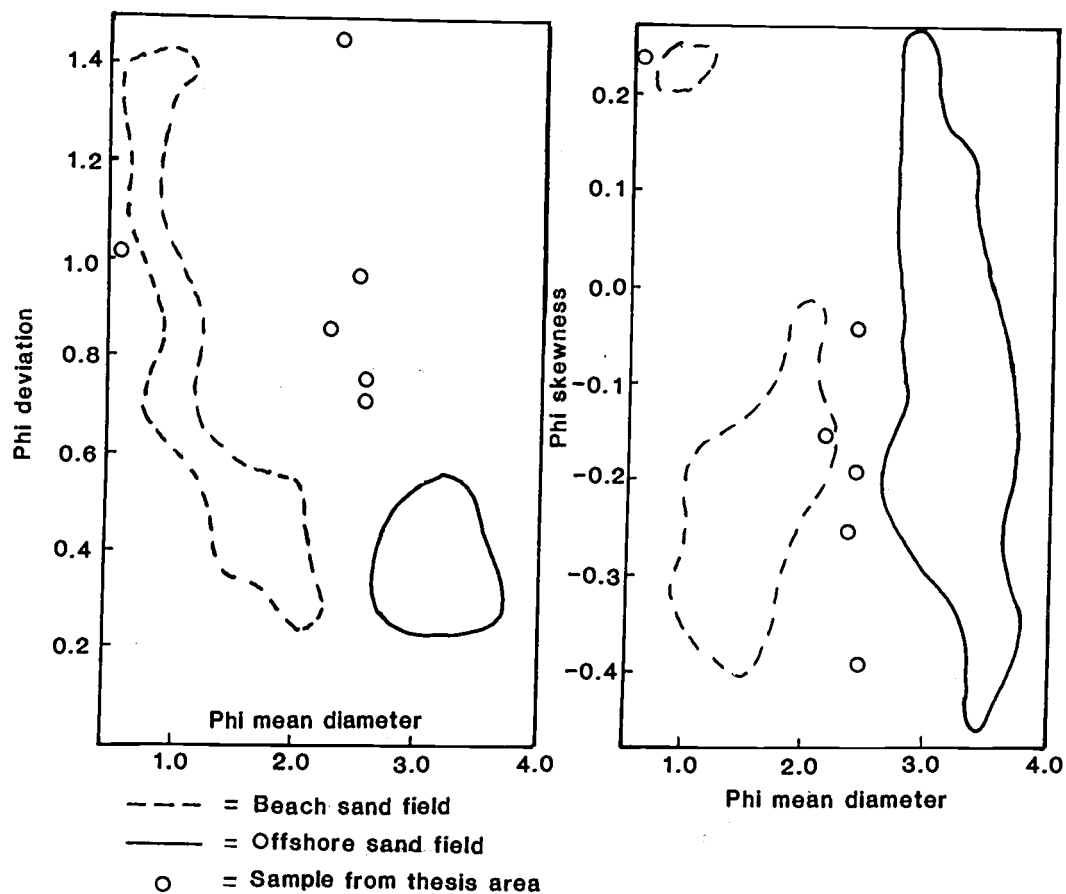
Figure 63. Grain size parameters of Sunset Highway member samples compared with modern beach and offshore sands analysed by Kulm and others (1975). Sunset Highway member sandstones have greater textural affinity with modern beach sands. A: Phi mean diameter vs. Phi deviation. B: Phi mean diameter vs. Phi skewness.

Figure 64: Sandstone samples from the Sunset Highway member plotted on the CM diagram of Passega (1957). The arkosic sandstone samples lie within or near the boundary of the beach field. A basaltic sandstone (■) sample plots in the turbidity current field.

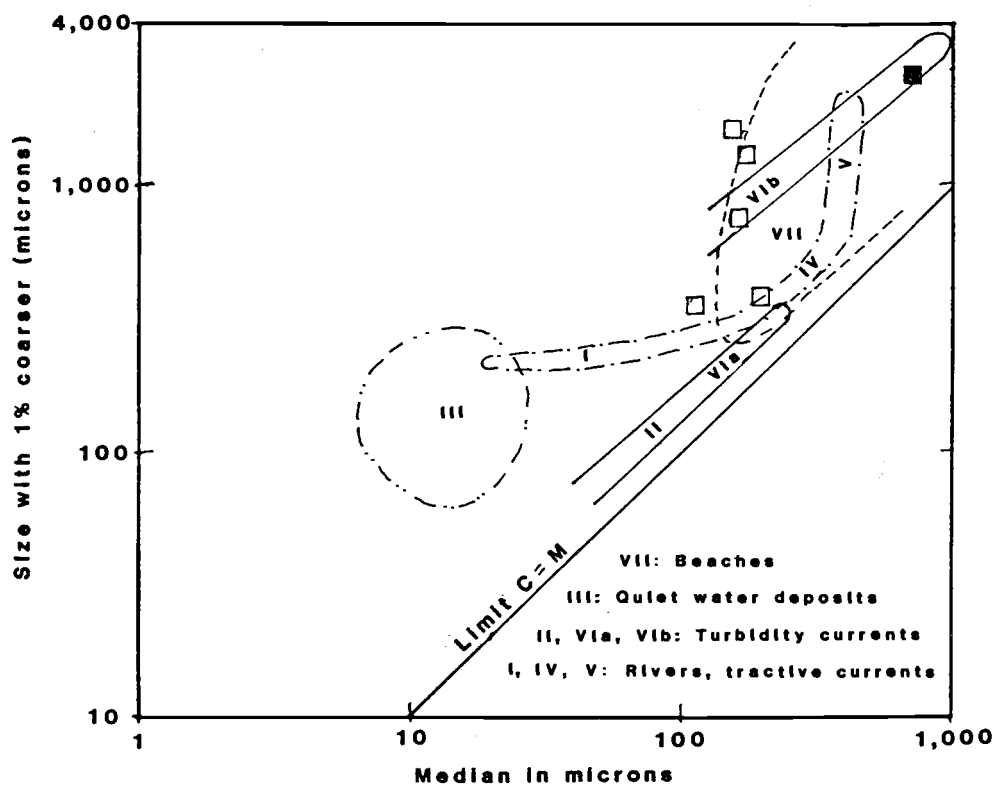tractive current fields. The beach environment is consistent with the known marine depositional environment of the Sunset Highway member. However, not enough data were generated to distinguish between traction or suspension transport of the sand. However, this diagram does indicate a narrow range of median grain sizes for the arkosic sandstones (100-100 microns) and the points out the much coarser character of basaltic sandstone in the Sunset Highway member.

Visher (1969) separated cumulative frequency curves into components representing grain subpopulations having different transport modes (saltation, suspension, traction). Cumulative frequency curves of Sunset Highway member sandstones indicate a poorly sorted grain population transported by traction, a moderately-well to well-sorted grain population transported by saltation, and little detritus in the grain population transported in suspension (figs. 59 and 60). These characteristics are fundamentally similar to curves established for beach sands.

Depositional Environment

The Sunset Highway member is interpreted to have been deposited in the transition to outer shoreface zone of an open shallow marine high energy shelf environment that was influenced or dominated by storms. A major river system (or systems) delivered extrabasinal arkosic sediments to the marine environment where they were reworked by longshore and wave-induced shelf currents. These sediments may have bypassed the littoral energy fence in several ways, including high discharge events related to storms and flooding, through flood-related plumes of fresh water discharged into the marine environment off a high energy delta, and storm surge ebb currents which eroded sediments from the beach and redeposited them on the shelf (Kulm and others, 1975). Basaltic sandstones, sandy conglomerates, and basaltic debris flows and breccias interbedded with the arkosic sandstones were derived from local volcanic edifices of the Tillamook Volcanics which may have been emergent and/or active. These interpretations are based on the following features:

1.) nearshore, shallow marine trace fossils and megafossils sandstones

2.) extensively bioturbated strata

3.) truncated low angle trough cross-bedded and hummocky-bedded fine- to medium grained sandstones and muddy siltstones.

4.) mudstone drapes over silty very fine-grained microcross-laminated sandstones and sand siltstones

5.) low angle trough cross-laminated and hummocky cross-stratified sandstones

6.) abundant carbonized plant debris

7.) no evidence of subaerial emergence

8.) regional facies relationships

The interstratified fine- to very-fine grained arkosic sandstones and silty mudstones of the Sunset Highway member are interpreted to have been deposited in a storm-influenced transition zone near fair weather wave base. These beds typically are typically discontinuously interstratified, reflecting variations in the "energy" of the depositional environment and sediment supply. Such fluctuations are associated with a transition zone at or near fair weather wave base (Reineck and Singh, 1980). Large storm-generated waves lower the fair weather wave base and generate suspension clouds of shore face and fore shore sediments (fine- to very-fine grained arkosic sandstones of the Sunset Highway member) which settle farther offshore in a normally low-energy shelf environment where muds and silts normally settle out of suspension (silty mudstones of the Sunset Highway member). Grain size analysis shows these sandstones area fine-grained, moderately to poorly sorted, generally coarse-skewed, and generally leptokurtic (Appendix II). These parameters are consistent with mixing of well-sorted sands eroded by storm surge ebb currents from the shore face and fore shore with finer-grained sediments of the outer shore face and transition zone. The coarse-skewed character of the sediments reflects the ability of the high energy storm events to transport coarser grained material.

Fossil evidence also supports this interpretation of the depositional environment. A fossilized pelecypod identified as Pitar? (Lamellichoncha) sp. by Dr. Ellen Moore (written communication, 1984)

was collected from low-angle trough cross-bedded sandstone of the
Sunset Highway member (locality 730-6, T. 4 N., R. 7 W., SE 1/4 sec.
5). Dr. Ellen Moore, U.S. Geological Survey (ret.), states that
"living eastern Pacific series assigned to LAMELLICONCHA live in warm
water (southern California and south) and depths of intertidal to 110
meters, with more species in the intertidal to 50 meter range."
(written communication, 1984). Other marine macrofossils (e.g.
Mytilus, identified by the author) and extensively burrowed strata
present in the Sunset Highway member are also consistent with such a
shallow marine depositional environment. Jackson (1983) reported
Pitar (a pelecypod) and Brisaster megafossils in the late Narizian
Cowlitz Formation in northwestern Washington and northeastern
Tillamook counties, both of which indicate shallow marine
environments.

Primary sedimentary structures and lithologic changes seen in the
Sunset Highway member are interpreted to record storm-generated
deposition. Large waves produced by episodic storms are thought to
have produced hummocky cross-stratification and low angle trough
cross-lamination (swales). Discontinuous microcross-laminated fine- to
very fine-grained sandstone lenses encased in mudstone drapes may
represent hummocky cross-stratification or sand deposited by
unidirectional ripple currents capped with fair weather muds. These
deposits also exhibit alternation of extensively burrowed and
unburrowed strata, which is consistent with fair weather shelf
sedimentation between storm events which produce hummocky cross-
stratification. During fair weather, infauna could bioturbate the
sandstone, which is typical of middle shelf depths. Dott and
Bourgeois (1982) have interpreted hummocky cross-stratified sequences
such as the middle Eocene Coaledo Formation as storm-influenced
deposition between the outer shelf and nearshore zones in water depths
ranging from 0 to 80 m. Parallel and low-angle trough cross
laminations are prevalent sedimentary structures in the Sunset Highway
member which could also be formed by storm-generated waves on the
shelf.

Storm events are thought to have also mobilized well-sorted
medium-grained micaceous arkosic sand from the inner shore-face to the

outer shore-face to offshore transition zone and moved the coarse-grained basaltic sands and gravels away from volcanic edifices of the Tillamook Volcanics. The medium-grained arkosic sandstones (e.g., locality 3812-1-7, August Fire road measured section) appear to be laterally persistent and have sharp basal contacts with underlying interstratified fine-grained sandstones and mudstones. These sandstones have little matrix, are moderately to moderately well sorted, and have a very leptokurtic grain size distribution (Sample 3812-1-7, Appendix II). Such characteristics are consistent with sands of the shore-face which have been transported to the outer shore face to transition zone by high energy storm events. Jackson (1983) reported similar sheet sandstones in his heterolithic lithofacies (lower Cowlitz Formation, a possible Sunset Highway member analog) which have erosive bases with occasional shell concentrates and parallel to low-angle trough cross-lamination. These features were not seen in the field area, but this may be due to extensive burrowing of the relatively thin (<2.5 m) sheet sandstones exposed in the field area.

Thick interbeds and lenses of coarse-grained basaltic sandstone, grits, and conglomerates to matrix-supported breccias in the Sunset Highway member are interpreted to have been shed from local volcanic edifices of the Tillamook Volcanics. The presence of these coarser grained beds in finer grained micaceous arkosic sandstones deposited in the transition to outer shore face requires mobilization of the coarse basaltic detritus from shallow water (foreshore or beach zone locally developed around volcanic edifices) into deeper middle to outer shelf depths. Grain size analysis was performed on one basaltic interbed in the upper Sunset Highway member (sample locality 715-4, T. 4 N., R. 7 W. NE 1/4 sec. 10). The statistics indicate that this sample is a poorly sorted, leptokurtic, strongly fine-skewed granule-bearing coarse sand. The poor sorting and presence of granules reflects the proximity of the sediment source and deposition under high energy conditions. The leptokurtic character may be due to initial sorting of the basaltic detritus in a high energy beach environment around a volcanic headland or sea stack. The strongly fine-skewed character is probably partly due to mixing of the coarse-

grained basaltic sediment with the fine-grained arkosic sand and partly due to diagenetic clays produced after burial.

Fossil evidence also indicates a shallow water environment for the source of the basaltic sands and gravels. A fossilized crab identified as Raninoides cf. R. fulgidus by Ross E. Berglund (written communication, 1986) was collected from a poorly sorted coarse-grained basaltic sandstone in the upper Sunset Highway member (Sunset Highway type section, locality 715-4, T. 4 N., R. 7 W., NE 1/4 sec 10). Raninoides is a sand crab which lives on the shore in wave-washed sand (Dr. Ellen Moore, written communication 1984). Some of the basaltic sandstone interbeds (e.g., upper Sunset Highway type section, fig. 51) exhibit distinct burrows, most of which are cylindrical (1-3 cm diameter) and vertical to subvertical, which indicate relatively shallow water (Reineck and Singh, 1980). The trace fossils strongly resemble those reported by Timmons (1981) and Jackson (1983) in Cowlitz Formation strata of similar age, lithology, and stratigraphic position east of the thesis area. The Cowlitz Formation trace fossils were identified as Thalassinoides and Rosselia-Cylindricus. These trace fossils are indicative of nearshore marine environment.

The matrix supported basaltic breccia in the upper part of the type Sunset Highway member may be a debris flow (fig. 51). Thicker debris flows with basaltic boulders in the Sunset Highway member (reported by Safley, in prep.) may have been generated by continuing eruption of the Tillamook Volcanics activity or severe storms that undermined sea cliffs or generated flash floods. The debris flows may have followed river channels and prograded out of the river mouth into the shallow shelf beyond the beach zone and below fair weather base to be preserved. These deposits are thicker and more numerous towards Green Mountain (T. 5 N., R. 6 W., sec. 35), making it one likely source area for the basaltic detritus (Safley, in prep.). Geochemical analyses of volcanic rocks from the Green Mountain area show greater fractionation (i.e. higher SiO_2 and K_2O), indicating volcanic activity may have been somewhat more prolonged, if not ongoing during Sunset Highway deposition, in this area (Olbinski, 1983; Safley, in prep). Slightly younger basaltic flows (Goble Volcanics) are interbedded with shallow marine arkosic sandstones of the Cowlitz Formation in Columbia

County and in Lewis County (southwestern Washington) which documents
active volcanism during the late Narizian east of the thesis area
(Wilkinson and others, 1945; Van Atta, 1971; Timmons, 1981).
Therefore, intermitted volcanic activity between the main eruptive
stage of the Tillamook Volcanics and that of the Goble Volcanics is
reasonable. The proximal source of the basaltic sediment would result
in poorly sorted basaltic sandstones with angular clasts when the
sediments were remobilized by strong storm waves into deeper parts of
the basin.

Diagenesis

    A diagenetic model for the development of cements and pore
evolution of the "cleaner" moderately- to well-sorted micaceous
arkosic sheet sandstones (see lithology section) of the Sunset Highway
member was composited from paragenetic relationships observed in thin
section and with a scanning electron microscope. As previously noted,
petrographic investigation of clay-rich sandstones of the Sunset
Highway member was severely hampered (thin sections could not be made
due to abundant expandable clays) and a complete diagenetic sequence
was not established for these "dirtier" arkosic and basaltic
sandstones.

    Relatively matrix-free micaceous arkosic sandstones of the Sunset
Highway member exhibit distinct but limited effects of diagenesis.
These sandstones are weakly cemented, and, therefore, friable.
Diagenetic processes have produced overgrowth cements which reduce
intergranular porosity and permeability, but the sandstones retain
large (100 to 200 micron) primary intergranular pores which are
effectively interconnected. The pore system has been slightly
increased by dissolution of unstable grains, particularly plagioclase
feldspars, which has created secondary intraparticle pores that are
connected to primary intergranular pores.

    The diagenetic sequence for the these sandstones consists of five
stages. Stage 1 is some reduction of initial intergranular porosity
due to burial pressure as evidenced by minor mechanical compaction
features such as better grain packing and crenulation of micas and

carbonaceous debris between framework grains. Stage 2 is represented
by corrosion and dissolution (?) of plagioclase feldspar resulting in
the formation of secondary interparticle porosity. Stage 3 is minor
development of smectite clay coats on detrital grains. Stage 4 is
represented by overgrowths of potassium feldspar on detrital
feldspars. Stage 5 is represented by telogenetic weathering and
oxidation of iron-bearing minerals to form hematite cement.

Mechanical compaction features are not very pronounced in the
sandstones of the Sunset Highway member. Detrital grains are not
fractured or broken, and grain contacts are largely tangential.
Pressure solution was not observed. Compaction due to lithostatic
loading has caused crenulation and slight deformation of ductile mica
flakes and carbonized plants debris pinched between more brittle
framework grains such as quartz an feldspar. Feathered ends of
compacted micas can flare out into pore throats and reduce porosity.

Stage 2 corrosion and dissolution of plagioclase feldspar is
pronounced in these sandstones and can result in formation of
secondary interparticle porosity. Potassium feldspar grains appear to
be much less affected. Samples impregnated with blue-dyed epoxy show
secondary porosity (?) developed along cleavage planes (fig. 65). It
is possible that some of this represents grain plucking when thin
sections were made. Scanning electron microscopy shows intraparticle
micropores to be up to 250 microns long that are well-connected to
primary intergranular pores (fig. 66). Corrosion of detrital
feldspars in arkosic sandstones of the Cowlitz Formation has also been
reported by Timmons (1981) and Nelson (1985).

Figures 66, 67, and 68 show authigenic clay coatings on detrital
grains which exhibit a webby, highly crenulated and honeycombed
morphology that resembles authigenic smectite illustrated by Welton
(1984). The energy dispersive spectrum of the clay shows Si, Al, Ca,
Mg, Fe, and K, which are the major elements of smectite (fig. 67B).
This indicates that the clay is smectite. The clays line and locally
bridge pores which results in reduced permeability. Van Atta (1971)
reported smectite to be a common clay in late Eocene arkosic
sandstones in northwestern Oregon.

Potassium feldspar overgrowths on detrital grains are fairly

Figure 65. Thin section photomicrographs of a relatively matrix free sandstone in the upper part of Sunset Highway member. The rock is a moderately sorted subarkose containing quartz (Q), corroded plagioclase feldspar (P), altered potassium feldspar (K), biotite (B), and zircon (Z). Blue-dyed epoxy fills intraparticle and interparticle (?) pore space, which totals about 7%. Note primary intergranular porosity (I), secondary intraparticle porosity in plagioclase feldspar (S), and clear euhedral potassium feldspar overgrowth (O) on altered detrital feldspar grain. A: plane polarized light. B: crossed polars. Field of view in approximately 1.31 mm. Sample locality 3812-1 near top of August Fire road measured section (T. 4 N., R. 7 W., NE 1/4 sec. 16).

A.

1mm
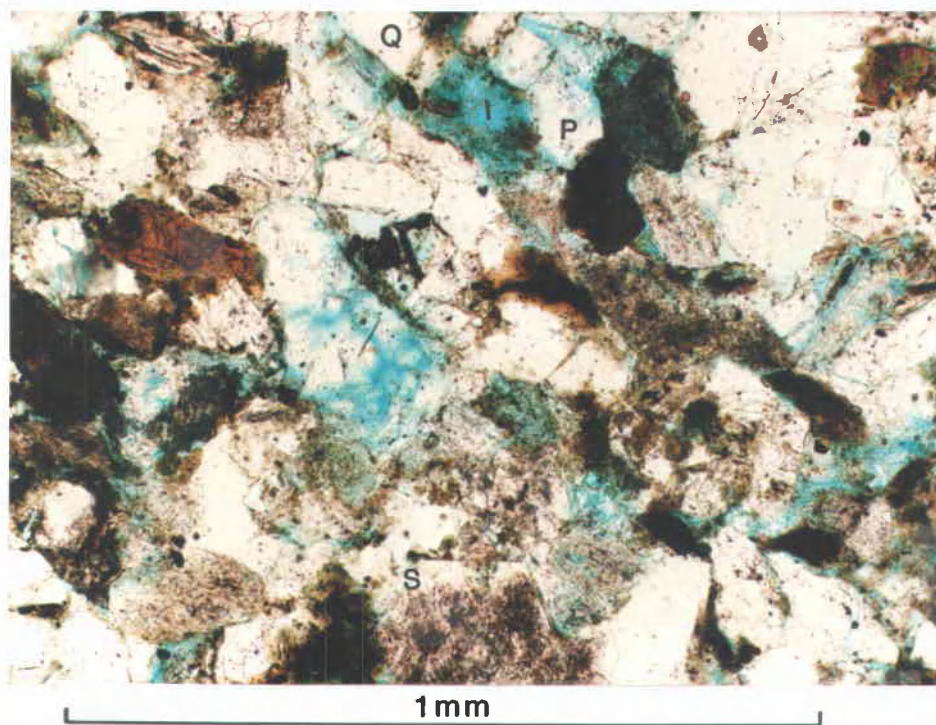
B.
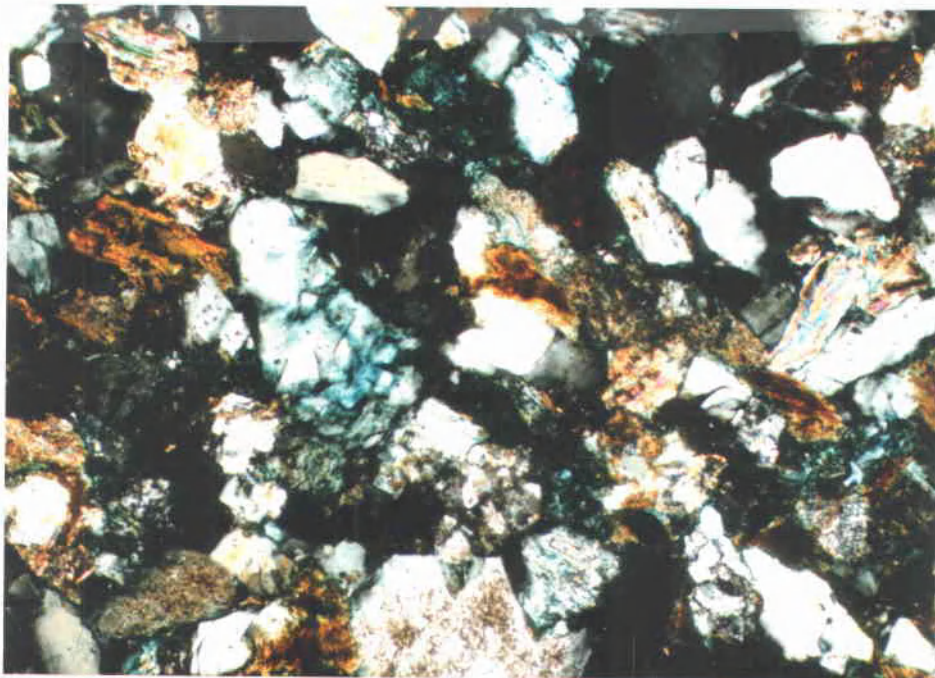
Figure 65.

Figure 66: Scanning electron photomicrographs of "clean" arkosic sheet sandstone in the upper Sunset Highway member. A: Note open sliver-like pore throats, large intergranular pore (center), corrosion of feldspar along cleavages creating secondary intraparticle porosity, thin clay coats, and blocky potassium feldspar overgrowths (upper and lower left). B: Note large (100μ) intergranular pore, webby and highly crenulated morphology of thin clay coats (smectite), and blocky overgrowths of authigenic potassium feldspar on grain along left edge of photograph. Both from locality 3812-1, near the top of the August Fire road measured section (T. 4 N., R. 7 W., NE 1/4 sec. 16).

A.
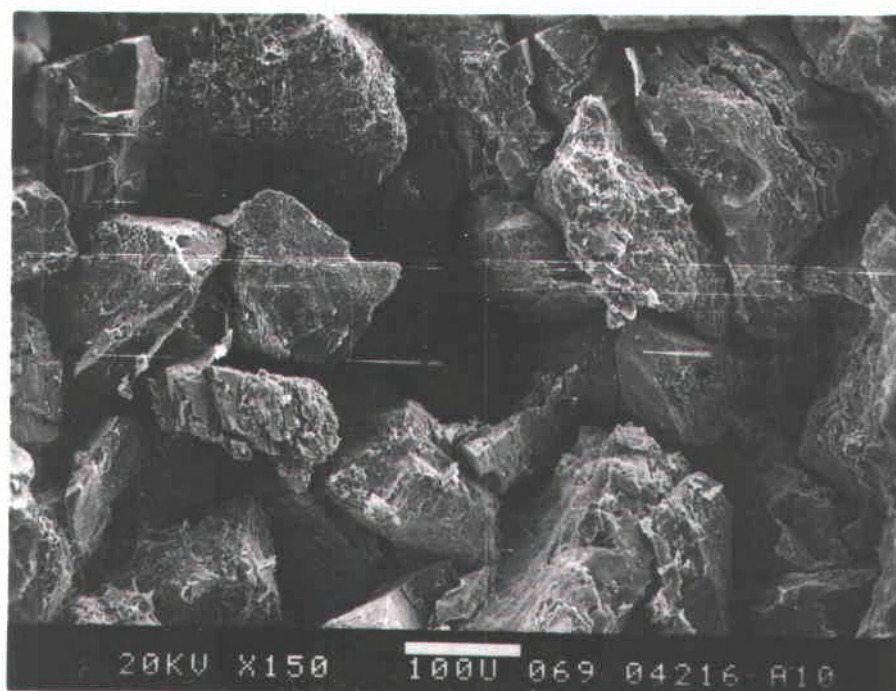
B.
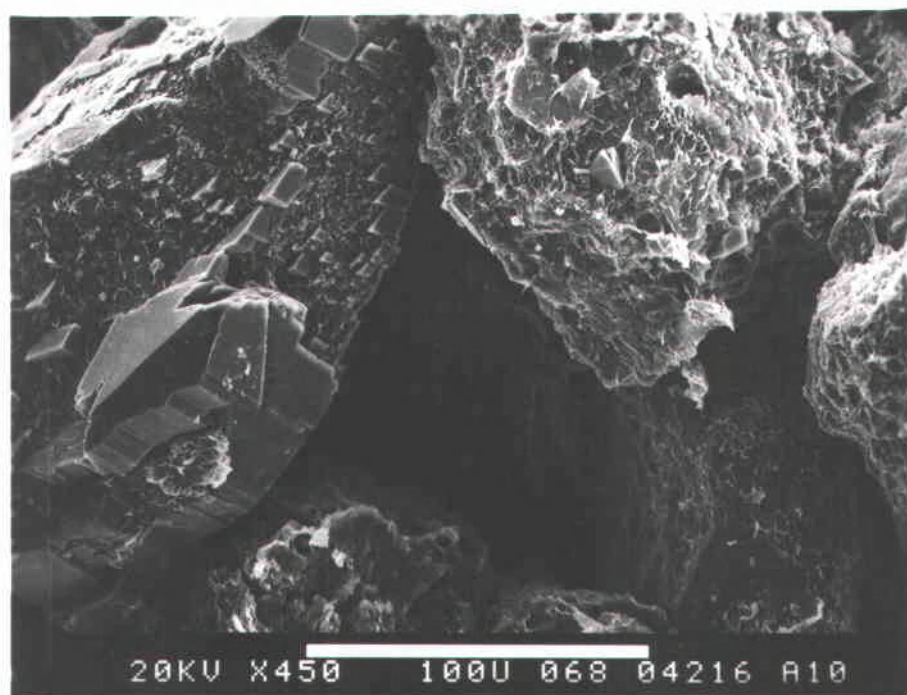
Figure 66.

Figure 67. Morphology and EDX analysis of authigenic clay coats on
detrital grain in arkosic sandstone from upper part of
the Sunset Highway member. A: Scanning electron
photomicrograph showing highly crenulated, webby,
honeycombed morphology of thin clay coating commonly
exhibited by smectite. B: Energy dispersive analysis of
circled point in A shows the major elements of smectite
(Si, Al, Ca, Mg, Fe, and K). The relatively large amount
of K may be derived from an underlying detrital K-
feldspar. Sample locality 3812-1 near the top of the
August Fire road measured section (T. 4 N., R. 7 W., NE
1/4 sec. 16)

A.

20KV X3300   10U 696 04107 A10
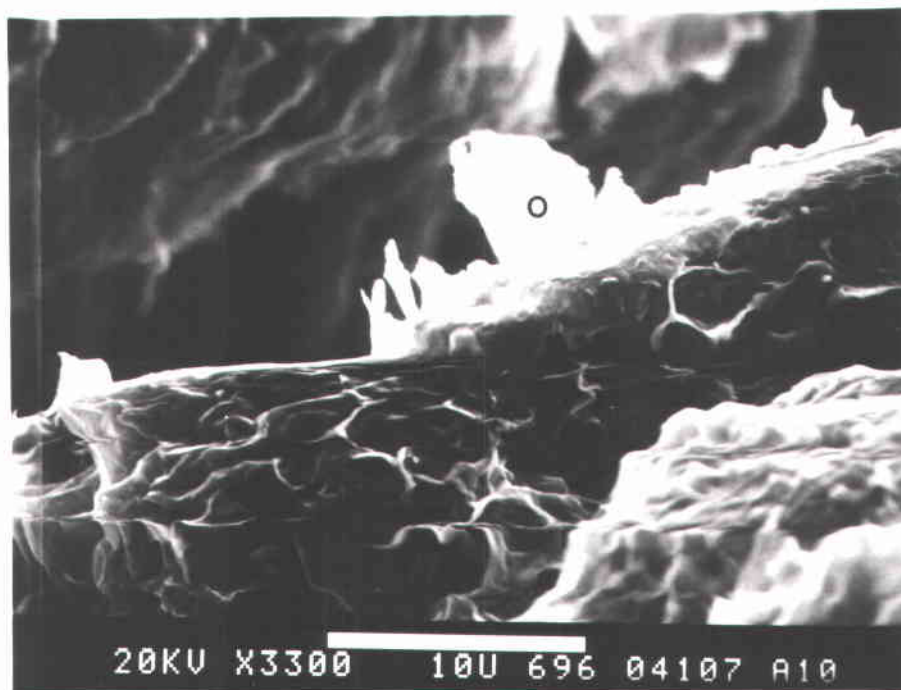
B.
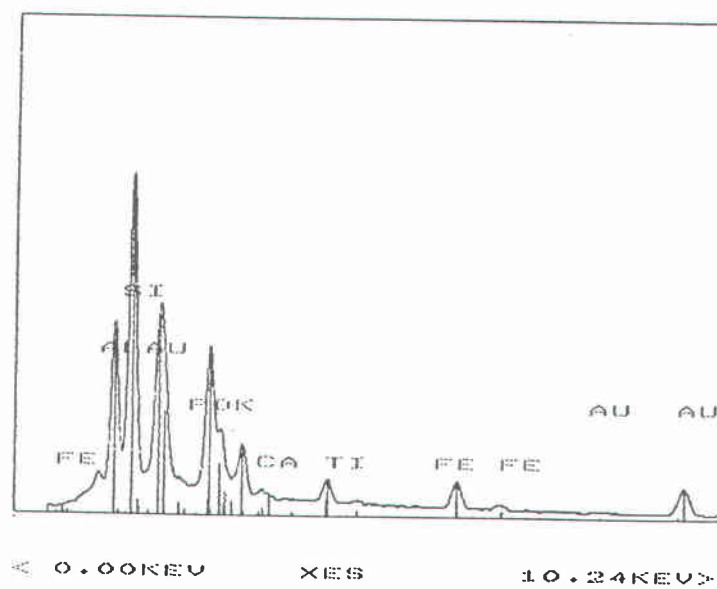
Figure 67.

common in the relatively matrix-free sandstones of the Sunset Highway
member. In thin section the overgrowths form relatively inclusion
free, unaltered, euhedral crystal faces in optical continuity with
partially altered detrital feldspar cores (fig. 65). It is not
possible to determine the composition of the altered cores with
certainty, but the character of alteration is usually associated with
potassium feldspar grains. For this reason, it is felt that the
overgrowths are preferentially developed on detrital potassium
feldspar grains. The blocky morphology of potassium feldspar
overgrowths seen with the SEM is not diagnostic (figs. 66 and 68), and
identification is based on analysis of the major elements, and
particularly the relative abundance of potassium, determined with the
EDX system (fig. 68B). Potassium feldspar overgrowths appear to be
growing over grain surfaces coated with stage 3 smectite, and these
clay coats prevent EDX analysis of the detrital grain cores (figs. 66
and 67). Although it is felt that potassium feldspar overgrowths have
developed preferentially, if not exclusively, on potassium feldspar
cores, it is possible that some authigenic potassium feldspar has
developed on plagioclase feldspar. Welton (1984) illustrated
potassium feldspar overgrowths on both potassium and plagioclase
feldspars. Galloway (1979) interpreted feldspar overgrowths to
represent a relatively advanced stage of diagenesis in Tertiary
volcaniclastic sandstones from the Pacific Northwest that is developed
during deep burial (greater than 1,000 to 3,000 m).

The final stage of diagenesis, stage 5, is related oxidation of
iron-bearing minerals by surface weathering and groundwater during
subaerial exposure in the telogenetic zone. Iron oxides cements
developed in this stage weakly lithify the sandstones and impart an
orange hue in weathered outcrops but otherwise do not strongly affect
the character of the rock.

Other diagenetic features were observed in muddy very fine-
grained arkosic sandstone in the Sunset Highway member but cannot be
placed in the diagenetic sequence of the more matrix free sandstones
with available data. These features include local calcite concretions
which are probably controlled by local compositional variations and
formed relatively early in the diagenetic sequence. Calcite

concretions in the overlying Sweet Home Creek member plastically deform the enclosing mudstones and thin turbidite sandstones. This demonstrates that the concretions formed early in the compaction history of these beds. Authigenic zeolites were observed in an arkosic sandstone sample from the lower part of the Sunset Highway member in thin section and with the scanning electron microscope. These zeolites have the morphology and EDX pattern of clinoptilolite illustrated by Welton (1984) and hexagonal erionite examined by Sheppard (1987) (fig. 69). Clinoptilolite and erionite commonly forms through the devitrification of volcanic ash (Welton, 1984; Sheppard, 1987). Tuffaceous material was not observed in the Sunset Highway member and it is more likely that the pore fluids which formed the authigenic zeolites originated in basaltic sandstones of the underlying Roy Creek member, in which authigenic heulandite-clinoptilolite has developed, or from an interbedded basaltic sandstone in the Sunset Highway member. Galloway (1979) interpreted the development of pore-filling zeolites in volcaniclastic sandstones to be a relatively advanced stage of diagenesis that occurs at intermediate depths of burial (1,000 to 3,000 m).

The diagenetic history of the relatively matrix-free arkosic sandstones in the Sunset Highway member is very different from the underlying basaltic sandstones, conglomerates, and breccias of the Roy Creek member. This reflects differences in pore fluid chemistry related to different compositions of the two members. It also indicates little exchange of pore fluids between the two members. This is interpreted to partly result from the more unstable composition of the Roy Creek member. Basaltic rock fragments of the Roy Creek member rapidly altered during early burial and lithification and produced pore fluids which deposited extensive secondary pore-lining and pore-filling calcite, smectite (nontronite), chlorite, and clinoptilolite-heulandite. In this way basaltic rock fragments became isolated from further alteration and interaction with pore fluids, and, therefore, could not significantly affect diagenesis of the arkosic Sunset Highway member. A similar early "self-sealing" diagenetic history is envisioned for the basaltic sandstones and debris flows in the Sunset Highway member. It is also probable that

Figure 68. Scanning electron photograph and EDX analysis of authigenic potassium feldspar overgrowths on a detrital feldspar grain. A: Blocky overgrowths appear to be growing over Stage 3 clay coats (webby material on grain surface). B: Energy dispersive spectra of circled area on A shows the major elements of potassium feldspar (Si, Al, and K). The absence Ca indicates a relatively pure K-feldspar composition. Locality 3812-1 (T. 4 N., R. 7 W., NE 1/4 sec. 16).

A.
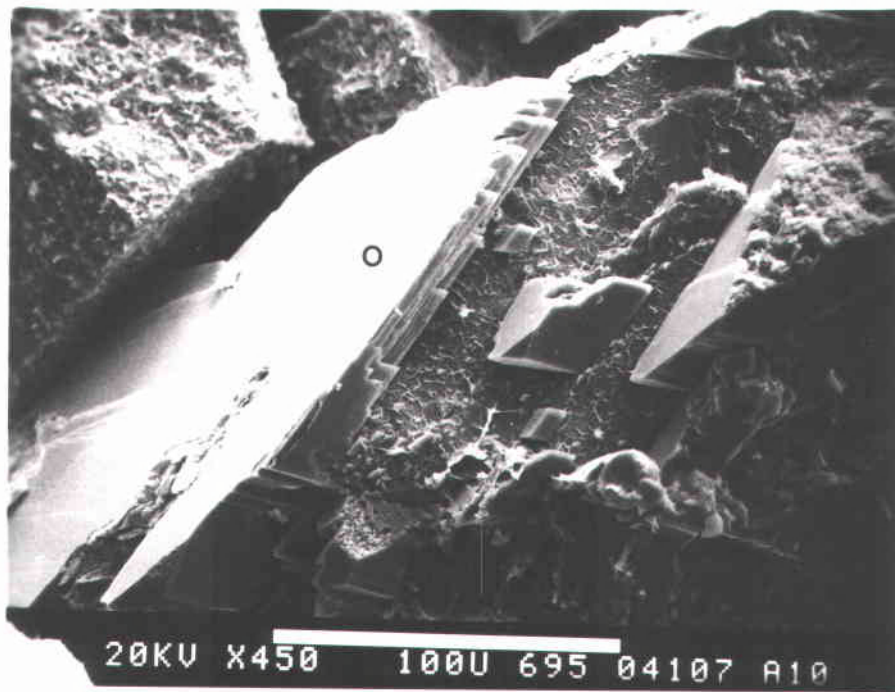
B.
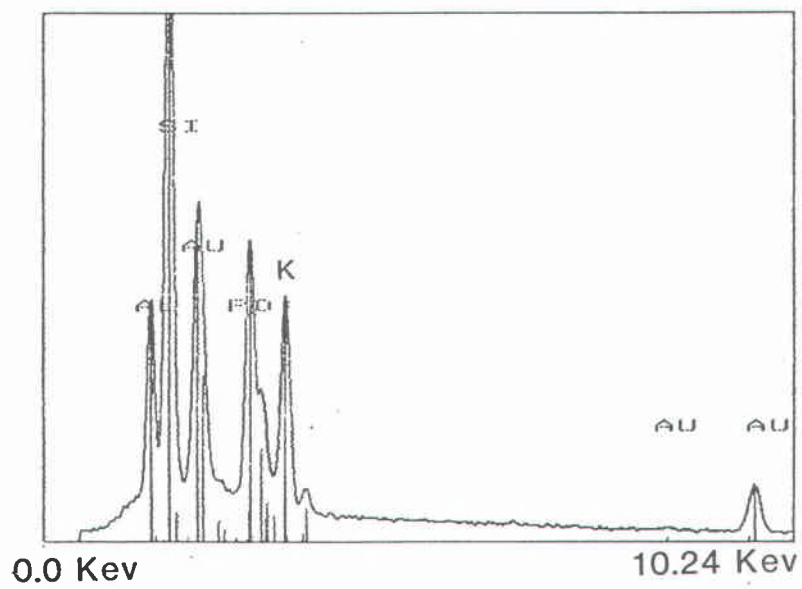
Figure 68.
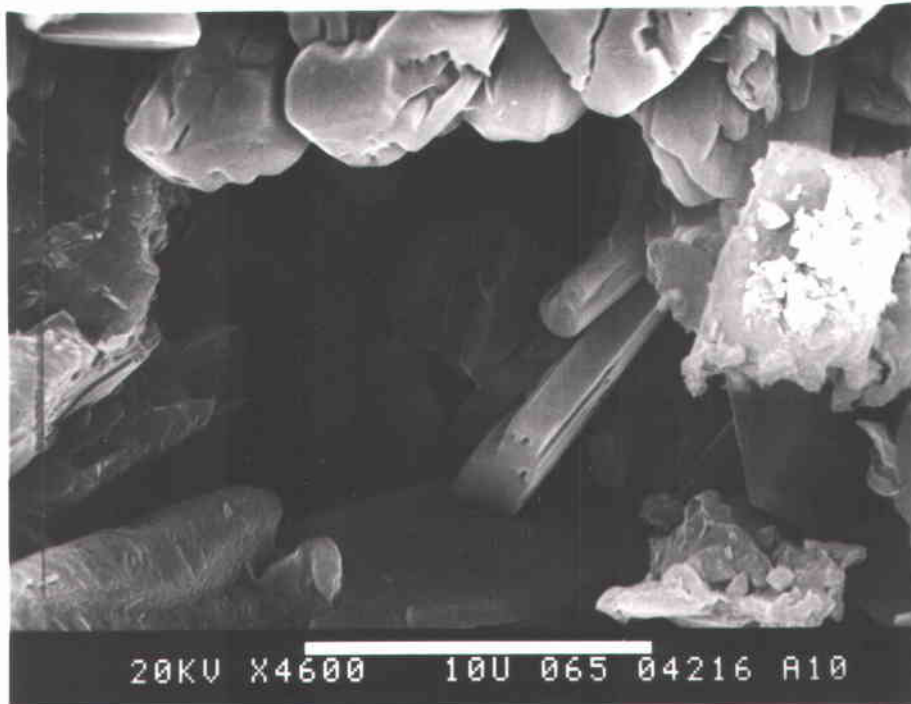
Figure 69. Scanning electron photograph of a diagenetic mineral in
muddy, very fine-grained arkosic sandstone of the Sunset
Highway member. The morphology compares favorably with
both clinoptilolite-heulandite illustrated by Welton
(1984) and hexagonal erionite illustrated by Sheppard
(1987).

muddy very fine-grained sandstones and siltstones in the lower Sunset Highway member severely impeded fluid exchange between the Sunset Highway and Roy Creek members.

Age and Correlation

The two identifiable macrofossils in the Sunset Highway member are not age diagnostic (Dr. Ellen Moore, U.S. Geological Survey, written communication, 1984). However, mudstones of the Sweet Home Creek member, which overlie the Sunset Highway member in the thesis area, contain foraminiferal assemblages assigned to the middle to late Narizian stage by Rau (written communication, 1984) and late Narizian to early Refugian stages by McDougall (written communication, 1984). These foraminiferal stages are late middle to late Eocene in age.

Rarey (1986) collected a number of age diagnostic foraminiferal and calcareous nannofossil assemblages from the Sweet Home Creek member west of the thesis area. In his area, the Sunset Highway member is absent and mudstone in the lower part of the Sweet Home Creek member is considered to be age equivalent to the Sunset Highway member (Rarey, 1986). All foraminiferal assemblages from this member were assigned to the late Narizian (late middle to late Eocene). Calcareous nannofossils (coccoliths) from the lower to upper middle part of the Sweet Home Creek member were assigned to subzone CP-14a, which is correlative to the late Narizian foraminiferal stage (Rarey, 1986). This indicates an upper middle Eocene for the Sunset Highway member. The upper Tillamook Volcanics are probably no younger than about 42 Ma (see Age section of the Tillamook Volcanics). This restricts the Sunset Highway member to an upper middle Eocene age.

Based on the stratigraphic position of the Sunset Highway member and age restrictions imposed by foraminiferal and calcareous nannofossil assemblages of the Sweet Home Creek member, the following units in northwestern Oregon are age equivalent to the Sunset Highway member: the Sweet Home Creek member of the Hamlet formation (Rarey, 1986), the Nestucca Formation, the Spencer Formation, and the Cowlitz Formation (fig. 7). The Sunset Highway member is also time correlative with the Cowlitz Formation of southwest Washington as

originally defined by Weaver (1912).

On a more specific local scale, the Sunset Highway member is correlative to the lower part of the Cowlitz Formation as defined by previous workers in Clatsop, Columbia, Washington, and northeastern Tillamook Counties. This includes the lower sandstone member (Tc_2 and Tc_3) of Olbinski (1983) and Nelson (1985), and heterolithic lithofacies of Jackson, 1983). The Sunset Highway member is slightly older than the cross-bedded shallow marine arkosic sandstone of the upper Cowlitz Formation (Tc_5 = upper sandstone member of Olbinski, 1983, and Nelson, 1985, and sandstone lithofacies of Jackson, 1983).

Sweet Home Creek member

The Sweet Home Creek member is a 100 to 400 m -thick mudstone-dominated unit of the Hamlet formation informally named by Rarey (1986) after a proposed type section in Sweet Home Creek immediately west of the thesis area (T. 4 N., R. 8 W., sec 20 and 29). Although the unit is primarily mudstone, it contains some siltstones, a few beds of fine- to coarse-grained moderately to poorly sorted basaltic sandstone, and local (e.g. along Sunset Highway in the northeastern part of the thesis area) micaceous arkosic turbidite sandstones (figs. 70 and 71).

Distribution

The Sweet Home Creek member has been mapped in southeastern Clatsop County, northwestern Tillamook County, and western Columbia County (Niem and Niem, 1985; Rarey, 1986; Safley, in prep.; Berkman, in prep.). In eastern Clatsop County, Sweet Home Creek member mudstones and turbidite sandstones overlie Sunset Highway member arkosic sandstones. The Sunset Highway member pinches out in central Clatsop County (at about the longitude of the Nehalem River in the thesis area). To the west of the pinchout the Sweet Home Creek member overlies fine-grained basaltic sandstones and siltstones of the Roy Creek member (Rarey, 1986; Niem and Niem, 1985). Because the Hamlet formation is an informal unit which has only recently been proposed, others workers have not as yet used the name (e.g., Bruer and others, 1984). Therefore, the distribution of the Sweet Home Creek member in Columbia, Washington, and northeastern Tillamook counties is incompletely known.

In the study area, the Sweet Home Creek member is well-exposed along Sunset Highway (locality 371-1, T. 4 N., R. 7 W., SE 1/4 sec. 3), in cut banks of the Nehalem River (localities 829-1 and 829-2, both T. 4 N., R. 7 W., NE 1/4 sec. 9), in stream cut banks of Humbug Creek near the confluence with the Nehalem River (localities 925-7 and 925-8, T. 4 N., R. 7 W., SW 1/4 sec. 5), and in road cuts along the lower Nehalem River north of Lukarilla (localities 74-4 and 74-5, T. 4

N., R. 7 W., SW 1/4 sec. 7; Plate I).

Lithology

Most of the Sweet Home Creek member consists of micro-micaceous and carbonaceous dark gray (N 3) to grayish black (N 2) mudstone which weathers moderate yellowish brown (10YR 6/4) to light brown (5YR 6/4). The mudstones are typically faintly laminated to thin-bedded and commonly contain small hook-shaped Helminthoida trace fossils. Small (5-15 cm) spheroidal to cone-shaped calcite- and/or pyrite-cemented concretions are common in the unit. Sweet Home Creek mudstones can be differentiated compositionally from those of the overlying Jewell member (Keasey Formation), which are generally similar, by the greater abundance of very fine-grained mica, carbonaceous debris, an laminations. In addition, Sweet Home Creek member mudstones lack the tuffaceous and glauconitic components of the Jewell member (Rarey, 1986) and also tend to contain more silt.

Locally, thin beds of basaltic turbidite sandstone are present in the lower part of the Sweet Home Creek member (e.g. localities 716-9, T. 4 N., R. 7 W., SW 1/4 sec. 3; 829-1 and 829-2, T. 4 N., R. 7 W., NW 1/4 sec. 9). These beds consist of moderately to poorly sorted medium- to coarse-grained basaltic rock fragments in a muddy matrix and contain fragmented gastropod and small pelecypod shells, echinoid spines, and fish scales (McDougall, written communication, 1984). Mudstones associated with the basaltic interbeds contain middle bathyal benthic Foramininfera with considerable amounts of transported outer shelf material (Dr. Kristin McDougall, written communication, 1984).

Thin (1-15 cm), even, rhythmically bedded arkosic turbidite sandstones in the lower part of the Sweet Home Creek member are well exposed in the northeastern part of the study area along Sunset Highway (locality 371-1, T. 4 N., R. 7 W., SE 1/4 sec. 3; figs. 70 and 71) and in a road cut along a Spur off Fishhawk Falls highway about one km. south of Jewell Junction (locality 627-2, T. 4 N., R. 7 W. SE 1/4 sec. 4). A 6 m measured section was made at the Sunset Highway locality (fig. 70). At this locality the thicker sandstones (>2 cm

Thick, structureless carbonaceous and micro-micaceous dark gray mudstone with four very thin beds of very fine-grained arkosic sandstone. Locally bioturbated. Vertical to subvertical cylindrical sand-filled burrows (fig. 75B). Spherical (10 cm diameter) calcite-cemented concretions.

Thinly interbedded carbonaceous and micro-micaceous very fine-grained arkosic sandstone and dark gray micro-micaceous and carbonaceous mudstone. Sandstones are locally calcite cemented and have well-preserved flute marks and load casts (fig. 73A). Basal part of sandstone beds are parallel laminated and upper parts exhibit microcross-laminations (Bouma B, C sequences). Sparse spherical (1/2 cm diameter) pyrite concretions. Thin discontinuous laminae and lenses of very fine-grained arkosic sandstone in the mudstone. Ledge-forming calcareous concretionary ledge.

Thinly interbedded micro-micaceous and carbonaceous very fine-grained micaceous arkosic sandstone and dark gray carbonaceous and micro-micaceous mudstone. Sandstones have sharp basal contacts with flute marks and exhibit parallel laminations near the base and microcross-laminations near the top. Carbonaceous plant debris concentrated at the tops of sandstone beds. Sparse, small (1/2 cm diameter) spherical pyrite concretions. Local zones of Helminthoida burrows in mudstones. Rare subvertical to vertical sand-filled calcite cemented cylindral burrows.

Structureless dark gray carbonaceous and micro-micaceous mudstone. Rare 1 cm thick calcareous concretions. Minor discontinuous very fine-grained sandstone laminae (starved ripples). Large foraminifers (Cyclamina pacifica).

Thinly interbedded micro-micaceous and carbonaceous very fine-grained arkosic sandstone and carbonaceous and micro-micaceous dark gray mudstone. Ledge-forming sandstones have sharp basal contacts, are very thinly parallel laminated in the lower part and discontinuously micro-scale cross-laminated and convolute bedded in the upper part (Bouma B, C seqences (fig. 72B). Mudstone locally bioturbated. Small (1/2 cm. diameter) spherical pyrite concretions.

Very thinly laminated with starved ripples of carbonaceous and micro-micaceous siltstone and very fine-grained arkosic sandstone. Thin discoidal calcareous concretions.
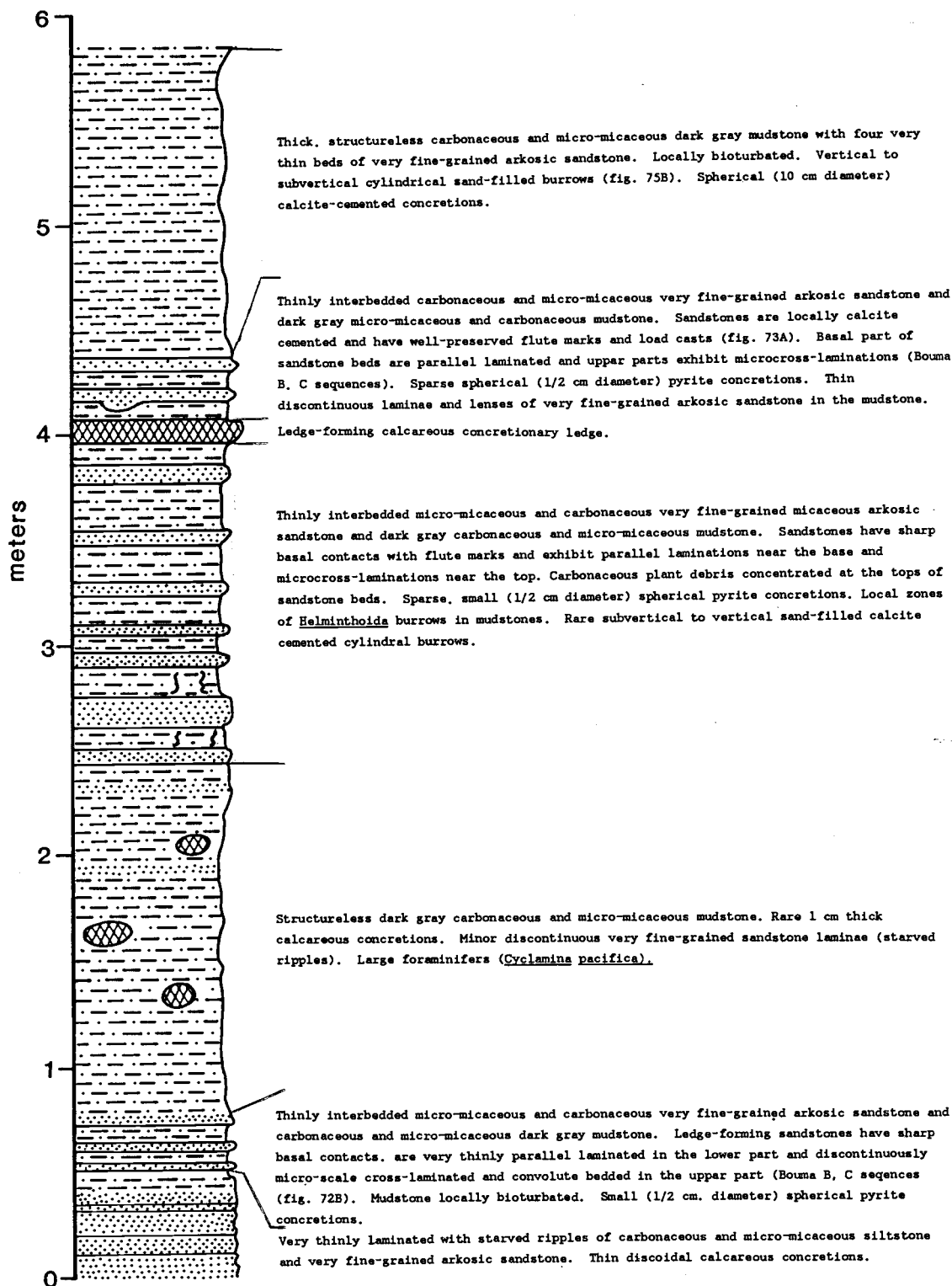
Figure 70. Measured section of thin bedded turbidite sandstones in the lower part of the Sweet Home Creek member. U.S. 26 Slump section, exposed along Sunset Highway. Locality 371-1, T. 4 N., R. 7 W., SE 1/4 sec. 3.

thick) are continuous and can be traced over the entire length of the outcrop (fig. 71A) while many of the thinner sandstones (≤2 cm thick) are discontinuous and pinch out over a distance of 10-15 m.   The sandstones are carbonaceous, micromicaceous, weakly normal graded, and parallel to convolute to microcross-laminated (fig. 71B). They have sharp basalt contacts and gradational upper contacts (fig. 71B). Flute marks preserved as flute and load casts are well-preserved on the bases of the thicker calcite-cemented sandstone beds (fig. 72A). All of these features are typical of turbidite deposition (Middleton and Hampton, 1973). Vertical to subvertical cylindrical burrows and large foraminifers (e.g., Cyclamina pacifica) are common in some mudstone beds and bioturbation completely disrupts bedding in places (fig. 72B). At this locality the ends of many of the discontinuous sandstone beds arch slightly upwards, and some are distinctly thicker in the middle. These features suggest that the turbidites were deposited in shallow paleochannels. Although the unit is not well exposed, similar sandstones were not observed elsewhere in the thesis area, which also indicates that distribution of the sandstones may be controlled by paleochannels.   Safley (in prep.) has also recognized these thin bedded turbidite sandstone in Clatsop County. Based on a limited number of measurements, the orientation of paleochannel axes (approximately S20°W) is approximately perpendicular to that of flute molds (approximately N782°W). The reason for this disparity is probably related to difficulty in accurately picking the orientation of low-angle paleochannel axes. No upward thinning or coarsening sequences of turbidite sandstones that are typical of channel abandonment were recognized (Walker, 1973).

Petrography

Turbidite sandstone beds from two localities were examined petrographically in thin section. Grain mounts of heavy mineral (specific gravity ≥2.85) grain mounts of the 3ϕ and 4ϕ size fractions of two samples from these localities were also studied. One turbidite sandstone was briefly examined with the scanning electron microscope. The sample from locality 627-2 (T. 4 N., R. 7 W., SE 1/4 sec. 4) is a

A.

B.

Figure 71: Photographs of micaceous arkosic turbidite sandstones in the upper part of the Sweet Home Creek member exposed along Sunset Highway. A. Outcrop of light gray, thin, rhythmically-bedded arkosic sandstones in dark gray mudstones. Note erosionally resistant ledge of calcite-cemented sandstone in the upper part of the outcrop. B: Close-up of normally graded sandstone bed. Note sole marks, load casts, and sharp bottom contacts, and convolute carbonaceous laminae and sand-filled burrows in upper part. Locality 371-1 (T. 4 N., R. 7 W., SE 1/4 sec. 3) along Sunset Highway approximately 3.5 km east of Jewell Junction.

A.

B.

Figure 72: Features of the thin-bedded turbidite sandstone-mudstone section in the lower part of the Sweet Home Creek member. A: Flute molds on the base of calcite-cemented turbidite arkosic sandstone. B: Long, cylindrical subvertical sand-filled burrows in mudstone. Note very thin, discontinuous lenses and wisps of sandstone (starved ripples). Locality 371-1 (T. 4 N., R. 7 W., SE 1/4 sec. 3) along Sunset Highway about 3.5 km east of Jewell Junction.

well sorted, fine-grained concretionary sandstone which classifies as an arkose (fig. 41). In thin section the rock is tightly cemented with sparry carbonate (probably calcite) which forms about 34% of the rock. Detrital framework grains with angular to ragged boundaries appear to be floating in the carbonate cement which has partially replaced feldspars and pried apart mica folia. It is probable that at least some of the finer-grained detrital feldspar, and especially the calcic plagioclase feldspars, have been completely replaced by carbonate cement. Detrital framework constituents of the sample are monocrystalline quartz (8%), potassium feldspar (22%), albite twinned plagioclase feldspar (11%), biotite and chloritized biotite (11%), muscovite (9%), opaques and carbonized plant debris (5%), and polycrystalline quartz (trace). Potassium feldspar in the sample is highly altered. No overgrowths were observed, indicating relatively early calcite cementation of the rock. The pervasive calcite cementation and replacement of detrital grains precludes assessment of compositional and textural maturity.

The sample from locality 371-1 (T. 4 N., R. 7 W., SE 1/4 sec. 3) is a muddy, fine-grained sandstone which plots as an arkose (fig. 41). A point count of 650 grains yields the following modes: 40% monocrystalline quartz, 24% plagioclase feldspar, 4% potassium feldspar, 18% total muscovite, biotite, and chloritized biotite, 6% carbonate cement (probably calcite), 2% pyrite, and 6% matrix clays. The rock is texturally immature (> 5% matrix) and compositionally mature (dominantly quartz, feldspar, and mica without rock fragments) (Folk, 1974). Although no overgrowths were seen, a trace amount of an intergranular authigenic mineral having the petrographic characteristics of zeolite mineral is present. This mineral is tentatively identified as mordenite based on the columnar morphology of the crystals observed with the scanning electron microscope. The morphology resembles mordenite specimens examined by Welton (1984), but the crystals are somewhat large. EDX and X-ray analysis, which were not performed in this study, would be required make a positive identification.

The heavy mineral assemblage from locality 627-2 (T. 4 N., R. 7 W., SE 1/4 sec. 4) is almost completely composed of muscovite and

biotite with a few grains of green and brown hornblende. The heavy
mineral assemblage from locality 371-1 (T. 4 N., R. 7 W., SE 1/4 sec.
3) is more diverse and contains abundant to very abundant muscovite
and biotite, very common pyrite, common chlorite, occasional opaque
oxides (magnetite, ilmenite, and leucoxene), rare diopside (?),
apatite, and epidote, and very rare hypersthene, zircon, and colorless
garnet.

Provenance

Framework minerals of micaceous arkosic turbidites in the Sweet
Home Creek member are petrographically similar to clean micaceous
arkosic sandstones of the underlying Sunset Highway member and they
also to have a similar heavy mineral suite. The clay mineral fraction
of Sweet Home Creek mudstones contains some illite (fine-grained mica)
which is thought to be detrital. This indicates a common acid
plutonic and high-rank metamorphic source area for the two units.
Rare basaltic turbidite sandstone beds in the Sweet Home Creek member
contain abundant basaltic rock fragments which indicate a local
volcanic source area ("Tillamook Island"). Rarey (1986) reported that
textural characteristics of basaltic rock fragments and the size and
composition of plagioclase crystals in basaltic sandstones of the
Sweet Home Creek member are similar to the Tillamook Volcanics and
interpreted the Tillamook Volcanics to be the source area for these
beds. Clay minerals in Sweet Home Creek mudstones include kaolinite
and smectite which are probably were derived from weathering of a
volcanic source area (see clay mineralogy section). Therefore, the
sandstones in the Sweet Home Creek member have a local mixed basaltic
and extrabasinal granitic-metamorphic provenance similar to the Sunset
Highway member.

Clay Mineralogy

X-ray diffraction analysis of the clay mineral fraction of three
mudstone samples from the Sweet Home Creek member was performed
according to the methodology of Harward (1976) (Appendix X). The clay

mineral assemblage of these samples consists of kaolinite, illite (fine-grained mica) and smectite.

Kaolinite is recognized by a basal spacing of about 7.2 Å which is insensitive to drying, treatment with ethylene glycol and glycerol, and moderate heating, but which collapses on heating above 500°C due to destruction of the kaolinite structure (fig. 73). Illite (fine-grained mica) is recognized by a 10 to 10.5 Å peak which is not changed with drying, heating, or treatment with ethylene glycol or glycerol, but which becomes more intense as water layers are removed. Smectite minerals are swelling clays and are identified by this expansive character. Potassium-saturated (K- on figs. 73, 74, and 75) smectites at 54% relative humidity have basal spacings of about 11.5 to 12 Å. Treatment with ethylene glycol expands the basal spacing to about 17 or 18 Å (fig. 73). Glycerol treatment expands beidellite to about 15 Å and montmorillonite to about 17.5 Å. When oven dried to moderate to high temperatures (300 to 550°C) smectites collapse and have basal spacing of about 10 Å (fig. 73).

The X-ray diffraction pattern of the clay mineral fraction of mudstone from locality 716-9 (T. 4 N., R. 7 W., SW 1/4 sec. 3) displays large and broad smectite (montmorillonite) peaks, small kaolinite peaks, and very small illite peaks (fig. 73). Non-clay (but clay sized) minerals in this sample include quartz, plagioclase, and possible zeolite. The X-ray diffraction patterns of the clay mineral fractions of mudstones from localities 829-2 (T. 4 N., R. 7 W., NW 1/4 sec. 9) and 371-1 (T. 4 N., R. 7 W., SE 1/4 sec. 3) are similar in having strong kaolinite and illite peaks with weaker smectite (montmorillonite) reflections (figs. 74 and 75). The non-clay mineral fractions from these localities contain quartz.

Based on a limited number of samples, the clay mineralogy of the Sweet Home Creek member appears to differ from the Jewell member (Keasey Formation) in containing kaolinite and greater amounts of illite (see Jewell member clay mineralogy section). The greater amount of illite reflects the micro-micaceous character of the Sweet Home Creek member mudstones which is visible in hand specimens.

Kaolinite clays have been reported to develop during weathering of basaltic to intermediate volcanic terrains in tropical and humid
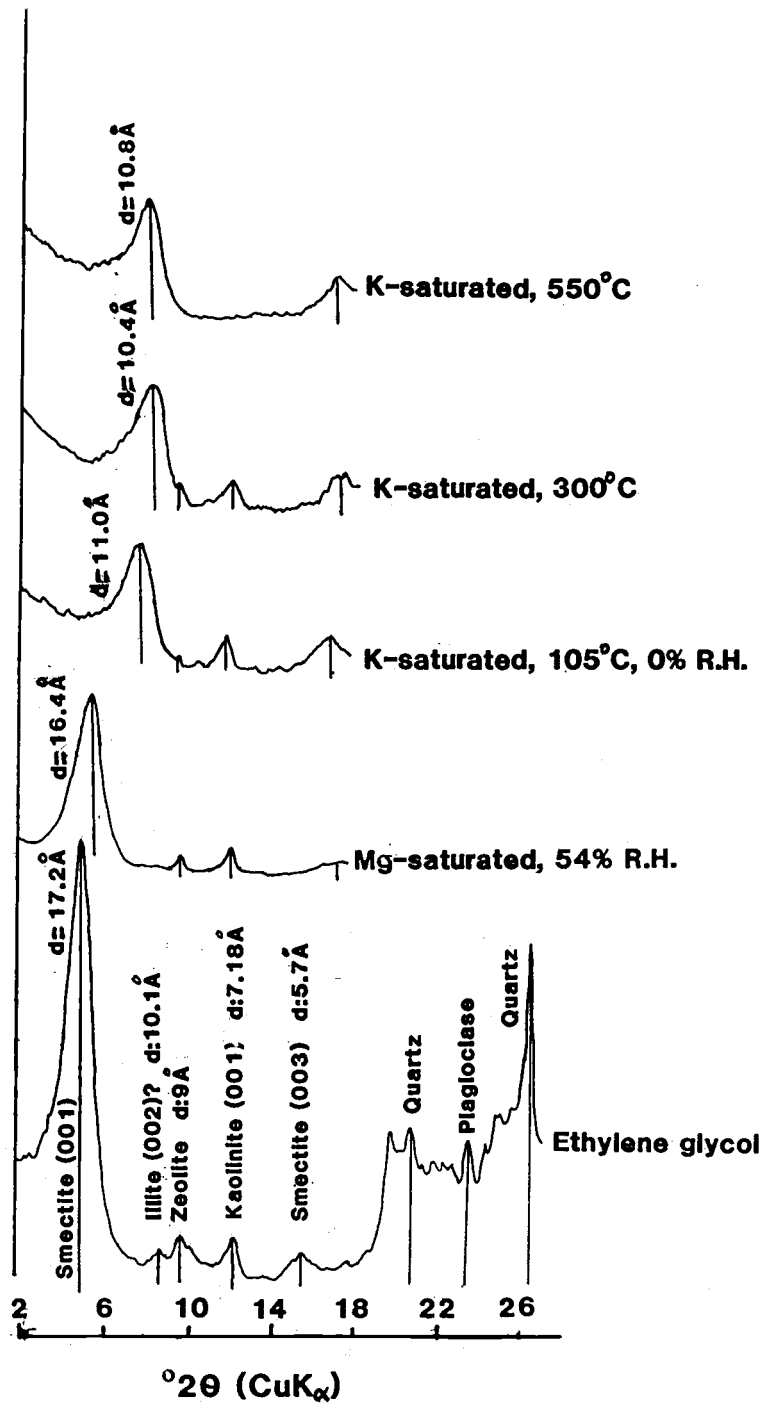
Figure 73. X-ray diffraction patterns of mudstone clay fraction from locality 716-9. Note shift of smectite (montmorillonite) peak with different treatments and collapse of small kaolinite peak at 550°C. Sample location T. 4 N., R. 7 W., SW 1/4 sec. 3 along Sunset Highway about 2 km east of Jewell Junction (Plate I).

Figure 74. X-ray diffraction patterns of mudstone clay fraction from locality 829-2. Note strong kaolinite peaks which collapse at 550°C, sharp illite peaks which remain essentially unchanged, and changes in smectite peaks (different d-spacings) with various treatments. Sample location T. 4 N., R. 7 W., NW 1/4 sec. 9 along the Nehalem River about 2 km south of Jewell Junction (Plate I).

202
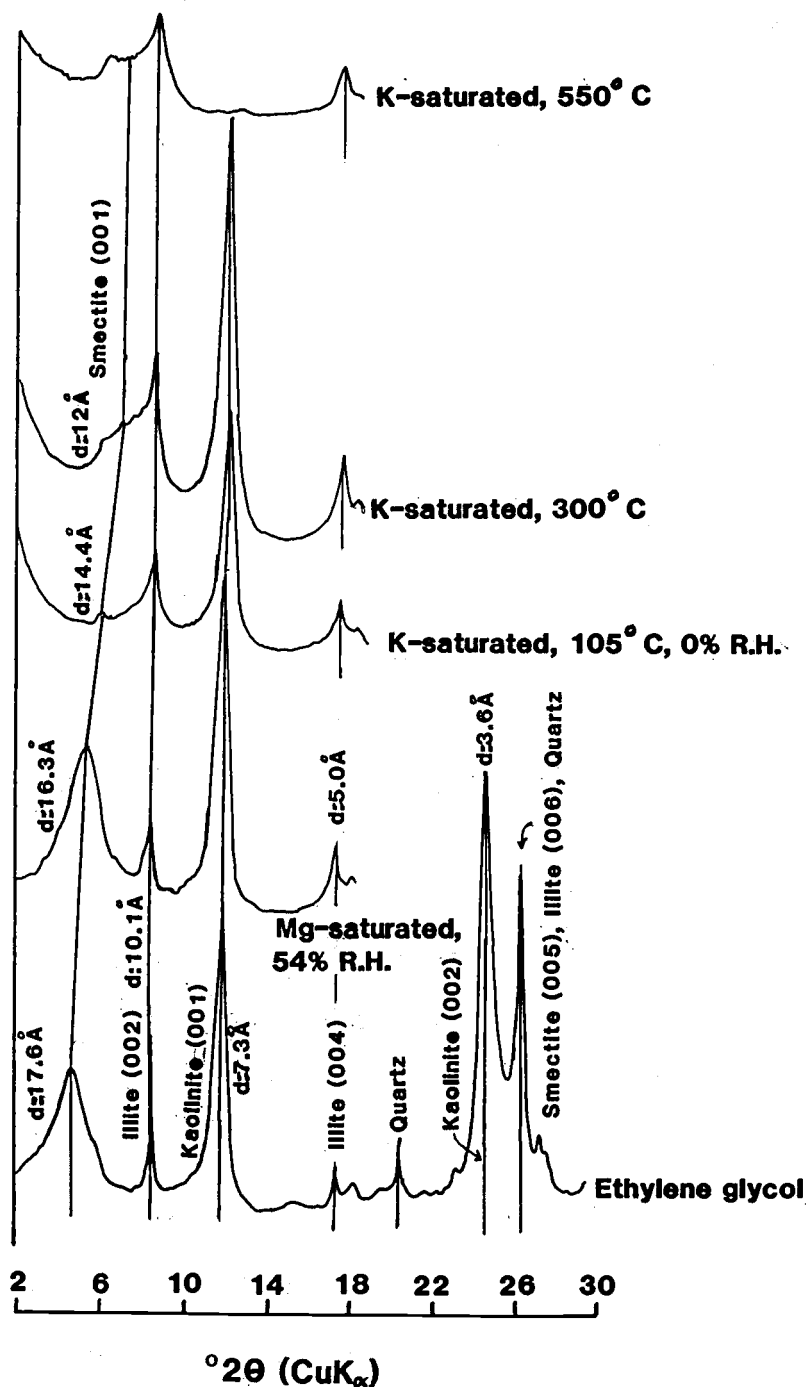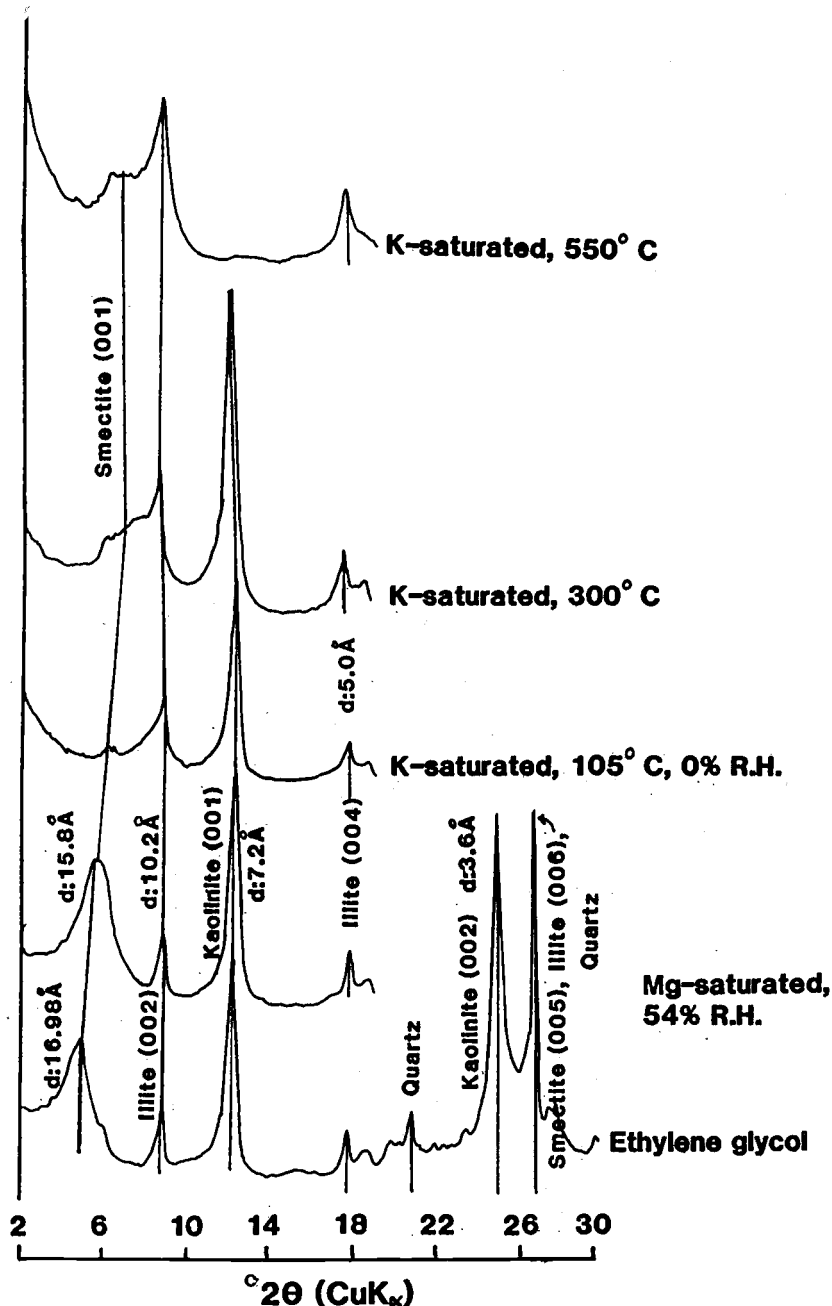

Figure 75. X-ray diffraction patterns of mudstone clay fraction from
locality 371-1. Note strong kaolinite peaks which
collapse at 550°C, sharp illite peak which become more
intense with heating, and changes in smectite
(montmorillonite) peaks with various treatments. Sample
locality T. 4 N., R. 7 W., NE 1/4 sec. 10 along Sunset
Highway (Plate I).

temperate climates (Glasmann, 1982; Glasmann and Simonson, 1985; Eswaran and DeConinck, 1971 in Glasmann, 1982). Smectites can also be transformed to kaolinite by extensive leaching and wetting and drying cycles in tropical soil microenvironments (Eswaran and DeConinck, 1971 in Glasmann, 1982). The presence of kaolinite in Sweet Home Creek mudstones is thought to reflect extensive tropical weathering of late Eocene volcanic units (such as the Tillamook Volcanics) in the source area of the Hamlet formation during the late middle and early late Eocene. Plant fossils in the Hamlet and Cowlitz formations and in interbeds in the lower Tillamook Volcanics indicate a humid subtropical climate (Cameron, 1980; Jackson, 1983). Basaltic sandstone beds in all three members of the formation are also thought to reflect this local source area.

Smectite also commonly forms during weathering of poorly drained soils developed on volcanic bedrock in tropical and humid temperate climates (Glasmann, 1982; Glasmann and Simonson, 1985). The presence of smectite in Sweet Home Creek member mudstones is also thought to reflect the presence of a late Eocene volcanic source terrain for part of the Hamlet formation.

Illite in Sweet Home Creek member is thought to be a detrital fine-grained mica weathered and transported from an acid plutonic source area. Micas are large and abundant in the underlying Sunset Highway member arkosic sandstones and the presence of megascopically-visible fine sand-sized mica flakes is a distinguishing characteristic of Sweet Home Creek mudstones. Therefore, it is likely that illite, or degraded mica, in the Sweet Home Creek member simply reflects clay-sized micas transported into a deep water (bathyal) depositional basin and represents a different provenance than the kaolinite and smectite constituents.

Contacts

The contact of the Sweet Home Creek member with the underlying Roy Creek and Sunset Highway members is thought to be conformable and gradational for the following reasons: 1) there is no significant change in bedding attitude between mudstones assigned to the Sweet

Home Creek member and arkosic sandstones of the Sunset Highway member. (e.g. August Fire road measured section); 2) there is no significant age difference between the Sweet Home Creek member and underlying members of the Hamlet formation; 3) turbidite sandstones in the Sweet Home Creek member are compositionally similar to those of the Sunset Highway member; 4) Sweet Home Creek mudstones contain foraminiferal assemblages indicating downslope transportation of outer shelf species (Sunset Highway member depositional environment) to middle bathyal depths; and 5) the transgressive Roy Creek member-Sunset Highway member-Sweet Home Creek member sequence documents uninterrupted sedimentation in progressively deeper water.

The overlying Cole Mountain basalt (sills, dikes, and submarine pillow basalt flows) exhibits features such as pillows and irregular intrusive contacts with the Sweet Home Creek member that suggest a conformable to intrusive contact between the two units (e.g., locality 74-4 and 74-5, T. 4 N., R. 7 W., SW 1/4 sec. 7). No evidence was found in the thesis area to indicate an unconformity between the two units.

The contact between the Sweet Home Creek member and Jewell member (Keasey Formation) was never recognized in the field area. North and east of the thesis area the Keasey Formation (Refugian) has been reported to be unconformable on the upper Narizian Cowlitz Formation which, in part, is a lateral equivalent of the Sweet Home Creek mudstone (Kadri, 1982; Nelson, 1985; Olbinski, 1983; Bruer and others, 1984). In the thesis area, Sweet Home Creek member mudstones and Jewell member mudstones (Keasey Formation) do not appear to be separated by a major unconformity. Both units have similar bedding attitudes, and the upper Sweet Home Creek member and lower Jewell member are essentially the same age (late Narizian/early Refugian). However, the base of the Keasey Formation is marked by a glauconitic facies (Rarey, 1986; Martin and other, 1985 in Niem and Niem, 1985; Dr. Niem, OSU geology dept., personal communication 1988) and at one locality in the thesis area (3624-3, T. 4 N., R. 7 W., NW 1/4 sec. 17; Lost Lake Creek) glauconite rip-ups in tuffaceous mudstone were observed. This can be interpreted to represent intrabasinal erosion and supports the existence of at least a minor unconformity or diastem

between the Hamlet formation and Keasey Formation. Glauconite usually forms in areas with low sedimentation rates under slightly reducing conditions due to alteration of fecal organic clay-rich material and can indicate an unconformity. In addition, environmentally diagnostic foraminiferal assemblages indicate a slight shallowing trend in the upper part of the Sweet Home Creek member which may be related to the unconformity at the base of the Keasey Formation (see depositional environment section). Late Narizian arkosic sandstones (Tc$_5$, of Olbinski, 1983, and Nelson, 1985) which overlie Sweet Home Creek member mudstones (Tc$_4$ of Olbinski, 1983, and Nelson, 1985) north and east of the thesis area are thought to missing in the thesis area due to a depositional pinch-out rather than erosion related to the unconformity at the base of the Keasey Formation. The unconformity between the Refugian Keasey Formation and late Narizian Cowlitz Formation is probably more pronounced north and east of the thesis area because of shallower strata were deposited in this area.

Age and Correlation

Nine samples from seven different localities in the thesis area yielded age-diagnostic foraminiferal assemblages (Appendix V). McDougall (U.S. Geological Survey, written communication, 1984) assigned five of the seven assemblages to the late Narizian to early Refugian and four assemblages (three from the same locality) to the Refugian. Rau (Washington Dept. of Natural Resources, written communication, 1984) interpreted all assemblages to be Narizian, with four of nine assemblages representing diagnostic Narizian assemblages. Evidently the two micropaleontologists (who examined identical assemblages from the same localities) have slightly different interpretations of the age significance of taxa present in these samples.

Smear slides of mudstones (for calcareous nannofossils) were prepared for five of the seven localities which yielded age-diagnostic foraminiferal assemblages. None contained key zonal taxa necessary for precise age assignment (David Bukry, U.S. Geological Survey, written communication, 1984; Appendix VI). However, three contained

Pemma stradneri Chang which is limited to the late middle Eocene or early late Eocene and has previously been reported from the Tillamook Volcanic Series (Bukry, written communication, 1984). This agrees with calcareous nannofossil subzones CP-14a and CP-14b reported by Rarey (1986) for the Sweet Home Creek member. These subzones are correlative to the middle to late Narizian foraminiferal stage (fig. 7) and indicates that the late Narizian is a good chronostratigraphic stage for the Sweet Home Creek member.

As part of this investigation foraminiferal assemblages were picked from two samples from the type area of the Yamhill Formation along Mill Creek in the central Oregon Coast Range (Appendix V). One of the samples contained a "Yamhill" fauna which is distinct from the "Cowlitz" fauna and was assigned to the lower or middle part of the Narizian stage (Rau, written communication, 1984). The other sample had only a general Narizian fauna. This indicates that the Sweet Home Creek member is younger than most or all of the Yamhill Formation. This is unlike Bruer and others (1984) who called strata equivalent to most of the Sweet Home Creek member of the Hamlet formation the Yamhill Formation in the subsurface of Columbia and Clatsop counties.

The following units in northwestern Oregon are in part time correlative with the Sweet Home Creek member: the Sunset Highway member of the Hamlet formation, the Cowlitz Formation (upper part), and the Spencer Formation. Rarey (1986) showed that the Sweet Home Creek member is time-equivalent with the type Cowlitz Formation of southwestern Washington and indicated that it is directly correlative to the lower part of the Unit B siltstones of Wolfe and McKee (1973) in southwest Washington.

Depositional Environment

Fairly accurate paleoenvironmental determinations were possible because nearly 100 different species of foraminifera were identified in Sweet Home Creek member mudstones, with up to 34 different species identified in samples with very diverse assemblages (Appendix V). Nine samples from seven different localities yielded environmentally diagnostic foraminiferal assemblages. McDougall (written

communication, 1984) and Rau (written communication, 1984) both consider most of the faunas to be indicative of an upper to middle bathyal depositional environment, with a range from outer neritic to possibly lower middle bathyal.

Both micropaleontologists made similar depth interpretations. The shallowest faunas are from the lower part of the Sweet Home Creek member and represent outer neritic (100 to 200 m) to upper bathyal (100 to 500 m) depths. Faunas from the middle part of the unit were interpreted to be the deepest, at middle bathyal depths (500 to 1200 m). The upper part of the unit is interpreted to have been deposited at upper to upper middle bathyal depths (200 to 500 m), which is somewhat shallower than the middle part of the Sweet Home Creek member. These interpretations indicate a deepening trend followed by a slight shallowing trend which may be related to an unconformity reported at the base of the Keasey Formation (see contacts section). In any case, the foraminiferal faunas indicate deposition of the Sweet Home Creek member in an outer shelf to "middle" slope (outer neritic to middle bathyal) environment.

All five samples of Sweet Home Creek mudstones examined for calcareous nannofossils contain pentalith taxa (coccoliths) which indicate relatively shallow water deposition (David Bukry, U.S. Geological Survey, written communication, 1984). Although this interpretation of water depth is not as precise as those obtained from environmentally diagnostic Foraminifera, it is in general agreement.

Other evidence which indicates deposition in a low energy outer shelf to middle slope environment include the following: 1) common Helminthoida burrows, 2) lithologic similarity to modern upper slope deposits (Kulm and others, 1975), 3) preservation of delicate ornamentations on microfossil tests indicating little, if any, transportation and post-depositional alteration, and 4) a slightly reducing environment indicated by preserved carbonaceous material and pyrite.

Rhythmically bedded fine-grained arkosic sandstones in the lower part of the Sweet Home Creek member are interpreted as turbidite deposits which originated on the shelf. The sandstones exhibit features such as sharp basal contacts with flute marks, faint normal

grading, thin parallel laminations and convolute to microcross-laminations in the upper part which are characteristically associated with Bouma A-B-C and B-C sequences in turbidite deposits (Middleton and Hampton, 1973; figs. 71 and 72). This is consistent with the depositional environment interpreted from foraminiferal data because turbidity currents are the most important mode of sediment transport onto the slope (Blatt and others, 1980). Turbidites in the Sweet Home Creek member may have been storm-generated because the lithology and sedimentary structures (e.g., hummocky cross-stratification) of the underlying Sunset Highway member are consistent with a storm-influenced or storm-dominated depositional environment (Dott and Bourgeois, 1982).

Basaltic sandstones in the Sweet Home Creek member are interpreted as turbidite deposits which originated around volcanic edifices in the depositional basin. The basaltic sandstones consist of moderately to poorly sorted medium- to coarse-grained basaltic rock fragments in a muddy matrix and contain fragmented gastropod and small pelecypod shells, echinoid spines, and fish scales (Dr. Kristin McDougall, U.S. Geological survey, written communication, 1984). These beds also have sharp bases on underlying mudstone and exhibit normal grading. Mudstones associated with the basaltic interbeds contain middle bathyal benthic Foraminifera with considerable amounts of transported outer shelf material (Dr. Kristin McDougall, U.S. Geological Survey, written communication, 1984). These features are indicative of turbidity currents of basaltic detritus originating from volcanic island and redeposited by gravity flows to a deep-water environment.

COLE MOUNTAIN BASALT

Nomenclature

One of the major contributions of detailed geologic mapping associated with this study, with that of Rarey (1986), and that of Safley (in prep.) was the recognition and delineation of an approximately 200 m -thick unit of upper Eocene basaltic intrusions and invasive (?) submarine pillow basalts underlying approximately 60 km^2 in southern Clatsop and northern Tillamook counties. Initially, this unit was informally referred to as Cougar Mountain basalt (Wells and others, 1983) after good exposures of the unit in the vicinity of Cougar Mountain in the thesis area (T. 4 N., R. 8 W, sec. 11). However, the name "Cougar Mountain" has been formally adopted a stratigraphic unit in the Washington Cascade mountains (Dr. A. R. Niem, OSU Dept. of Geology, personal communication, 1986) and an alternative type section at Cole Mountain (T. 4 N., R. 9 W., sec. 12) was proposed by Rarey (1986) in order to avoid future problems with formalizing a name for the unit. Therefore, this informal unit is now referred to as the Cole Mountain basalt (Niem and Niem, 1985; Rarey, 1986).

Detailed geologic mapping, biostratigraphic constraints, petrography, lithology, and geochemistry demonstrate that the Cole Mountain basalt is distinct from other volcanic units in the area. Cole Mountain intrusion and minor submarine volcanics are approximately positioned between upper Narizian Sweet Home Creek member mudstones (Hamlet formation) and upper Narizian/lower Refugian Jewell member mudstones (Keasey Formation) which demonstrates that the unit is younger than the underlying Tillamook Volcanics (fig. 7; Plates I and II). The upper contact of the Cole Mountain basalt is the base of the Keasey Formation (Rarey, 1986) and is older than most, if not all, of this overlying unit. This stratigraphic position constrains the Cole Mountain basalt to a late Narizian to early Refugian (late Eocene) age, which is substantially older than the middle Miocene intrusions of the Columbia River Basalt Group.

Rarey (1986) reported that the Cole Mountain basalt is stratigraphically, petrographically, and geochemically similar to the type area Goble Volcanics. However, type area Goble Volcanics lithologically differ from the Cole Mountain basalt primarily in consisting of subaerial basalt to andesite flows and debris flow breccias with minor pyroclastic and interbedded sedimentary rocks (Henriksen, 1956; Livingston, 1966). Geologic mapping (Olbinski, 1983) and subsurface correlation of wells (Bruer, 1984) in the area between the outcrop belts of Goble Volcanics (northeastern Columbia County) and Cole Mountain basalt (southern Clatsop County) show that volcanic rocks of similar stratigraphic position and geochemistry are essentially absent (only small intrusions of limited areal extent). Timmons (1981) mapped Goble Volcanics in southeastern Clatsop and southwestern Columbia counties but Safley (in prep.) and Berkman (in prep.) found that most of these volcanic rocks are fault blocks of Tillamook Volcanics or Cole Mountain basalt intrusions. The apparent geographic separation and lithologic differences of the Goble Volcanics and Cole Mountain basalt support use of the informal Cole Mountain basalt nomenclature in southern Clatsop and northern Tillamook counties.

However, there are remaining problems with regard to formally naming the Cole Mountain basalt. Preliminary geochemical studies of the Cole Mountain basalt and Goble Volcanics indicate that the two units are closely related (Rarey, 1986). This indicates that the Cole Mountain basalt may be a submarine facies of "invasive" dikes and sills derived from the type Goble Volcanics (see Mode of Emplacement). Such a relationship is analogous to that of the middle Miocene intrusions of Coastal Basalts (Depoe Bay and Cape Foulweather basalts of Snavely and others, 1973) and nearby subaerial flows of the Columbia River Basalt Group in northwestern Oregon and southwestern Washington (Beeson, 1979). Therefore, formal naming of the Cole Mountain basalt will require additional field and geochemical studies beyond the scope of this investigation to determine the relationship between these two genetically related units.

Distribution

Cole Mountain basalt has been mapped over 60 km^2 in southern Clatsop, southwestern Columbia, and northernmost Tillamook counties (Wells and others, 1983; Niem and Niem, 1985). This outcrop belt includes areas which had previously been mapped as undifferentiated sedimentary rocks (Warren and Norbisrath, 1945; Beaulieu, 1973), Goble Volcanics (Timmons, 1981), subaerial flows of the middle to late Eocene Tillamook Volcanics (Warren and Norbisrath, 1945; Jackson, 1983), or as undifferentiated late Eocene intrusions and middle Miocene intrusions of the Columbia River Basalt Group (Beaulieu, 1973).

The Cole Mountain basalt is well-exposed in the thesis area. In the northwestern and northeastern parts of the study area the unit is a generally tabular, sill-like body that is roughly concordant with enclosing mudstones (plates I and II). In the east-central part of the study area erosion has removed the upper part of the unit and remaining outcrops are scattered and have a dike-like plan view (plates I and II).

The pillowed base of the unit is well exposed along the lower Nehalem River road at localities 73-8 (T. 4 N., R. 7 W., SW 1/4 sec. 5) and 74-5 (T. 4 N., R. 7 W., SW 1/4 sec 7). Highly vesicular zones in the upper part of the unit are well exposed in the vicinity of Cougar Mountain (localities 99-5, T. 4 N., R. 8 W., NW 1/4 sec. 10 and 99-6, T. 4 N., R. 8 W., NW 1/4 sec. 11). The unit is also well exposed at Jewell Junction (T. 4 N., R. 7 W., NE 1/4 sec. 4) and in the George Creek drainage (T. 4 N., R. 8 W., secs. 1, 2, 11, and 12).

Lithology

The characteristic lithology of the unit is altered vesicular and/or amygdaloidal plagioclase- and pyroxene-porphyritic basalt to relatively fresh basaltic andesite with a dark glassy groundmass. Fresh exposures are dark gray (N 2), but the vesicular character of the rock promotes extensive chemical weathering which results in

light gray (N 4) to medium gray (N 3) colors with reddish-brown
hues. As a result, typical exposures of Cole Mountain basalt are
highly weathered. Vesicles and amygdules typically have oval to
spherical shapes, range from §1 to 15 mm in diameter, and are
generally randomly distributed. At one locality (74-3, T. 4 N., R.
7 W., SW 1/4 sec. 7) near the base of the unit the concentration of
vesicles into 2 cm - to 4 cm - thick sheets results in a thin-bedded
appearance. Field estimates indicate that vesicles and/or amygdules
comprise up to 35% of the volume of highly vesicular and/or
amygdaloidal outcrops. The upper part of the Cole Mountain basalt
is particulary vesicular and in places displays a frothy appearance.
Vesicle-filling materials include chalcedonic silica, calcite,
fibrous zeolites, and chloritic clays. In most outcrops one
amygdule mineralogy predominates but it is not uncommon for two or
more different minerals to be present. Chloritic clays and calcite
are the most common amygdules; with silica and zeolites are much
less common.

Plagioclase phenocrysts range from about 2 to 25 mm in length,
typically form about 25% of the rock and are commonly weathered to
light gray to greenish clays. Plagioclase phenocrysts are generally
larger and more abundant in more vesicular parts of the upper Cole
Mountain basalt. Pyroxene (augite) phenocrysts range from about 1
to 4 mm across and typically form about 5% of the rock. Sparse
glomerophenocrysts of plagioclase and pyroxene up to 10 mm across
are visible in some outcrops.

Irregular thin dikes and thick sills (fig. 76) and thin beds
(1 to 2 m) of pillow basalt in Sweet Home Creek member mudstones
characterize the basal part of the Cole Mountain basalt (fig. 77).
The basal contact of the main Cole Mountain basalt "sill" exhibits a
glassy chilled margin and large (up to 4 m long) oblong pillow-like
features that are interpreted to be collapsed lava tubes (fig. 78).
Otherwise, the lower and middle part of the unit have a massive
appearance. Large-scale, radially arranged "war-bonnet" jointing
suggestive of large pillows or lava tubes, and interpillow
hyaloclastite (fig. 79) were observed at one locality (73-8, T. 4
N., R. 7 W., SW 1/4 sec. 5) in the middle to upper part

Figure 76.   Outcrop showing thin, irregular dikes and apophyses of
             Cole Mountain basalt intruding chippy-weathering thin-
             bedded mudstone of the Sweet Home Creek member.   The
             dikes originate in the upper part of a larger sill-like
             intrusion exposed in lower left of photograph. Geologic
             pick for scale.   Locality 74-5 (T. 4 N., R. 7 W., SW 1/4
             sec. 7) along the lower Nehalem River road.

Figure 77. Outcrop of pillowed Cole Mountain basalt intrusion near
the basal contact. The erosionally-resistant lower
parts of the outcrop are Cole Mountain basalt (Tcm).
The talus-covered parts of the outcrop are baked
mudstones of the upper Sweet Home Creek member (Hamlet
formation) (Thshc). Note pillows with interpillow
hyaloclastite and mudstone inclusions in upper part of
photograph. Locality 74-5 (T. 4 N., R. 7 W., SW 1/4
sec. 7) along the lower Nehalem River road.

Figure 78. Exposure of contact between resistant, altered Cole
Mountain basalt and underlying brown, softer mudstone of
the upper Sweet Home Creek member (Hamlet formation). A
large, oblong pillow in central right of the photograph
is defined by a chilled margin and a thin selvage of
mudstone on the top and sides. This pillow has a dark
medial line that is typical of a collapsed lava tube or
large collapsed pillow. Note conjugate shears
immediately below and to the left of the "Rocks" sign.
Locality 74-4 (T. 4 N., R. 7 W., SW 1/4 sec. 7) along
the lower Nehalem River road.

Figure 79. Photograph of pillow breccia and hyaloclastite in upper Cole Mountain basalt. Note glassy rinds on brecciated pillows and angular, glassy fragments of interpillow hyaloclastite. Geologic pick for scale. Locality 73-8 (T. 4 N., R. 7 W., SW 1/4 sec. 5) along the lower Nehalem River road.

of the unit. Peperites were observed at localities 74-2 (T. 4 N.,R.
7 W., SW 1/4 sec. 7) and 7320-1 (T. 4 N., R. 7 W., NW 1/4 sec. 20).
These features all suggest that the Cole Mountain basalt formed in
part from submarine basalt flows or was injected and steam-blasted
into uncompacted, water-laden sediments near the water-sediment
interface to form near surface pillowed dikes and sills. Such near-
surface Cole Mountain basalt pillowed sills have been recognized by
Rarey (1986). The vesicular character of the unit also suggests
that lithostatic and hydrostatic pressures were too low to contain
volatiles dissolved in the magma (Williams and McBirney, 1979).

Light brownish gray sugary-textured to smooth chert nodules
(up to 25 cm diameter) with conchoidal fracture and sparry quartz
associated with the nodules are locally present in the upper part of
the Cole Mountain basalt (e.g., locality 629-3, T. 4 N., R. 7 W., NE
1/4 sec. 4). Berkman (in prep.) has also recognized these nodules
in pillowed Cole Mountain basalt in western Columbia County where
they contain about 1% disseminated pyrite. This suggests a
hydrothermal origin for the siliceous nodules. The silica composing
the nodules was not identified with an X-ray diffraction pattern,
but is probably chalcedony based on physical characteristics.

West of the thesis area Rarey (1986) reported a thin bed (1 m
thick) of locally derived hyaloclastite in upper Sweet Home Creek
member mudstone at the uppermost contact of Cole Mountain basalt.
The hyaloclastite bed consists of calcite-cemented fine- to coarse-
grained, angular, highly vesicular, glassy, basaltic rock fragments
with a few siltstone rip-up clasts.

Petrography

Petrographic examination of the Cole Mountain basalt was
limited to eight thin sections from six different localities (Plate
I). In addition, one peperite associated with unit was examined
petrographically and one basalt sample was examined briefly with an
AMRAY scanning electron microscope. Modal abundances were
determined for seven of the samples by point-counting 650 points
(Table 8). A visual estimate of mineral abundances was made for the

<u>Minerals</u>   <u>Sample</u>

Minerals	630-4-1[1]	73-2-1[2]	730-1-5[3]	730-1-2[3]	730-2-2[4]	730-3-2[5]	730-3-3[5]
Plagioclase							
phenocrysts	22	57	23	22	20	19	18
microlites	36	(total)	30	25	25	26	31
Augite							
phenocrysts	4	4	6	10	4	8	3
groundmass	13	3	11	13	14	15	6
Opaques	7	5	6	5	7	6	8
Glass	7	*	4	16	16	17	6
Secondary minerals	4	31	17	4	13	9	14
Vesicles/ Amygdules	7	<1	4	5	1	0	6

Table 8. Petrographic modal analyses of selected Cole Mountain basalts (650 points counted). [1]T. 4 N., R. 7 W., NW 1/4 sec. 4. [2]T. 4 N., R. 7 W., SW 1/4 sec. 4. [3]T. 4 N., R. 7 W., NE 1/4 sec. 4. [4]T. 4 N., R. 7 W., NE 1/4 sec. 4. [5]T. 4 N., R. 7 W., NE 1/4 sec. 4.

other two thin-sections. Samples selected for thin sections are
biased towards those exhibiting the least alteration, which
effectively eliminates highly vesicular and amygdaloidal samples
common to many exposures of Cole Mountain basalt. However, all
samples have been affected to some extent by weathering and deuteric
(hydrothermal) alteration, as reflected by the abundance of secondary
minerals (Table 8). This precludes accurate petrographic and
geochemical analysis of highly altered samples.

Texturally, all samples are porphyritic and/or glomeroporphyritic
with plagioclase and/or augite phenocrysts set in an intersertal to
hyalopilitic groundmass (fig. 80). Six of the eight samples are
plagioclase porphyritic with plagioclase phenocrysts ranging from 0.4
to 3 mm in length and groundmass microlites ranging from 0.05 to 0.12
mm in length. In the other two samples (73-2-1 and 74-5-5) no
distinct break in the size of plagioclase crystals is visible, which
defines a seriate rather than porphyritic texture with regard to
plagioclase. However, these samples do contain distinct augite
phenocrysts. All samples also contain sparse glomerophenocrysts up to
2 mm in diameter. These usually consist of large, intergrown
plagioclase and augite phenocrysts or only of intergrown plagioclase
phenocrysts, but some contain opaque oxides (magnetite-ilmenite) as
well.

Plagioclase phenocrysts are euhedral to subhedral and commonly
exhibit resorption features, pronounced normal oscillatory zoning, and
partial alteration to secondary clay minerals. Polysynthetic and/or
Carlsbad twinning is ubiquitous among plagioclase phenocrysts.
Maximum extinction angles (Michel-Levy method) of albite-twinned
plagioclase phenocrysts indicate a labradorite composition ranging
from An_{54} to An_{59}. Only a few zoned crystals were properly oriented
for determination of core and mantle compositions, and these have
labradorite cores (An_{58}) and calcic andesine rims (An_{47}). Alteration
to greenish to moderate brown clay minerals is most intense in the
calcic cores of strongly zoned phenocrysts and along polysynthetic
twin lamellae. These secondary clay minerals have petrographic
characteristics of chlorite and nontronite. One sample of altered
Cole Mountain basalt was briefly

Figure 80.   Photomicrographs of the late middle Eocene Cole Mountain
             basalt. Abundant labradorite and light greenish-gray
             augite phenocrysts and glomerophenocrysts are set in a
             groundmass consisting of randomly oriented plagioclase
             microlites, small augite crystals, opaque oxides, glass,
             and secondary clays. Note normal oscillatory zoning of
             albite twinned labradorite phenocrysts (look closely) and
             alteration of phenocryst cores, twinning of augite
             phenocrysts, and abundant vesicles filled with radiating
             nontronitic clays. Field of view 6.7 mm. A: plane
             polarized light. B: crossed polarizers. Locality 730-1,
             T. 4 N., R. 7 W., NE 1/4 sec. 4 along U. S. 26 at Jewell
             Junction.

A.

1 mm

B.

Figure 80.
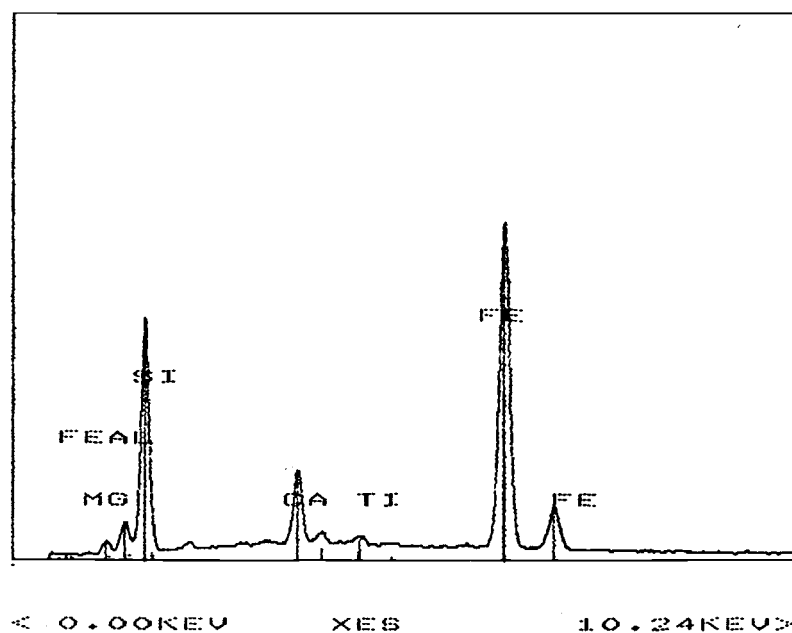
Figure 81. Energy dispersive spectra of clay alteration mineral on
labradorite phenocryst in Cole Mountain basalt. Strong
Fe, Si, and Ca peaks are consistent with nontronite
analyzed and illustrated by Welton (1984).

examined with the scanning electron microscope to aid in identifying
the alteration products. Under high magnification the secondary
minerals did not exhibit distinctive morphologies, but energy
dispersive spectra (EDX) collected from the sample have strong iron
peaks with lesser amounts of silicon and calcium (fig. 83) which
compares favorably with nontronite (an iron-rich smectite) analyses by
Welton (1984). Secondary iron oxides visible in thin section and hand
samples are attributed to surficial weathering and oxidation of iron-
bearing minerals. Two thin sections showed a minor amount of
secondary calcite after plagioclase.

Plagioclase microlites range from 0.06 to 0.12 mm in length and
are too small for compositional determinations by optical methods.
Rarey (1986) reported that groundmass plagioclase of Cole Mountain
basalt has the composition of labradorite (An_{50} to An_{60}). Most
microlites exhibit a single Carlsbad twin and are set in groundmass
glass or secondary minerals after the basaltic glass. In one sample
(730-1-2) axiolitic plagioclase appear to have formed from devitrified
glass.

Augite phenocrysts range from about 0.2 to 3.5 mm across (average
about 1 mm) and form 3 to 10% of thin sectioned samples (Table 8).
They are euhedral to subhedral and are commonly twinned. In one
sample (730-3-2) augite phenocrysts exhibit distinct zoning at the
margin and are mantled with a thin rim of clinopyroxene (pigeonite?).
This is interpreted to represent two episodes of crystallization.
Augite phenocrysts are commonly altered to a dusky green chloritic (?)
clay, particularly when in association with plagioclase in
glomerophenocrysts.

Groundmass clinopyroxene has the same appearance as larger
clinopyroxene phenocrysts and is probably augite. These crystals
range from about 0.02 to 0.09 mm across and form between 3% and 15% of
thin sectioned samples (Table 8). They are set in glass or clay
altered glass along with plagioclase microlites.

Opaque iron oxides are the only other major mineral constituents
of thin sectioned samples. Minute opaques contained in groundmass
glass result in a dusty appearance. Larger crystals in the groundmass
range from 0.01 to 0.3 mm across, with an average size of about 0.1

mm. The small size of these crystals, along with surficial weathering and oxidation, makes it extremely difficult to make mineral identifications.

Opaque basaltic glass (tachylite), partially devitrified glass, and alteration products after glass are major constituents of thin sectioned Cole Mountain basalt samples (Table 8). Fresh basaltic glass is characteristically black to moderate brown in color. In one sample (730-1-2) brownish glass has partially devitrified and axiolitic feldspars have formed. In all samples examined most of the secondary alteration products have formed from preexisting glass rather than primary minerals. This is reflected in Table 8 by the inverse correlation between abundances of glass and secondary minerals (i.e., samples with the least glass have the greatest amount of secondary minerals). Secondary minerals formed through alteration of glass have the petrographic characteristics of fine-grained chlorite and nontronite and commonly exhibit a colloform or radiating fibrous habit, particularly around vesicles and/or amygdules.

Vesicles and amygdules are common to abundant in Cole Mountain basalt but occupy only 0 to 7% of the volume of thin sectioned samples (Table 8.). This is due to sampling bias toward less altered rocks which have fewer vesicles and amygdules. In thin section vesicles and amygdules range in diameter from 0.2 to 4.5 mm. In outcrop they are commonly much larger than this. Essentially all vesicles have at least a thin lining of secondary chlorite and are, therefore, technically amygdules. Amygdule constituents identified in hand sample and in thin section are chlorite, calcite, iron oxides/hydroxides, glass, and zeolites. Chlorite is the most common amygdule mineral, followed by sparry calcite and zeolite. Chlorite in amygdules usually exhibits a colloform or radiating habit. Other amygdules usually have at least a thin chlorite lining. Zeolite in amygdules has a fibrous, radiating habit and was petrographically identified as thompsonite. Rarey (1986) identified thompsonite in a zeolite amygdule in Cole Mountain basalt with an X-ray diffraction pattern and considered it to be the most common zeolite of the unit.

The Cole Mountain basalt is petrographically distinct from subaerial flows of the Tillamook Volcanics and dikes and sills of the

Columbia River Basalt Group in the thesis area. The Tillamook
Volcanics usually contain only sparse plagioclase and augite
phenocrysts, generally lack significant amounts basaltic glass, have
an intergranular groundmass, commonly exhibit a pilotaxitic flow
texture, and contain much greater abundances of opaque oxides (fig.
19). Dikes and sills of the Grande Ronde Basalt member of the
Columbia River Basalt Group in the thesis area do not contain abundant
labradorite and augite phenocrysts and glomerophenocrysts, lack
abundant glass, are not vesicular and/or amygdaloidal, and do not
exhibit the alteration characteristics of Cole Mountain basalt.

Petrochemistry

Eight samples from widely spaced localities in the Cole Mountain
basalt were analyses for major oxides by X-ray fluorescence. The
analyses were made under the direction of Dr. Peter Hooper at
Washington State University using the international basalt standard.
Sample preparation prior to shipment involved crushing the sample,
picking approximately 10 grams of the freshest sample chips (visually
screened with a binocular microscope), and ultrasonically cleaning the
chips. Major oxide values are presented in Table 9. Sample locations
are shown on Plate I and are listed in Appendix I. An effort was
made to select the least altered samples for major oxide analysis, but
all samples have been altered to some extent by deuteric and/or
weathering processes. Modal analyses of samples from localities 73-2
and 730-3 show relatively high abundances of secondary alteration
minerals (31% and 9% respectively) (Table 8). The smallest amount of
secondary minerals, determined by modal analysis, is 4% (Table 8).
Despite the variable degree of alteration, which one would expect to
variably affect major oxide chemistry, the analytical results are
relatively consistent for all samples (Table 9).

In the thesis area the Cole Mountain basalt varies in SiO_2 content
from 55.74% to 58.62% and the mean for all samples is 57.15%. Various
SiO_2 ranges have been proposed for classifying basalt, basaltic
andesite, and andesite. Priest and others (1983) utilized the
following SiO_2 ranges in the definition of volcanic rocks in western

Major Oxide				Sample					
	3624-1-1	73-2-1	99-6-1	630-1-3	730-4-2	730-3-4	73-7-3	717-10-3	Av.
SiO_2	58.00	56.41	56.86	58.62	56.93	58.10	56.51	55.74	57.15
Al_2O_3	15.81	16.42	17.75	16.53	15.92	15.92	15.08	16.93	16.30
TiO_2	1.47	1.42	1.55	1.51	1.47	1.45	1.40	1.50	1.47
FeO*	8.57	8.70	7.88	8.10	9.27	8.82	9.03	9.48	8.73
MnO	0.18	0.15	0.10	0.12	0.17	0.17	0.16	0.13	0.15
MgO	3.80	4.29	3.32	3.26	3.98	3.61	4.02	3.80	3.76
CaO	7.55	8.15	8.22	6.93	7.85	7.28	9.01	8.12	7.89
Na_2O	3.29	3.16	2.96	3.44	3.21	3.56	3.34	2.87	3.23
K_2O	0.60	0.60	0.70	0.78	0.41	0.35	0.69	0.70	0.60
P_2O_5	0.31	0.27	0.27	0.33	0.33	0.32	0.31	0.26	0.30

Table 9. Major oxide values of Cole Mountain basalt.

and central Oregon: basalt >53%, basaltic andesite ≥53% and ≤57%, and andesite ≥57% and ≤63%. In this classification scheme six samples are basaltic andesite and two are andesite. In the chemical classification scheme of Irvine and Baragar (1971) all samples plot in the basalt field near the basalt/andesite boundary (fig. 85). These workers did not distinguish a basaltic andesite field. This indicates a more basaltic than andesitic chemical affinity which is also supported by petrographic evidence such as plagioclase composition (labradorite rather than andesine phenocrysts and groundmass microlites) and the absence of hydrous minerals such as hornblende or biotite which are more common in andesitic rocks (Hughes, 1982). However, the plagioclase phenocrysts exhibit strong normal zoning which is common in andesites (Hughes, 1982). In any case, major oxide values and petrographic characteristics are transitional between basalt and andesite and it is felt that basaltic andesite is the most appropriate rock name.

Approximate ranges of other major oxides are: Al_2O_3 15-18%, FeO* (total Fe as FeO) 8-10%, TiO_2 1.4-1.6%, CaO 7-9%, MgO 3.3-4.3%, Na_2O 2.9-3.6%, K_2O 0.35-0.8%, and P_2O_5 0.26-0.33%. These compositional ranges are fairly well constrained and indicate chemical homogeneity of the Cole Mountain basalt (fig. 82). The major oxide analyses are characterized by intermediate silica values (average 57.15%), moderately high Al_2O_3 (average 16.3%), low TiO_2 (average 1.47%), and low K_2O (average 0.60%). These elements provide a chemical fingerprint which distinguishes Cole Mountain basalt from other Eocene and Miocene volcanic units in the area (e.g., Tillamook Volcanics and Grande Ronde Basalt Member of the Columbia River Basalt Group)(fig. 82).

Normative (C.I.P.W.) minerals calculated form major oxide values of the Cole Mountain basalt are given in Appendix IX. All samples contain significant amounts of normative quartz (10.6% to 15.5%), diopside (3.9% to 15.2%), and hypersthene (9.9% to 14.2%) and, therefore plot well within the quartz tholeiite field of the Ol-Di-Hy-Qz quadrilateral (not shown).

Major oxide values are represented by the mineralogy of the Cole Mountain basalt. The relatively elevated SiO_2 and Al_2O_3 values

reflect abundant labradorite phenocrysts and microlites and more siliceous basaltic glass. Moderate MgO contents are primarily due to augite in phenocrysts and in the groundmass. The FeO* (all iron expressed as FeO) and TiO$_2$ contents of Cole Mountain basalt samples are substantially lower than those of the Tillamook Volcanics and Columbia River Basalt Group and this is reflected by a much lower abundance of opaque oxides. Petrographically determined plagioclase compositions (An$_{54}$ to An$_{59}$) agree fairly well with normative plagioclase compositions (An$_{46}$ to An$_{56}$) but tend to be somewhat more calcic. Although all analyses have normative quartz and hypersthene neither of these minerals was observed in thin section. This is not unusual because normative minerals are predicated on equilibrium conditions which could not be sustained upon emplacement and cooling of the Cole Mountain basalt.

Figure 82 shows Al$_2$O$_3$, FeO*, TiO$_2$, K$_2$O, and CaO silica variation diagrams for all major oxide analyses of igneous units in the area. Silica contents of the late Eocene Cole Mountain basalt and middle Miocene Grande Ronde Basalt Member of the Columbia River Basalt Group are comparable and are distinctly greater than the Tillamook Volcanics. The Grande Ronde Basalt in the thesis area can be chemically distinguished from the Cole Mountain basalt by much higher FeO* values, slightly higher TiO$_2$ values, and distinctly lower Al$_2$O$_3$ values. The Tillamook Volcanics have distinctly higher FeO* and TiO$_2$ values and generally have higher CaO values than the Cole Mountain basalt. One sample of Tillamook Volcanics (and a duplicate sample) has SiO$_2$, TiO$_2$, Al$_2$O$_3$, and FeO* values which overlap those of the Cole Mountain basalt, but it can be distinguished by distinctly greater K$_2$O, Na$_2$O, and P$_2$O$_5$ values and smaller MgO and CaO values (fig. 82). These plots graphically demonstrate the distinct chemical groupings of igneous units in the thesis area. Although the sample base for each unit is relatively small, it is felt that the distinct groupings are valid and may be used to help identify these igneous units outside the thesis area

Figure 82. FeO*, Al$_2$O$_3$, CaO, K$_2$O, and TiO$_2$ silica variation diagrams
of all igneous units in the thesis area. Symbols: crosses
= Tillamook Volcanics, open circles = Cole Mountain basalt,
open boxes = Grande Ronde Basalt member of the Columbia
River Basalt Group. Note distinct grouping of samples from
each unit and high K$_2$O, low CaO of high SiO$_2$ sample (and
duplicate) from the Tillamook Volcanics.
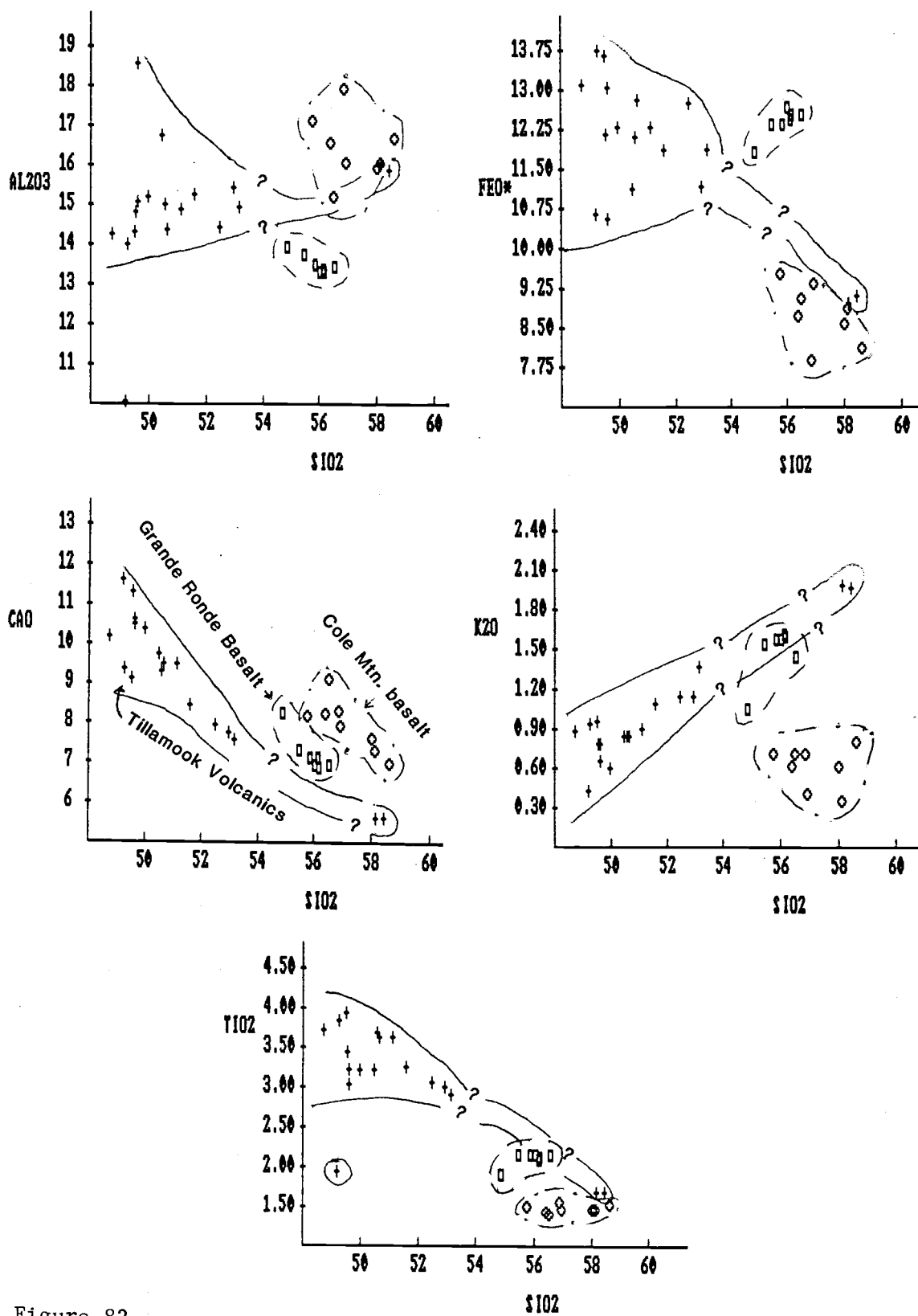
Figure 82.

when the stratigraphic position is unknown. Rarey (1986) reported minimal overlap of the Tillamook Volcanics and Cole Mountain basalt grouping with a compiled database of over 100 analyses.

Chemical Classification

Irvine and Baragar (1971) proposed a chemical classification for common volcanic rocks which is used in this study. A more detailed account of this classification scheme is presented in the earlier discussion of the Tillamook Volcanics. None of the samples contain normative acmite, which is indicative of peralkaline rocks (high Na and K contents), and are, therefore, alkaline or subalkaline. Figure 83 shows that Cole Mountain basalt samples plot well within the subalkaline field.

Figure 84 shows that the samples plot close to, and on both sides of, the boundary between the calc-alkaline and tholeiitic fields defined on the AFM and normative plagioclase composition versus Al_2O_3 diagrams. On the Al_2O_3 versus normative plagioclase content diagram (fig. 84A), which is best for basalts, five samples plot in the calc-alkaline field and three plot in the tholeiitic field. On the AFM diagram (fig. 84B) six samples plot in the calc-alkaline field and two plot in the tholeiitic field. This indicates that the Cole Mountain basalt is transitional between the two trends but is more closely allied with the calc-alkaline series. Rarey (1986) also noted the transitional but mildly calc-alkaline character of the Cole Mountain basalt.

Irvine and Baragar (1971) assigned names to subalkaline rocks on the basis of normative color index versus normative plagioclase composition. According to this plot all Cole Mountain basalts are basalts (fig. 85). As noted previously, it is felt that basaltic andesite best conveys the chemical and petrographic character of the Cole Mountain basalt. However, basaltic andesite is not recognized in this classification scheme.
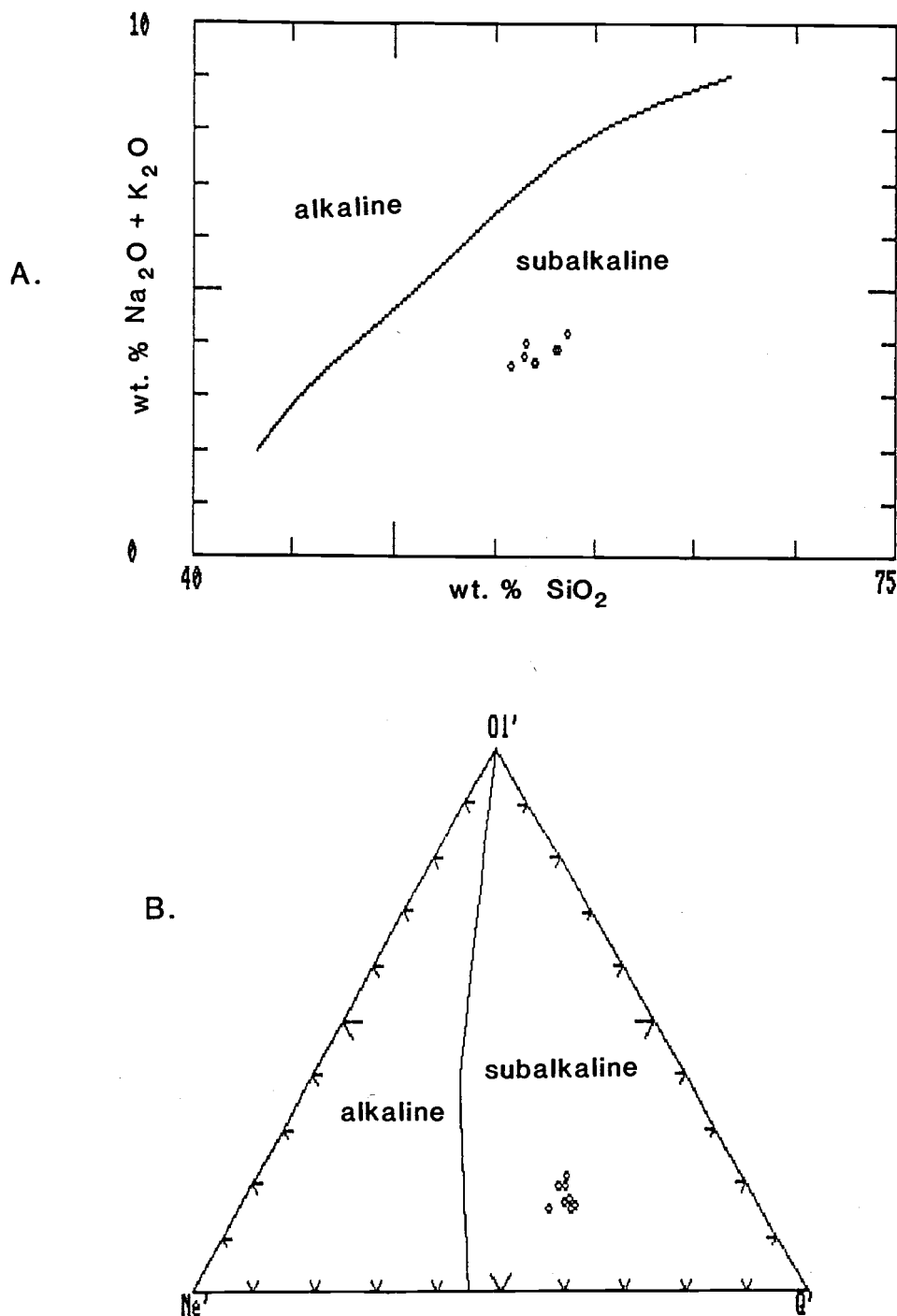
Figure 83. Irvine and Baragar (1971) alkaline/subalkaline classification of samples of the Cole Mountain basalt from the thesis area. A: total alkalies ($Na_2O + K_2O$) versus SiO_2. B: contents of normative Di-Ol-Ne-Q tetrahedron projected from Di apex onto basal Ol'-Ne'-Q' triangle.

231
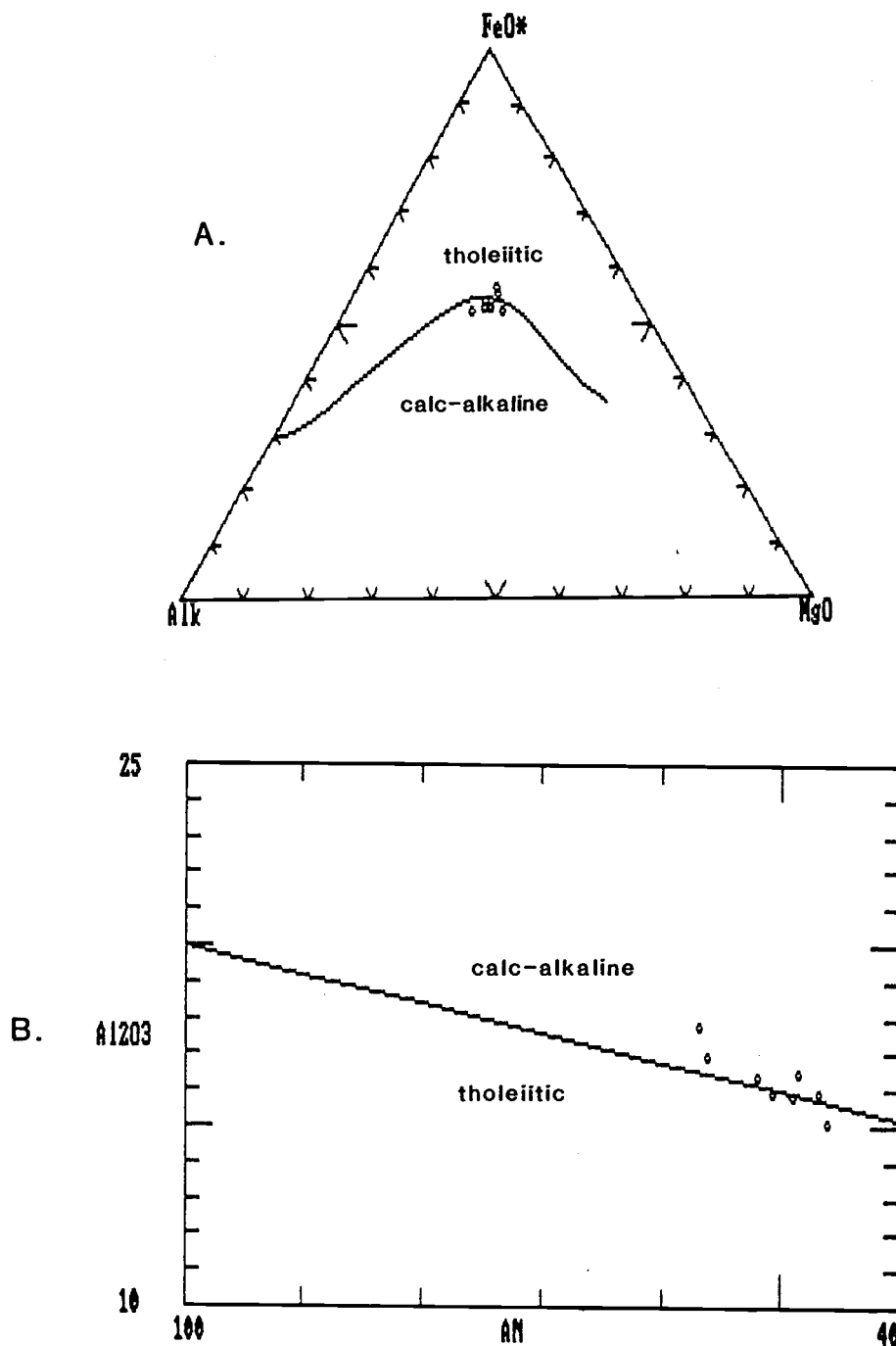
Figure 84. Irvine and Baragar (1971) tholeiitic/calc-alkaline
classification of samples of Cole Mountain basalt from
the thesis area. Samples plot near the tholeiitic/calc-
alkaline boundary on both diagrams, but fall mainly in
the calc-alkine field. A: total alkalies ($Na_2O + K_2O$)-
FeO* (all Fe as FeO)-MgO. B: weight per cent Al_2O_3
versus normative plagioclase composition.
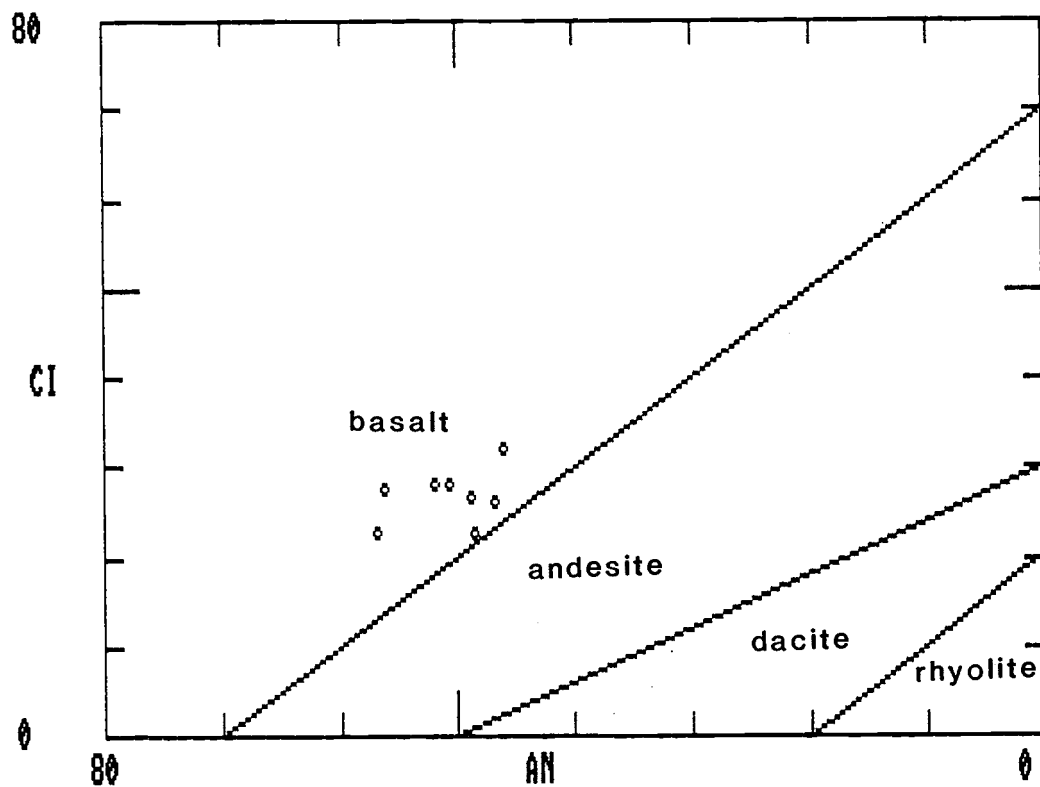
Figure 85. Irvine and Baragar (1971) classification of samples from
the Cole Mountain basalt in the thesis area. All samples
classify as basalt on this plot of normative color index
versus normative plagioclase composition.

Magnetic Polarity

The polarity of the Cole Mountain basalt was determined at 14 widely spaced localities with a fluxgate magnetometer (Plate I; Appendices I and VIII). An effort was made to correct for structural orientation and regional tectonic rotations. Samples from 12 localities showed a strong normal polarity. Weak responses indicating reversed polarity were obtained at the other two localities. The two weak reversed polarity responses are thought to be due to weathering and/or deuteric alteration, incorrect structural and tectonic rotation corrections, and possibly thermal disturbance related to middle Miocene dikes and sills. Nelson (1985) reported a normal polarity for cores magnetically cleaned with a spinner magnetometer from locality 730-3 in the thesis area (site GV3 of Nelson). A normal polarity at this locality was also obtained with the fluxgate magnetometer. Rarey (1986) determined the polarity of 11 Cole Mountain basalt localities immediately west of the thesis area with a fluxgate magnetometer. He reported normal polarity for 10 of the 11 sites and one questionable reversed polarity. Therefore, it is likely that the Cole Mountain basalt has normal magnetic polarity. Rarey (1986) tentatively assigned the Cole Mountain basalt to normal magnetic epochs 16 or 17 of Ness and others (1980). This was based on correlation of coccolith ages obtained from mudstone units above and below the Cole Mountain basalt.

Age and Correlation

The age of the Cole Mountain basalt is well constrained by biostratigraphic and lithologic evidence. K-Ar radiometric age determinations, however, have not been reliable or reproducible. The Cole Mountain basalt intrudes and overlies mudstone of the middle to upper Narizian (late middle to late Eocene) Sweet Home Creek member (Hamlet formation) and is overlain by tuffaceous mudstone of the upper Narizian to lower Refugian (late Eocene) Jewell member (Keasey Formation) (fig. 7; Plates I and II).

Field evidence which indicates that upper Sweet Home Creek member

(Hamlet formation) sediments were water-saturated and semilithified at the time of emplacement of the Cole Mountain basalt includes the following: 1) soft sediment deformation features such as load structures at the base of sills, 2) local development of peperite, 3.) irregular basal contact of the Cole Mountain basalt, and 4) local pillow basalts with incorporated mudstone at the base of the Cole Mountain basalt (fig. 77). These features demonstrate that a significant amount of time did not elapse between deposition of the Sweet Home Creek member sediments and emplacement of the Cole Mountain basalt. Therefore, the Cole Mountain basalt is about the same age or slightly younger than these enclosing sediments. Foraminiferal assemblages from the upper Sweet Home Creek member have been assigned to the upper Narizian (see age and correlation section of the Sweet Home Creek member of the Hamlet formation), which correlates to the late middle to late Eocene. Rarey (1986) reported calcareous nannofossil assemblages (coccoliths) from the middle and upper Sweet Home Creek member which were assigned to subzones CP-14a and CP-14b which also correlates to the upper Narizian (late middle Eocene) (fig. 7).

The upper contact of the Cole Mountain basalt also provides age constraints because it is stratigraphically fixed in the lowest part of the Jewell member (Keasey Formation) over a large region in southeastern Clatsop County (Rarey, 1986). In the thesis area foraminiferal assemblages from the lower Keasey Formation immediately overlying the Cole Mountain basalt (locality 73-4, T. 4 N., R. 7 W., NW 1/4 sec. 5) were assigned to upper Narizian to lower Refugian.

Therefore, the age of the Cole Mountain basalt is late middle Eocene to late Eocene. Berggren and others (1985) correlate these epochs to the geochronometric time scale at about 38 to 40 Ma (fig. 7).

Whole-rock potassium-argon radiometric age determinations of Cole Mountain basalt by Leda Beth Pickthorn (U.S. Geological Survey) and Kristin McElwee (Oregon State University) have not been reliable. A sample collected from locality 73-5 (T. 4 N., R. 7 W., SW 1/4 sec. 5) initially yielded and age determination of 40.7 +/- 0.5 Ma but lost both K and Ar upon acid treatment (to rid the sample of alteration

products), which resulted in an age determination of 18.1 +/- 0.1 Ma (Kris McElwee, personal communication 1987). A sample collected west of the thesis area was analyses by Leda Beth Pickthorn and yielded an age determination of 42 Ma prior to acid treatment and 24 Ma after acid treatment (Kristin McElwee, personal communication, 1987). Brief visual inspection of two radiometrically dated samples showed considerable amounts of secondary alteration minerals which are suspected to be responsible for the lack of reproducible K-Ar ages.

An Ar_{39}/Ar_{40} analysis of a Cole Mountain basalt sample yielded and age determination of 34.3 +/- 2.1 Ma with and overlapping isochron age of 36.0 +/- 1.7 Ma (Kris McElwee, written communication in Niem and Niem, 1985). This radiometric age determination approximates the biostratigraphically constrained age of the Cole Mountain basalt. The "maximum" age of 37.7 Ma is slightly young in comparison with benthic foraminiferal stages correlated to the absolute time scale (Armentrout, 1983; fig. 7). However, the position of the Narizian/Refugian boundary and its relationship to the absolute time scale has recently been revised several times (Armentrout, 1981, Armentrout and others, 1983, Prothero and Armentrout, 1985; fig. 12). In addition, extremely detailed correlation of the biostratigraphic and radiometric time scales in this area may not be possible.

Wilkinson and others (1945) reported that the type area Goble Volcanics in eastern Columbia County, Oregon and southwestern Washington were conformable on and intercalated with upper Narizian sedimentary rocks and the Cowlitz Formation in particular. Rarey (1986) conducted reconnaissance field work and sampling of several volcanic units, including the type area Goble Volcanics, outside his map area and concluded that the Cole Mountain basalt is stratigraphically and chemically correlative with the type area Goble Volcanics along the Columbia River. However, the Goble Volcanics are lithologically dissimilar to the Cole Mountain basalt in primarily consisting of subaerial flows and flow breccias.

Mode of Emplacement

Lithologic features of the Cole Mountain basalt and enclosing mudstones indicate intrusive emplacement of the lower part of the unit and shallow-level intrusion and possible subaqueous eruption of the upper part. In the lower and middle part of the Sweet Home Creek mudstone (Hamlet formation) the Cole Mountain basalt occurs predominantly as dikes with peperite developed along the intrusive contact. Peperites form by steam blasting as hot magmas intrude water saturated and unconsolidated sediments (Snavely and others, 1973). This indicates only partial compaction and lithification of Sweet Home Creek member sediments during intrusive emplacement of the Cole Mountain basalt. Large dikes in the east-central part of the thesis area (e.g. locality 717-10, T. 4 N., R. 7 W., NE 1/4 sec. 20 and in the Flat Iron Mountain area) and east of the thesis area (Safley, in prep.) exhibit a fine-grained gabbroic to microgabbroic texture which also suggests intrusion and slow cooling. West of the thesis area Rarey (1986) reported Cole Mountain basalt dikes and discrete sills with baked upper and lower contacts in the lower part of the Sweet Home Creek member which indicate intrusion into compacted and at least partially lithified sediments.

Soft sediment deformation features associated with the Cole Mountain basalt are present in the upper Sweet Home Creek mudstone. In addition, basalt in this part of the section is glassy and locally pillowed, has an irregular basal contact that is locally associated with peperites, and locally contains siliceous nodules between pillows that are interpreted to have formed hydrothermally (figs. 77, 78, and 79). These features suggest eruption onto the ocean floor but can also be produced by magma emplacement into water-saturated, semi-consolidated or unconsolidated sediments near the sea water/sediment interface (Hanson and Scheickert, 1982; Kokelaar, 1982; Snyder and Fraser, 1963). The fact that Cole Mountain basalt is only locally pillowed and does not contain volumetrically significant hyaloclastite, which one would associate with subaqueous eruption, favors the interpretation of magma emplacement into wet, unconsolidated sediments near the sediment/sea water interface for

most of the Cole Mountain basalt.

Rarey (1986) reported a local, normally graded, 0.5 m-thick hyaloclastite deposit directly overlying the upper part of the Cole Mountain basalt immediately west of the thesis area. The deposit consists primarily of angular, glassy basalt fragments which are petrographically identical to the Cole Mountain basalt with minor extrabasinal materials (glauconite, hornblende, and granitic rock fragments). He interpreted the composition and bedded character of the deposit to document subaqueous extrusion and concomitant fragmentation of Cole Mountain, resulting in gravity-induced sedimentation off a submarine "volcano". Bedded hyaloclastite was not observed in the thesis area, but the upper part of the Cole Mountain basalt in the vicinity of Cougar Mountain (T. 4 N., R. 8 W., sec. 10, 11, and 12) is exceedingly vesicular. This indicates that lithostatic and hydrostatic pressure was insufficient to contain dissolved volatiles and is consistent with very shallow level intrusion or subaqueous eruption. Williams and McBirney (1979) suggest that vesicular basaltic eruptions would represent water depths less than 500 m. In any case, it is easy to envision development of a hyaloclastite through breaching of the sediment/water interface by a rapidly cooling viscous magma exsolving copious quantities of volatiles.

Therefore, it appears that the Cole Mountain basalt was emplaced largely as shallow-level intrusions and perhaps in places formed through subaqueous eruption onto the ocean floor. Rarey (1986) showed that such an emplacement history favorably compares with that documented by Einsele (1982) for basaltic sills in the Guyamas basin in the Gulf of California. Einsele (1982) showed that in a sequence of shallow basaltic sills, younger sills generally intrude above baked and indurated sediments overlying older sills. This leads to formation of a series of sills alternating with relatively thin, discontinuous screen of sedimentary rocks. In this manner magma will eventually breach the sediment/water interface as long as soft sediments with lower bulk density does not accumulate faster than sills are emplaced. In the thesis area stratigraphically discontinuous, thin mudstone pods and bodies are locally present

between Cole Mountain basalt sills (e.g., locality 74-4, T. 4 N., R. 7
W., SW 1/4 sec. 7) which is consistent with the model of Einsele
(1982). The overall glassy character of the Cole Mountain basalt
suggests rapid cooling of multiple units (emplacements) which one
would not anticipate in a 75 to 300 m-thick sill emplaced in one
event. The previously noted hyaloclastite described by Rarey (1986)
documents a minor build-up of the volcanic pile above the sea floor.
No large Cole Mountain basalt edifices have been found in southern
Clatsop County, however.

The nature of the magma source, i.e. of invasive versus local
origin, which fed the Cole Mountain basalt is debatable. Rarey (1986)
conducted reconnaissance work which indicates that the Cole Mountain
basalt is stratigraphically, petrographically, and chemically
equivalent to the type area Goble Volcanics. This suggests that the
Cole Mountain basalt may represent an invasive facies of the Goble
Volcanics. That is, some western Cascades derived subaerial flows of
the Goble Volcanics may have flowed from the Columbia River area in
Columbia County into the forearc basin and foundered into water
saturated sediments of the Sweet Home Creek member. (This invasive
process was suggested by Beeson and others (1979) and documented by
Wells and Niem (1986) and Pfaff and Beeson (1986) for plateau-derived
flows of the Columbia River Basalt Group that invaded sediments in
Clatsop County and southwestern Washington in the Miocene). An
invasive origin is also suggested by the absence of Cole Mountain
basalt dikes in Tillamook Volcanics (Rarey, 1986). However, subaerial
flows of the Goble Volcanics and Cole Mountain basalt intrusions have
not been connected by surface mapping or subsurface correlations of
exploratory wells in eastern Clatsop and western Columbia counties
(Olbinski, 1983; Timmons, 1981; Bruer and others, 1984; Martin and
others, 1985 in Niem and Niem, 1985; Berkman, in prep.). This does
not disprove an invasive origin, however, because the late Eocene
section has been partially or wholly removed by erosion over large
areas east of the thesis area as indicated by the unconformity at the
base of the Keasey Formation (Bruer and others, 1984).

Evidence suggesting a local source includes the following: 1) the
thick fine-grained gabbroic dikes and sills in eastern Clatsop County

(Timmons, 1981; Safley, in prep); 2) apparent physical separation of
Cole Mountain basalt intrusions and Goble Volcanics subaerial flows
without any connecting flows in the Columbia County subsurface (Bruer
and others, 1984); and 3) the presence of a hyaloclastite which is
interpreted to be locally derived in central Clatsop County (Rarey,
1986).

One possibility is that the large intrusive bodies in eastern
Clatsop and western Columbia counties represent the invasion points of
now eroded subaerial flows into partially lithified Hamlet formation
sediments. Such large intrusion may have fed shallow-level invasive
flows and reemerged as submarine basalt flows on an irregular
submarine topography farther west (western part of field area and area
of Rarey (1986). Invasive basalts of the Columbia River Basalt Group
apparently did this in middle Miocene time (Dr. A. R. Niem, OSU Dept.
of Geology, personal communication, 1988). The absence of a thick
breccia pile, which one would associate the postulated piercing point
argues against this model, but this absence may be due to erosion
associated with an unconformity at the base of the Keasey Formation
(Kadri, 1983; Bruer and others, 1984).

The origin of the Cole Mountain basalt and its relationship with
the Goble Volcanics remains an interesting topic for further regional
investigation that is beyond the scope of this study.

Plate Tectonic Setting

Foraminiferal assemblages collected from mudstones enclosing the
Cole Mountain basalt represent middle bathyal to outer neritic
depositional environments (Kristin McDougall, U.S. Geological Survey,
and Weldon Rau, Washington Dept. of Natural Resources, written
communication, 1984). This indicates emplacement of the Cole Mountain
basalt on the upper continental slope to outer shelf. A middle
bathyal to outer neritic environment is also indicated by glauconite
in the lower part of the Jewell member (Keasey Formation) which
overlies the Cole Mountain basalt. Kulm and others (1975) found that
glauconite formation is enhanced by low sedimentation rates in
slightly reducing marine environments such as elevated areas on the

modern outer continental shelf.

The timing of Cole Mountain basalt volcanism is coeval with the oldest rocks of the western Cascades (Wells and others, 1984; Wells and Heller, 1988). The unit was emplaced in the developing forearc region of the Cascade Volcanic arc which was rotating westward in response to late Eocene plate reorganization and back arc spreading in the Great Basin (Wells and others, 1984; Wells and Heller, 1988). This is somewhat unusual because the forearc region is supposedly characterized by an absence of volcanism (Best, 1982). However, this tectonic setting is not unique to the Cole Mountain basalt because there are many volcanic units in the Oregon Coast Range (such as the Tillamook Volcanics, Goble Volcanics, Nestucca Volcanics, Cascade Head Volcanics, and Oligocene camptonite breccias and nephelite syenite sills) which were emplaced in the forearc (Wells and others, 1984; Wells and Heller, 1988; Snavely and others, 1968).

Cole Mountain basalt and Goble Volcanics trace element chemistries are relatively "primitive" (low abundances of rare earth elements) and resemble those of early western Cascades rocks more than the highly fractionated upper Tillamook Volcanics (Timmons, 1981; Rarey, 1986; Kristin McElwee, personal communication, 1987).

A Peacock diagram is a plot of $CaO/(Na_2O + K_2O)$ versus SiO_2. A calc-alkali index is defined on this diagram by the SiO_2 value where the curve intercepts a ratio value of 1.0. Christiansen and Lipman (1982) used this index for plutonic rocks to distinguish compressional tectonic suites having high indices (60-64) from extensional suites having low indices (50-56). The estimated index of Cole Mountain basalt samples from the thesis area is 62 and is consistent with a compressional tectonic setting (fig. 86). The estimated index for the Tillamook Volcanics is roughly 55, which indicates an extensional setting. This also suggests a stronger relationship of the Cole Mountain basalt with compressional calc-alkaline arc rocks of the western Cascades than with the tholeiitic Tillamook Volcanics.

Rarey (1986) proposed the following models for Cole Mountain
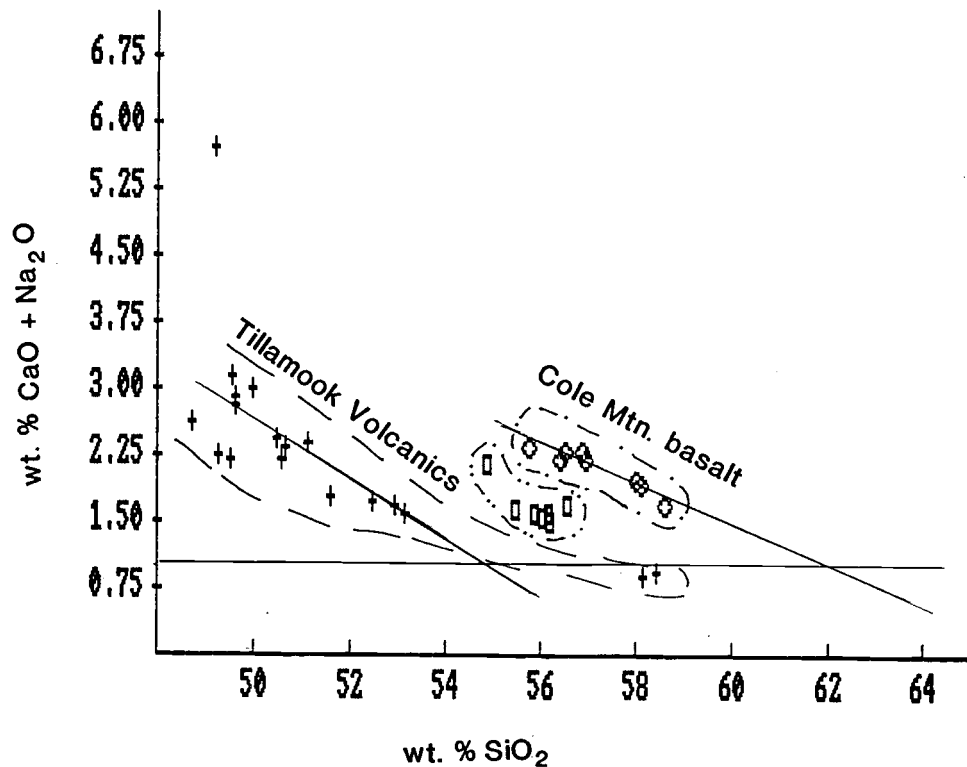
Figure 86. CaO/(Na₂O + K₂O) versus SiO₂ variation (Peacock) diagram for samples of all igneous rocks in the thesis area. Petro and others (1979) used this plot to graphically estimate a calc-alkali index and compressive versus extensional plate tectonic regime for plutonic rocks. The Tillamook Volcanic have an "extensional" index of approximately 55 whereas the Cole Mountain basalt has a "compressional" index of about 62.

basalt petrogenesis: 1) continued subduction of remaining parts of the Kula-Pacific ridge, 2) early Cascade arc magmatism and westward migration of magmas up the subducting slab into the forearc, and 3) early Cascade arc magmatism with the Cole Mountain basalt representing an "invasive" facies of the Goble Volcanics. He concluded that physical and stratigraphic constraints made model 3 unlikely and favored models 1 and 2, but deferred further petrogenetic speculation pending more detailed regional petrologic and tectonic data. However, Rarey (1986) also presented evidence which indicates that the Goble Volcanics and Cole Mountain basalt are closely related petrogenetically, chemically, stratigraphically and temporally and, since the mechanism(s) of emplacement for "invasive" dikes and sills is/are only poorly known, and it would appear that further study is required to discount this model.

In any case, both the Cole Mountain basalt and the Goble Volcanics (as well as other post-late Eocene volcanic units in northwestern Oregon and southwestern Washington) were erupted in the forearc region of the Cascade arc (Rarey, 1986; Wells and others, 1984; Wells and Heller, 1988). Therefore, further study of forearc volcanism, particularly in northwestern Oregon and southwestern Washington, is needed to understand and further constrain petrogenetic models for the Cole Mountain basalt.

KEASEY FORMATION

Nomenclature

Schenk (1927, 1928) originally described reference sections of stratified tuffaceous and locally glauconitic siltstones and mudstones exposed along Rock Creek near Vernonia (between Tara and Keasey Stations) in western Columbia County, Oregon to define the Keasey Formation. Weaver (1937) appended a younger sequence of tuffaceous siltstone overlying the originally defined type sections and listed some characteristic molluscan fossils. Warren and Norbisrath (1946) subdivided the expanded definition into three informal members: 1) a lower shale member (type Keasey); 2) a thick middle tuffaceous and concretionary siltstone member; and 3) a thin upper member of stratified tuffaceous sandy shales. In the vicinity of Sunset Tunnel along the Sunset highway (US 26) the Keasey Formation is approximately 520 m thick (Warren and Norbisrath, 1946).

The Jewell member of the Keasey Formation was informally proposed by Olbinski (1983) and Nelson (1985 for a sequence of Refugian laminated to thinly bedded, locally glauconitic mudstones exposed in the vicinity of Jewell in eastern Clatsop County, Oregon. The Jewell member is lithologically similar to the lower two members of the Keasey Formation of Warren and Norbisrath (1946) but is thinner and contains clastic dikes of arkosic sandstone. This study follows the nomenclature of Olbinski (1983) and Niem and Niem (1985) who restricted the Keasey Formation to the Jewell member in eastern Clatsop County. The Jewell member is the youngest sedimentary formation in the thesis area

Distribution

The Jewell member is well exposed in the extreme northwestern and north-central parts of the thesis area (fig. 5 and Plate I). The unit is topographically expressed as low, undulating hills because it is easily eroded and prone to landsliding. The best

exposures of the unit are in road cuts along US highway 26 (e.g., locality 625-1, T. 4 N., R. 7 W., NE 1/4 sec. 6), in the scenic garbage dump pit of the hamlet of Elsie (locality 94-2, T. 5 N., R. 7 W, SE 1/4 sec 31), in stream cut banks along Humbug Creek, and at locality 73-4 (T. 4 N. R. 7 W, NW 1/4 sec. 5) along the lower Nehalem River road (Plate I). Nelson (1985) used this last locality as a reference section for the Jewell member of the Keasey Formation. Other accessible road cut exposures are scattered along logging roads in the northwest part of the thesis area. Less accessible exposures of the unit are present in the central part of the thesis area in the vicinity of Lost Lake and Spruce Run Lake (both T. 4 N., R. 7 W., sec. 17). Approximately 300 meters of the lower part of the Jewell member is exposed in the thesis area (based on bedding attitude and area of outcrop distribution). Rarey estimated a thickness of 500 to 800 m west of the thesis area, and Olbinski (1985) reported a thickness of 365 m northeast of the thesis area. Martin and others (1985 in Niem and Niem, 1985) show a thickness of over 900 m in the subsurface of central Clatsop County.

Lithology and Petrography

In the thesis area the Jewell member predominantly consists of chippy weathering laminated and thin-bedded tuffaceous mudstone with rare clastic dikes of arkosic sandstone and very thin tuff beds in the lower part (fig. 87) and thin tuff beds in the upper part. Fresh mudstone exposures are dark gray (N 3) to medium gray (N 4). More common weathered exposures are very pale orange (10 YR 8/2) to grayish yellow (5Y 8/4). Thin tuff beds are typically light gray (N 8).

Small to large (0 to over 100 cm across) ovoid to irregularly shaped calcite-cemented concretions are commonly concentrated in layers parallel to bedding, particularly in the lower part of the member (fig. 87). Concretions are usually relatively small (< 5 cm in diameter) but locally approach 1 m in diameter. Trace fossils are common in the Jewell member. Hook-shaped Helminthoida trace fossils are locally abundant; larger, less numerous subvertical

Figure 87. Exposure of lower part of Keasey Formation (Jewell member). Note clastic dike of arkosic sandstone in chippy weathering mudstone, and small, white, calcareous concretions developed along bedding plane (upper left of photograph). Fresh mudstones are dark gray while upper slope is typically very pale orange due to deep chemical weathering. Tom Berkman for scale. Locality 73-4 (T. 4 N., R. 7 W., NE 1/4 sec. 5) along the lower Nehalem River road approximately one km south of Elsie.

cylindrical burrows (not identified) occur most commonly in the lower part of the unit (e.g., locality 73-4, T. 4 N., R. 7 W., NW 1/4 sec. 5). Large foraminfers such as Cyclamina and micro-molluscs such as Dentalium (a scaphopod) are often visible in fresh samples.

Thin (1 to 5 cm-thick), light colored tuff beds are a distinctive feature of Jewell member mudstones and emphasize the bedded character of the unit. In the lower part of the unit pumice fragments are concentrated in tuff beds but are also disseminated in the mudstones. Pumice fragments are generally larger and more abundant in the middle to upper part of the unit (e.g., locality 910-9, T. 4 N., R. 8 W., NW 1/4 sec. 14).

Thin sandy mudstone and siltstone beds (1/2 m thick) with very coarse sand to granule-sized glauconitic rip-up clasts were observed at two closely spaced localities (3624-3, T. 4 N., R. 7 W., NW 1/4 sec. 17 and 3624-6, T. 4 N., R. 7 W., NE 1/4 sec. 18) very near the base of the Jewell member. The dark green glauconitic clasts are angular and mostly in matrix support but are locally clast-supported in small (1 m by 5 cm) sandy lenses. This glauconitic facies is very thin in the thesis area but appears to be a regional feature of the basal Keasey Formation (Martin and others, 1985 in Niem and Niem, 1985; Rarey, 1986; Berkman, in prep.). This thin but regionally extensive glauconitic facies is significant because it may reflect an unconformity or period of slow deposition at the base of the Keasey Formation.

Fine-grained, moderately sorted, micaceous and carbonaceous arkosic sandstone was found in several places in the "lower middle" part of the Jewell member but in most exposures it was not possible to determine the geometry of the sandstone bodies. A lens of sandstone is exposed at locality 98-8 (T. 4 N., R. 8 W., NW 1/4 sec. 2). It is finely laminated and is interpreted to represent a small paleochannel. Thin (1/2 m thick), approximately vertical, clastic dikes were observed at localities 74-4 (T. 4 N., R. 7 W., NW 1/4 sec. 5, fig. 87), 94-3 (T. 5 N., R. 7 W., SW 1/4 sec. 31) and 94-6 (T. 4 N., R. 7 W., NW 1/4 sec. 5). Sandstones in the clastic dikes and in the small channel appear to be lithologically identical. Therefore, it is probable that the clastic dikes formed through

rapid loading and liquefaction of the sandstone lenses. Nelson
(1985) and Rarey (1986) have reported similar sandstone bodies in
the Jewell member north and west of the thesis area, respectively.
The micaceous arkosic sandstone may have been derived from erosion
of the "C and W" Cowlitz Formation sandstone or the Sunset Highway
member (Hamlet formation) or may represent rare Columbia River
derived channelized turbidites that reached the Keasey depositional
basin.

A few thin, evenly bedded fine-grained basaltic sandstones were
found in the "upper middle" part of the Jewell member above Spruce
Run Lake (T. 4 N., R. 7 W. sec. 17, fig. 88). The sandstones are
normally graded and are interpreted to be turbidites. Modal
analysis (650 counts) of one thin section shows the following
composition: 68% basaltic rock fragments, 17% plagioclase feldspar,
14% replacive calcite, 1% sparry calcite cement, and trace potassium
feldspar, which classifies the sample as a litharenite or volcanic
arenite (fig. 42). Both the feldspars and rock fragments are
angular to subangular. Therefore, the rock is texturally submature
to immature and compositionally immature. The abundant basaltic
rock fragments document the presence of a local volcanic source in
the Keasey depositional basin. However, they are highly altered so
that it is difficult to positively determine whether they have
greater affinity to the Tillamook Volcanics or Cole Mountain basalt.
The glassy nature and presence of numerous plagioclase
microphenocrysts suggests the latter source. Olbinski (1983) and
Martin and others (1985) reported basaltic sandstones near the base
of the Jewell member which also indicates a local minor source of
basaltic detritus.

The Jewell member can be distinguished from the underlying
Sweet Home Creek member of the Hamlet formation by its tuffaceous
composition and more obvious stratified appearance. Where present,
clastic dikes and small lenses of arkosic sandstone, and glauconitic
layers are also diagnostic of the Jewell member as these features
have not been observed in the underlying Sweet Home Creek member.
Micas and carbonaceous debris are also much less abundant and finer
grained in the Jewell member than in the Sweet Home Creek

A.
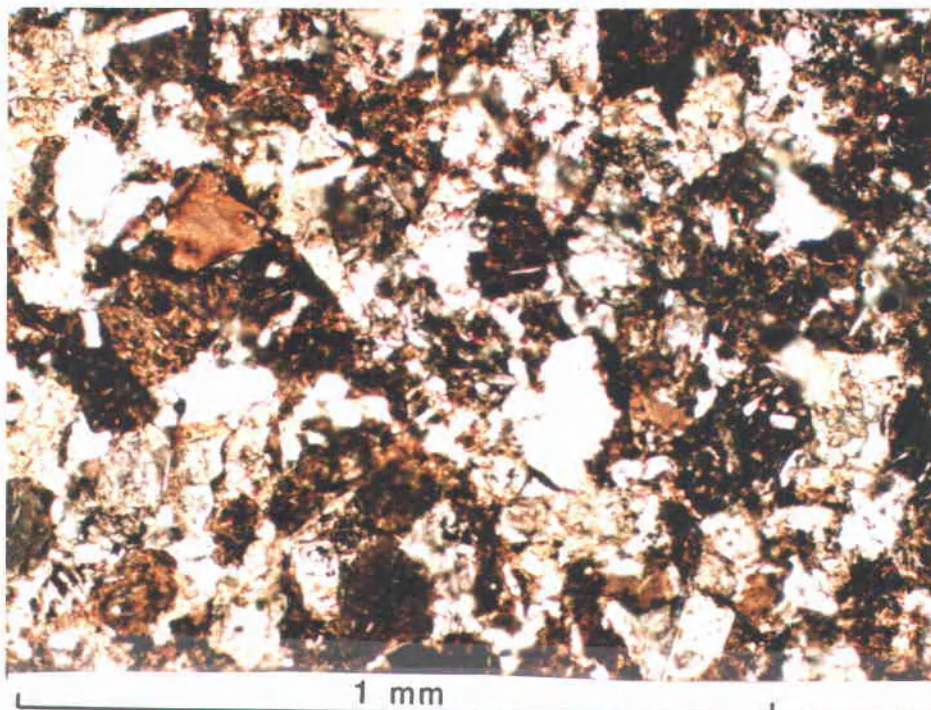
B.
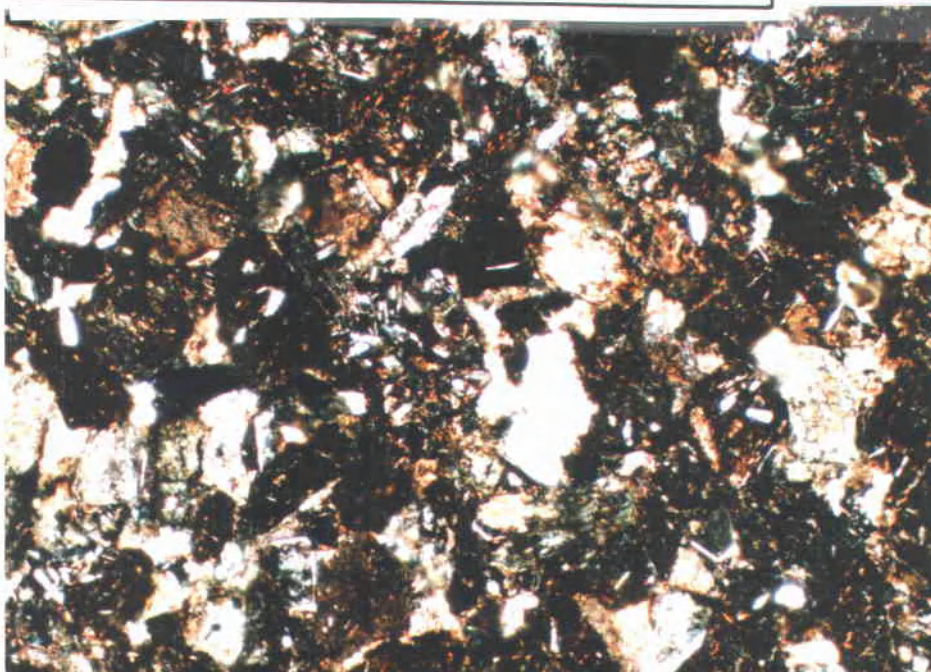
Figure 88.   Photomicrographs of a local, very fine-grained basaltic
sandstone in the Jewell member. Note abundant basaltic
rock fragments and pervasive calcite cement. Field of
view 1.31 mm. A: plane polarized light. B: crossed
polars. Locality 3715-2 (T. 4 N., R. 7 W., SE 1/4 sec.
17) above Spruce Run Lake.

member. Therefore, it is generally possibly to lithologically distinguish the Jewell member from the Sweet Home Creek member. In addition, the Cole Mountain basalt is generally positioned between the two units in southeast Clatsop County.

Contact Relationships

Bedding attitudes and the relative ages of the lower Jewell member and the upper part of the underlying Sweet Home Creek member (Hamlet formation) do not significantly differ and there is no strong evidence indicating a major unconformity between the two units in the thesis area (Plate I). However, a regional glauconitic facies in Clatsop County (this study; Rarey, 1986; Niem and Niem, 1985) at the base of the Jewell member is thought to mark a minor unconformity or diastem between the Jewell member and the underlying Cole Mountain basalt and Sweet Home Creek member (Hamlet formation). This contact is described in more detail in the Contacts section of the Sweet Home Creek member. A pronounced regional unconformity between the Keasey Formation and underlying upper Narizian strata has been reported northeast of the thesis area (Kadri, 1982; Bruer and others, 1984). The upper contact of the Jewell member of the Keasey Formation is not exposed in the thesis area.

Age

Four samples from two localities in the Jewell member yielded over 60 benthic foraminifera species which were identified by Dr. Kristin McDougall (U.S. Geological Survey) and Weldon Rau (Wash. Dept. of Natural Resources) (Appendix V). Three of the samples from the same locality (73-4, T. 4 N., R. 7 W., NW 1/4 sec. 5) near the base of the Jewell member yielded age diagnostic assemblages which were assigned to the upper Narizian to lower Refugian (Kristin McDougall, U.S. Geological Survey and Weldon Rau, Washington Dept. Natural Resources, written communication, 1984). Other foraminiferal assemblages collected from this locality by Nelson (1985) and Dr. Niem (personal communication, 1984) were assigned to

the lower Refugian by Dr. McDougall and Daniel McKeel (consulting micropaleontologist, Otis, Oregon). Coccoliths in a smear slide from this locality are sparse, but the was dated as late middle Eocene to earliest Oligocene on the basis of the overlap of Dictyoccoccites bisectus (Hay et al.) and Reticulofenestra reticulata (Gartner and Smith) by David Bukry (U.S. Geological Survey). Similar age assignments have been obtained from the type section of the Jewell member (Dr. Niem, OSU Dept. of Geology, personal communication, 1984). Therefore, it appears that the lower Jewell member straddles the upper Narizian/lower Refugian (Eocene/Oligocene) boundary. Nelson (1985), Niem and Niem (1985), and Rarey (1986) reported a lower Refugian age for the remainder of the Jewell member.

The age assignments of the Jewell member are identical to the type Keasey Formation in western Columbia County, Oregon (McDougall, 1975). She concluded that the lowest part of the Keasey Formation is late Narizian with the remaining part of the unit being Refugian.

Correlation

The Jewell member is lithologically and biostratigraphically equivalent to the lower and middle parts of the type Keasey Formation as originally defined by Warren and Norbisrath (1946) in western Columbia County. The Keasey Formation is age equivalent to the basal part of the Lincoln Creek Formation of southwestern Washington, the basal part of the Alsea Formation of the central Oregon Coast Range, and the upper part of the Bastendorff sandstone and lower part of Tunnel Point sandstone in the southern Oregon Coast Range (fig. 7).

The lowest part of the Jewell member may be partly correlative to a thick section of late Narizian mudstone in the subsurface of Clatsop and Columbia counties (upper mudstone member of the Cowlitz Formation as depicted in subsurface correlations by Bruer and others, 1984). In the subsurface of Clatsop County Martin and others (1985) assigned some of these upper Narizian mudstones to the Jewell member.

Clay Mineralogy

The clay-sized fraction of three samples from the lower and middle and upper middle Jewell member were analyzed by X-ray diffraction according to the methodology of Harward (Appendix X). Identification of clay minerals by X-ray diffraction is discussed in the clay mineralogy section of the Sweet Home Creek member. The clay mineral fraction throughout the Jewell member samples appear to be dominated by smectite (montmorillonite) (figs. 89, 90, and 91). A sample from the basal part of the Jewell member also contains a trace amount of illite (fine-grained mica) and kaolinite (fig. 89), which is similar to the Sweet Home Creek member. Non-clay minerals in the clay-sized fraction are zeolite, quartz, plagioclase, calcite, and possibly opal CT.

X-ray diffraction patterns of Jewell member mudstones do not exhibit the strong illite and kaolinite peaks present in X-ray diffraction patterns of the clay minerals of Sweet Home Creek member mudstones (figs. 73, 74, and 75). In addition, zeolite is present in all Jewell member samples but was detected in only one sample from the Sweet Home Creek member. The strongest zeolite peaks were obtained from a highly tuffaceous sample containing abundant pumice fragments in the upper middle to upper middle part of the Jewell member (fig. 91). The d-spacings calculated from these peaks are consistent with heulandite-clinoptilolite.

Smectite commonly forms during weathering of poorly drained soils developed on volcanic bedrock in tropical and humid temperate climates such as in the western Cascades arc (Glasmann, 1982; Glasmann and Simonson, 1985). The presence of smectite in Sweet Home Creek member and Jewell member mudstones is thought to reflect such a volcanic source terrain. Devitrification and alteration of ash in the Jewell member may also have contributed to formation of smectite clays as well as zeolite.

Depositional Environment

Three samples from one locality (73-4, T. 4 N., R. 7 W., NW 1/4
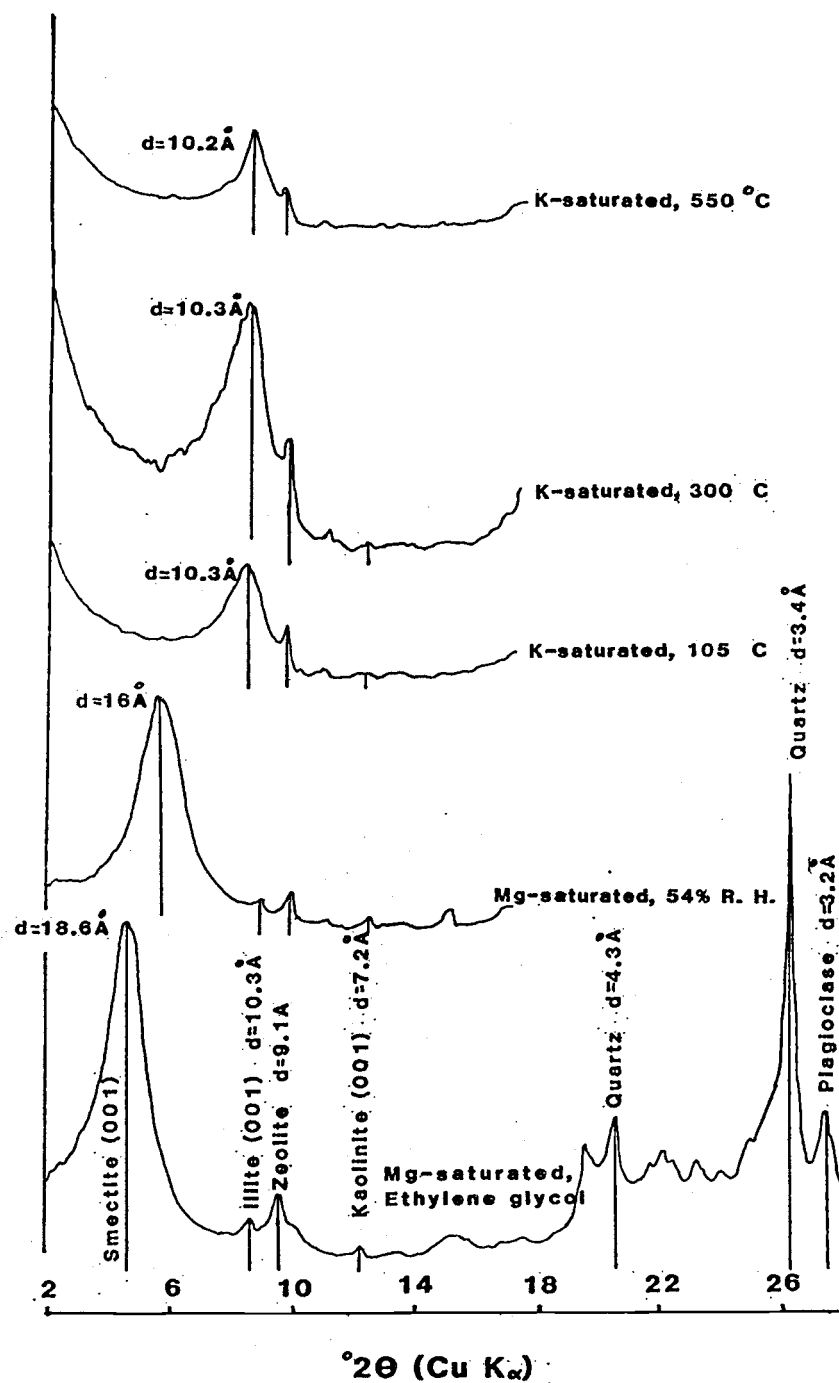
Figure 89. X-ray diffraction patterns of mudstone from the lower part of the Jewell member. Note shift of smectite peak with various sample treatments and the small illite, kaolinite, and zeolite peaks. Locality 73-4 (T. 4 N., R. 7 W., NE 1/4 sec. 5) along lower Nehalem River road about 1 km south of Elsie.
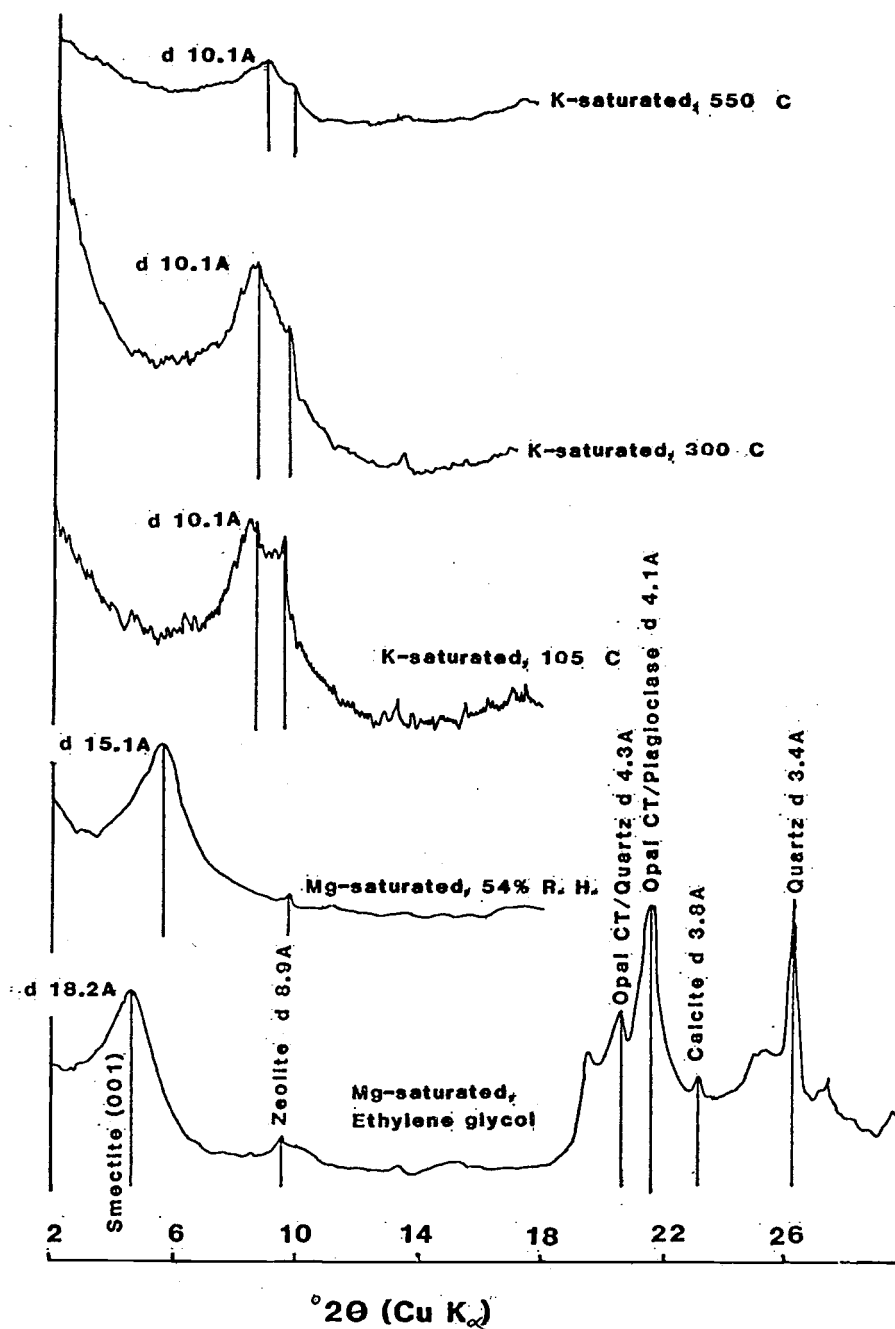
Figure 90. X-ray diffraction patterns of mudstone from the upper middle Jewell member. Note shift and collapse of smectite peak and the small zeolite peak. Locality 625-1 (T. 4 N., R. 7 W., NE 1/4 sec. 6) along US 26 southeast of Elsie.
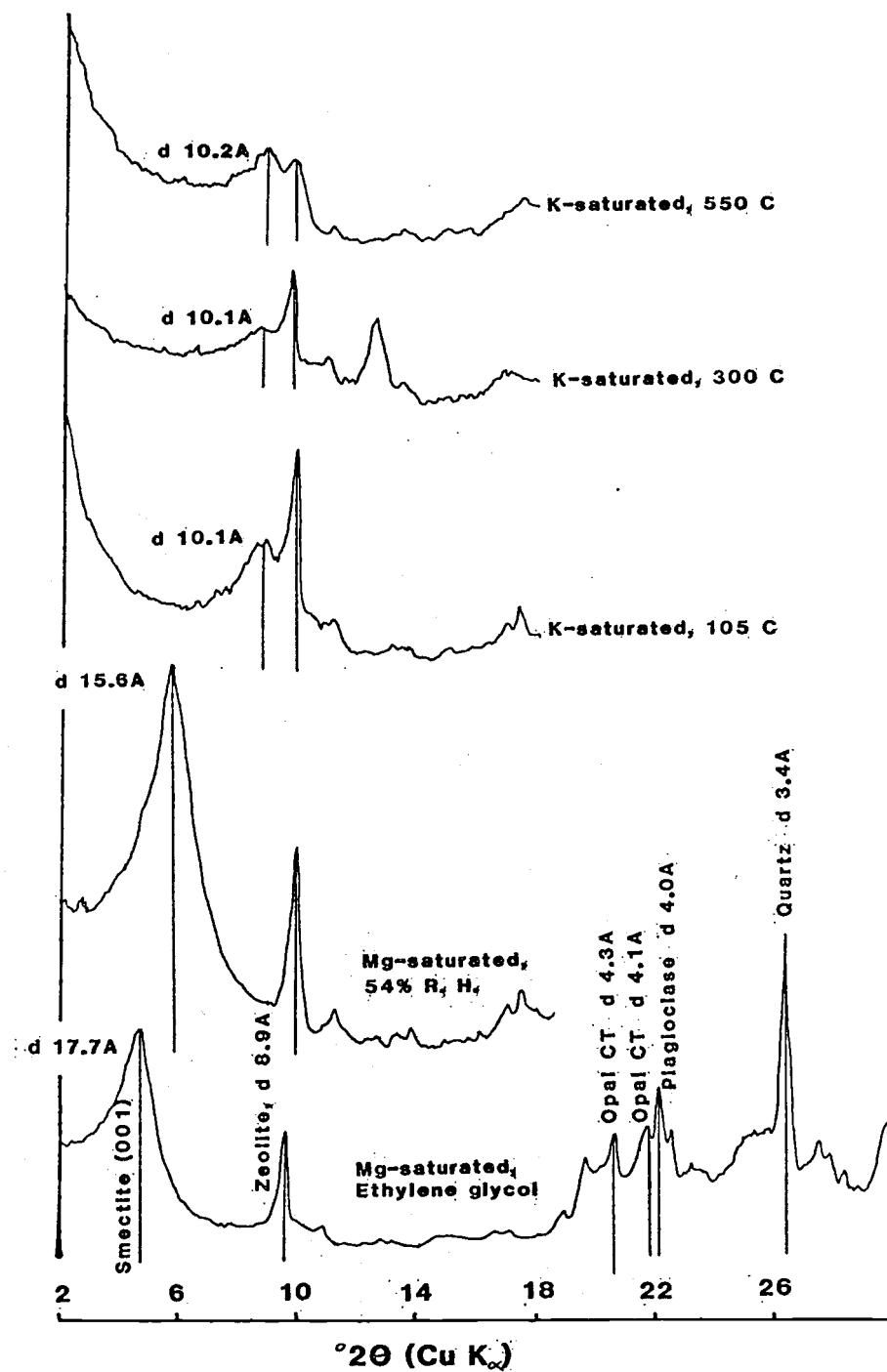
Figure 91. X-ray diffraction pattern of mudstone from highly
tuffaceous bed in the upper middle Jewell member. Note
shift and collapse of smectite peak and the strong
zeolite peak. Locality 910-9 (T. 4 N., R. 8 W., SW 1/4
sec. 14).

sec. 5) in the basal part of the Jewell member contained foraminiferal assemblages diagnostic of a lower middle to lower bathyal (1200 to 2000 m) environment of deposition (Kristin McDougall, U.S. Geological Survey and Weldon Rau, Washington Dept. of Natural Resources, written communication, 1984). The assemblages contain considerable numbers of shelf and upper slope species which were transported into the deeper water environment (Dr. Kristin McDougall, U.S. Geological Survey, written communication, 1984). A bathyal setting is also consistent with Helminthoida trace fossils which are locally abundant in the unit (Chamberlain, personal communication to Nelson, 1985).

Glauconite rip-ups in sandy mudstones at the base of the Jewell member are interpreted to have been transported from the upper slope to outer shelf into a deeper water (bathyal) environment. Glauconite formation is favored by slightly reducing conditions and low sedimentation rates, such as on uplifted area or topographic highs on the outer continental shelf (Kulm and others, 1975). Arkosic sandstones in the lower part of the Jewell member are interpreted to represent small channels which served to transport outer shelf sands onto the middle and lower slope. Rarey (1986) interpreted thin, sheet-like arkosic sandstone beds in the Jewell member to represent deposition from turbidity currents which flowed down small channels. Graded basaltic sandstones in the Jewell member represent sediment gravity flows shed off local volcanic highs and deposited on the middle to lower slope. The smectitic tuffaceous composition of the Jewell member, as well as the presence of thin tuff beds, documents explosive silicic calc-alkaline volcanism in the developing western Cascade arc east of the depositional basin.

Therefore, the Jewell member depositional environment is characterized by a middle to lower slope setting in which hemipelagic sedimentation was intermittently interrupted by turbidity currents off both the outer shelf and local volcanic highs. The tuffaceous character of the unit reflects settling of fine ash through the water column and discrete tuff beds may represent contourite turbidity currents of very fine silicic ash,

dust, and water-logged pumice.

COLUMBIA RIVER BASALT GROUP

Introduction

Tholeiitic flood basalts of the Columbia River Basalt Group are a remarkable geologic feature of the Pacific Northwest. The sequence covers a huge area (over 200,000 km^2) in Oregon, Washington and Idaho to an average depth of over 1 km (Mangan and others, 1986). This represents a volume of approximately 300,000 km^3 which was erupted over an 11 m.y. time span, mainly in the middle Miocene (Reidel and others, 1982). Approximately 85% of the Columbia River Group is composed of the Grande Ronde Basalt (Reidel and others, 1982), one of the five formations recognized in the Columbia River Group (fig. 92). This voluminous unit was erupted during a brief period between 14 and 16.5 m.y. B. P. (Watkins and Baksi, 1974) from north-northwest-trending fissure systems (Chief Joseph dike swarm) in northeastern Oregon and southeastern Washington (Taubeneck, 1970; Waters, 1961). Swanson and others (1979) subdivided the Grande Ronde Basalt into four units based on magnetostratigraphy. Mangan and others (1986) further subdivided the unit into five main chemical types, two of which are present in the thesis area.

Rarey (1986) and Goalen (1988) have recently discussed the distribution and probable mode of emplacement of Columbia River Basalt Group subunits in northwestern Oregon in considerable detail. Therefore, in this study, detailed discussion of the Columbia River Basalt Group is limited to the two magneto-chemical types of Grande Ronde Basalt in the thesis area

Nomenclature

Columbia River Basalt Group of the Columbia Plateau

Russell (1893) was first to describe Eocene to Recent basaltic lavas cropping out in parts of eastern Washington, eastern Oregon, southern Idaho, and northern California. In 1901 he used the term "Columbia River basalt" in reference to Miocene and older basalts (in

Waters, 1961). Merriam (1901) and Lindgren (1901) favored restriction
the Columbia River basalt terminology to middle and upper Miocene
basaltic flows on the Columbia Plateau. Waters (1961) delineated two
major units in the Columbia River Basalt, the older Picture Gorge
Basalt and the younger Yakima Basalt, through detailed geologic
mapping, petrography, and chemical composition. He also recognized
"Late Yakima" flows (post-early Pliocene) but did not subdivide them
into a separate major unit. Wright and others (1973) identified
eleven chemical types in the Columbia River Basalt (based on $MgO-SiO_2$
variation) and erected an informal four unit nomenclature (Picture
Gorge basalt and lower, middle and upper Yakima basalt). Swanson and
others (1979) conducted an exhaustive stratigraphic, geochemical,
paleomagnetic, and K-Ar age study of the Columbia River Basalt and
formally revised the stratigraphic nomenclature of the unit. The
Columbia River Basalt was raised to Group status, the Yakima Basalt
was elevated to the subgroup level, the term Grande Ronde Basalt (as
first suggested by Taubeneck, 1970) replaced the lower Yakima basalt
of Wright and others (1973), and the entire sequence was subdivided
into five formations. From oldest to youngest the formations are: the
Imnaha Basalt, the Picture Gorge Basalt, the Grande Ronde, the Wanapum
Basalt, and the Saddle Mountains Basalt (fig. 92). The Grande Ronde
Basalt, Wanapum Basalt, and Saddle Mountains Basalt are three
formations of the Yakima Basalt Subgroup. In addition, four
magnetostratigraphic units were established in the Grande Ronde
Basalt; from youngest to oldest these units are designated N_2, R_2, N_1,
and R_1 (fig. 92). The Wanapum and Saddle Mountains Basalts were
subdivided into numerous members (fig. 92).

Columbia River Basalt Group of Coastal Oregon and Washington

Of the five formations and numerous members of the Columbia River
Basalt Group present on the Columbia Plateau, only the Grande Ronde
Basalt, the Frenchman Springs Member and Priest Rapids Member of the
Wanapum Basalt, and the Pomona Member of the Saddle Mountains Basalt
have been recognized in western Oregon and Washington (Beeson and
Moran, 1979; Rarey, 1986; Anderson and others, 1987). Snavely and

Series		Group	Sub-group	Formation	Member	K-Ar age (m. y.)	Magnetic polarity
MIOCENE	Upper Miocene	Basalt	Yakima Basalt Subgroup	Saddle Mountains Basalt	Lower Monumental Member	6[2]	N
					Erosional unconformity		
					Ice Harbor Member		
					Basalt of Goose Island	8.5[2]	N
					Basalt of Martindale	8.5[2]	R
					Basalt of Basin City	8.5[2]	N
					Erosional unconformity		
					Buford Member		R
					Elephant Mountain Member	10.5[2]	N, T
					Erosional unconformity		
					Pomona Member	12[2]	R
					Erosional unconformity		
	Middle Miocene				Esquatzel Member		
					Erosional unconformity		
					Weissenfels Ridge Member		
					Basalt of Slippery Creek		N
					Basalt of Lewiston Orchards		N
					Asotin Member		N
					Local erosional unconformity		
					Wilbur Creek Member		N
					Umatilla Member		N
					Local erosional unconformity		
		River		Wanapum Basalt	Priest Rapids Member		R₃
					Rozo Member		R₃ T
					Frenchman Springs Member		N
					Eckler Mountain Member		
					Basalt of Shumaker Creek		N₂
					Basalt of Dodge		N₂
					Basalt of Robinette Mountain		N₂
	Lower Miocene	Columbia River		Grande Ronde Basalt	Basalt of Dayville / Basalt of Monument Mountain / Basalt of Twickenham [1]	14-16.5[3] (14.6-15.8)[1,3]	N₂
							R₂
							N₁
							R₁
				Picture Gorge Basalt -?-?-			
				Imnaho Basalt		R₁ T	
							R₀ ?

Figure 92. Stratigraphic nomenclature, age, and magnetic polarity of the Columbia River Basalt Group from Mangan and others (1986). N, normal magnetic polarity; R, reversed, T, transitional. [1]Information in parentheses refers to Picture Gorge Basalt. [2]Data from McKee and others (1977). [3]Data mostly from Watkins and Baksi (1974). Bar indicates units recognized in the Elsie-lower Nehalem River area.

others (1973) subdivided lower and middle Miocene basalts along the central to northern Oregon Coast and southern Washington coast into three petrologic types based on lithology, petrography, major element chemistry, and isotopic composition. From oldest to youngest these are the Depoe Bay Basalt, the Cape Foulweather Basalt, and the Basalt of Pack Sack Lookout. Snavely and others (1973) correlated the Coastal and Plateau basalts as follows:

Plateau Units	Coastal Units
Pomona Member	Basalt of Pack Sack Lookout
Wanapum Basalt	Cape Foulweather Basalt
Grande Ronde Basalt	Depoe Bay Basalt

These workers concluded that magmas of the coastal and plateau basalts were cosanguinous, but were erupted from distinct vents. This genetic interpretation supported their use of a different stratigraphic nomenclature for the coastal units.

Beeson and others (1979) reconsidered the evidence and concluded that the coastal units represented plateau eruptions which flowed down an ancestral Columbia River drainage through lows in the Oregon Coast Range into the marine coastal embayment where they formed large breccia piles, foundered in the unconsolidated sediments, and formed "invasive" dikes and sills. Subsequent research has supported the "one vent" hypothesis (see Age, Correlation, and Origin section), and, therefore, Columbia River Basalt Group nomenclature is used for the Miocene coastal basalt units in this study (Peterson, 1984; Nelson, 1985; Niem and Niem, 1985; Pfaff and Beeson, 1987; Wells and Niem, 1987; Anderson and others, 1987; Goalen, 1988).

Grande Ronde Basalt Petrologic Types

Murphy (1981), Peterson (1984), Nelson (1985), Rarey (1986), and Goalen (1988) have subdivided Grande Ronde Basalt flows and invasive dikes and sills in northwestern Oregon (Clatsop County) into four subunits on the basis of MgO and TiO_2 content and magnetic polarity. From oldest to youngest the subunits are: 1) R_2, low MgO-high TiO_2

(Tgr1); 2) R_2, low MgO-low TiO_2 (Tgr2); 3) N_2, low MgO-low TiO_2 (Tgr3); and 4) N_2, high MgO (Tgr4). Because Grande Ronde Basalt occurs as intrusions in the thesis area which cannot be physically traced into a stratigraphic section of Columbia River Basalt, the two magneto-chemical types of Grande Ronde Basalt in the thesis area (Tgr3 and Tgr4) are referred to as petrologic types in this study.

Distribution in the Thesis Area

Two geographically separated Grande Ronde Basalt petrologic types are present in the thesis area. Irregular dikes and sills in the central and east central parts of the study area have major oxide values and the magnetic polarity of petrologic type Tgr3 (N_2, low MgO, low TiO_2) (Plate I; Table 11). This unit is the most commonly encountered petrologic type in the thesis area. It is well exposed in numerous small quarries and borrow pits (e. g. west end of Flat Iron Mountain, T. 4 N., R. 7 W., NW 1/4 sec 22; junction of Lost Lake road and August Fire road, T. 4 N., R. 7 W., NW 1/4 sec. 16) as well as in a spectacular landslide exposure above Spruce Run Lake (fig. 93, T. 4 N., R. 7 W., SE 1/4 sec. 17).

One major oxide analysis from a dike at locality 97-7 (T. 4 N., R. 8 W., NW 1/4 sec 3) in the extreme northwestern part of the thesis area is indicative of petrologic type Tgr4 (N_2, high MgO) (Table 11). Other irregular dikes and sills in the vicinity of the headwaters of Big Creek (mainly T. 4 N., R. 8 W., NW 1/4 sec. 3) are lithologically similar to the analyses dike and are thought to be petrologic type Tgr4. No reversely polarized low MgO Grande Ronde Basalt intrusions were recognized.

Lithology

The two petrologic types of Grande Ronde Basalt in the thesis area are lithologically similar. Both units are usually fresh, nonvesicular, finely crystalline (aphyric to very sparsely microphyric), and dark gray (N 2) to black (N 1). Petrologic type Tgr4 (N_2, high MgO) tends to be slightly but distinctly more coarsely

crystalline than petrologic type Tgr3 (N_2, low MgO, low TiO_2). This difference has also been reported by Peterson (1984), Nelson (1985), and Rarey (1986) and appears to be a widespread characteristic. However, this distinction is not always evident, particularly in small, quickly chilled intrusions and the chilled margins of larger intrusions.

Jointing characteristic vary with the size of Grande Ronde Basalt intrusions such that small bodies (1 to 3 m thick) are usually highly fractured whereas thick intrusions (>10 m) usually display columnar jointing oriented perpendicular to cooling surfaces. A thick, irregular intrusion above Spruce Run Lake (T. 4 N., R. 7 W., SE 1/4 sec. 17) exhibits a basal colonnade (fig. 93) and upper platy entabulature. In thick intrusions columnar joints commonly extend a short distance outward from the contact into thermally metamorphosed mudstone (hornfels). Most Grande Ronde Basalt intrusions in the thesis area are of intermediate thickness (3 to 10 m) and typically exhibit blocky and/or platy jointing patterns.

Glassy cooling margins are present in thick intrusions in the thesis area but these are very thin (§10 cm) and usually at least partially altered to clay. Otherwise, these intrusions exhibit a generally homogeneous aphanitic texture from the margin to the core.

Mudstone is usually bleached light gray (N 7) along intrusive contacts. Baking and induration of mudstone away from intrusive contacts varies with the size of the intrusion. Most contact metamorphic effects are limited to a 10 to 20 cm-thick zone. However, mudstones have been baked and indurated 15 to 20 m from the approximately 30 m-thick intrusion above Spruce Run Lake (locality 3715-2, T. 4 N., R. 7 W., SE 1/4 sec. 17; fig. 93).

The form of Grande Ronde Basalt intrusions is typically irregular. Figure 93 shows a thick intrusion (petrologic type Tgr3) change from a discordant dike to a concordant sill. Similar changes in Tgr4 intrusions in the northwestern part of the thesis area cannot be unequivocally demonstrated in the thesis area. However, both dikes and sills are present in this area and are suspected to be connected in the subsurface. In the thesis area the Grande Ronde Basalt intrudes middle to upper Narizian Sweet Home Creek member (Hamlet

A.

B.

Figure 93. Photographs of a middle Miocene Grande Ronde Basalt
intrusion or invasive flow. A: Note columnar jointing of
concordant sill in upper left and the transition to a
discordant dike (upper right). B: Detail of transition
from sill to dike. Note bleached contact with thin-bedded
Jewell member mudstone (with thin, nearly horizontal
basaltic sandstone turbidites) and induration of the
mudstone caused by baking by the intrusion. The intrusion
is petrologic type Tgr3. Locality 3715-2 above Spruce Run
Lake (T. 4 N., R. 7 W., SW 1/4 sec. 17).

formation) or uppermost Narizian and Refugian Jewell member (Keasey
Formation) mudstones. These intrusions are generally tabular but do
abruptly change in thickness and orientation. They do not appreciably
deform enclosing strata. These intrusions do not cut the late Eocene
Cole Mountain basalt or the middle Eocene Tillamook Volcanics.
Olbinski (1983) and Rarey (1986) reported that Grande Ronde Basalt
intrusions higher in the stratigraphic section, which has been eroded
from the thesis area, tend to be highly irregular with pod-like
apophyses, suggesting emplacement in less lithified sediments.

Petrography

Four thin sections from widely spaced localities were examined
with a petrographic microscope. Modal analyses were made by point
counting 650 points with a mechanical stage (Table 10). Three of the
thin sections are of the Tgr3 petrologic type and one is a Tgr4
petrologic type. Tgr3 intrusions contain very sparse (2%) andesine
(An$_{45}$) and augite microphenocrysts set in an intersertal to
hyalopilitic groundmass (fig. 94). Andesine microphenocrysts measure
about 0.8 mm in length and are subhedral, show slight normal
compositional zoning, may contain zonally arranged apatite crystals
(fig. 95), and some are associated with trace amounts of secondary
fine-grained clay (saucerite). Clinopyroxene microphenocrysts are
identified as augite based on color and a $2V_z$ of about 50°. These
microphenocrysts measure about 0.6 mm across, are anhedral to
subhedral, are rarely twinned, and have a slight pinkish cast
suggesting a high titanium content. Chlorophaeite or chloritic clays
usually rims a few of the augite crystals. In one thin section
(locality 77-13, T. 4 N., R. 7 W., NE 1/4 sec. 17) a thin reaction rim
of hornblende (?) is present on a few of the augite microphenocrysts.

The groundmass of Tgr3 intrusions consists of plagioclase
microlites (44% to 55%), clinopyroxene (27% to 37%), opaque oxides (6%
to 13%), basaltic glass and clay-altered glass (4% to 8%) (Table 10).
Subhedral plagioclase microlites usually display a single
polysynthetic twin and average about 0.1 mm in length. Compositional
determinations by the Michel-Levy method indicate a sodic andesine

Sample Locality

Mineral	------low MgO, low TiO$_2$; Tgr3 ----			High Mgo; Tgr4
	77-13	3623-8	79-12	97-7
Plagioclase	54			46
	(total)			(total)
Phenocrysts		2	2	
Microlites		55	44	
Augite	27			44
	(total)			(total)
Phenocrysts		2	2	
Groundmass		27	37	
Opaque Oxides	13	9	6	5
Glass/ Altered glass	6	4	8	
Hornblende		trace	1	trace
Biotite	trace			trace

Table 10. Modes of petrographically examined Grande Ronde Basalt petrologic types from the thesis area.

Figure 94. Photomicrographs of low MgO–low TiO_2 Grande Ronde Basalt. Sparse andesine (An_{45}) and augite microphenocrysts are set in an intersertal-to-hyalopilitic groundmass predominantly composed of plagioclase microlites, intergranular clinopyroxene crystals, and opaque oxides. A: plane polarized light. B: crossed polars.

A.

B.
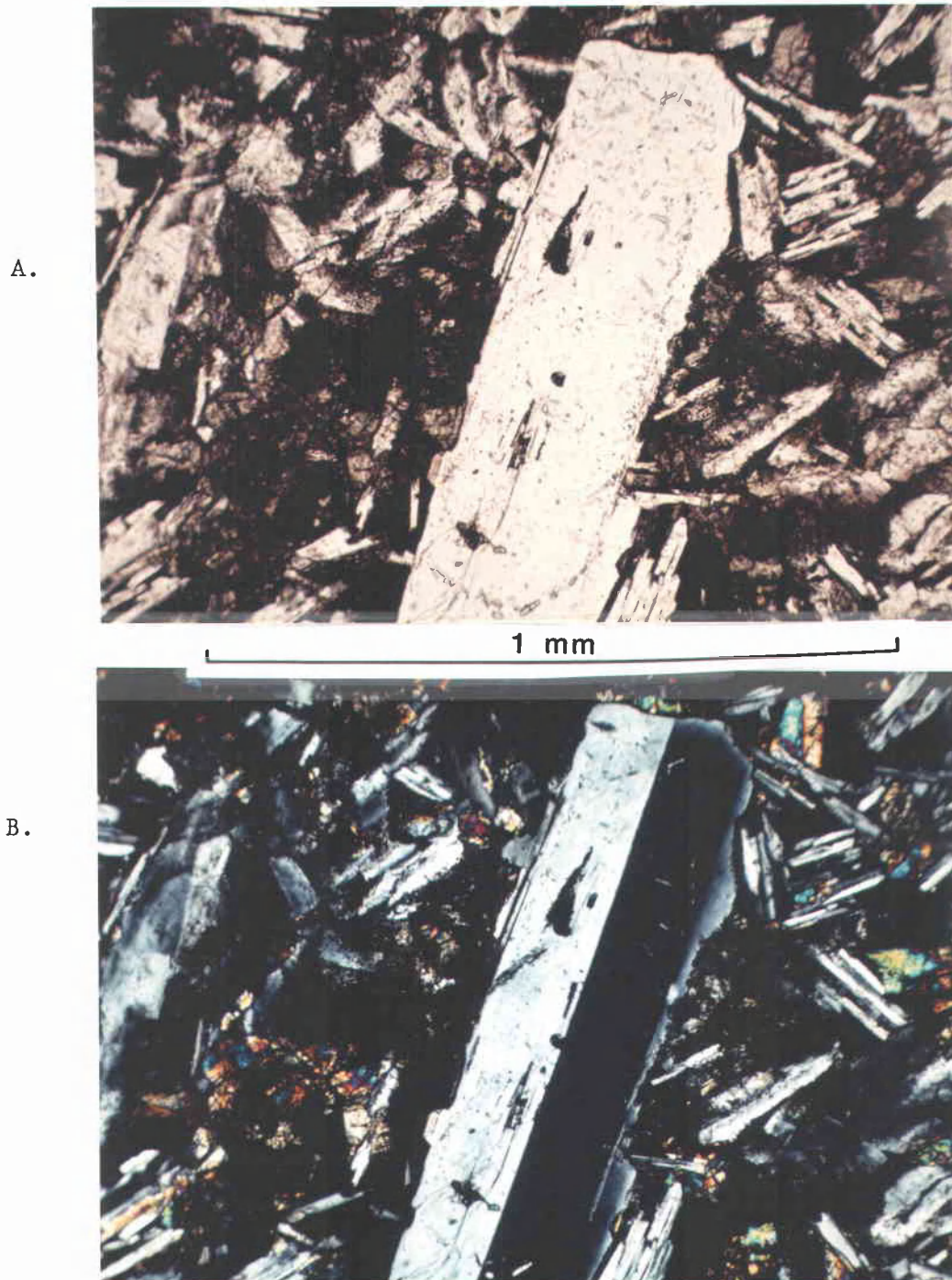
Figure 95.   Photomicrographs of low MgO—low TiO$_2$ Grande Ronde Basalt.
Note zonally arranged apatite crystals in plagioclase
microphenocryst.   A: plane polarized light.   B: crossed
polars.

composition (An_{40}-An_{44}). Groundmass clinopyroxene forms small subhedral to anhedral intergranular crystals averaging about 0.2 mm across, and is probably augite. Opaque oxides, most likely magnetite and ilmenite, occur as very small intergranular crystal averaging about 0.05 mm across and as a finely disseminated "dust" in basaltic glass, which is dark colored (nearly black or very dark brown).

The Tgr4 basalt examined in thin section consists of very sparse plagioclase-augite microglomerophenocrysts set in a holocrystalline intersertal groundmass (fig. 96). The groundmass consists of seriate calcic andesine (An_{46}) to sodic labradorite (An_{52}) microlites (46%), intergranular clinopyroxene (44%), opaque oxides (5%), and trace amounts of biotite and hornblende associated with trace mixtures of quartz and potassium feldspar silicic residuum in the groundmass (fig. 97). Plagioclase microlites display polysynthetic and/or Carlsbad twins and ranges from about 0.01 mm to 0.7 mm in length. Augite ranges from <0.01mm to about 0.5 mm across and is locally rimmed with chlorophaeite. Opaque oxides, probably magnetite and ilmenite, occur as small subhedral to anhedral crystals averaging about 0.04 mm across.

This limited petrographic study concurs with the petrographic comparisons of low MgO and High MgO Grande Ronde Basalt intrusions made by Rarey (1986) in that 1) low MgO intrusions tend to contain significant amounts of glass (tachylite or siderolomane), and 2) high MgO intrusions contain less plagioclase and more clinopyroxene than low MgO intrusions. Rarey (1986) also noted that low MgO intrusions are generally more finely crystalline than high MgO intrusions of comparable thickness. This is evident in hand samples from the thesis area but was not visible in thin section, probably because the thin section sample of the high MgO intrusion was collected from a chilled margin. Goalen (1988) studied both extrusive and intrusive parts of six Grande Ronde Basalt chemical subtypes and did not observe (or recognize) any major petrographic differences between the low MgO and high MgO petrologic types.

Snavely (1973) compared the petrographic characteristics of the Grande Ronde Basalt on the Columbia Plateau and the Depoe Bay Basalt along the coast and reported that the two units are essentially the

1 mm
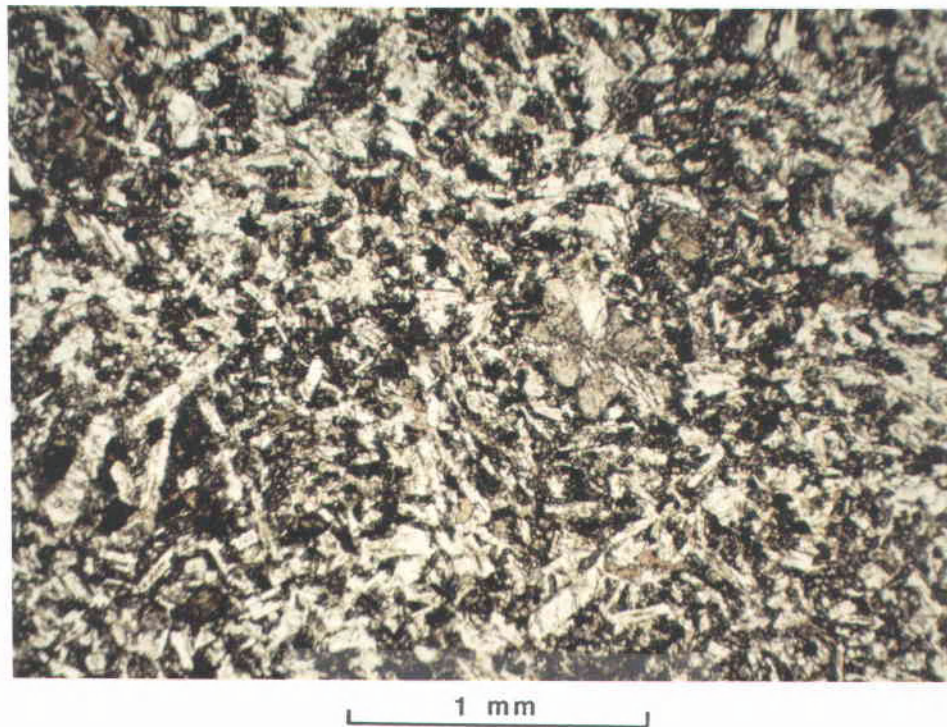
Figure 96. Photomicrograph of high MgO Tgr4 Grande Ronde Basalt intrusion. Note plagioclase-augite microglomerophenocryst in center of photograph (approx. 0.25 mm across), and seriate calcic andesine to sodic labradorite microlites with intergranular clinopyroxene and opaque oxides. Plane polarized light. Field of view 3.3 mm. Locality 97-7 (T. 4 N., R. 8 W., NW 1/4 sec. 3)

1 mm
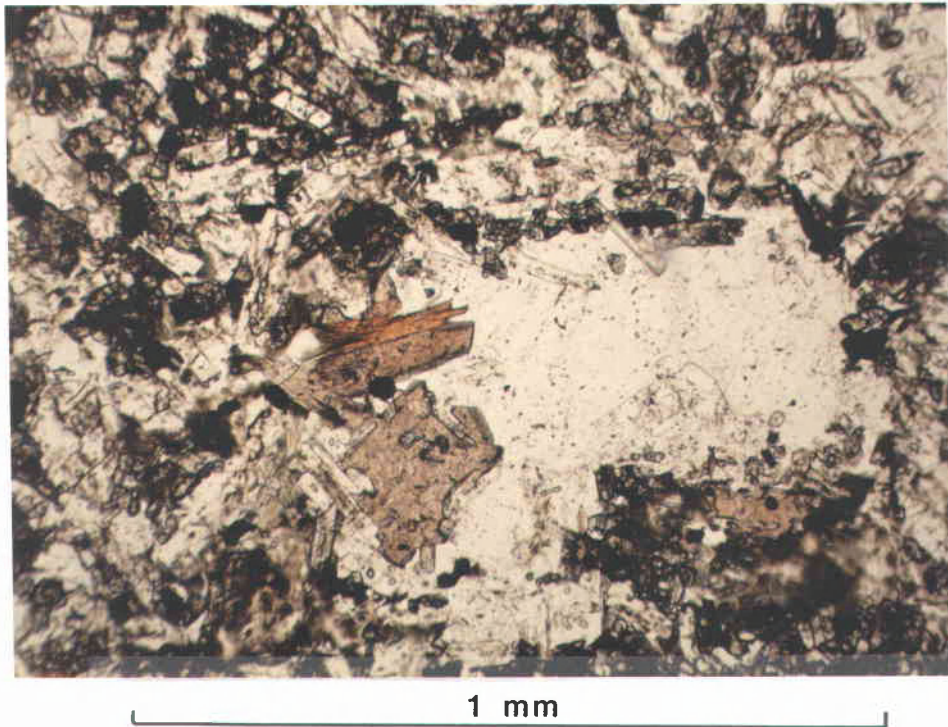
Figure 97. Photomicrograph of high MgO Tgr4 Grande Ronde Basalt dike.
Note quartz-alkali feldspar residuum with associated
biotite and hornblende. Plane polarized light. Field of
view 1.31 mm. Locality 97-7, T. 4 N., R. 8 W., NW 1/4
sec. 3.

same. The petrographic similarity of these two units has been further substantiated by Tolson (1976), Penoyer (1977), Coryell (1978), Murphy (1981), Olbinski (1983), Peterson (1984), Nelson (1985), Rarey (1986), and Goalen (1988).

Magnetostratigraphy

A fluxgate magnetometer was used to determine the magnetic polarity of Grande Ronde Basalt samples from seven locations in the thesis area. Polarities, sample locations, and outcrop remarks are given in Appendix I. Five localities have normal polarity, one locality has an indicated (weak response) reverse polarity, and one locality has indeterminate polarity.

Swanson and Wright (1978) and Swanson and others (1979) divided the Grande Ronde Basalt into R_1, N_1, R_2, and N_2 magnetostratigraphic units (fig. 92). The N_1, R_2, and N_2 units occur both on the Columbia Plateau and in western Oregon whereas the R_1 unit has been identified only on the Columbia Plateau and Willamette Valley (Beeson and Moran, 1979; Goalen, 1988).

Beeson and Moran (1979) and Peterson (1984) documented both normally polarized (Tgr3 of Peterson, 1984) and reversely polarized (Tgr2 of Peterson, 1984) low MgO-low TiO_2 Grande Ronde Basalt in western Oregon. All normally polarized localities belong to the low MgO-low TiO_2 group and, therefore, classify as the Tgr3 petrologic type (N_2, low MgO, low TiO_2).

A weak reverse polarity was obtained from one locality which has high MgO content. However, detailed magnetostratigraphic studies on the Columbia Plateau and in western Oregon have shown that high MgO Grande Ronde Basalt is normally polarized (Swanson and others, 1979). Therefore, the weak reverse polarity of the high MgO basalt in the thesis area is spurious, probably because of structural disturbance and/or tectonic rotations that were not taken into account during sample orientation and collection. This appears to be likely because the sample locality is near the northwestern extension of the Gales Creek fault (Plate I). In any case, high MgO Grande Ronde basalts are generally normally polarized.

Grande Ronde Basalt in the thesis area appears to be restricted to the normally polarized low MgO-low TiO_2 and normally polarized high MgO subtypes. The combination of magnetic polarity and chemical composition, particularly MgO, TiO_2, and P_2O_5, is useful for identifying specific petrologic types of Grande Ronde Basalt.

Petrochemistry

Seven samples from intrusions of Grande Ronde Basalt were analyses for major oxides by X-ray fluorescence at Washington State University under the direction of Dr. Peter Hooper. Preliminary sample preparation was identical to previously described samples of the Tillamook Volcanics and Cole Mountain basalt. Analyses were standardized against the U. S. Geological Survey BCR-1 silicate standard (Columbia River Basalt standard) which has been utilized almost exclusively for published analyses. Therefore, analyses in this report, which are presented in Table 11, can be directly compared with most published analyses.

Snavely and others (1973) established compositional fields on silica variation diagrams for middle Miocene basalts of coastal Oregon. Samples from the thesis area plot in the Grande Ronde Basalt (Depoe Bay Basalt) compositional field, which is primarily distinguished from the other fields by a higher SiO_2 (fig. 98).

One sample (locality 97-7, T. 4 N., R. 8 W., NW 1/4 sec. 3) from the thesis area has a significantly higher MgO content compared to the other six samples. This sample also contains greater CaO and less SiO_2 and K_2O than the other Grande Ronde Basalt samples. Other workers (e.g. Peterson, 1984, Nelson, 1985, Rarey, 1986, Goalen, 1988) have associated these chemical characteristics with the Tgr4 petrologic type (N_2, high MgO). The low MgO Grande Ronde Basalt samples from the thesis area also have low TiO_2 (all less than 2.15 wt. %) and belong to the Tgr3 petrologic type (N_2, low MgO, low TiO_2).

Mangan and others (1986) established a regional correlation of Grande Ronde Basalt stratigraphy through geochemical analysis and magnetic polarity of over 350 samples from 47 stratigraphic sections on the Columbia Plateau and Columbia River Gorge. These workers

Sample Locality

Major
Oxide

Major Oxide	low MgO-low TiO$_2$; Tgr3						Av. Chem. type 5[1]	high MgO -Tgr4- 97-7	Av. Chem. type 1[1]
	3630-2	718-1	3715-2	77-13	78-4	79-12			
SiO$_2$	56.53	55.47	56.02	55.84	56.18	56.13	55.73	54.85	54.74
Al$_2$O$_3$	13.37	13.64	13.22	13.44	13.25	13.30	14.11	13.86	14.42
FeO*[2]	12.38	12.21	12.54	12.20	12.39	12.30	11.32	11.72	10.99
MgO	3.31	3.57	3.49	3.61	3.41	3.42	3.88	4.56	4.60
CaO	6.92	7.24	6.87	7.07	6.83	7.06	7.38	8.17	8.40
Na$_2$O	2.83	3.07	3.02	3.02	3.09	2.95	3.10	2.85	2.77
K$_2$O	1.40	1.50	1.54	1.53	1.55	1.58	1.76	1.02	1.30
TiO$_2$	2.12	2.13	2.14	2.13	2.11	2.08	1.96	1.88	1.80
P$_2$O$_5$	0.36	0.37	0.37	0.38	0.38	0.37	0.31	0.32	0.36
MnO	0.19	0.21	0.19	0.20	0.019	0.20	0.18	0.20	0.16

Table 11. Major oxide values of Grande Ronde Basalt intrusions from the thesis area compared with average major oxide values of chemical types 1 and 5 from Mangan and others (1986). [1]Mangan and others (1986). [2]All Fe expressed in reduced form.
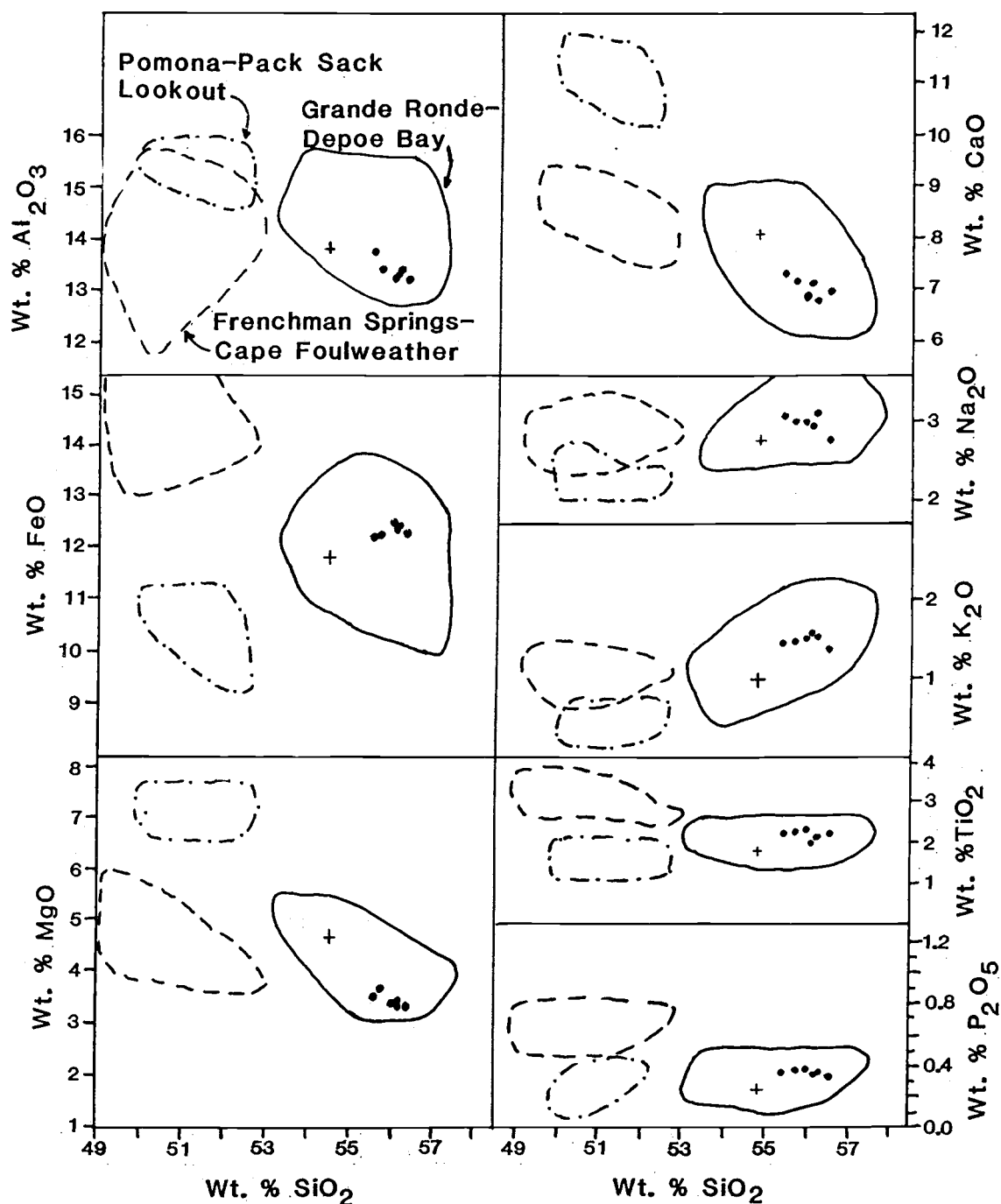
Figure 98. Major oxide values of Grande Ronde Basalt samples from the thesis area plotted on silica variation diagrams. Fields for Pomona Basalt (Basalt of Pack Sack Lookout), Grande Ronde Basalt (Depoe Bay Basalt), and Frenchman Springs Member of the Wanapum Basalt (Cape Foulweather Basalt) from Snavely and others (1973). Note that all samples plot in the Grande Ronde Basalt geochemical fields.

subdivided the Grande Ronde Basalt on the Columbia Plateau into five main chemical types based on variations in MgO, TiO_2, and P_2O_5 content (fig. 99). Chemical types 2 and 5 of Mangan and others (1986) have lower MgO contents (< 4.5 wt. %) than chemical types 1, 3, and 4. Chemical type 2 is distinguished from chemical type 5 by higher P_2O_5 and higher TiO_2 contents. Of the high MgO chemical types, type 3 is distinguished from type 1 by lower P_2O_5 contents and from type 4 by lower P_2O_5 and lower TiO_2.

Six samples from the thesis area plot in the field of chemical type 5 and one Tgr4 sample plots in the field of chemical type 1 (fig. 99). Mangan and others (1986) reported that only flows of subunits 2D, 5C, 5A, 4A, 3A, and 1A of the Grande Ronde Basalt, which are the most widespread subunits, occur west of the Cascades. All samples from the thesis area have been assigned to the N_2 magnetic polarity subzone. Therefore, Tgr3 samples correspond to subunit 5A (subunit 5C is transitional but reversely polarized in western Oregon) and the Tgr4 sample corresponds to subunit 1A.

Goalen (1988) also reported a N_2, low MgO, low TiO_2 Grande Ronde Basalt in northwestern Oregon correlative to subunit 5A of Mangan and others (1986). In the Plympton Ridge Section (Elk Mountain-Porter Ridge area of Clatsop County), Goalen correlated N2, high MgO Grande Ronde Basalt flow(s) to subunit 4A of Mangan and others (1986). This indicates that at least two distinct N_2, high MgO Grande Ronde Basalt units (chemical types 1A and 4A of Mangan and others (1986), are present in northwestern Oregon. Beeson and Moran (1979) and Murphy (1981) previously documented the existence of two distinct N_2, high MgO Grande Ronde Basalt flows in northwestern Oregon.

Age, Correlation, and Origin of the Grande Ronde Basalt

Age

Swanson and others (1979) radiometrically dated the Grande Ronde Basalt on the Columbia Plateau between 16.5 and 14.5 Ma. Snavely and others (1973) reported virtually identical K-Ar ages ranging from 14 +/- 2.7 Ma to 16 +/- 0.6 Ma for the Depoe Bay Basalt (Grande Ronde
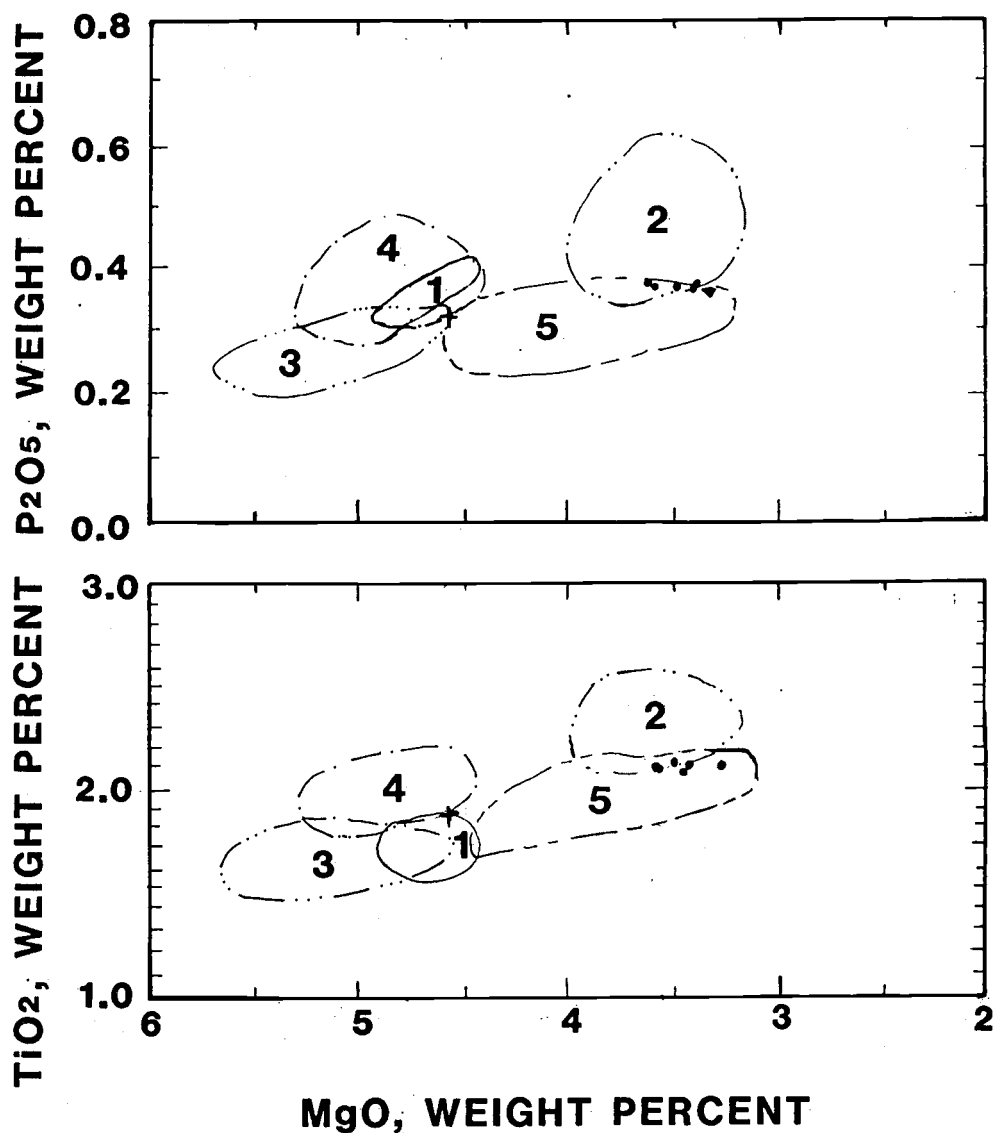
Figure 99. Major oxide values of Grande Ronde Basalt samples from the thesis area plotted on P_2O_5-MgO and TiO_2-MgO bivariate diagrams. Fields for chemical types 1 through 5 from Mangan and others (1986). Six samples of petrologic type Tgr3 plot in the field of chemical type 5 and one sample of petrologic type Tgr4 plots in the field of chemical type 1.

Basalt) of coastal Oregon. Niem and Cressy (1973) reported a radiometric age of 15.9 +/- 0.3 Ma. for a very thick, gabbroic low MgO Grande Ronde Basalt sill which forms Neahkahnie Mountain along the northern Oregon Coast. These radiometric age determinations demonstrate the age equivalence of the Grande Ronde Basalt in both the coastal region and on the Columbia Plateau.

Correlation and Origin

The correlation of Columbia River Basalt Group units in the coastal regions of northwestern Oregon and southwestern Washington with the Columbia Plateau sequence has strong implications for the origin of these coastal basalts. Warren and Norbisrath (1946) tentatively correlated subaerial flows of Columbia River Basalt exposed on the eastern flank of the Oregon Coast Range in northwestern Oregon with the subaerial sequence exposed on the Columbia Plateau and supported a plateau origin for these flows. However, these workers invoked a local vent origin for the generation of middle Miocene intrusions and related basaltic extrusive west of the "westernmost margin" of the subaerial flows. Snavely and others (1973) demonstrated that the "coastal basalts", including intrusive dikes and sills, were stratigraphically, geochemically, and petrographically correlative to "plateau basalts" of the Columbia River Basalt Group. Snavely and others (1973), however, supported the idea that these basalts were erupted from local vents. Evidence cited by these and other workers to suggest local eruption included intrusions (dikes, ring dikes, sills) and subaerial eruptive features such as "volcanic bombs". These workers concluded that the "coastal basalts were erupted from vents positioned along a 260 km-long north-south trending fracture system extending from Waldport, Oregon to Grays Harbor, Washington. Snavely and others (1973) recognized obvious problems with the "two vent" hypothesis (e.g. having the same tholeiitic magma erupted at the same time and in the same stratigraphic sequence from vents approximately 500 km. apart and on either side of the intervening calc-alkaline Cascades arc). These workers reasoned that the magma reservoir associated with the two widely separated vent

areas must have been very widespread and geochemically homogeneous, and that eruptions must have occurred rapidly and simultaneously on either side of the Cascade arc from deep extensional fractures. Snavely and others (1973) proposed three petrogenetic-plate tectonic models compatible with these constraints: 1) partial melting of refractory eclogite subducted with the Juan de Fuca Plate beneath the leading edge of the North American Plate and migration of magma up the subduction zone to deep seated coastal fractures, 2) partial melting related to a broad region of horizontal shear at the base of the North American Plate (lithosphere-asthenosphere boundary) and magma migration to the two widely spaced fracture systems, and 3) partial melting of homogeneous eclogite (Juan de Fuca Plate) in the mantle and lateral spread of magma to deep-seated fractures. However, these workers pointed out two major shortcomings of all three models. One inadequacy is that concurrent calc-alkaline magmatism of the Cascade arc between the two postulated mafic vent areas is not explained. The other problem is that all models call upon large-scale magma migration from source regions to the two postulated eruptive sites without crustal contamination. Therefore, these petrogenetic/plate tectonic models are inadequate.

Beeson and others (1979) noted the inadequacies inherent in the petrogenetic models of Snavely and others (1973) and challenged the "two vent" hypothesis. As an alternative model, these workers posited that the intrusive parts of the "coastal basalts" represented the distal ends of voluminous basaltic lava flows which were erupted from vents on the Columbia Plateau, flowed down the ancestral Columbia River drainage to the Miocene coastal embayment (i.e. Astoria Basin), and foundered into and interacted with less dense, unconsolidated and unlithified marine sediments. This model explains the following: 1) the occurrence of pillow-palagonite and breccia piles at the margin of the subaerial flows, 2) the association and distribution of dikes and sills with the pillow-palagonite and breccia complexes, 3) the same eruptive sequence on both the Columbia Plateau and in the coastal regions, 4) the identical major and trace element geochemical characteristics, 5) the identical age of the rocks, and 6) the absence of local feeder dikes in the volcanic basement rocks of northwestern

Oregon and southwestern Washington. This "one vent" hypothesis has been supported by subsequent detailed studies which have geophysically, geochemically, magnetically, and stratigraphically demonstrated the correlation of Grande Ronde Basalt flows and intrusions in northwestern Oregon with the flow sequence on the Columbia Plateau (Beeson and Moran, 1979; Murphy, 1981; Pfaff, 1981; Peterson, 1984; Nelson, 1985; Rarey, 1986; Anderson and others, 1987; Wells and Niem, 1987; Goalen, 1988). Invasive flows of the Columbia River Basalt Group have been documented on the Columbia Plateau (Byerly and Swanson, 1978; Swanson and Wright, 1979; Byerly and Swanson, 1987) and in the Coast Range of northwestern Oregon and southwestern Washington (Wells and Niem, 1987; Pfaff and Beeson, 1987). Goalen (1988) has documented detailed field, geochemical, and magnetic evidence demonstrating the transition from subaerial flows to pillow-palagonite complexes to "invasive" flows in the Elk Mountain-Porter Ridge area of northern Clatsop County, Oregon. Murphy (1981) documented the transition of subaerial flows of Grande Ronde Basalt and Frenchman Springs Member to palagonite-pillow lava delta complexes and then into dikes and sills in the Big Creek area of Clatsop County, Oregon. Therefore, it is thought that Grande Ronde Basalt dikes and sills in the thesis area are directly correlative and the same age as subaerial flows of Grande Ronde Basalt on the Columbia Plateau and in northwestern Oregon. However, the exact mechanics of invasion or invasiveness are not understood at this time (Wells and Niem, 1987).

QUATERNARY DEPOSITS

Quaternary deposits of the thesis area consist of terrace alluvium (Qt), modern stream and river alluvium (Qal), slump and landslide debris (Qls), and colluvium (not mapped)(Plate I). Alluvial terrace deposits are distributed along the Nehalem River (e.g. Pope Corner area, south of Jewell Junction, and the Lukarilla area), and along Humbug Creek (Elsie area). These terrace deposits are 1 to 5 m thick and consist of rounded, poorly sorted basaltic cobbles, pebbles, and boulders in a sandy matrix. All of the larger terraces (e.g., Pope Corner and Lukarilla areas) are utilized for agricultural and housing purposes. Most recent alluvial deposits consist of poorly sorted basaltic cobbles in a sandy matrix. The steep Cronin Creek drainages (north, middle, and south forks), which are entirely developed in the Tillamook Volcanics, contain angular basalt boulders up to 5 m in diameter. However, the majority of smaller creeks and streams in the thesis area does not contain mappable quantities of stream alluvium. In the Spruce Run Lake area the Qal map unit represents lacustrine deposits of clay, peat, silt and sand which are filling in sag pods.

Three major areas of recently active slumps and landslides were delineated from field mapping and aerial photographs (Plate I). In the northeastern part of the thesis area along U.S. 26 about 1.6 km east of Jewell Junction an area of approximately 0.75 km^2 is actively slumping and required stabilization measures in 1984. In this area Sweet Home Creek member mudstones are slumping southwestward off a topographic high composed of Cole Mountain basalt. This mass movement is marked by hummocky topography, tilting of trees, phacoidal mudstone developed along small thrust faults, and progressive offset of the Sunset Highway (U. S. 26) pavement. Another major landslide area of at least 2.6 km^2 extends into the northeastern part of the thesis area from about Flat Iron Mountain to the Quartz Creek drainage. This landslide is marked by hummocky topography, the tilting of trees, sag pods (Bloom Lake) and an active toe in Quartz Creek which consists of blocks of mudstone up to 10 m in diameter with admixed basalt cobbles, trees, and shrubs. This landslide is also developed in Sweet Home

Creek mudstone which is thought to have slid off of the Flat Iron Mountain topographic high, which is predominantly composed of Cole Mountain basalt. A third major landslide is located immediately southeast of Lost Lake in the central part of the thesis area. This landslide largely consists of a coherent block of Grande Ronde Basalt and thermally indurated Jewell member mudstone that has slid into the Spruce Run Creek drainage over Jewell member mudstone which is not thermally indurated. Numerous smaller slumps and landslides exist in the thesis area but were not mapped. Sweet Home Creek member and Jewell member mudstones are especially prone to mass wasting.

STRUCTURE AND TECTONICS

Structure of the Oregon Coast Range

Introduction

Warren and Norbisrath (1946) generalized the structure of the Coast Range as a geanticline. Snavely and Wagner (1964) described it as a regional anticlinorium that plunges north and is complicated by northwest-, northeast-, and east-trending faults. However, this is misleading because the requisite synclinal and anticlinal structures are either difficult to trace out or are absent (Niem and Van Atta, 1973). It is probably best described as a basement uplift cut by many faults. The central and northern parts are cored by the 15,000 to 20,000 foot thick lower to middle Eocene Siletz River Volcanics and middle Eocene Tillamook Volcanic Series, respectively (Snavely and Wagner, 1964) Younger Tertiary strata homoclinally dip away from the nose and flanks of the basement uplift (Snavely and Wagner, 1964).

The axis of the northward plunging structural high, called the Nehalem arch, trends through the southern part of the thesis area and is nearly coincident with the border of Clatsop and Columbia counties (Wells and Peck, 1961). It separates the Astoria basin to the west from the Nehalem (or Willamette) basin to the east (Wells and Peck, 1961; Bruer and others, 1984; Armentrout and Suek, 1985). Uplift of the Oregon Coast Range began in the middle to late Miocene (Snavely and Wagner, 1963; Snavely and others, 1980) and is reflected by rapid shallowing of the Astoria basin from bathyal to shelf water depth (Nelson, 1985).

Summary of Tectonic Events

Since the Eocene, the Oregon Coast Range and adjacent continental shelf and slope have undergone numerous episodes of compression, uplift, and extension (Snavely and others, 1980). Oblique plate convergence and subduction of the Juan de Fuca and Farallon plates beneath the North American continent has created low angle, eastward

dipping, imbricate thrust faults and folds along the Oregon continental slope (Kulm and Fowler, 1974; Silver, 1978; Snavely and others, 1980; Wells, 1981; Magill and others, 1981, 1982; Niem and Niem, 1984). Episodic underthrusting has been postulated during the middle Eocene, middle late Eocene, late middle Miocene, Pleistocene, and Holocene by Snavely and others (1980). Underthrusting episodes were interrupted by periods of major right lateral strike slip faulting in the late middle Eocene and early late Eocene and by periods of extension during the late Eocene to late middle Miocene, and late Miocene to early (?) Pleistocene (Snavely and others, 1980). Nelson (1985) interpreted four phases of structural development in Clatsop County: 1) late Eocene block faulting; 2) latest Eocene and middle Oligocene to early Miocene uplift of the Coast Range; 3) middle Miocene northwest-southeast oriented extension; and 4) post middle Miocene north-south compression creating conjugate oblique slip faults and associated north-dipping east-west oriented thrust faults.

Structures in Northwestern Oregon

In Clatsop County two dominant trends of faulting have been mapped: 1) east-west trending high angle faults, and 2) a conjugate set of northeast-trending left lateral and northwest-trending right lateral oblique-slip faults (Olbinski, 1983; Peterson, 1984; Nelson, 1985; Niem and Niem, 1985; Rarey, 1986; this study). Less prominent structures include north-south-trending high angle faults, and east-west-trending thrust faults, and en echelon northwest-trending open folds associated with oblique left lateral east-west-trending faults (Olbinski, 1983; Peterson, 1984; Nelson, 1985; Niem and Niem, 1985, Rarey, 1986). The rare folds that are present are highly disrupted by intrusions and numerous northwest- and northeast-trending oblique slip faults (Niem and Niem, 1985). In southeastern Clatsop County, northwest-trending horsts and grabens bounded by high angle oblique-slip faults trend into the thesis area and juxtapose upper middle to late Eocene Hamlet formation strata against the main body of middle Eocene Tillamook Volcanics to the south and a smaller uplifted block of Tillamook Volcanics to the north (Green Mountain outlier)

(Warren and Norbisrath, 1946; Niem and Niem, 1985; Safley, in prep.; this study).

Regionally, faults in northwestern Oregon are generally compatible with that of a major zone of distributed right lateral shear and associated small block clockwise rotation (Wells and others, 1984). In this interpretation rare north-south and more common northwest-trending oblique slip dextral faults are the primary expressions of dextral shear in basement rocks (wrench faults), east-west trending oblique slip sinistral faults are R' (Reidel prime) shears which undergo substantial clockwise rotation, and the northeast trending high angle faults are R (Reidel) shears. Pull-apart basins and high angle normal faults form along oblique strike slip faults at releasing bends where divergence occurs (Wilcox and others, 1973). The northwest-southeast oriented graben in southeast Clatsop County may be such a pull-apart basin because northwest-trending right lateral oblique-slip faults turn more westerly in this region (Jackson, 1983; Wells and others, 1983); Niem and Niem, 1985). Nelson (1985) paleomagnetically documented significant small block rotation of middle Miocene Grande Ronde Basalt dikes in Clatsop County and attributed it to distributed shear between northwest-trending right lateral and northeast-trending left lateral oblique-slip faults. Wells and Coe (1985) also attributed clockwise tectonic rotations in southwestern Washington to a model of simple shear, and suggested that tectonic rotations in the Oregon Coast Range might be caused by the same mechanism.

However, application of the idealized model to the observed fault pattern is complicated by the fact incomplete definition of the faulting history (e.g., faults of different ages have not always been delineated and tied to different tectonic episodes). Earlier formed structures would no doubt influence the development of subsequent structures. However, greater offset of upper Eocene and lower Oligocene strata along high angle east-west-trending faults is more evident than offset of younger Miocene strata. The greater offset of upper Eocene rocks and lesser offset of Miocene units and middle Miocene volcanics along these major east-west-trending faults suggests that dip slip (?) motion may have been initiated in the late Eocene

and that these faults were reactivated in post middle Miocene time with left lateral oblique slip motion (Niem and Niem, 1985). A predominantly left lateral sense of offset along northeast-trending faults in Clatsop County is indicated by offset of Miocene dikes which have been used as piercing points (Peterson, 1984; Nelson, 1985; Niem and Niem, 1985). This is inconsistent with the expected right lateral offset for R faults in the simple dextral shear model. The author also documented a predominantly left lateral sense of motion along of northeast-trending faults in the thesis area.

Faults in the Thesis Area

Faults in northwestern Oregon are largely concealed by lush vegetation and extensive weathering. Other obstacles in delineating structural elements include the paucity of suitable stratigraphic markers, such as bedding planes, in massive mudstone units to determine strike and dip, and anomalous structural attitudes caused by deformation, loading and disruption by numerous intrusive bodies, and unrecognized slumps. Offset of generally vertical and linear trends of middle Miocene basalt dikes has been used by earlier workers to identify piercing points and relative motion along strike-slip faults (Olbinski, 1983; Peterson, 1984; Nelson, 1985; Niem and Niem, 1985). This was not possible in the thesis area because most exposed intrusions are highly irregular and prone to rapid changes in orientation and stratigraphic position (e.g., fig. 93).

Faults in the study area were mapped on the basis of 1) direct observation of stratigraphic offset, slickensides on shear surfaces, and gouge zones; 2) juxtaposition of stratigraphic units; and 3) anomalous regional dip directions and angles. In addition, lineaments and linear features interpreted on 1983 high altitude SLR imagery, Landsat imagery, high altitude black and white aerial photographs, and USGS topographic maps were field checked for evaluation of structural significance. Slickensides on shear surfaces and fault gouge were most commonly observed in the Tillamook Volcanics. Stratigraphic offset was most easily detected in thin distinctive units such as the Roy Creek and Sunset Highway members of the Hamlet formation. In many

instances subparallel synthetic faults were used to determine the orientation, sense of displacement, and approximate position of concealed major faults. Although several significant faults were mapped, the author suspects numerous smaller faults were not detected. This would create a more complex structural pattern than depicted on figures 100 and 103. Faults not discussed below lack evidence for significant displacement such as development of fault gouge and juxtaposed stratigraphic units.

East-West Faults

Four east-west trending high angle faults were mapped in the thesis area see (fig. 100; Plate I). Two are major faults which traverse the entire width of the thesis area (11-14.5 km) and have considerable vertical separation (200-300 m) The other two are less prominent and demonstrate significantly less throw (10-60 m) All are offset by NW trending strike-slip faults. Stepped slickensides on shear surfaces generally indicate latest oblique strike-slip motion. From south to north these faults are identified as: 1) the God's Valley-God's Valley extension fault; 2) the Sweet Home Creek fault; 3) the Cole Mtn.-Quartz Creek fault; and 4) the Jewell Junction-Jewell Junction fault extension.

The God's Valley-God's Valley extension fault extends across the southern portion of the study area. God's Valley fault is well exposed in cliffs of Tillamook Volcanics along the lower Nehalem River highway in the SE 1/4 sec. 34 and SW 1/4 sec. 35, T. 4 N., R. 8 W. (localities 731-1,2,3; fig. 100). It controls the east-west course of the Nehalem River in this area. The fault plane strikes N62-76E to N62-68W, dips steeply to the north (62-90°, with 75-90° most prevalent), and have "steps" which indicate latest right lateral motion. Slickensides plunge 7-11° east. The shear zone in this region is approximately 20 meters wide, and at locality 731-3 (SE 1/4 sec. 34, T. 4 N., R. 8 W.) fault gouge along one shear plane is roughly 4 m thick. Less prominent conjugate shears trend N30-32E and dip steeply NW.

Rarey (1986) named and mapped the God's Valley fault over a 12 km
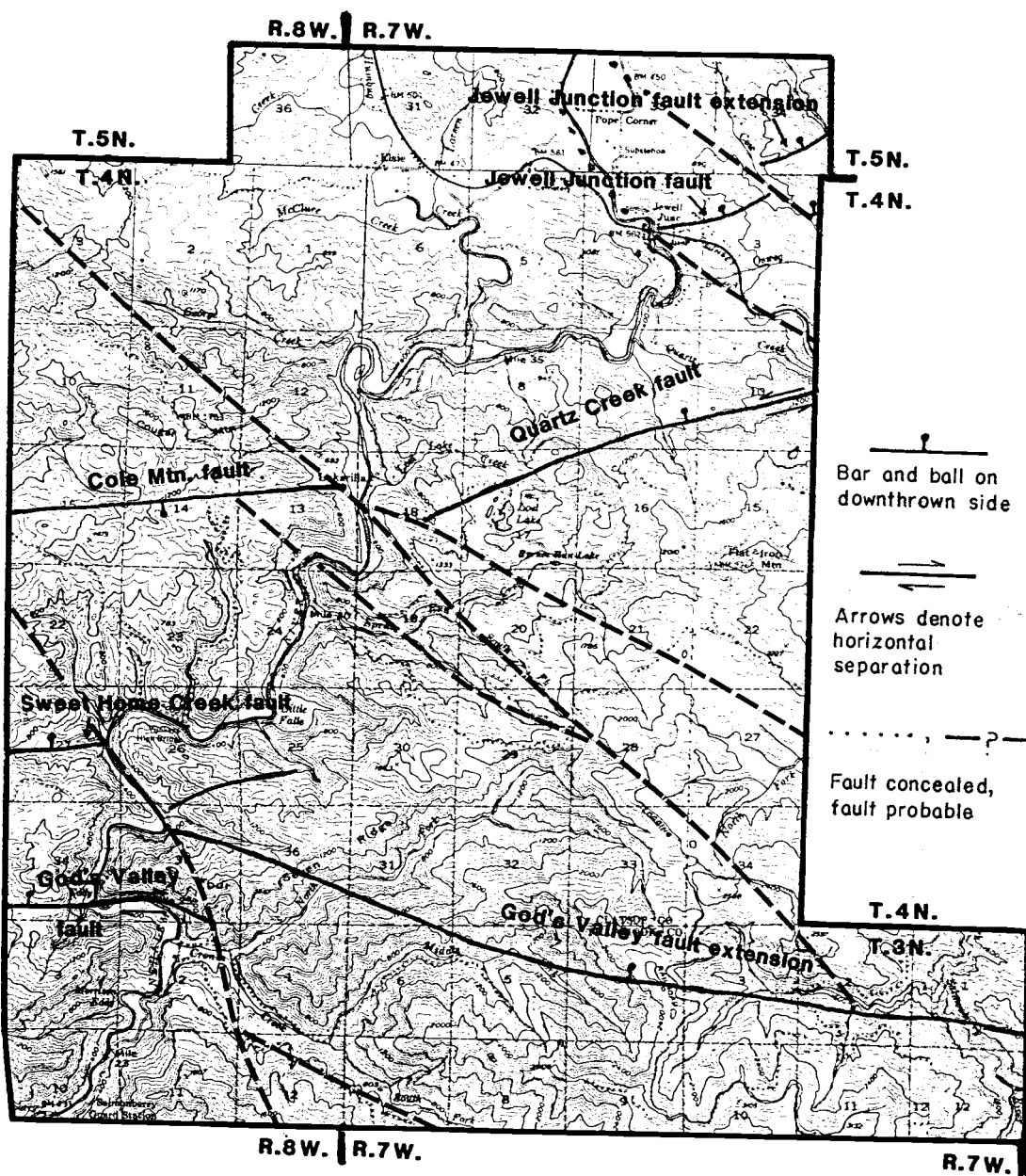
Figure 100. Location map of east-west-trending faults in the Elsie-lower Nehalem River area. Major faults are offset by northwest-trending strike-slip faults (dashed).

A.

B.

Figure 101. Exposures of God's Valley fault. A: Looking west along
subhorizontal mullion features on a natural cliff
exposure of Tillamook Volcanics. Hammer in crack in
lower left for scale. B: close up showing eastward
plunge of slickensides with "steps" indicating latest
right lateral motion. Hammer for scale. Both from
locality 731-2 (T. 4 N., R. 7 W., SW 1/4 sec. 35).

distance west of the thesis area. He found Jewell member mudstone of the Refugian Keasey Formation faulted against middle Eocene Tillamook Volcanics which demonstrates roughly 200 meters of vertical separation. He observed "steps" in the fault zone indicating latest left lateral oblique strike-slip motion. This fault forms a prominant escarpment between ridge-forming erosionally resistant basalts (Tillamook Volcanics) to the south and less resistant valley-forming mudstone to the north.

West of the area mapped by Rarey (1986), the God's Valley fault is on trend with a major east-west fault mapped by Cressy (1974). Niem and Niem (1985) show this fault abruptly cutting middle Miocene basalt and the middle Miocene Astoria Formation at the coast line and extending offshore.

In the thesis area, the God's Valley fault appears to be offset or terminated by a NW trending oblique left lateral fault (Cronin Creek fault) in sec. 35, T. 4 N., R. 8 W. (fig. 100). A possible extension of the God's Valley fault, originating in the NW 1/4 sec. 35, T. 4 N., R. 7 W., has been mapped into the SE part of the field area where it parallels a part of logging road 101 (Plate I). Evidence for extending God's Valley fault consists of observed on-trend synthetic faults, gouge zones, and continuation of linear features observed on aerial photographs and SLR imagery. On strike with the fault, at outcrop locality 923-9 (SE 1/4 sec. 4, T. 3 N., R. 7 W.), a well-exposed normal fault in Tillamook Volcanics strikes N70W and dips 72NE (fig. 102). However, there is only 5.5 meters of vertical separation at this location, and evidence for strike-slip motion is lacking, suggesting that the God's Valley fault dies out to the east. Alternatively, this normal fault may be a small en echelon Reidel fault formed at an acute angle to the major east-west God's Valley fault system with is to be expected in a wrench tectonic system (Wilcox and others, 1973). It is also possible that the God's Valley fault terminates against the previously mentioned NW-trending Cronin Creek fault and that it is unrelated to the God's Valley fault extension. In any case, the God's Valley fault is a major structure which has been mapped over a distance of at least 27 kilometers.

The Sweet Home Creek fault mapped by Rarey (1986) trends into the

Figure 102. Normal fault in the middle Eocene upper Tillamook
Volcanics. Note offset of less erosionally resistant
flow top breccia and discoloration (MnO_x and FeO_x) of
fault zone. Banded pole is 180 cm long. Locality 923-9
(T. 3 N., R. 7 W., SE 1/4 sec 4) on spur off logging road
#100.

southwest part of the study area in sec. 27, T. 4 N., R. 8 W.. It has been extended into the thesis area on the basis of an on-trend saddle and stream drainage (fig. 100). The fault appears to terminate against the same NW trending strike-slip fault that offsets God's Valley fault 2.4 km to the south (Cronin Creek fault) because no evidence for its existence has been found east of this point. Rarey (1986) mapped the Sweet Home Creek fault as a south-dipping high angle normal fault and estimated 60 meters of vertical displacement.

The Cole Mtn.-Quartz Creek fault is another major structure in northwestern Oregon that has been mapped over a 34 km distance (Niem and Niem, 1985). It trends across the central part of the thesis area and is offset by the northwest-trending oblique right lateral strike-slip Gales Creek fault near Lukarilla, in the center of the thesis area (fig. 100; Plate I). West of the Gales Creek fault, it is referred to as the Cole Mtn. fault. East of the Gales Creek fault it is called the Quartz Creek fault. Exposures of the fault plane were not found in the thesis area, but approximately 200 meters of vertical separation is indicated by juxtaposition of Sweet Home Creek mudstone and Tillamook Volcanics in the vicinity of Lukarilla (T. 4 N., R. 7 W., NW 1/4 sec. 18). The fault is expressed topographically. South of the fault the Nehalem River is entrenched in a steep-walled canyon because it is confined by the erosionally resistant Tillamook Volcanics. North of the fault the river valley river is much broader and the surrounding topography is subdued because less resistant sedimentary rocks predominate. Rarey (1986) mapped the continuation of the east-west-trending Cole Mtn. fault west of the study area and documented 200 meters of vertical separation. Niem and Niem (1985) terminate the Cole Mtn. fault roughly 14.5 km west of the thesis area against a northwest trending fault along Buchanan Creek.

East of the Gales Creek fault offset, in the Lost Lake Creek area, Hamlet formation and Keasey Formation strata north of the Quartz Creek fault dip 35-45° into the fault plane. This is consistent with drag along a high angle fault with considerable throw. In the NE part of the map area (sec. 9 and 10, T. 4 N., R. 7 W.), the fault forms a prominent escarpment because the erosionally resistant Tillamook Volcanics to sky out over less resistant Hamlet formation due to

juxtaposition along the fault. This escarpment is pronounced on aerial photographs, topographic maps, and SLR imagery. Vertical offset in this area is approximately 300 meters.

Immediately east of the map area the Quartz Creek fault has been mapped by Safley (in prep.). Shearing along the fault is evident in Tillamook Volcanics and Roy Creek member conglomerate just north of the U.S. 26 bridge over Quartz Creek and has formed slickensides consistent with latest left lateral oblique slip movement (Safley, in prep). An exploratory adit with roughly 30 m of underground drifts and cross-cuts explore the 15 m-wide Quartz Creek fault shear zone which has been mineralized with quartz, calcite, pyrite, and minor arsenopyrite. Similar mineralization was observed in subparallel shears to the Quartz Creek fault in exposures of Tillamook Volcanics in near the base of the August Fire road measured section (sec. 16, T. 4 N., R. 7 W. and along the Cow Creek Fault. Quartz Creek probably was named after the abundant open space filling sparry quartz that has weathered out of the shear zone. The mineralization suggests that the Quartz Creek fault extends to considerable depth and has acted as a conduit for hydrothermal fluids.

The sense of displacement changes along the length of the Cole Mtn.-Quartz Creek fault. The change is suspected to occur at a north-south oriented normal fault in sec. 9, T. 4 N. R. 7. W. (fig. 103, Plates I and II). West of the north-south fault strata on the north side are uplifted along the Quartz Creek fault, whereas east of the north-south fault strata along the Quartz Creek fault are uplifted on the south side. Different senses of displacement are expected along oblique-slip transcurrent faults that have accommodated substantial movement and have been affected by displacements along adjacent synthetic and antithetic faults (Freund, 1974). The Quartz Creek fault appears to be a major structural zone like the God's Valley fault.

The Jewell Junction fault is located in the northeast part of the thesis area near the US highway 26 overpass over the Nehalem River. Nearly vertical shears exposed in a road cut along Luukinin road in Cole Mountain basalt sill strike N75E (locality 630-9; NE 1/4 sec. 4, T. 4 N., R. 7 W.). At outcrop locality 629-2 (also NE 1/4 sec. 4,

T. 4 N., R. 7 W.) the fault strikes N70E and dips 65° SE. No evidence
for sense of displacement was observed at either locality, but reverse
faulting is suggested by the outcrop pattern (south side uplifted).
Throw is estimated to be 60-70 meters. This fault is truncated on
both ends by northwest-striking faults.

The Jewell Junction fault extension may be an eastward extension
of the Jewell Junction fault that has been offset in a left lateral
sense by a northwest-trending fault. The fault is exposed in Cow
Creek in the northeastern part of the study area (SW 1/4 sec. 34, T. 5
N., R. 7 W.) where it trends N55E and juxtaposes Tillamook Volcanics
and sheared Roy Creek member basaltic conglomeratic sandstone against
lower Sweet Home Creek member mudstone. This relationship indicates
roughly 60 meters of stratigraphic separation. Conglomeratic
sandstone caught in the two meter-wide fault zone has been
hydrothermally altered, silicified, and mineralized with pyrite and
minor arsenopyrite. Immediately northwest of the fault zone, in Cow
Creek, Sweet Home Creek member mudstone has been sheared out as
waxy-surfaced phacoidal blocks along a plane slightly oblique to
bedding, indicative of a thrust fault. This observation supports the
interpretation of this fault being an offset extension of the Jewell
Junction reverse fault.

Northwest- and Northeast- Trending Faults

Four major northwest-trending high angle faults have been mapped
in the thesis area (see Plate 1 and fig. 103). Conjugate high angle
northeast-trending faults are associated with the northwest-trending
faults but are generally less significant. From southwest to
northeast these faults are informally referred to as 1) the Cronin
Creek fault; 2) the Gales Creek fault; 3) the Sunset Highway fault;
and 4) the Cow Creek fault (fig. 103).

The Cronin Creek fault is named after numerous N15-30W-trending
shear planes in Tillamook Volcanics observed along logging roads
paralleling the south fork of Cronin Creek. The gouge zone observed
at outcrop locality 824-2 (NE 1/4 sec. 12, T. 3 N., R. 7 W.) is nearly
vertical, strikes N17W, and contains slickensides consistent with

Bar and ball on
downthrown side

Arrows denote
horizontal
separation

....., —P—
Fault concealed,
fault probable
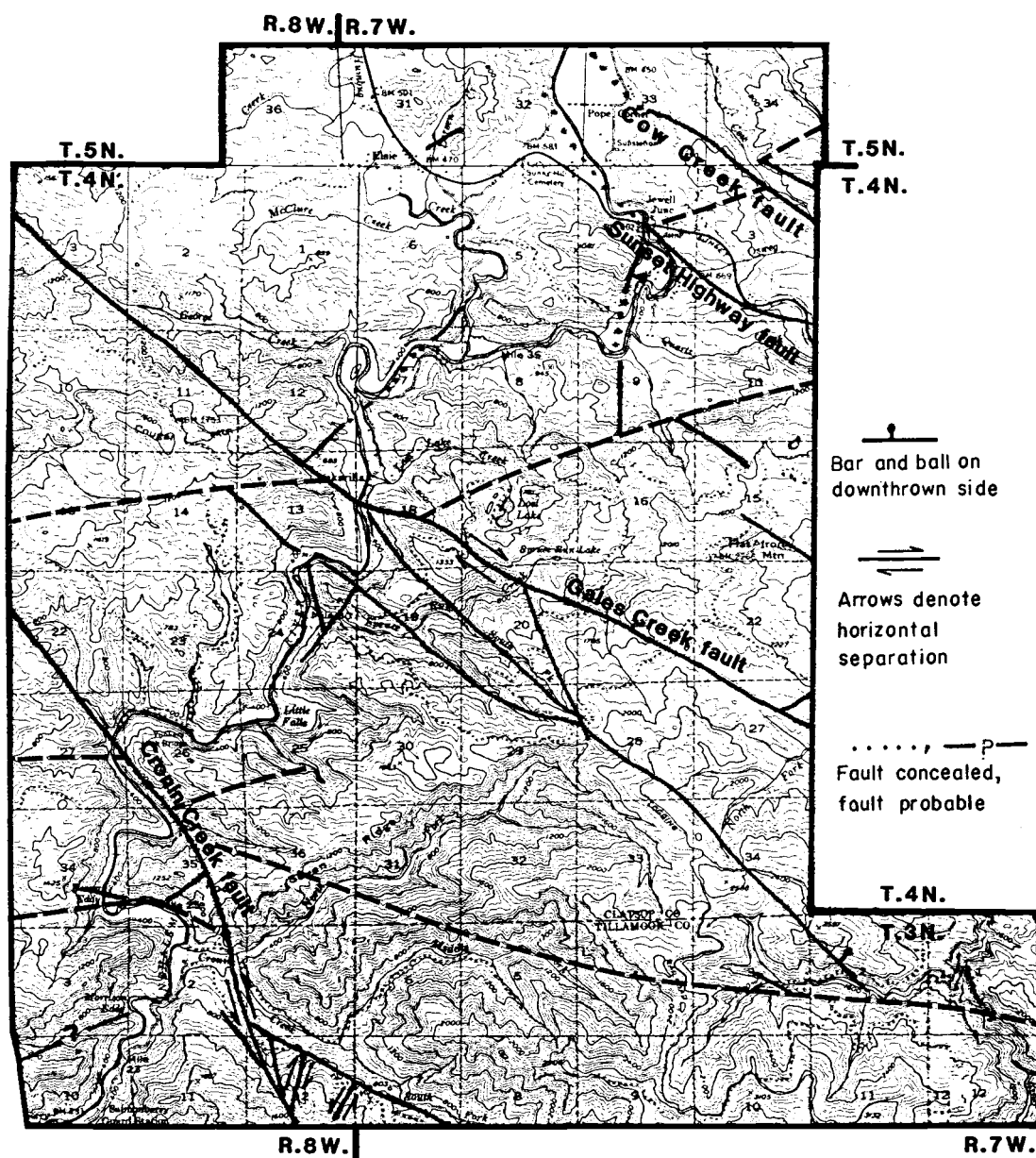
Figure 103.   Location map of northwest- and northeast-trending faults
in the Elsie-lower Nehalem River area.

latest oblique left lateral strike-slip motion. Synthetic subparallel shears strike north to N19W and have vertical to 53° NE dips. Stepped slickensides in the gouge zones are indicative of normal faulting (down to the east). Conjugate shears in this area are vertical and strike N30-37E and have slickensides indicating latest left lateral strike-slip motion.

At outcrop locality 732-8 (NW 1/4 sec. 35, T. 4 N., R. 8 W.) nearly vertical shears strike N46-64W and have stepped slickensides consistent with latest oblique left lateral strike-slip motion. This fault controls the northwest-southeast course of the Nehalem River over a 1.6 km segment and has been mapped as a continuation of the Cronin Creek fault on the basis of similar orientation and sense of displacement.

The Cronin Creek fault offsets God's Valley fault in a left lateral sense and terminates Sweet Home Creek fault (Plate I). Approximately one kilometer of left lateral horizontal separation is indicated by the interpretation of God's Valley fault continuing east of the Cronin Creek fault (the God's Valley fault extension).

The Gales Creek fault mapped by Wells and Peck (1961) in the northeastern Oregon Coast range was extended farther to the northwest by Jackson (1983), Wells and others (1983) and Safley (in prep). It enters the southeast part of the study area near Camp Olson (SW 1/4 sec. 29, T. 4 N., R. 7 W.) and trends N50-70W across the entire map area (Plate I). Southeast of the thesis area this major structure controls the course of the North Fork of the Salmonberry River and forms prominent lineaments on aerial photographs and topographic maps. North of the Cole Mtn.-Quartz Creek fault, the Gales Creek fault is difficult to locate and it appears to die out approximately one km north of the study area. This suggests that significant strain may have been taken up by the Cole Mtn.-Quartz Creek fault (reactivation?).

Although no outcrop of the actual fault zone were observed in the thesis area, the location of the Gale's Creek fault south of the Quartz Creek fault is constrained by juxtaposition of different stratigraphic units. For instance, in the Spruce Run-Lost Lake area (sec. 17, T. 4 N., R. 7 W.) lower Roy Creek member conglomeratic

sandstone crops out less than one-half km from lower Jewell member
mudstones. This indicates roughly 200 m of vertical separation. A
right lateral sense of motion is indicated by offset of the Cole
Mtn.-Quartz Creek fault trend. Strike-slip movement is also suggested
by steeply dipping mudstones at outcrop locality 3630-1 (SE 1/4
sec. 17, T. 4 N., R. 7 W.) which have been affected by drag and strike
parallel to the fault.

Two small subparallel faults have been mapped 0.7 and 1.4 km
southwest of the Gales Creek fault. The closer one trends N50W down
the south fork of Spruce Run Creek. This fault is not exposed, but
its location is tightly constrained in the SE 1/4 sec. 20, T. 4 N.,
R. 7 W. where uplifted Tillamook Volcanics on the southwest side of
the south fork of Spruce Run Creek are juxtaposed against lower Roy
Creek member conglomeratic sandstone, which strikes into the
volcanics, on the northeastern side of the drainage (Plate I). The
location of this fault farther northwest is mapped on the basis of
on-trend topographic features such as a saddle in the NE 1/4 sec. 19,
T. 4 N., R. 7 W. and an unnamed on-trend tributary to the Nehalem
River in the SW 1/4 sec. 18, T. 4 N., R. 7 W.. Vertical separation is
estimated to be less than 20 meters. The other subparallel fault 1.4
km south of the Gales Creek fault also controls a N50W-trending stream
valley. The fault plane is exposed at outcrop locality 76-2 (SE 1/4
sec. 13, T. 4 N., R. 7 W.) where it strikes N70W and dips 58° SW.
Stepped slickensides indicate latest oblique left lateral strike-slip
motion. This opposite sense of displacement suggests that it may be
an antithetic fault to the right lateral Gales Creek fault.

A N20W-trending splay off the Gales Creek fault has been mapped
in sec. 20, T. 4 N., R. 7W.. The location of this suspected fault is
poorly constrained by sparse outcrops which require juxtaposition of
uplifted Roy Creek member sandstone and Sweet Home Creek member
mudstone. Throw on this fault is estimated to be less than 60 meters.

The Sunset Highway fault is located in the northeastern part of
the study area (Plate I and fig. 103). Stepped slickensides on shear
surfaces at outcrop locality 627-1 (NE 1/4 sec. 4, T. 4 N., R. 7
W.) in a Cole Mountain basalt sill strike N60W, are nearly vertical,
and indicate latest left lateral strike-slip motion. This fault

crosses US highway 26 near outcrop locality 371-1 (sec. 3 and 10, T. 4. N., R. 7 W.) where Sweet Home Creek member turbidites are juxtaposed against Sunset Highway member interbedded arkosic and basaltic sandstones, indicating approximately 70 meters of vertical separation. Drag along the fault has affected strata so that they strike is parallel to the fault.

The Cow Creek fault is located 3.7 km northeast of the Sunset Highway fault and controls the orientation of the Cow Creek drainage. A cliff outcrop at locality 3810-1 in Cow Creek, sheared Roy Creek conglomeratic sandstone is faulted against Tillamook Volcanics, creating a scenic waterfall. The fault zone strikes N60W and dips 79°NE. Mullion features suggest dominant dip-slip motion. However, the N60W orientation is consistent with other NW-trending strike-slip faults. The sense of offset of the Jewell Junction-Jewell Junction fault extension by the Cow Creek fault is left-lateral.

Stereonet of faults and fractures in the thesis area

Figure 104 is a contoured stereonet of 102 fault and fracture plane s-poles from the Elsie-lower Nehalem River area. It displays four point maxima which correspond to different fault sets in the thesis area. The greatest point density is associated with N30E-trending faults that dip steeply to the SE. Other maxima correspond to sets of high-angle faults trending N50E, N75E, and N60W. This agrees reasonably well with mapped faults (Plate I, figs. and 100 and 103), except that field observations and structural relationships indicate that NW- and east-west-trending faults are much more significant than NE-trending faults. This apparent discrepancy is probably due to crushing and alteration along east-west and northwest-trending major fault zones which renders them more susceptible to erosion and concealment in natural exposures than the small northeast-trending faults. However, N10E- to N30E-trending right lateral strike-slip faults (Reidel shears) are expected to preferentially form adjacent to dextral wrench faults (Freund, 1974), and the point maxima for N30E-trending faults and fractures is compatible with this expectation. The point maxima for the N75E and
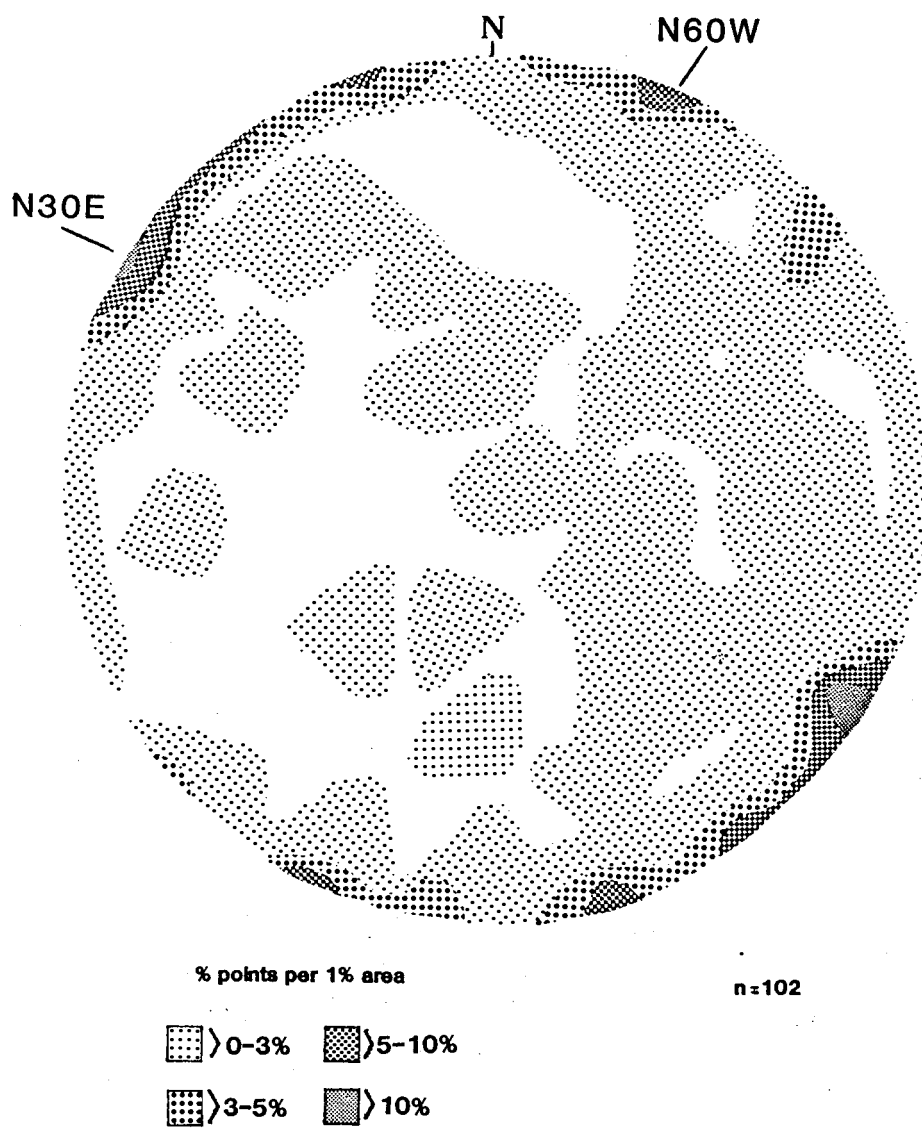
Figure 104.   Contoured stereonet of s-poles of 102 fault planes in the
Elsie-lower Nehalem River area.   Most faults strike N30E
and dip steeply SE.   Note submaxima of faults with N60W
strike and steep Ne and SW dips.

N70W-trending faults and fractures is compatible with that expected for antithetic left lateral strike-slip faults (conjugate Reidel shears) related to simple dextral shear (Wilcox and others, 1973).

REGIONAL TECTONICS AND PLATE ROTATIONS

Structural Setting of the Western Cordillera

Regional right-lateral shear of the western continental margin of North America with respect to adjacent oceanic plates of the Pacific basin was first proposed by Carey (1958) as a mechanism responsible for the fundamental structure of the western Cordillera. Subsequent paleomagnetic investigations in the western Cordillera demonstrated systematic discordance of paleomagnetic pole positions away from the expected reference pole for the stable North American continent for the Mesozoic and Tertiary into the general area of the Atlantic Ocean (Beck, 1976,1980). Various tectonic models have been proposed to account for the discordance, but a dextral shear mechanism is common to all of them (Beck,1980). These paleomagnetic studies indicate that the western Cordillera consists of a collage of allochthonous continental and oceanic fragments or microplates that have undergone accretion, rotation, and in some instances, significant northward translation since the Mesozoic (Atwater,1970; Beck,1976; Jones and others, 1977; Simpson and Cox,1977; Irving,1979; Stone and Packer,1979; Beck,1980; Bates and others,1981; Globerman and others,1982; Magill and others,1982; Schultz,1983; Beck,1984; Wells and others,1984; Wells,1984; Wells and Coe,1985). Understanding the mechanism(s) responsible for tectonic rotation is essential for paleogeographic reconstructions. In western Oregon and Washington, paleomagnetic pole positions indicate systematic clockwise rotation of the region without statistically significant northward transport (fig. 105; for an exception to this see Beck, 1984).

Paleomagnetic Investigations in Oregon and Washington

Oregon Coast Range

Cox (1957) first reported aberrant pole positions for the lower to middle Eocene Siletz River Volcanics of the Oregon Coast Range

Figure 105. Tectonic rotations of Tertiary rocks in the Pacific Northwest, grouped by age. (slightly modified from Wells, 1984). WASHINGTON: BH - Eocene Crescent Formation, Black Hills (Globerman and others, 1982); BP - Eocene volcanic rocks at Bremerton-Port Ludlow (Beck and Engebretson, 1982); CR - Frenchman Springs Member of the Wanapum Basalt of the Yakima Basalt Subgroup of the Columbia River Basalt Group (Simpson, Wells, and Bentley, unpublished data); GS - Miocene Snoqualmie batholith (Beske and others, 1973); GV1 - Goble Volcanics (Beck and Burr, 1979); GV2 - upper Eocene Goble Volcanics (Wells and Coe, 1985); PO1 - upper Miocene basalt of Pack Sack Lookout correlative with Pomona Member of the Saddle Mountains Basalt of the Yakima Basalt Subgroup of the Columbia River Basalt Group (Wells and others, 1982); PO2 - intracanyon Pomona Member of the Saddle Mountains Basalt of the Yakima Basalt Subgroup to the Columbia River Basalt Group (Wells, Simpson, and Beeson, unpub. data); SP - Eocene Sanpoil Volcanics (Fox and Beck, 1985); WH - Crescent Formation, Willapa Hills (Wells and Coe, 1985)

OREGON: CF - Eocene and Oligocene Clarno Formation (Beck, 1980); EI - Eocene intrusions (Beck and Plumley, 1980); G - Ginkgo Member of the Saddle Mountains Basalt of the Yakima Basalt Subgroup of the Columbia River Basalt Group (Sheriff, 1984); OI - Oligocene intrusions (Beck and Plumley, 1980); SR - Eocene Siletz River Volcanics (Simpson and Cox, 1977); TF - Eocene Tyee Formation (Simpson and Cox, 1977); TV - Eocene Tillamook Volcanics (Magill and others, 1981); WC1 and WC2 - Oligocene and Miocene volcanic rocks of the western Cascade Range (Magill and Cox, 1980); WC3 - Western Cascade Range Series of northern California (Beck and others, 1984); YB - upper Eocene Yachats Basalt (Simpson and Cox, 1977).

Figure 105.

PRE-ACCRETION ROCKS
(Mostly middle Eocene)

POST-ACCRETION ROCKS
(Mostly Eocene and Oligocene)

MIOCENE ROCKS

301a
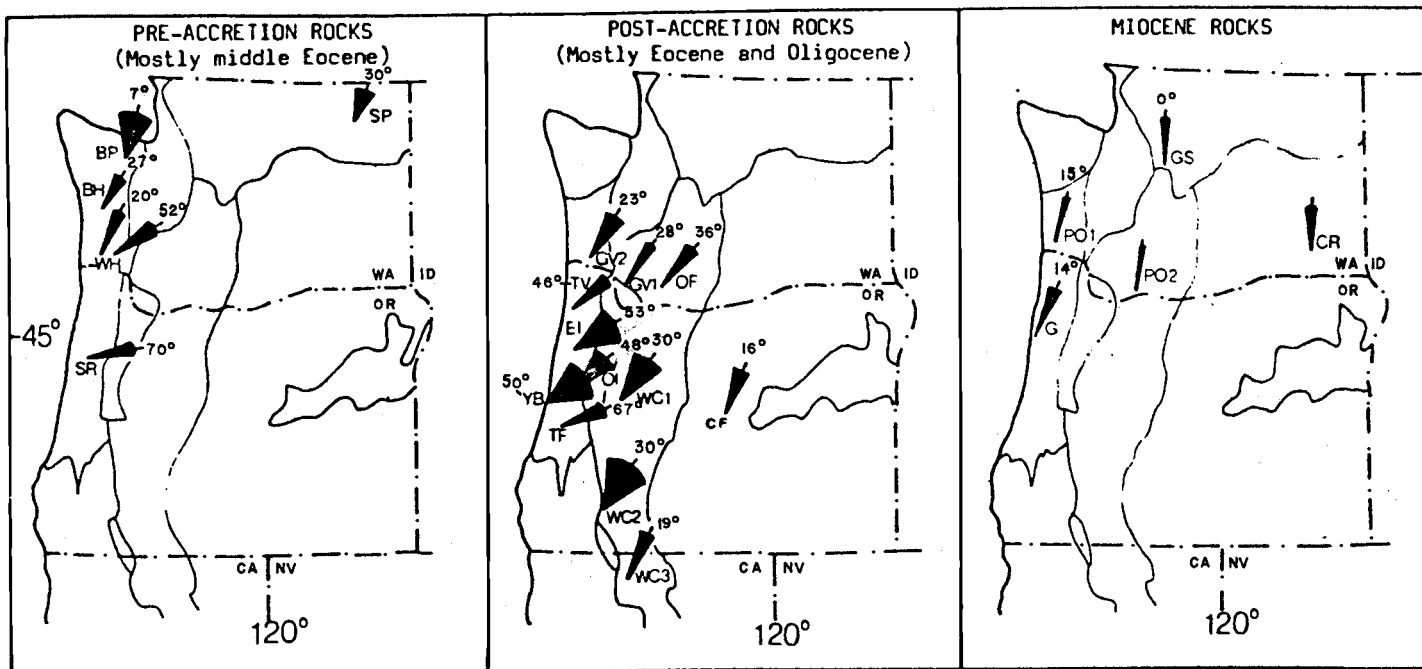
which indicated approximately 75° of clockwise rotation from the expected Eocene field direction. (However, he did not attribute the aberrant pole position to tectonic rotation at the time). Further paleomagnetic investigations were not pursued for about 20 years, when a better understanding of accretionary plate tectonics made rotation of the region seem reasonable and researchers began determining the size of rotated blocks, the timing of rotation, and proposing mechanisms of rotation.

Simpson and Cox (1977) investigated the lower to middle Eocene Siletz River Volcanics, sedimentary rocks of the early to middle Eocene Tyee and Flournoy formations, and the upper Eocene Yachats volcanic rocks of the Oregon Coast Range, and reported pole positions 50-70° east of the expected Eocene field direction. This confirmed Cox's earlier work and expanded the region of known rotation to a 225 km-long block extending from immediately north of the Klamath Mountains to beyond Newport, Oregon.

Magill and others (1981) determined 46° of clockwise rotation for the lower part of the Eocene Tillamook Volcanic Series which further extended the region of known rotation northward approximately 125 km north of Newport, into northern Tillamook County, Oregon.

Nelson (1985) conducted a preliminary study of the upper part of the upper Eocene Tillamook Volcanics and upper Eocene Cole Mountain basalt (one site in the study area of this investigation) in southern and central Clatsop County which indicated 48° of clockwise rotation. This is nearly identical with the clockwise rotation reported by Magill and others (1981) and extends the region of rotation still farther north almost to the Columbia River.

Washington Coast Range

Paleomagnetic studies of Tertiary rocks in the Washington Coast Range demonstrate significantly less clockwise rotation than correlative rocks in the Oregon Coast Range (Beck and Burr, 1979; Wells and Coe, 1980; Globerman and others, 1982; Wells and Coe, 1985). Wells and Coe (1985) conducted an investigation of the lower to middle Eocene Crescent Formation in southwest Washington

(correlative with the Siletz River Volcanics of the Oregon Coast Range) and interpreted local discordance of paleomagnetic directions to represent small block rotation between strike-slip faults. Gravity contours show sharp amplitude discontinuities which also indicate a more complicated and disrupted basement than is present in the Oregon Coast Range (Bromery and Snavely, 1964; Berg and Thiruvathukal, 1967).

Cascade Range

In 1979, initial investigations of Cascade Range rotation were undertaken in southwestern Washington. Beck and Burr (1979) determined 25° +/- 13° of clockwise rotation for the upper Eocene to Oligocene Goble Volcanic Series. They suggested that rotation of the may have been independent of the more rotated Oregon Coast Range. Bates and others (1979) reported 23° +/- 16° of clockwise rotation for the Oligocene Ohanapecosh Formation. Further paleomagnetic investigations of the Ohanapecosh and two other Oligocene Formations in southwestern Washington determined 35° +/- 14° of clockwise rotation (Bates and others, 1981).

Magill and Cox (1980) computed a post Oligocene average of 27° +/- 7° of clockwise rotation for the western Cascade Range from data reported by Beck (1962), Beck and Burr (1979), Bates and others (1979) and from their own study of Oligocene rocks the western Cascades of Oregon.

Post-Eocene kinematic histories of the Cascade Range in Oregon and Washington are evidently quite similar, but pre-Oligocene histories are different, indicating that these two regions were separate blocks prior to their accretion to the North American continent (Wells and Coe, 1985). The contact between these regions of differing early rotational histories is located near the Columbia River and is marked by a change in structural geometry as indicated by geophysical studies (Silver, 1978). Wells (1984) has stated that the course of the lower reach of the Columbia River appears to be at least partially fault controlled.

Discussion of Mechanisms for Tectonic Rotation

The three fundamental mechanisms proposed for tectonic rotation of the Pacific Northwest have been summarized by Wells (1984) and are depicted in figure 106. They are: 1) simple shear rotation; 2) rigid microplate rotation; and 3) microplate rotation during Basin and Range extension.

Simple Shear Rotation

Beck (1976; 1980) proposed that roughly equant crustal blocks or microplates caught in a dextral shear couple developed between the generally northward moving plates of the Pacific basin and the North American continent would rotate clockwise in a ball-bearing fashion (fig. 106a).

In a detailed investigation of Eocene volcanic rocks in southwestern Washington, Wells and Coe (1985) identified domains of rotation within fault blocks separated by major northwest- and northeast-trending faults. They observed a post-late Eocene fault pattern compatible with one described by Freund (1974) for regions caught in a shear couple along transcurrent fault zones. In this model strain is accommodated by a conjugate set of secondary strike-slip faults which differentially rotate in response to the external shear couple (fig. 106b). One set, called Reidel shears (R) forms at a low angle (10°-30°) to the transcurrent fault (Wilcox and others, 1973). Another set, called conjugate Reidel shears (R'), forms at a high angle (70°-90°) to the transcurrent fault (Wilcox and others, 1973). Either set of shears may be active under moderate shear strains, but it is the R' shears or faults that experience considerable clockwise rotation because they are more orthogonal to the external shear direction (Freund, 1974; see fig. 107). In the Pacific Northwest the right-lateral shear couple is thought to be created by partial coupling of the forearc region with oblique subduction of the Farallon plate (Wells and Coe, 1985) (Figs. 106a and 107).
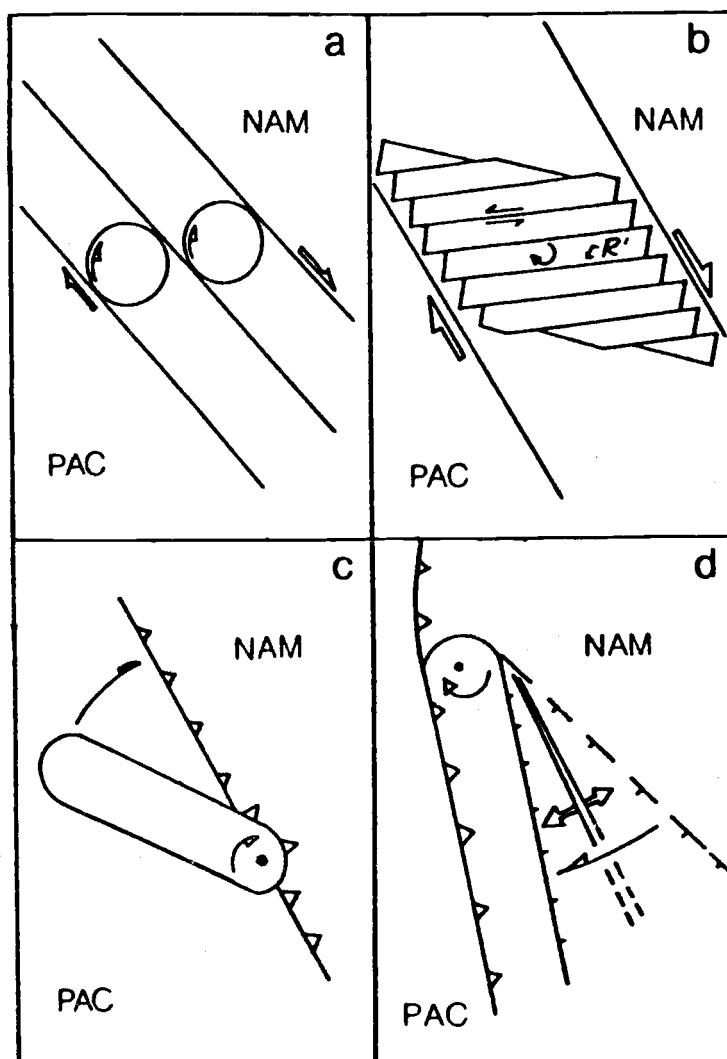
Figure 106. Proposed rotation models for terranes along the western
North American Continental margin. (From Wells, 1984).
a.) ball-bearing model of rotation for terranes caught
in a dextral shear couple.
b.) Rotation of elongate crustal slices bounded by
rotated sinistral R' Reidel shears associated with a
dextral shear couple. Also see Figure 107.
c.) Rigid microplate rotation during oblique subduction.
d.) rotation related to asymmetric extension in the
Basin and Range Province (back arc spreading).

Rigid Microplate Rotation

Simpson and Cox (1977) suggested that elongate blocks of microplates, such as a seamount chain, would rotate upon oblique collision with and subsequent accretion to the continent (fig. 106c). They presented two models for tectonic evolution of the Pacific Northwest. Model 1 proposes clockwise rotation of the block about a pivot point near its southern end during subduction beneath North America (fig. 106c). Model 2, which extended the block northward to include the Olympic Peninsula, proposed northeastward transport of the block, seaward shift of an early Eocene subduction zone caused by choking of the trench with anomalously thick oceanic crust, and southwestward rotation of western Oregon and Washington about a pivot near the Olympic Mountains due to continental rifting (e.g., back-arc spreading, see fig 106d). Magill and others (1981) refined and quantified this model of rotation with a two phase model of rigid plate rotation. Phase one postulates roughly 50° of clockwise rotation about a southern pivot prior to accretion of the Coast Range in the Eocene (50 m.y.b.p.). This is similar to Model 1 of Simpson and Cox (1977)(fig. 106c). Phase two calls upon 27° of post 20 m.y.b.p. rotation about a pivot point near the Washington/Oregon border as a result of Basin and Range extension (fig. 106d).

The idea that the Oregon Coast Range microplate, which extends from just north of the Klamath Mountains to the Columbia River, has behaved as a rigid block during Tertiary clockwise rotations has been advanced by many workers (Clark, 1969; Cox and Magill, 1977; Simpson and Cox, 1977; Beck and Plumley, 1980; Magill and others, 1981). These workers believe that internal coherence of the Oregon Coast Range block is indicated by similar amounts of rotation for coeval rocks in different parts of the Oregon Coast Range, the lack of observable deformation of laterally continuous sedimentary formations in the Coast Range (e.g., Tyee-Flournoy), consistent orientation of paleocurrent indicators recorded in turbidites within some formations (Snavely and others, 1964; Lovell, 1969), and a pronounced gravity high extending the length of the Oregon Coast Range block (Bromery and Snavely, 1964) that displays smooth contours indicative of undisrupted
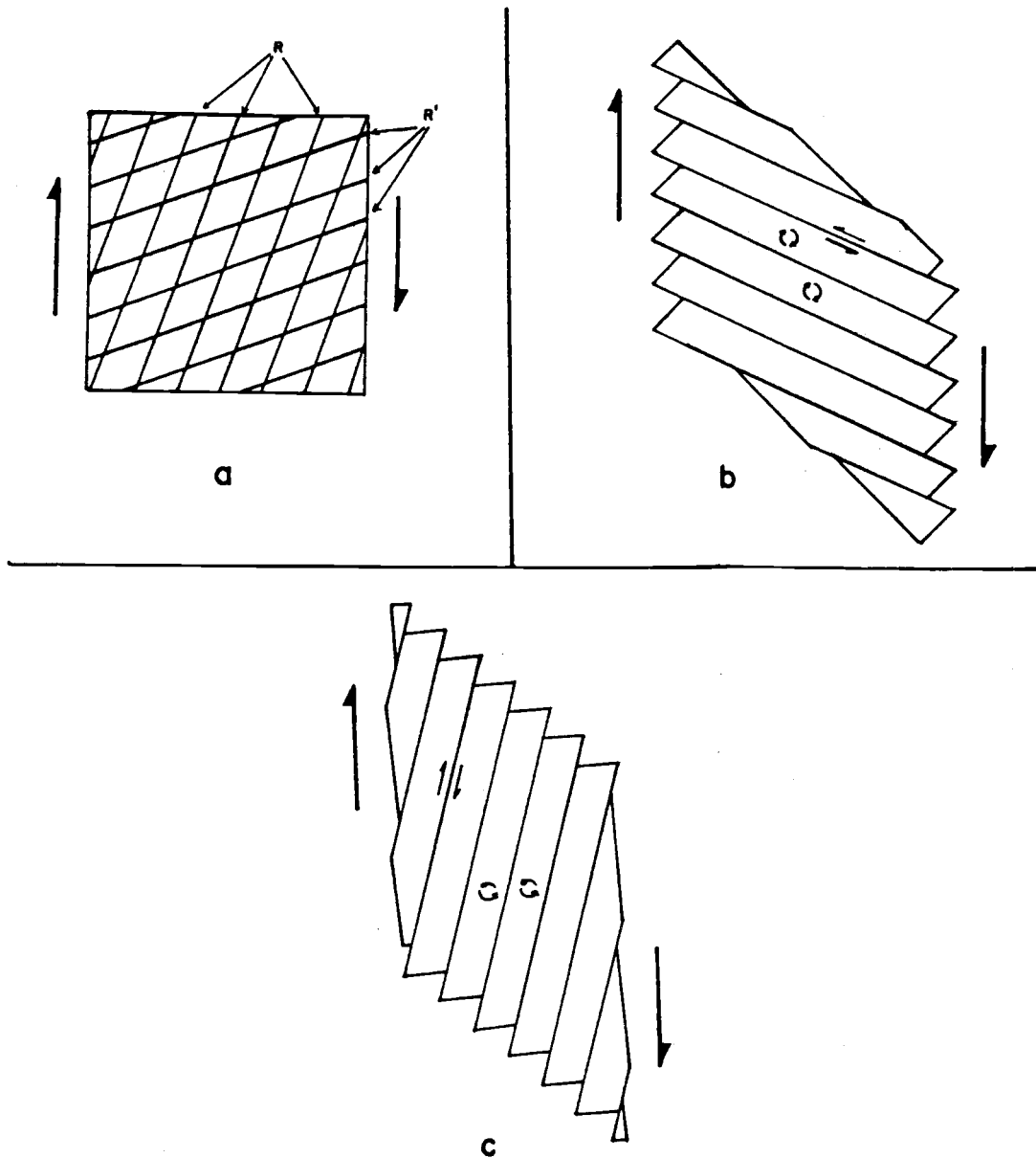
Figure 107. Simple shear model of Freund (1974).
　　　　　　a.) Initial orientation of R and R' Reidel shears
　　　　　　　　related to dextral shear couple.
　　　　　　b.) Substantial clockwise rotation of sinistral R'
　　　　　　　　shears and bounded elongate area with progressive
　　　　　　　　dextral shear.
　　　　　　c.) Limited counterclockwise rotation of R shears with
　　　　　　　　progressive dextral shear.

basement rocks. Recently, Wells and Coe (1985) have questioned the
rigid plate behavior of the Oregon Coast Range on a number of grounds.

<u>Microplate Rotation during Basin and Range Extension.</u>

Model 2 of Simpson and Cox (1977) suggested that the last 28° of
clockwise rotation of western Oregon and Washington took place about a
northern pivot near the Olympic Peninsula in response to asymmetric
late Miocene extension in the Basin and Range province. (See Figure
106d.) Magill and others (1981) revised this model by proposing 27°
of post 20 m.y. Basin and Range extension about a pivot point near
the Oregon and Washington border.

Discussion of Rotation Mechanisms

Wells (1984) and Wells and Coe (1985) argue that plate
reconstructions and tectonic rotations of western Oregon and
Washington are not compatible with the model of rigid microplate
rotation. They observed that post-accretion rotations of middle Eocene
units in the Oregon Coast Range are nearly as large as rotations in
the early to middle Eocene oceanic basement. Therefore, little, if
any rotation of the supposed rigid microplate occurred before
collision and accretion of the microplate to the North American
continent. Three related lines of evidence support their
contention: 1) plate motions are incompatible with formation of
basement rocks on an aseismic ridge (seamount province) and subsequent
rotation during docking and accretion (Wells and others, 1984); 2)
detailed analysis of basement rocks in the Washington Coast Range
(Crescent Formation) demonstrates that early deformation of these
rocks during docking against the continental margin preceded tectonic
rotation (Wells and Coe, 1985); and 3) the middle Eocene Tyee
Formation, which covers the contact between the Oregon Coast Range and
pre-Tertiary rocks of the Klamath Mountains, is only mildly deformed
but highly rotated. This requires docking of the microplate prior to
rotation, at least at the southern end of the Oregon Coast Range.
Wells and Coe (1985) favor the simple shear mechanism and suggest that

the Oregon Coast Range may be more significantly disrupted than is currently believed stating that "lack of faulting in western Oregon and Washington ... is only apparent, a result of dense cover and incomplete coverage of detailed geologic mapping". Snavely and Wagner (1964) made almost the same statement over 20 years earlier after preliminary field mapping in the Oregon Coast Range: "west to northwest trending faults with lateral separation (strike slip) may be more common than was previously recognized.".

If rotation of a rigid microplate during oblique collision with the North American continent is eliminated as a plausible rotation mechanism, simple shear and Tertiary extension in the Basin and Range province are left as viable mechanisms for rotations observed in Oregon and Washington (fig. 106d). Some constraints on the proportion of rotation due to these two mechanisms are provided by paleomagnetic directions recorded in rocks of the Clarno Formation in central Oregon. The Clarno Formation has been assigned to the Eocene and Oligocene. However, this time span Clarno may be the result of hasty field work and sampling procedures; the preferred age of the Clarno Formation is middle Eocene (Dr. Edward Taylor, OSU Dept. of Geology, personal communication, 1988). Rocks of the Clarno Formation appear to have been rotated clockwise only 16° relative to North America which precludes more that 30° of rotation in western Oregon due to Basin and Range extension (Wells, 1984). However, this apparent lower degree of rotation may be related to inappropriate sampling as some paleomagnetic investigations of the Clarno Formation reportedly have included highly altered rocks and even boulders in debris flows (Dr. Edward Taylor, OSU Dept. of Geology, personal communication, 1988). In any case, coeval and younger rocks in the Oregon Coast Range demonstrate nearly twice as much clockwise rotation which implies that small block rotation due to simple shear may be responsible for nearly half the observed rotations (Wells, 1984). Although tectonic rotation related to a simple shear model seems likely for southwestern Washington, not enough paleomagnetic data have been generated to evaluate the regional contribution of the mechanism.

Magill and others (1982) investigated correlative late Miocene volcanic rocks assigned to the basalt of Pack Sack Lookout in

southwestern Washington and the Pomona member of the Columbia River
Basalt Group east of the Cascade Range in Oregon and Washington.
These rocks are believed to represent erosional remnants of a single
12 m.y.b.p. flow. Their study provided evidence for progressive
clockwise rotation toward the coast ($16°$ in the Coast Range, $0°$ east
of the Cascade Range) which supports the model of simple shear
rotation for the western margin of Oregon and Washington proposed by
Wells and Coe (1985). Sheriff (1984) reported a nearly identical
amount of rotation ($14°$) for Ginkgo flows of the Wanapum Basalt
Subgroup of the Columbia River Basalt Group in western Oregon. The
boundary between the rotated and unrotated regions of Oregon and
Washington (at least during the past 12 m.y.) is coincident with the
active Cascade Range arc which makes it suspect locus of tectonic
decoupling (Magill and others, 1982).

GEOLOGIC HISTORY

The Siletz River Volcanics and Crescent Formation form the core of the Coast Range of northern Oregon and western Washington (Wells and others, 1983). These volcanics represent basaltic oceanic islands which were accreted to the North American continent by seafloor spreading and subduction during the middle Eocene (Wells and others, 1984). Accretion of the seamounts terrain and associated trench deposits (e.g., Umpqua Formation) is thought to have "plugged" the subduction zone, resulting in westward shift of the subduction zone and associated volcanic arc (Wells and others, 1984). In the developing forearc region a thick sequence of early to middle Eocene bathyal mudstones and delta-fed sandy turbidites (e.g., Yamhill Formation) were deposited over the accreted seamounts (Wells and others, 1984, Heller and Ryberg, 1983; Dott and Chan, 1983).

Volcanism in the developing late middle Eocene forearc produced a large volcanic island complex represented by the tholeiitic Tillamook Volcanics, which are the oldest rocks exposed in the thesis area. Major oxide analyses and petrographic characteristics from this study indicate that the Tillamook Volcanics were erupted in an extensional tectonic environment and that the upper part of the Tillamook Volcanics are highly fractionated.

Volcanic activity in northwestern Oregon rapidly lessened in the late middle Eocene, resulting in rapid cooling and associated thermal subsidence and transgression. The deepening, transgressive trend is marked by the following sequence of Narizian to early Refugian Hamlet formation lithologies: 1) basal basaltic conglomerates and sandstones (Roy Creek member) deposited around rocky headlands of the Tillamook Volcanics in a high energy, near shore environment; 2) micaceous, arkosic and lithic arkosic hummocky-bedded sandstones (Sunset Highway member) deposited on a storm-dominated shelf; 3) bioturbated, structureless to thin-bedded mudstones and thin turbidite sandstones (Sweet Home Creek member) deposited at bathyal depths on the outer shelf and upper slope. The micaceous arkosic sandstones of the Sunset Highway member represent a different and distinct provenance of continentally derived quartzo-feldspathic material delivered by an

ancestral Columbia River drainage to the shallow marine Hamlet basin.
Minor, local basaltic submarine debris flow deposits in the upper part
of the shallow marine Sunset Highway member attest to some intrabasin
contribution from topographically elevated, and possibly active,
volcanic edifices or islands. North and east of the thesis area a
thick sequence of arkosic, nearshore to shelf sandstones of the
Cowlitz Formation (as restricted by Wells, 1983 and Niem and Niem,
1985) were deposited during a late Narizian regression or progradation
of the "Cowlitz Delta" of southwest Washington. The Cowlitz sandstone
did not reach the thesis area but correlates to the upper part of the
bathyal Sweet Home Creek member mudstone. Coal beds in the Cowlitz
Formation, as well as the carbonaceous character of the underlying
Hamlet formation, indicate lush vegetation and subtropical climatic
conditions.

Emplacement of possible submarine flows and intrusions of the
calc-alkaline Cole Mountain basaltic andesite followed deposition of
the upper part of the Sweet Home Creek member and prior to deposition
of the Keasey Formation. The origin of this basaltic unit is not yet
known, but it may represent an "invasive" submarine facies of the
geochemically, petrographically, and stratigraphically correlative
Goble Volcanics to the east.

Disconformably overlying the Hamlet Formation, Cowlitz Formation,
and Cole Mountain basalt, is a thick sequence uppermost Narizian and
Refugian tuffaceous and locally glauconitic bathyal mudstones and
minor small arkosic sandstone channels and basaltic turbidites of the
Keasey Formation (Jewell member). The tuffaceous character and
presence of discrete tuff beds in the Keasey Formation records
explosive silicic volcanic activity in the developing calc-alkaline
Cascade arc to the east.

Flood basalts of the Columbia River Basalt Group were erupted on
the Columbia Plateau of eastern Oregon, southeastern Washington, and
western Idaho in the middle and late Miocene and flowed down the
ancestral Columbia River drainage to the Astoria embayment of
northwestern Oregon (Snavely and Wagner, 1963; Murphy, 1981). At the
interface with the marine environment the voluminous flows interacted
with less dense, unconsolidated and unlithified sediments to form

pillow-palagonite and pillow breccia complexes (Penoyer, 1977; Wells and Niem, 1987; Goalen, 1988). In the thesis area dikes and sills of two Grande Ronde Basalt petrologic types occur in host rocks that are interpreted to have been only partially lithified at the time of intrusion; this suggests that they, too, were emplaced through autoinvasive mechanisms.

Major uplift of coastal Oregon and Washington began in the late Miocene and is still continuing (Snavely and Wagner, 1963; Curt Peterson, OSU School of Oceanography, personal communication, 1988). This has resulted in the development of the Coast Range forearc ridge. Considerable erosion of rock units in the thesis area has taken place because of this uplift.

Numerous east-west-trending faults and conjugate high angle northwest- and northeast-trending strike-slip faults in the thesis area may be related to late Miocene to Pliocene north-south oriented compression and shear generated by oblique subduction and partial coupling of the Juan de Fuca plate with the North American plate (Wells and others, 1984). Major east-west-trending normal faults may be related to an earlier middle to late Eocene period of extensional tectonics, perhaps related to thermal subsidence and/or an increased angle of subduction.

ECONOMIC GEOLOGY

Introduction

The value of Oregon's mineral production between 1977 and 1987 is presented in Table 12. The table shows that rock materials (sand, gravel and crushed stone) generate the lion's share of mineral revenues, generally being about twice that of metals (primarily placer gold and nickel) and industrial minerals (e.g., limestone, pumice, diatomite). Of 595 active mine sites in the state in 1987, only 30 were involved in metals and industrial minerals with the remainder sand, gravel, and stone operations (Ramp, 1987). The table also reflects the 1979 discovery of the Mist Gas field, located in Columbia County approximately 16 km northeast of the thesis area, and production revenues in ensuing years.

Crushed Rock

Basaltic rocks, and particularly middle Miocene basalt intrusions of the Columbia River Basalt Group, are frequently quarried in northwestern Oregon. In the thesis area this material is locally utilized to macadamize logging roads. Outside the thesis area quarries supply rip-rap for use in jetties, stream bank reinforcements, and slump stabilization. Transportation costs dictate local utilization of crushed rock from quarries in Clatsop County. Major population centers in the Willamette Valley (i.e. Portland) are supplied with locally produced crushed rock and, therefore, do not rely on quarry operations in Clatsop County.

In the thesis area, Grande Ronde Basalt intrusions are fresher than other volcanic units and are best suited for use as road aggregate. Grande Ronde Basalt intrusions have been quarried on a small scale in several locations in the thesis area (e. g. west end of Flat Iron Mountain, junction of the August Fire Road and Lost Lake Road)(Plate I). A few quarries have also been developed in

MINERAL PRODUCTION OF OREGON

in millions of dollars

YEAR	ROCK MATERIALS	METALS AND INDUSTRIAL MINERALS	NATURAL GAS	TOTAL
1977	74	35	0	109
1978	84	44	0	128
1979	111	54	0	165
1980	95	65	12	172
1981	85	65	13	163
1982	73	37	10	120
1983	82	41	10	133
1984	75	46	8	129
1985	91	39	10	140
1986	96	30	9	135
1987	102	52	6	160

Table 11. Value of Oregon's mineral production in millions of dollars between 1977 and 1987. From Ramp (1988).

thick Cole Mountain intrusions for use as stream bank rip-rap (e.g. in Humbug Creek approximately 1 km south of Elsie along the lower Nehalem River road) and slump stabilization (along U.S. 26 east of the Quartz Creek bridge). In general, however, Cole Mountain basalt is extensively weathered (particulary the highly vesiculated upper part) and is not suitable for use as road aggregate. Because basalt intrusions in the area occur in areas predominantly underlain by mudstone, which drains poorly and is susceptible to slumping, dikes and sills suitable for quarrying are frequently exploited. The Tillamook Volcanics, which underlie the southern third of the thesis area are better drained and much less prone to slumping than sedimentary units in the area. Therefore, roads in this part of the thesis area are generally not macadamized. However, the unit has been locally quarried for logging road aggregate. Vesiculated flow tops and interstratified flow breccias of the Tillamook Volcanics are prone to weathering and are of marginal quality for roadbeds. Thick columnar jointed sills and dikes make the best road aggregate.

Hydrocarbon Resources and Potential

The Pacific Northwest remains a frontier area with regard to hydrocarbon exploration. The density of deep wells (¶5,000 m) in Cenozoic basins of the region is about one for each 1,000 km^2 so that the area largely remains be to adequately tested for hydrocarbon accumulations (Armentrout and Suek, 1985). The first discovery in Washington was the small Grays Harbor Ocean City field which produced about 12,000 bbls of high paraffin oil and some gas between 1946 and 1957 (Armentrout and Suek, 1985). In Oregon, approximately 80 years of hydrocarbon exploration came to fruition in 1979 with the discovery of commercial quantities of natural gas near Mist in Columbia County (Newton, 1979; Bruer, 1980). The Mist gas field is located approximately 16 km northeast of the thesis area. As of March, 1987 ARCO had 13 producing wells in the Mist gas field (Wermiel, 1987). Production from the field in 1986 totaled approximately 4.6 billion cubic feet with a value of about $9.2 million (Wermiel, 1987). Cumulative production from the Mist gas field through the end of 1986

was 27.9 billion cubic feet (Wermiel, 1987). Reservoir sandstones in the Mist area are micaceous arkosic sandstones of the middle to late Eocene Cowlitz Formation. Gas production has primarily been from the informal "Clark and Wilson" sand (or C and W sand), which has a porosity between 18 and 32% (average 25%) and permeability of 19 to over 1,500 millidarcies (average 200 millidarcies) (Armentrout and Suek, 1985).

A goal of this study was to correlate facies of the Cowlitz Formation exposed in the thesis area with the target sands in the Mist gas field. As explained in the nomenclature section of the Hamlet formation, arkosic sandstones positioned between the Tillamook Volcanics and Keasey Formation in the thesis area which previously had been included in the Cowlitz Formation (e.g. Warren and Norbisrath, 1945) have been reassigned to the Sunset Highway member of the Hamlet formation. These sandstones are older than Cowlitz Formation sandstones as defined by Wells (1981), Bruer and others (1984), and Niem and Niem (1985). Target sandstones of the Cowlitz Formation pinch out approximately 8 km northeast of the study area into bathyal mudstones of the Sweet Home Creek member, which overlies the Sunset Highway member (Rarey, 1986). Therefore, the C and W sandstone is not a potential exploration target in the thesis area.

Sandstones units in the thesis area are basaltic sandstones of the Roy Creek member, arkosic sandstones of the Sunset Highway member, thin arkosic sandstones in the Sweet Home Creek member, and small arkosic sandstone channels and very thin basaltic turbidites in the Jewell member. Thin section petrography and scanning electron microscopy show that Roy Creek member basaltic sandstones are tightly cemented with diagenetic clays (chlorite and nontronite) and zeolite (clinoptilolite-heulandite). These pore-filling cements have reduced the porosity to only a few percent which eliminates further consideration of these sandstones as hydrocarbon reservoirs.

Most of the arkosic sandstones of the Sunset Highway member are very fine-grained, silty, and contain a significant percent of swelling (smectite) clays. Point counted intergranular pore space amounts to only a few percent in these sandstones. These sandstones also have fair effective porosity (17.6%) but very low permeability

(0.88 md), probably due to diagenetic clays clogging pore throats (Safley, in prep.). Therefore, these sandstones are considered to be unsuitable reservoirs. The Sunset Highway member also contains a few very friable fine- to medium-grained well-sorted arkosic sandstones which have several percent porosity. Porosity and permeability of these relatively matrix free sandstones has been reduced by diagenetic smectite coats on detrital framework grains and authigenic potassium feldspar overgrowths. Interestingly, these sandstones also exhibit some secondary intraparticle porosity in plagioclase feldspar grains. These arkosic sandstones have the best potential for natural gas reservoirs in the thesis area but are not as attractive as Cowlitz Formation sandstones due to lower porosity (petrographically determined to be about 5% to 10%) and limited thickness (3 to 5 m). In addition, erosion has breached Sunset Highway member sandstones in the thesis area. Permeability studies of these sandstones have not been conducted. Washburne (1914, p. 49) reported natural gas escaping from "micaceous clay shale" exposed in the riverbed of the Nehalem River in the vicinity of Lukarilla which was mapped as Sunset Highway member in this study (plate I). The Gales Creek and Cole Mountain-Quartz Creek faults cross the Nehalem River in this area and it is possible that this observation is related to migration of natural gas from a relatively matrix free arkosic sandstone reservoir along fault and fracture planes. However, I did not see any evidence of this reported gas seep.

The Sunset Highway member is thought to be equivalent to the Clatskanie sand of the Yamhill Formation which underlies the C and W sand in the Mist field (Robert Deacon, personal communication, 1985 in Niem and Niem, 1985). Armentrout and Suek (1985) refer to this sand as the "lower Cowlitz sandstone" and state that it is a friable, low-porosity, nonpermeable sandstone in the Mist gas field. However, these workers may not have examined the cleaner sandstones in the unit. Therefore, parts of the Sunset Highway member may locally be viable exploration targets. Although there is a question regarding sufficient source of source rock beneath Sunset Highway member sandstones, juxtaposition of Sweet Home Creek and Jewell member mudstones by faulting could potential provide suitable source rock-

reservoir rock configurations.

Arkosic turbidite sandstones of the Sweet Home Creek member are thin, fine-grained, contain significant quantities of clays, are locally tightly cemented by carbonate, and have very low porosities. Total and effective porosities of two Sweet Home Creek member arkosic turbidite sandstones were determined by nuclear magnetic resonance. One sample of a turbidite sandstone (locality 371-1 along U.S. 26, T. 4 N., R. 7 W., SE 1/4 sec. 3) has a total porosity of 25.9% with an effective porosity of 14.2% (Terry Mitchell, personal communication to Dr. Alan Niem, 1984). The permeability of this sample (calculated from experimentally derived equations) is 0.71 md (Jill Schlaefer, written communication, 1984). Another Sweet Home Creek turbidite sandstone from locality 627-2 (T. 4 N., R. 7 W., SE 1/4 sec. 4), which is tightly cemented with carbonate (calcite) has a total porosity of 8.5% and an effective porosity of only 2% (Terry Mitchell, personal communication to Dr. Alan Niem, 1984). This sample has a calculated permeability of only 0.1 md. Therefore, these sandstones are clearly unattractive hydrocarbon reservoirs.

Arkosic sandstone channels in the Jewell member are small (less than 3 m thick and 3 to 5 m wide). Sandstone in the channels is fine-grained and contains substantial diagenetic clay matrix (Rarey, 1986). Basaltic Jewell member turbidite sandstones are very thin (2 to 4 cm) and are tightly cemented with diagenetic clays associated with abundant basaltic rock fragments. For these reasons Jewell member sandstones are not viable exploration targets.

Two samples of Sweet Home Creek member mudstone and one sample of lower Jewell member mudstone were analyzed for source rock geochemistry by AMOCO Production Company. Samples were collected from fresh stream cut, road cut, and landslide scarps. The analytical results are presented in Table 13.

According to Dickey and Hunt (1972), a potential source rock must have a minimum TOC of 0.5 wt. percent. All three mudstone samples have TOC values well above this minimum.

Law and others (1984) showed that organic matter in source rocks of Oregon and northern California is predominantly type III kerogen (i.e., terrestrial, woody debris) and that "better" source rocks were

Table 12. Source Rock Geochemistry of selected mudstone samples.

Sample Locality	% TOC	V.R. % RO	Visual Kerogen Type	Kerogen Kerogen	Generation Stage of TypeRating Diagenesis Oil/Gas
371-1[1]	1.2	0.50		S	GasNon-source Pre-Gener.
716-9[1]	0.9	**		*	GasNon-source Pre-Gener.
3715-2[2]	1.1	**		*	GasNon-source Early Peak Gas

S = Structured
[1]Sweet Home Creek member
[2]Jewell member

capable of generating gas but little or no oil. Samples from the thesis area also have kerogen types that can produce gas but little or no oil. Type III kerogen has bee widely reported from late Eocene and younger strata in northwestern Oregon (e. g. Armentrout and Suek, 1985; Goalen, 1988).

Armentrout and Suek (1985) concluded that gas in the Mist field was thermogenically generated because it is isotopically light (C in methane -42.5 to -43.8) and has ethane values typical of thermally generated hydrocarbons. Armentrout and Suek (1985) utilized Lopatin plots to predict the maturation behavior of potential source rocks and concluded that potential source beds in the Cowlitz Formation and underlying strata in the northern Willamette basin could produce such hydrocarbons if buried to depths of at least 3,000 m. However, these workers reported that samples of potential source rocks from the Cenozoic sequence exposed along the Canyon River in the Grays Harbor basin of southwest Washington, which are considered to be representative of potential source rocks near the Mist gas field, are thermally immature (R_o 0.5%) despite having been buried to depths of 3,000 m. These workers predicted gas generation at shallower burial depths in areas affected by higher heat flow. Potential source rocks in the Hamlet formation, Keasey Formation, Smuggler Cove formation and Astoria Formation are buried to depths of at least 3,000 m in the Astoria basin of western Clatsop County (Niem and Niem, 1985). If the source rock maturation predictions of Armentrout and Suek are correct,

then these rocks are potential gas sources.

Summer and Verosub (1987) showed that sediment maturation profiles in the Pacific Northwest are unusually steep and concluded that the dominant maturation process is due to elevated geothermal gradients related to hydrothermal fluids associated with volcanic activity. These workers concluded that vitrinite reflectance data from the region cannot be interpreted by conventional methods such as Lopatin plots, which is based on a calculated time-temperature interval, because of short-term thermal perturbations which would overprint the maturation data. This suggests that the source rock maturation predictions of Armentrout and Suek (1985) may be incorrect.

According to Reverdatta and Melenevskii (1983), "significant" quantities of thermogenic gas can be generated from immature mudstones by heating associated with dike and sill emplacement. Niem and Niem (1985) showed that thick, gabbroic sills of middle Miocene Grande Ronde Basalt in the Astoria basin caused thermal maturation of several hundred meters of overlying Jewell member mudstone (fig. 108). Similarly, a sample collected approximately 10 m below a thick (approximately 30 m) Grande Ronde Basalt intrusion in the thesis area (locality 3715-2, T. 4 N., R. 7 W., SE 1/4 sec. 17) was rated as "early peak gas" with regard to stage of diagenesis. Intrusions have also been linked to thermal maturation of Sweet Home Creek member mudstones in Clatsop County (Safley, in prep.). These findings support the maturation hypothesis or Summer and Verosub (1987). The Cowlitz Formation of northwestern Oregon and southwestern Washington also contains thick coal beds which may have served as in situ hydrocarbon sources for adjacent sandstones, rendering other source rocks unnecessary. Intrusions in these area could generate enough local heat to produce gas for the Mist field.

Washburne (1914) was probably the first to report hydrocarbon generation in the Pacific Northwest related to basaltic intrusions. He reported a "chunk of dull black hydrocarbon" in an area of "Astoria shale and intrusive basalt" near Knappton, Washington, "black, shiny, brittle hydrocarbon" infilling vesicles in a weathered vesicular basalt on the north shore of the Youngs River near Astoria, Oregon, and similar material "in pores on the east margin of the large dike in

Thermal Maturation (R$_O$)

Boise Cascade 11-14 well
thermally immature
equivalent & older
Paleogene strata

Crown Zellerbach 31-17 well
Paleogene strata thermally
matured by underlying
gabbroic sills

thick gabbroic sills
in CZ 31-17 well
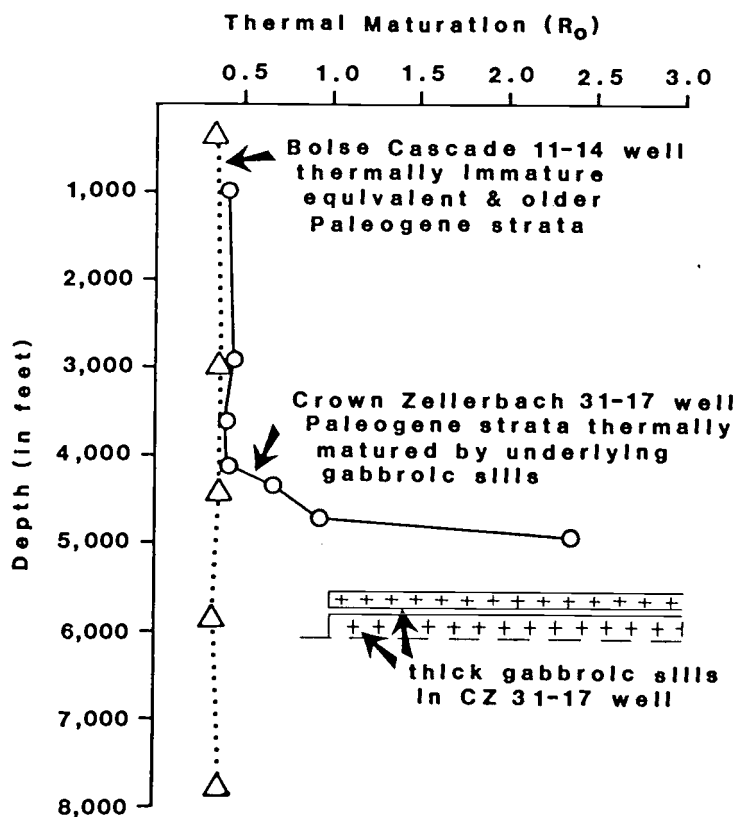
Figure 108. Thermal maturation (R$_O$) of Jewell member mudstone in the CZ 31-17 well related to thick middle Miocene sills. Note equivalent age strata in the Boise Cascade 11-14 well are thermally immature and are not associated with intrusions. From Niem and Niem, 1985.

the southwestern part of Ilwaco, Wash., near the shore of Columbia
River". The author found identical amygdule-forming asphaltic
hydrocarbons in Goble Volcanics near Woodburn, Washington and has seen
similar hydrocarbon retorting associated with intrusions in tuffaceous
and carbonaceous Tertiary sandstones at Shale City in southwestern
Oregon (Jackson County).

In any case, it seems likely that gas in the Mist gas field was
produced by thermal maturation of source rocks caused by basaltic
intrusions. Because intrusions of the late Eocene Cole Mountain
basalt and Goble Volcanics and middle Miocene Columbia River Basalt
Group are quite common in the region, further hydrocarbon exploration
based on the model of the Mist gas field is warranted. Thick sections
of late Eocene deltaic arkosic sandstones, which are widespread on
both sides of the Cascade Range in northern Oregon and southern
Washington, are the most attractive exploration targets in the region.
Initial exploration of these potential reservoirs should include the
identification of structural and stratigraphic traps similar to those
of the Mist gas field.

Mineralization

Two distinct systems of mineralization were identified in the
thesis area. One consists of quartz-carbonate-sulfide veins in shear
zones. The other is thought to be related to hydrothermal alteration
associated with Cole Mountain basalt intrusions.

A partially caved adit is located immediately east of the thesis
area near the Quartz Creek bridge along U.S. 26 in the vicinity of the
confluence of the north and south forks of Quartz Creek (T. 4 N., R. 7
W., center section 11). The adit explores thin veins (10 to 20 cm-
thick) of quartz-carbonate-sulfide mineralization in the approximately
15 m-wide shear zone of the Quartz Creek fault. Gouge in the shear
zone consists of Roy Creek member basaltic sandstone and conglomerate
and brecciated basalt flows of the Tillamook Volcanics. Pyrite is the
dominant sulfide and is associated with a small amount of
arsenopyrite. Quartz Creek probably was named for sparry vein-filling
quartz in the drainage which has weathered out from this mineralized

fault zone.

Timmons (1981) related this mineralization to a hydrothermal system associated with emplacement of a thick intrusion (Cole Mountain basalt) exposed approximately 100 m east of the Quartz Creek bridge. Geologic relationships in the thesis area demonstrate that this is incorrect. Mineralization in the shear zone of the Quartz Creek fault must post-date emplacement of the intrusion because the Cole Mountain-Quartz Creek fault offsets Cole Mountain basalt in the western part of the thesis area (Plate I). Similar mineralization in the Tillamook Volcanics is exposed further west along the Quartz Creek fault at the base of the August Fire road measured section (T. 4 N., R. 7 W., NE 1/4 sec. 16) and in sheared Tillamook Volcanics and Roy Creek member basaltic sandstone along the Jewell Junction fault extension in Cow Creek (T. 4 N., R. 7 W., NE 1/4 sec. 3). Neither of these areas is spatially associated with intrusions of Cole Mountain basalt. It is probable that similar mineralization is present along other major east-west-trending faults in the area.

A sample of quartz-carbonate-sulfide vein material taken from the mineralized Quartz Creek fault zone at the base of the August Fire road measured section was geochemically analyzed by Bondar-Clegg & Co., Ltd. in Vancouver, B. C.. Results of the analysis are as follows: 56 ppm Cu, < 5 ppm Pb, 100 ppm Zn, 14 ppm Mo, 1172 ppm As, 0.6 ppm Ag, and <5 ppb Au. Except for arsenic, none of these metals appears to be present in anomalous concentrations. Safley (in prep.) has obtained similar results for samples from the mineralized shear zone under the Quartz Creek bridge. This limited sampling indicates that these mineral occurrences do not contain economically attractive concentrations of metals and, therefore, are not considered to be viable exploration targets.

A second type of mineral occurrence in the thesis area is associated with Cole Mountain basalt intrusions. Supergene chrysocolla in fractured Jewell member mudstone near the basal contact of an overlying Cole Mountain basalt intrusion was found in the northwestern part of the thesis area (locality 910-13, T. 4 N., R. 8 W., NW 1/4 sec. 22). The chyrsocolla probably formed through weathering and supergene concentration of hydrothermally deposited

sulfides in the Cole Mountain basalt. Disseminated pyrite in chalcedonic silica nodules associated with pillowed Cole Mountain basalt has been found in widely scattered localities in Clatsop and Columbia counties (Timmons, 1981; Berkman, in prep., this study). However, the hydrothermal system which deposited the sulfides is thought to be very localized because rocks in the mineralized areas are not obviously bleached or silicified. A sample of the supergene chrysocolla mineralization was sent to Bondar-Clegg & Co., Ltd, Vancouver, B.C. for geochemical analysis. Results of the analysis are: 20,000 ppm Cu (21.6%), 166 ppm Pb, 29 ppm Zn, 212 ppm Mo, 165 ppm As, 50 ppm Ag (3.5 opt), and 500 ppb Au. This analysis confirms the copper-rich nature of the sample (chrysocolla) and indicates that all elements except Zn are present in anomalous concentrations. The copper, silver, and gold values are particularly interesting but are almost certainly related to supergene enrichment.

Timmons (1981) reported pyrite, bornite, quartz, and arsenopyrite concentrated in veins and fractures associated with brecciated margins of subaqueous flows of the Goble Volcanics (which are geochemically, petrographically, and stratigraphically equivalent to the Cole Mountain basalt; Rarey, 1986) in the Columbia County Quarry. Therefore, copper mineralization associated with these equivalent volcanic units has been reported from widely spaced localities (e.g. Timmons, 1981; this study) but it is not a universal association. For example, Rarey (1986) mapped widespread intrusions of Cole Mountain basalt but did not report any mineralization associated with the unit. The mineralized outcrop in the thesis area is quite small (§2 m across) and was the only one of its kind observed in the thesis area. Although the geochemical values of the analyzed sample are quite interesting and warrant some follow-up exploration, it is considered highly unlikely that economic reserves of any metal will be found in this area.

Lucia (1953) recounted the tale of the Lost Indian mine which is fabled to be a great gold deposit in the Coast Range mountains of northwestern Oregon. According to Indian legend, directions to the mine from the northern Oregon coast are "Go three suns to the white, white mountain. Where water runs to a lake in a black canyon you will

find it" (Lucia, 1953, p. 2). Indians reportedly brought gold nuggets from a mine in the area that is now the Tillamook Burn country and used it in trading and commerce along the coast and in the Willamette Valley (Lucia, 1953). Efforts by many settlers and explorationists to find this deposit have been fruitless.

Although the basaltic pile of the Tillamook Volcanics would appear to be an unlikely host for a gold deposit, mineralization associated with hydrothermal alteration is possible. Wells and others (1983) outlined areas of silicic volcanic rocks (andesites and dacites) in the Tillamook Volcanics which could potentially be associated with such a mineral deposit. These silicic rocks, and rare associated ash flows, are thought to represent highly differentiated magmas produced by fractional crystallization (Snavely, personal communication, 1987). If this is indeed the case, then there is no reason to suspect a link with mineralization. Alternatively, these rocks may represent more basaltic rocks which have been hydrothermally altered and silicified, a scenario is much more likely to be associated with mineralization. Numerous faults are present in the Tillamook Volcanics, and some have been mineralized by hydrothermal fluids (e.g. along the Quartz Creek fault in the thesis area). Therefore, one could speculate that larger-scale hydrothermal alteration and silicification may have occurred in more highly fractured rocks situated in a fault zone. Although this hypothetical geologic setting explains the possibility of a mineralizing system, it does not provide an adequate explanation for the ultimate source of the gold reported in the Tillamook Highlands. In any case, those afflicted with "gold fever" who choose to search for the metal in the northern Oregon Coast Range would be wise to investigate mapped faults in silicic volcanic rocks of the Tillamook Volcanics as a primary exploration target.

REFERENCES CITED

Addicot, W. O., 1976, Neogene molluscan stages of Oregon and Washington in Fritsche, A. E. et al., eds., Neogene Symposium: Soc. Econ. Paleon. Min., Pacific Sec., San Francisco, California, April, 1976, p. 95-115.

Addicott, W. O., 1981, Significance of pectinides in Tertiary biochronology of the Pacific Northwest: Geol. Soc. Am. Spec. Pap. 184, p. 17-37.

Augustithis, S. S., 1978, Atlas of the textural patterns of basalts and their genetic significance: Amsterdam, Elsevier Scientific Publishing Co., 323 p.

Al-Azzaby, F. A., 1980, Stratigraphy and sedimentation of the Spencer Formation in Yamhill and Washington counties, Oregon: unpub. M.S. thesis, Portland State Univ., Oregon, 104 p.

Alger, M. P., 1985, Geology; in Olmstead, D. L., Mist Gas field: exploration and development, 1979-1984: Oregon Dept. of Geology and Min. Ind. Oil and Gas Invest. 10, p. 6-9.

Anderson, J. L., 1978, The stratigraphy and structure of the Columbia River Basalt in the Clackamas River drainage: unpub. M.S. thesis Portland State Univ., Oregon, 136 p.

Anderson, J. L., Beeson, M. H., Bentley, R. D., Fecht, K. R., Hooper, P. R., Niem, A. R., Reidel, S. P., Swanson, D. A., Tolan, T. L., and Wright, T. L., 1987, Distributions maps of stratigraphic units of the Columbia River Basalt Group; in Schuster, J. E., ed., Selected papers in the geology of Washington: Washington Department of Natural Resources Bull 77., p. 183-195.

Armentrout, J. M., 1981, Correlation and ages of Cenozoic chronostratigraphic units in Oregon and Washington: Geol. Soc. Amer. Spec. Pap. 184, p. 137-148.

Armentrout, J. M., Hull, D. A., Beaulieu, J., D. and Rau, W. W., 1983, Correlation of Cenozoic stratigraphic unit of western Oregon and Washington: Oregon Dep. Geology and Mineral Industries, Oil and Gas Invest. 7, 90 p. and 1 chart.

Armentrout, J. M., McDougall, K. A., Jefferis, P. T., and Nesbitt, E., 1980, Geologic field trip guide for the Cenozoic stratigraphy and late Eocene paleoecology of southwestern Washington, in Oles, K. F. et al., eds.: Oregon Dept. Geol. Min. Ind. Bull. lol, p. 79-119.

Armentrout, J. M. and Suek, D. H., 1985, Hydrocarbon exploration in western Oregon and Washington: Amer. Assoc. Pet. Geol. Bull., v. 69, p. 627-643.

Atwater, Tanya, 1970, Implications of plate tectonics for the Cenozoic tectonic evolution of western North America: Geol. Soc. Amer. Bull., v. 81, p. 3513-3536.

Baldwin, E. M., 1976, 1981, Geology of Oregon: Dubuque, Kendall/Hunt Publ. Co., 170 p.

Barnes, M. A. W., 1981, The geology of Cascade Head, an Eocene volcanic center; unpub. M.S. thesis, Univ. of Oregon, Eugene, 94 p., map.

Bates, R. G., Beck, M. E., Jr., and Burmester, R. F., 1981, Tectonic rotations in the Cascade Range of southern Washington: Geology, v. 9, p. 184-189.

Bates, R. G., Beck, M. E., and Simpson, R. W., 1979, Preliminary paleomagnetic results from the southern Cascade Range of southwestern Washington (abs.), EOS Trans. AGU, v. 60, p. 816-817.

Beaulieu, J.D., 1973, Environmental geology of inland Tillamook and Clatsop counties, Oregon: Oregon Dept. Geol. Min. Ind. Bull. 79, 65 p.

Beck, M. E., Jr., 1962, Paleomagnetism of a thick Tertiary volcanic sequence in northern California: Rep AFCRL 62-821, U. S. Air Force Cambridge Res. Lab., 45p.

Beck, M. E. Jr., 1976, Discordant paleomagnetic pole positions as evidence of regional shear in the western Cordillera of North America: Amer. Jour. Sci., v. 276, p. 694-712.

Beck M. E. Jr., 1980, Paleomagnetic record of plate-margin tectonic processes along the western edge of North America: Jour. Geophys. Res., v. 85, p. 7115-7131.

Beck, M. E., Jr., 1984, Has the Washington-Oregon coast Range moved northward?: Geology, V. 12, P. 733-740.

Beck M. E. Jr. and Burr, C. D., 1979, Paleomagnetism and tectonic significance of the Goble Volcanic Series, southwestern Washington: Geology, v. 7, p. 175-179.

Beck, M. E., Jr., and P. W. Plumley, 1980, Paleomagnetism of intrusive rocks in the Coast Range of Oregon: microplate rotations in middle Tertiary time: Geology, v. 8, p. 573-577.

Beck, M. E., Jr. and Engebretson, D. C., 1982, Paleomagnetism of small basalt exposures in the West Puget Sound Area, and speculations on the accretionary origin of the Olympic Mountains: Jour. Geophys. Res., V. 87, no. B5, p. 3755-3760.

Beck, M. E., Jr., Burmester, R. F., Craig, D. E., Gromme, C. S., and Wells, R. E., 1986, Paleomagnetism of middle Tertiary volcanic rocks from the Western Cascade Series, northern California: timing and scale of rotation in the southern Cascades and Klamath Mountains: Jour. Geophys. Res., v. 91, p. 8219-8230.

Beeson, M. H. and Tolan, T. L., 1985, Regional correlations within the Frenchman Springs Member of the Columbia River Basalt Group: New insights into the middle Miocene tectonics of northwestern Oregon: Oregon Geology, v. 47, p. 87-92.

Beeson, M. H. and Morran, M. R., 1979, Columbia River Basalt Group stratigraphy in western Oregon: Oregon Geology, v. 41., no. 1, p. 11-14.

Beeson, M. H., Perttu, R. and Perttu, J., 1979, The origin of the Miocene basalts of coastal Oregon and Washington: An alternative hypothesis: Oregon Geology, v. 41, no. 10, p. 159-166.

Bently, R. D., 1977, Stratigraphy of the Yakima Basalt and structural evolution of the Yakima ridges in the western Columbia Plateau, in Brown, E. H., and Ellis, R. C., eds., Geological excursions in the Pacific Northwest: Bellingham, Western Washington Univ. Press, p. 339-389.

Berkman, T., M. S. candidate, OSU Dept. of Geology, Corvallis, OR

Berg, J. W. Jr., Tremble, L.,, Emilia, S. A., Hutt, J. R., King, J. M., Long, L. T., McKnight, W. R., Sarmah, S. K., Souders, R., Thiruvathukal, J. V., and Vossler, D. A., 1966, Crustal refraction profile, Oregon Coast Range: Seismol. Soc. Amer. Bull., v. 56, p. 1357-1362.

Bergrren, W. A., Kent, D. V., Flynn, J. J., and Van Couvering, J. A., 1985, Cenozoic geochronology: Geol. Soc. Amer. Bull., V. 96, no. 11, p. 1407-1418.

Beske, s. J., Beck, M./ E., Jr., and Noson, L., 1973, Paleomagnetism of the Miocene Grotto and Snoqualmie batholiths, central Cascades, Washington: Journal of Geophy. Res, v. 78, p.1 2601-2608.

Best, M. G., 1982, Igneous and metamorphic petrology: San Francisco, W. H., Freedman and Co., 630 p.

Blatt, H. E., Middleton, G. V., and Murray, R. C., 1980, Origin of sedimentary rocks: Prentice-Hall, New Jersey, 782 p.

Bluck, B. J., 1967, Sedimentation of beach gravels: Examples from South Wales: Jour. Sed. Pet., v. 37, p. 128-156.

Bourgeois, J., 1980, A transgressive shelf sequence exhibiting hummocky stratification: the Cape Sebastian Sandstone (Upper Cretaceous), southwestern Oregon: Jour. Sed. Pet., v. 50, p. 681-702.

Bridges, P. H., 1975, The transgression of a hard substrate shelf: the Llandovery (lower Silurian) of the Welsh borderland: Jour Sed. Pet., v. 45, p. 79-94.

Bromery, R. N., and Snavely, P. D., Jr., 1964, Geologic interpretation of reconnaissance gravity and aeromagnetic surveys in northwestern Oregon: U. S. Geol. Survey Bull., 1181-N, p. N1-N13.

Bruer, W. G., Alger, M. P., Deacon, R. J., Meyer, H. J., Portwood, B. B., and Seeling, A. F., 1984, Correlation section 24, northwest Oregon: Amer. Assoc. of Petrol. Geol. Pacific Sec., chart.

Bukry, D., Micropaleontologist, U.S. Geol. Survey, La Jolla Marine Geology Laboratory (A-015), La Jolla, CA, written communication, May 1, 1984.

Bukry, D., 1973, Low-latitude coccolith biostratigraphic zonation, in Edgar, N. T., Saunders, J. B., and others, eds., Initial reports of the Deep Sea Drilling Project, v. 15: Washington, D.C.., U.S. Government Printing Office, P. 685-703.

Bukry, D., 1975, Coccolith and silicoflagellate stratigraphy, north-western Pacific Ocean, Deep Sea Drilling Project 32, in Larson, R. L., Moberly, R., and others, eds., Initial reports of the Deep Sea Drilling Project, v. 32, Washington, D.C., U.S. Government Printing Office, p. 677-701.

Bukry, D., 1981, Pacific Coast coccolith stratigraphy between Point Conception and Cabo Corrientes, Deep Sea Drilling Project, Leg 63, in Yeats, R. S., Hag, B. U. et al., eds.: Initial reports, Deep Sea Drilling Project, Leg 63, Washington, D. C., U.S. Government Printing Office, p. 445-472.

Burns, L. K. and Ethridge, F. G., 1979, Petrology and diagenetic effects of lithic sandstones: Paleocene and Eocene Umpqua Formation, southwest Oregon, in Scholle, P. A. and Schluger, R. R., eds., Aspects of diagenesis: Soc. Ec. Paleon. Min. Sp. Pub. 26, p. 307-318.

Burr, C. D., 1978, Paleomagnetism and tectonic significance of the Goble Volcanics of southern Washington: unpub. M.S. thesis, Western Washington Univ., Bellingham, 66p.

Byerly, G. and Swanson, D., 1978, Invasive Columbia River Basalt flows along the northwestern margin of the Columbia Plateau, north-central Washington: Geol. Soc. Amer. Abstr. with programs, v. 10, p. 98.

Byrne, T., 1979, Late Paleocene demise of the Kula-Pacific spreading center: Geology, v. 7, p. 341-344.

Cameron, K. A., 1980, Geology of the south central margin of the Tillamook highlands; southwest quarter of the Enright quadrangle, Tillamook County, Oregon: umpub M.S. thesis, Portland State Univ., Oregon., 87 p.

Carey, S. W., 1958, The tectonic approach to continental drift, in Carey, S. W.,, ed., Continental drift - a symposium: Hobart, Australia, Univ. Tasmania, p. 177-358.

Carmichael, I., Turner, F., and Verhoogen, J., 1974, Igneous petrology: McGraw Hill, New York, 739 p.

Carter, J. W., 1976, The environmental and engineering geology of the Astoria Peninsula area, clatsop county, Oregon: unpub. M. S. thesis, Oregon State Univ., Corvallis, 138 p.

Chan, M. A. and Dott, R. H., Jr., 1983, Shelf and deep-sea sedimentation in an Eocene forearc basin, western Oregon - Fan or non-fan?: AAPG Bull., v. 67, p. 2100-2116.

Choiniere, S. R. and Swanson, D. A., 1979, Magnetostratigraphy and correlation of Miocene basalts of the northern Oregon coast and Columbia Plateau, southeast Washington: Jour. Amer. Sci., v. 279, p. 755-777.

Christiansen, R. L. and Lipman, P. W., 1972, Cenozoic volcanism and plate tectonic evolution of the western U.S., II. Late Cenozoic: Philos. Trans. R. Soc. London, Ser. A, v. 271 p. 249-284.

Clark, H. C., 1969, Remanent magnetism, cooling history, and paleomagnetic record of the Mary's Peak sill, Oregon: Jour. Geophys. Res., v. 74, p. 3143-3160.

Clifton, H. E., 1973, Pebble segregation and bed lenticularity in wave-worked vs. alluvial gravel: Sedimentology, v. 20, p. 173-187.

Coates, R. R., 1968, Basaltic andesites, in Hess, H. H., and Poldervaart eds., Basalts, vol. 1, John Wiley and Sons, New York, p. 689-736.

Conrad, T. A., 1849, Fossil shells from Tertiary deposits on Columbia River, near Astoria: Amer. Jour. Sci., ser. 2, v. 5., p. 432-433.

Cooper, D. M., 1981 Sedimentation, stratigraphy and facies variation within the early to middle Miocene Astoria Formation in Oregon: unpub. Ph.D. dissertation, Oregon State Univ., Corvallis, 433 p.

Coryell, G. F., 1978, Stratigraphy, sedimentation, and petrology of the Tertiary rocks in the Bear Creek-Wickiup Mountain-Big Creek area, Clatsop County, Oregon unpub. M.S. thesis, Oregon State Univ. Corvallis, 178p.

Cox, A. V., 1957, Remanent magnetization of lower to middle Eocene basalt flows from Oregon: Nature, v. 179, p. 685-686.

Cox, A. V., and Magill, J., 1977, Tectonic rotation of lower to middle Eocene basalt flows from Oregon (abstract): EOS Trans. Amer. Geophys. Union, v. 58, p. 1126.

Cox., K. G., Bell, J. D., and Pankhurst, R. J., 1979, The interpretation of igneous rocks: London, George Allen and Unwin, Ltd., 450 p.

Cressy, F. B., Jr., 1974, Stratigraphy and sedimentation of the Neahkahnie Mountain-Angora Peak area, Tillamook and Clatsop counties, Oregon: unpub. M.S. thesis, Oregon State Univ., Corvallis, 148 p.

Cushman, J. A. and Schenck, H. G., 1928, Two foraminiferal faunules from the Oregon Tertiary: Calif. Univ. Pubs., Dept. of Geol. Sci. Bull., v. 17, p. 305-324.

Dall, W. H., 1909, Contributions the the Tertiary paleontology of the Pacific coast, I. The Miocene of Astoria and Coos Bay, Oregon: U.S. Geol. Survey Prof. Pap. 59, 278 p.

Dana, J. D., 1849, Geological observations on Oregon and northern California: U.S. Explor. Exped., 1838-1842, under the command of Charles Wilkes: Geology, v. 10, chap. 17, p. 611-678, p.722-723, p. 729-730, atlas pls. 16, 17, 21.

Deacon, R. J., 1953, A revision of upper Eocene and lower Oligocene stratigraphic units in the upper Nehalem River basin, northwest Oregon: unpub. M.S. thesis, Oregon State Univ., Corvallis, 84 p.

Dickey, P. A., and Hunt, J. M., 1972, Geochemical and hydrogeologic methods of prospecting for stratigraphic traps: Amer. Assoc. of Petrol. Geol. Memoir 16, p. 137-167.

Dickinson, W. R. and Suczek, C. A., 1979, Plate tectonics and sandstone compositions: Amer. Assoc. Petrol. Geol. Bull., v. 63, p. 2164-2182.

Diller, J. S. 1896, Geological reconnaissance in northwestern Oregon: U.S. Geol. Survey 17th Ann. Rpt., p. 1-80.

Doell, R. R. and Cox, A., 1964, Determination of the magnetic polarity of rock samples in the field: U.S. Geol. Survey Prof. Pap. 450-D, p. 105-108.

Dott, R. H., Jr., and Bird, K. J., 1979, Sand transport through channels across an Eocene shelf and slope in southwestern Oregon, in Doyle, L. J. and Pilkey, O. H. Jr., eds., Geology of Continental Slopes: Soc. Econ. Paleon. Min. Spec. Pub. no 27, p. 247-264.

Dott, R. H., Jr. and Bourgeois, J., 1982, Hummocky stratification: significance of its variable bedding sequences: Geol. Soc. Amer. Bull., v. 93, p. 663-680.

Dougless, R. G. and Heitman, H. L., 1979, Slope and basin benthic foraminifera of the California borderland, in Doyle, L. J. and Pilkey, O. H. Jr., eds., Geology of Continental Slopes: Soc. Econ. Paleon. Min. Spec. Pub. no. 27, p. 247-264.

Duncan. R. A., 1982, A captured island chain in the Coast Range of Oregon and Washington: Jour. Geophys. Res., v. 87, no. B13, p. 10827-10837.

Einsele, G., 1982, Mechanism of sill intrusion into soft sediment and expulsion of pore water: Initial reports Deep Sea Drilling Project, Leg. 64, v. 64, p. 1169-1176

Einsele, G., Bieskes, J. M., and others, 1980, Intrusion of basaltic sills into highly porous sediments, and resulting hydrothermal activity: Nature, v. 283, no. 5746, p. 441-445.

Faure, G., 1977, Principles of Isotope Geology: John Wiley and Sons, Inc., Santa Barbara, CA., 464p.

Floyd, T. H. and Winchester, J. A., 1975, Magma type and tectonic setting discrimination using immobile elements: Earth Planet. Sci. Lett., v. 27, p. 211.

Folk, R. L., 1974, Petrology of sedimentary rocks: Austin, Texas, Hemphill Publishing Co., 182 p.

Folk, R. L., 1980, Petrology of sedimentary rocks: Austin, Texas, Hemphill Publishing Co., 182 p.

Folk, R. L. and Ward, W. C., 1957, Brazos River Bar: A study in the significace of grain size parameters: Jour. Sed. Pet., v. 27, p. 3-26.

Fox, K. F. and Beck, M. E., Jr., 1985, Paleomagnetic results for Eocene volcanic rocks from northeastern Washington and the Tertiary tectonics of the Pacific Northwest: Tectonic, v. 4, pt. 3, p. 323-341.

Freund, R. M., 1974, Kinematics of transform and transcurrent faults: Tectonophysics, v. 21, p. 93-104.

Friedman, G. M., 1962, Comparison for moment measures for sieving and thin section data in sedimentary petrologic studies: Jour. Sed. Pet., v. 32, p. 15-25.

Friedman, G. M., 1979, Address of the retiring president of the International Association of Sedimentologists; differences in size distributions of populations of particles among sands of various origins: Sedimentology, v. 26, p. 3-32.

Galloway, W. E., 1974, Deposition and diagenetic alteration of sandstone in northeast Pacific arc-related basins: implications for graywacke genesis: Geol. Soc. Amer. Bull., v. 85., p. 379-390.

Galloway, W. E., 1979, Diagenetic control of reservoir quality in arc-derived sandstones: Implications for petroleum exploration, in Scholle, P. A. and Schluger, R. R., eds., Aspects of Diagenesis: Soc. Econ. Paleon. Min. Spec. Pub. 26, p. 251-262.

Gaston, L. R., 1974, Biostratigraphy of the type Yamhill Formation, Polk County, Oregon: umpub. M.S. thesis, Portland State Univ., Oregon, 139 p.

Geist, D. J., McBirney, A. R., and Duncan, R. A., 1986, Geology and petrogenesis of lavas from San Cristobal island, Galapagos Archipelago: Geol. Soc. Amer. Bull., v. 97, no 5., p. 555-566.

Gerlach, A. C., ed., 1970, The national atlas of the United States of America: U.S. Geological Survey, Washington, D.C., 417 p.

Glasmann, J. R., 1982, Alteration of andesite in wet, unstable soils of Oregon's western Cascades: Clays and Clay Minerals, v. 30, no. 4, p. 253-263.

Glasmann, J. R., and Simonson, G. H., 1985, Alteration of basalt in soils of western Oregon: Soil Sci. Am. Jour., v. 49, p. 262-273.

Globerman, B. R., Beck, M. E., Jr., and Duncan, R. A., 1982,
Paleomagnetism and tectonic significance of Eocene basalts from
the Black Hills, Washington Coast Range: Geol. Soc. Amer. Bull.,
V. 93, p. 1151-1159.

Goalen, J., 1988, Geology of the Elk Mountain-Porter Ridge Area,
Clatsop County, northwest Oregon: unpub. M.S. thesis, Oregon
State Univ., Corvallis.

Gottardi, G., and Galli, e., 1985, Natural Zeolites: Springer-Verlag,
New York, 409 p.

Hamblien, A. P. and Walker, R. G., 1979, Storm-dominated shallow
marine deposits: The Fernie-Hootenary (Jurassic) transition,
southern Rocky Mountains: Can. Jour. Earth Sci., v. 16,
p. 1673-1690.

Hanson, R. E. and Scheickert, R. A., 1982, Chilling and brecciation of
a Devonian rhyolite sill intruded into wet sediments, northern
Sierra Nevada, California: Jour. of Geol. v. 90, p. 717.

Hardenbol, J., and Berggren, W. A., 1978, A new Paleogene numerical
time scale, in Cohee, G. V., and others, eds., Contributions to
the geological time scale: Amer. Assoc. Petrol. Geologists
Studies in Geology, no. 6, p. 213-234.

Harker, A., 1909, The natural history of igneous rocks: New York,
MacMillan Pub. Co. Inc., 384 p.

Harms, J. C., Southard, J. B., and Walker, R. G., 1982, Structures and
sequences in clastic rocks: Soc. Econ. Paleontologists and
Mineralogists Short Course No. 9, 249 p.

Harrison and Eaton (Firm), 1920, Report on investigation of oil and
gas possibilities of western Oregon: The Mineral Resources of
Oregon, v. 3, p. 1-37.

Heller, P. L. and Dickinson, W. R., 1985, Submarine ramp facies model
for delta fed, sand rich turbidite systems: Amer. Assoc. of
Petrol Geol. Bull., v. 69, p. 960-976.

Heller, P. L. and Ryberg, P. T., 1983, Sedimentary record of
subduction to forearc transition in the rotated Eocene basin of
western Oregon: Geology, v. 11, p. 380-385.

Henricksen, D. A., 1956, Eocene stratigraphy of the lower Cowlitz
River-eastern Willapa Hills area, southwestern Washington:
Wash. Div. Mines and Geology Bu.. 43, 122 p., 2 plates, including
map.

Hertlein, L. G., and Crickmay, C. H., 1925, A summary of the nomenclature and stratigraphy of the marine Tertiary of Oregon and Washington: Am Philos. Soc. Proc., v. 64, p. 224-282.

Heyl, A. V., Brock, M. R., Jolly. J. L., and Wells, C. E., 1966, Regional structue of the southeast Missouri and Illinois-Kentucky mineral districts: U.S. Geol. Survey Bull. 1202-B, p. 1-20.

Hill, D. W., 1975, Chemical composition studies of Oregon and Washington coastal basalts: unpub. M.S. thesis, Oregon State Univ., Corvallis, 99 p.

Howard, K., in prep, Hydrothermal vents of the Gorda Ridge, NE Pacific: Mineralogy and chemistry of sulfide chimneys, precipitates and alteration products, OSU School of Oceanography

Howe, H. V., 1926, Astoria: Mid-Tertic type of Pacific coast: Pan-Am Geologist, v. 45, p. 295-306.

Hughes, C. J., 1976, Igneous Petrology: Elsevier Scientific Publishing Co., New York, 551p.

Hyndman, D. W., 1985, Petrology of Igneous and Metamorphic Rocks, 2nd ed.: McGraw-Hill, San Francisco, 786p.

Irvine, T. N. and Baragar, W. R. A., 1971, A guide to the chemical classification of the common volclanic rocks: Can. Jour. Earth Sci., v. 8, p. 523-548.

Irving, E., 1979, Paleopoles and paleolatitudes of North America and speculations about displaced terrains: Canadian Jour. Earth Sciences, v. 16, P. 669-694.

Jackson, M. K., 1983, Stratigraphic relationships of the Tillamook Volcanics and the Cowlitz Formation in the Upper Nehalem River-Wolf Creek area, northwestern Oregon: unpub. M.S. thesis, Portland State Univ, Oregon, 112 p.

Jones, D. L., Silbering, N. S., and Hillhouse, J. W., 1977, Wrangellia: a displaced terrane in northwestern North America: Canadian Jour. Earth Sciences, v. 14, p. 2565-2577.

Kallendar, R. M., 1953, Problems of rehabilitating the Tillamook burn: unpub. M. S. thesis, Oregon State College, 85p.

Kadri, M. M., 1982, Structure and influence of the Tillamook uplift on the stratigraphy of the Mist area, Oregon: unpub. M.S. thesis, Portland State Univ., Oregon, 105 p

Kadri, M. M., Beeson, M. H., and Van Atta, R. O., 1983, Geochemical evidence for a changing provenance of Tertiary formations in northwestern Oregon: Oregon Geology, v. 45, p. 20-22.

Kelty, K. B., 1981, Stratigraphy, lithofacies, and environment of deposition of the Scappoose Formation in central Columbia County, Oregon: unpub. M.S. thesis, Portland State Univ., Oregon, 81 p.

Kerr, P. F., 1977, Optical Mineralogy, Fourth ed.: McGraw-Hill, San Francisco, CA, 492p.

Kienle, C. F., 1971, The Yakima basalt in western Oregon and Washington: unpub. Ph.D. thesis, Univ. of Calif. at Santa Barbara.

Kienle, C. F., Sheriff, S. D., and Bentley, R. D., 1978, Tectonic significance of paleomagnetism of the Frenchman Springs Basalt, Oregon and Washington: Geol. Soc. Am. Abst. with Prog., v. 10, p. 111-112.

Kokelaar, B. P., 1982, Fluidization of wet sediments during the emplacement and cooling of various igneous bodies: Jour. Geol. Soc., London, v. 139, p. 21-33.

Kosloff, E. N., 1976, Plants and animals of the Pacific Northwest: University of Washington Press, Seattle, 264 p.

Kulm, L. D., and Fowler, G. A., 1974, Oregon and continental margin structure and stratigraphy: a test of the imbricate thrust model, in Burk, C. A., and Drake, C. L., eds.: The geology of continental margins: New York, Springer-Verlag, p. 261-283.

Kulm, L. D. and Scheidegger, K. F., 1979, Quaternary sedimentation of the tectonically active Oregon continental slope, in Doyle, L. J. and Pilkey, O. H. Jr., eds., Geology of Continental Slopes: Soc. Econ. Paleon. Min. Spec. Pub. no. 27, p. 247-264.

Kulm, L. D., Roush, R. C., Harlett, J. G., Neudeck, R. H., Chambers, D. M., and Runge, E. J., 1975, Oregon continental shelf sedimentation: interrrelationships of facies distribtuion and sedimentary processes: Jour. Geol., v. 83, p. 145-175.

Larig, R. W., Stevens, R. E., and Norman, M. B., 1964, Staining of plagioclase feldspar with F.D. and C. Red no. 2: U.S. Geol. Survey Prof. Paper 501-B.

Law, B. E., Anders, D. E., Fouch, T. D., Pawllewicz, M. J., Lilckus, M. R., and Molenaar, C. M., 1984, Petroleum source rock evaluations of outcroop samples from Oregon and northern California: Oregon Geology, v. 46, no. 7, p. 77-81.

Leckie, D. A. and Walker, R. G., 1982, Storm-and-tide dominated shorelines in Cretaceous Moosebar-lower Gates Interval-outcrop equivalents of deep basin gas trap in western Canada: Amer. Assoc. of Petrol. Geol. Bull., v. 66, p. 138-157.

Lindgren, W., 1901, The gold belt of the Blue Mountains of Oregon: U.S.G.S. 22nd Ann. Rept., pt. 11, p. 551-776.

Livingston, V. E. Jr., 1966, Geology and mineral resources of the Kelso-Cathlamet area, Cowlitz and Wahkiakum counties, Washington: Wash. Div. of Mines and Geology Bull. 54, 110 p.

Loeschke, J., 1979, Basalts of Oregon and their geotectonic environment; petrochemistry of Tertiary basalts of the Oregon Coast Range: Nuess Jahrbuch Fur Minerologie Abhandlugen, v. 134, p. 225-247.

Long, P. E., Ledgewood, R. K., Myers, W. W., Reidel, S. P., and Landon, R. D., 1980, Chemical stratigraphy of Grande Ronde Basalt, Pasco Basin, southcentral Washington: Rockwell Hanford Operations, Contract No. DE-AC06-77RL01030; RHO-BWI-SA-32, Richland, Washington.

Lovell, J. P. B., 1969, Tyee Formation: undeformed turbidites and their lateral equivalents: mineralogy and paleogeography: Geol. Soc. Amer. Bull., v. 80, no. 1, p. 9-22.

Lucia, E., 1953, Lost Indian Mine of the Tillamook Country: Sunday Oregonian Magazine, Oregonian, August 30, 1953, p. 2-3.

Lucia, E., 1983, Tillamook Burn Country: Caxton Printers, Caldwell, ID, 305p.

MacDonald, G. A., 1972, Volcanoes: Prentice Halls, Englewood Cliffs, N.J., 450 p.

MacDonald, G. A. and Katsura, T., 1964, Chemical classification of Hawaiian lavas: Jour. Pet., v. 5, p. 82-133.

Mackin, J. H., 1961, A stratigraphic section in the Yakima Basalt and Ellensburg Formation in southcentral Washington: Wash. Div. Mines and Geol. Rept. Inv. 19, p. 45.

Magill, J. R., and Cox., A. V., 1980, Tectonic rotation of the Oregon Western Cascades: Oregon Dept. of Geol. and Min. Ind. Special Paper 10, 67p.

Magill, J. R., Cox, A. V., and Duncan, R. A., 1981, Tillamook Volcanic Series: further evidence for tectonic rotation of the Oregon Coast Range: Jour. Geophy. Res., v. 86, p. 2953-2970.

Magill, J. R., Wells, R. E., Simpson, R. W., and Cox, A. V., 1982, Post-12 m.y. rotation of southwest Washington: Jour. Geophys. Res., v. 87, no. 5, p. 3761-3776.

Mangan, M. T., Wright, T. L., Swanson, D. A., and Byerly, G. R., 1986, Regional correlation of Grande Ronde Basalt flows, Columbia River Basalt Group, Washington, Oregon, and Idaho: Geol. Soc. Amer. Bull, v. 97, no. 11, p. 1300-1318.

Manson, V., 1967, Geochemistry of Basaltic Rocks: Major elements in Hess, H. H. and Poldervaart, A., eds., Basalts: Interscience publishers, New York, v. 1, 482 p.

Martin, M., Kadri, M., Niem, A. R. and McKeel, D. R., 1985, Correlation of exploration wells, Astoria basin, NW Oregon, in Niem, A. R. and Niem, W. A., 1985, Oil and gas investigation of the Astoria basin, Clatsop and northernmost Tillamook counties, northwest Oregon: Oregon Dept. Geology and Mineral Industries Oil and Gas Invest. 14, plate 2.

Martini, E., 1970, The upper Brockenhurt bed: Geological magazine, v. 107, no. 3, p. 225-228

Martini, E., 1971, Standard Tertiary and Quaternary calcareous nannoplankton zonation, in Farinacci, A., ed. Proc. 2nd Planktonic Conf., Roma, Edizioni Technoscienza, p. 739-835.

McArthur, L. A., 1982, Oregon Geographic names, 5th ed.: Western Imprints, the press of the Oregon Historical Society, Portland, 839p.

McBirney, A. R., 1963, Factors governing the nature of submarine volcanicsm: Bull. Volcanol., v. 26, p. 455-469.

McDougall, K. A., 1975, The microfauna of the type section of the Keasey Formation of northwestern Oregon, in Weaver, D. W., Hornaday, G. R., and Tipton, A., eds., Future energy horizons of the Pacific Coast: Amer. Assoc. Petrol. Geol. Soc. Econ. Paleon. Min.-Soc. Econ. Geophys. Pacific Sections Ann. Mtg., Long Beach, Calif., p. 343-359.

McDougall, K. A., 1980, Paleoecologial evaluation of late Eocene biostratigraphic zonations of the Pacific coast of North America: Soc. Econ. Paleon. Min. Paleontological Mon. No. 2, 46 p.

McDougall, K. A., 1981, Systematic paleontology and distribution of late Eocene benthic foaminifers from northwestern Oregon and southwestern Washington: U.S. Geol. Survey Open-file Report 81-109, 501 p.

McDougall, K. A., Micropaleontologist, U.S. Geol. Survey, written communication, July 16, 1984.

McElwee, K. R. and Duncan, R. A., 1984, The chronolgy of volcanism in the Coast Range, Oregon and Washington: 1984 Pacific Northwest Metals and Minerals Conf., Abst., p. 22.

McKee, E. H., Swanson, D. a., and Wright, T. L., 1977, Duration and volume of Columbia River Bas;lt volcanism, Washington, Ortegon, and Idaho: Geol. Soc. Amer. Abstracts with Programs, v. 9 no. 4, p.1 463-464.

McKeel, D. R., 1983, Subsurface biostratigraphy of the east Nehalem Basin, Columbia County, Oregon: Oregon Dept. of Geol. and Min. Indust. Oil and Gas Invest 9, 34 p.

Merriam, J. C., 1901, A contribution to the geology of the John Day basin: Calif. Univ. Dept. Sci. Bull., v. 2, p. 269-314.

Middlemost, E. A. K., 1975, The basalt clan: Earth-Sci. Rev., v. 11, p. 337-364.

Middleton, G. V., and Hampton, M. A., 1976, Subaqueous sediment transport and deposition by sediment gravity flows, in D. J. Stanley and D. J. P. Swift, eds., Marine sediment transport and environmental management: New York, John Wiley and Sons, p. 197-217.

Miller, P., 1984, Geology of the Silverton area, western Oregon: Unpub. M. S. thesis, Univ. of Oregon.

Miller, P. R., and Orr, W. N., 1986, The Scotts Mills Formation: mid-Tertiary geologic history and paleogeography of the central western Cascade Range: Oregon, Oregon Geology, v. 48, no. 12, p. 139-151.

Milner, H. B., 1962, Sedimentary petrography: MacMillan, New York, 715 p.

Miyashiro, A., 1974, Volcanic rock series in island arcs and active continental margins: Amer. Jour. Sci., v. 274, p. 321-355.

Montanari, A., Drake, R., Bice, C./ M., Alvarez, W., and Curtis, G. H., 1985, Radiometric time scale for the upper Eocene and Olilgocene based on K/Ar and Rb/Sr dating of volcanic biotites from the pelagic sequence of Gubbio, Italy: Geology, v. 13, no. 13, p. 596-599.

Moore, E. J., 1976, Oligocene marine mollusks from the Pittsburg Bluff Formation in Oregon: U.S. Geol. Survey Prof. Pap. 922, 66 p., 17 plates.

Moore E. J., Molluscan paleontologist, U.S. Geol. Survey, written communication, May 7, 1984.

Moorhouse, W. W., 1959, The Study of Rocks in Thin Section, Harper and Row, New York, 514p.

Mullen, E. D., 1983, MnO/TiO$_2$/P$_2$O$_5$; a minor element discriminant for basaltic rocks of oceanic environments and it implications for petrogenesis: Earth and Planetary Sci. Letters, v. 62, p. 53-62.

Murphy, T. M., 1981, Geology of the Nicolai Mountain-Gnat Creek area, Clatsop County, northwest Oregon: unpub. M.S. thesis, Oregon State Univ., Corvallis, 355 p.

Neel, R. H., 1976, Geology of the Tillaook Head-Neacanicum Junction area, Clatsop County, northwest Oregon: unpub. M.S. thesis, Oregon State Univ., Corvallis, 204 p.

Nelson, D. E., 1985, Geology of the Jewell-Fishhawk Falls area, Clatsop County, northwest Oregon: unpub. M.S. thesis, Oregon State Univ., Corvallis, 420 p.

Nelson, D. O., and Shearer, B. B., 1969, The geology of Cedar Butte, northern Coast Range of Oregon: Ore Bin, v. 31, p. 113-130.

Nelson, M. P., 1978, Tertiary stratigraphy and sedimentation in the Lewis and Clark-Young's River area, Clatsop County, northwest Oregon: unpub. M.S. thesis, Oregon State Univ., Corvallis, 242 p.

Ness, G., Levi, S., and Couch, R., 1980, Marine magnetic anomaly timescales for the Cenozoic and late Cretaceous: A precise critique and synthesis: Reviews of Geophysics and Space Physics, v. 18, no. 4, p. 753-770.

Newton, V. C. Jr., and Van Atta, R. O., 1976, Prospects for natural gas production and underground storage of pipe-line gas in the upper Nehalem River basin, Columbia-Clatsop counties, Oregon: Oregon Dept. Geol. Min. Ind. Oil and Gas Invest. 5, 56 p.

Newton, V. C., Jr., 1979, Oregon's first gas well completed: Oregon Geology, v. 41, no. 6, p. 87-90.

Niem, A. R., 1976, Tertiary volcaniclastic deltas in an arc-trench gap, Oregon Coast Range: Geol. Soc. Amer. Abst. with Prog., v. 8, p. 400.

Niem, A. R. and Cressy, F. B., Jr., 1973, K-Ar dates for sills from the Neahkahnie Mountain and Tillamook Head areas of of northwestern Oregon coast: Isochron West, v. 7, no. 3, p. 13-15.

Niem, A. R., and Van Atta, R. O., 1973, Cenozoic stratigraphy of northwestern Oregon and adjacent southwestern Washington, in Beaulieu, J. D., ed., Geologic field trips in northern Oregon and southern Washington: Oregon Dept. Geol. and Min. Ind. Bull. 74, p. 75-89.

Niem, A. R. and Niem, W. A., 1984, Cenozoic geology and geologic history of western Oregon: Ocean margin Drilling Program, Regional Atlas Series, Atlas I: Western North American continental margin and adjacent ocean floor off Oregon and Washington, sheets 17 and 18: Marine Science International, Woods Hole, Massachusetts.

Niem A. R. and Niem. W. A., 1985, Oil and Gas investigation of the Astoria basin, Clatsop and northernmost Tillamook counties, northwest Oregon: Oregon Dept. Geol. and Min. Ind. Oil and Gas Invest. 14.

Niem A. R. and Van Atta, R. O., 1973, Cenozoic stratigraphy of northwestern Oregon and adjacent southwestern Washington, in Beaulieu, J. D., ed., Geologic field trips in northern Oregon and southern Washington: Oregon Dept. Geol. Min. Ind. Bull. 74, p. 75-89.

N.O.A.A., 1978, Climates of the States: Gale Research Co., Detroit, MI, 1185 p.

N.O.A.A., 1983, Climatological data; Oregon, v. 89, no. 7: Environmental Data and Information Service, National Climatic Center, Asheville, N. C., 41 p.

North American Commission on Stratigraphic Nomenclature, 1983, North American stratigraphic code: Am. Assoc. Petrol. Geol. Bull., v. 67, no. 5, p. 841-875.

Okada, H. and Bukry, D., 1980, Supplementary modification and introduction of code numbers to the low-latitude coccolith biostratigraphic zonation (Bukry, 1973, 1975): Marine Micropaleontology, v. 5, p. 321-325.

Olbinski, J. S., 1983, Geology of the Buster Creek-Nehalem Valley area, Clatsop County, northwest Oregon: unpub. M.S. thesis, Oregon State Univ., Corvallis, 231 p.

Passega, R., 1957, Texture as characteristic of clastic deposition: Amer. Assoc. of Petrol. Geol. Bull., v. 41, p. 1952-1984.

Paulis, P. L. and Bruhn, R. L., 1983, Deep-seated flow as a mechanism for the uplift of broad forearc ridges: Tectonics, v. 2, p. 473-479.

Pearce, T. H., 1976, Statistical analysis of major element pattens in
    basalts: Jour. of Petrol., v. 17 p. 15.

Pearce, T. H., Gorman, B. E., and Birkett, T. C., 1977, The
    relationship between major element chemistry and tectonic enviro-
    nment of basic and intermediate volcanic rocks: Earth and
    Planetary Sci. Let., v. 36, p. 121- 132.

Pearce, T. H., Gorman, B. E., and Birkett, T. C., 1975, The
    $TiO_2-K_2O-P_2O_5$ diagram: a method of discriminating between
    oceanic and non-oceanic basalts: Earth and Planetary Sci. Let.,
    v. 24, p. 419-426.

Penoyer, P. E., 1977, Geology of the Saddle and Humbug Mountain area,
    Clatsop County, northwest Oregon: unpub. M.S. thesis, Oregon
    State Univ., Corvallis, 232 p.

Perfit, M. R. and Fornari, D. J., 1983, Geochemical studies of abyssal
    lavas recovered by DSRV Alvin from eastern Galapogos Rift, Inca
    Transform, and Ecuador Rift; 2, phase chemistry and
    crystallization history: Jour. Geophy. Res., v. 88, no. 12, p.
    10530-10550.

Peterson, C. P., 1984, Geology of the Green Mountain-Young's River
    area, Clatsop County, northwest Oregon: unpub. M.S. thesis,
    Oregon State Univ., Corvallis, 215 p.

Peterson, C. P., Kulm, L. D., and Gray, J. G., 1985, Geologic
    Bibliography and index maps of the ocean floor off Oregon and the
    adjacent continental margin: Oregon Dept. Geol. and Min. Ind.
    GMS-39.

Petro, W. L., Vogel, T. A., and Wilband, J. T., 1979, Major element
    chemistry of plutonic rock suites from compressional and
    extensional plate boundaries: Chem. Geol. v. 26, p. 217-235.

Pfaff, V. J. and Beeson, M. H., 1987, Miocene Basalts of Coastal
    Oregon and Washington: Geochemical and geophysical evidence for
    Columbia Plateau origin: G.S.A. Abs. with Programs, No. 136146.

Pickthorn, L. B., Geochronologist, U.S. Geological Survey, personal
    communcation to Alan R. Niem, 1984.

Priest, G.A., Woller, N.M., and Black, G.W., 1983, Overview of the
    geology of the central Oregon Cascade Range, in, Priest, G.W.,
    and Vogt, B.F., eds., Geology and geothermal resources of the
    central Oregon Cascade Range: Oreg. Dept. Geol. Min. Ind. Spec.
    Paper 15, p. 3.28.

Prothero, D. R. and Armentrout, J. M., 1985, Magnetostratigraphic correlation of the Lincoln Creek Formation, Washington: implication for the age of the Eocene- Oligocene boundary: Geology, v. 13, p. 208-211.

Ramp, L., 1988, Exploration and mining activity in Oregon, 1987: Oregon Geology, v. 40, no. 4, p. 39-44.

Rarey, P. J., 1986, Geology of the Hamlet-north Fork of the Nehalem River area, southern Clatsop and northernmost Tillamook Counties, northwest Oregon: unpub Oregon State Univ. M. S. thesis, 426 p.

Rau, W. W., Paleontologist, Washington State Division of Natural Resourses, written communication to Dr. Alan Niem, October 12, 1984.

Reidel, S. P., Long, P. E., Myers, C. W., and Mase, J., 1982, Nedw evidence for greater than 3.2 km of Columbia River Basalt beneath the central Columbia Plateau: EOS, Amer. Geophys. Union Trans., v. 63, no. 8, p. 173.

Reineck, H. E. and Singh, J. B., 1980, Depositional sedimentary environments: Springer-Verlag, New York, 549 p.

Reverdatta, V. V. and Melenevskii, V. N., 1983, Magmatic heat as a factor in generation of hydrocarbons: the case of basalt sills: Soviet Geology and Geophysics, v. 24, p. 15-23.

Rierson, H., Retired forester, Elsie, Oregon, personal communication, 1982.

Rock-color Chart Committee, 1970, Rock-color chart: Geol. Soc. of Amer., Boulder, Colorado.

Royse, C. F., 1970, An introduction to sediment analysis: Tempe, Arizona, 180 p.

Russel, I. C., 1901, Geology and water resources of Nez Perce County, Idaho: U.S.G.S. Water Supply Paper, No. 53, p. 28-85.

Safley, L. E., in prep., Geology of the Green Mountain-Military Creek area, Clatsop and Tillamook counties, northwestern Oregon: unpub. M.S. thesis, Oregon State Univ., Corvallis.

Schenck, H. G., 1927, Stratigraphic and faunal relations of the Keasey Formation of the Oligocene of Oregon: Geol. Soc. Amer. Bull., v. 44, no. 1, 217 p.

Schlicker, H. G. and Deacon, R. J., 1967, Engineering geology of the Tualatin Valley region, Oregon: Oregon Dept. Geology and Mineral Industries Bull. 60, 103 p.

Schlicker, H. G., Deacon, R. J., Beaulieu, J. D., and Olcott, G. W., 1972, Environmental geolgy of the coastal region of Tillamook and Clatsop counites, Oregon: Oregon Dept. Geol. Min. Ind., Bull. 74, 164 p.

Schlaefer, J., Geologist, AMOCO Production Co., Denver, Colorado, written communication, March 28, 1984.

Schmincke, H. U., 1967, Stratigraphy and petrography of four upper Yakima Basalt flows in southcentral Washington: Geol. Soc. Amer. Bull., v. 78, p. 1385-1422.

Schmincke, H. U., 1967, Fused tuff and peperites in south-central Washington: Geol. Soc. Amer. Bull. v. 78, p. 319-330.

Schultz, K. E., 1983, Paleomagnetism of Jurassic plutons in the central Klamtath Mountains, southern ORegon and northern California: unpub. M.S. thesis, Oregon State Univ., Corvallis

Shaw, N. B., 1986, Biostratigraphy of the Cowlitz Formation in the upper Nehalem River Basin, northwest Oregon: unpub. M. S. thesis, Portland State Univ., Portland, OR., 110p.

Sheppard, R. A., 1987, Field trip guide to the Sheaville and Rome zeolite deposits, southeastern Oregon: Oregon Geology, v. 49, no. 1, p. 3-10.

Sheriff, S. D., 1984, Paleomagnetic evidence for spatially distributed post-Miocene rotation of western Washington and Oregon: Tectonics, v. 3, p. 397-408.

Silver, E. A., 1978, Geophysical studies and tectonic development of the continental margin off the western United States, lat. 34° to 48° N, in Smith, R. B., and Eaton, G. P., eds., Cenozoic tectonics and regional geophysics of the western Cordillera: Geol. Soc. Amer. Memoir 152, p. 251-262.

Simpson, R. W. and Cox, A. V., 1977, Paleomagnetic evidence for tectonic rotation of the Oregon Coast Range: Geology, v. 5, p. 585-589.

Smith, G. A., 1986, Coarse-grained nonmarine volcaniclastic sediment: Terminology an depositional process: G.S.A. Bull., v. 97, no 1. p 1-10.

Smith, T. N., 1975, Stratigraphy and sedimentation of the Onion Peak area, Clatsop County, Oregon: unpub. M.S. thesis, Oregon State Univ., Corvallis, 190 p.

Snavely, P. D., Jr., 1984, Sixty years of growth along the Oregon continental margin, in Clarke, S. H., ed., Highlights in marine research: U.S. Geol. Survey Circular 938, p. 9-18.

Snavely, P. D., Jr., MacLeod, N. S., and Rau, W. W., 1969, Geology of the Newport area, Oregon: Ore Bin, v. 31, p. 25-48.

Snavely, P. D., Jr. and MacLeod, N. S., 1974, Yachats Basalt - An upper Eocene differentiated volcanic sequence in the Oregon Coast Range, U.S. Geol. Survey J. Res., 2, p. 395-405.

Snavely, P. D., Jr., MacLeod, N. S., and Rau, W. W., 1970, Geologic Research Recannaissance mapping Tillaook highlands: U.S. Geol. Survey Prof. Pap. 650A, p. A47.

Snavely, P. D., Jr., MacLeod, N. S., and Wagner, H. C., 1973, Miocene tholeiitic basalts of coastal Oregon and Washington and their relations to coeval basalts of the Columbia Plateau: Geol. Soc. Amer. Bull., v. 84, p. 387-421.

Snavely, P. D., Jr., MacLeod, N. S., Rau, W. W., Addicott, W. O., and Pearl, J. E., 1975, Alsea Formation - an Oligocene marine sedimentary sequence in the Oregon Coast range: U.S. Geol. Survey Bull. 1395-F, p. F1-F21.

Snavely, P. D., Jr., Pearly, J. E., and Lander, D. L., 1977, Interim report on petroleum resources potential and geologic hazards in the outer continental shelf - Oregon and Washington Tertiary province: U.S. Geol. Survey Open-file Rept. 77-282, 64 p.

Snavely, P. D., Jr. and Voker, H. E., 1949, Geology of the coastal area between Cape Kiwanda and Cape Foulweather, Oregon: U.S. Geol. Survey Oil and Gas Invest., prelim. map 97, scale 1:62,500.

Snavely, P. D., Jr. and Wagner, H. C., 1963, Tertiary geologic history of western Oregon and Washington: Washington Div. Mines Geol., Rept. Inv. No. 22, 25 p.

Snavely, P. D., Jr. and Wagner, H. C., 1964, Geologic sketch of northwestern Oregon: U.S. Geol. Survey Bull. 1181-M, p. 1-17.

Snavely, P. D., Jr. and Wagner, H. C., 1968, Tholeiitic and alkalic basalts of the Eocene Siletz River Volcanics, Oregon Coast Range: Amer. Jour. Sci., v. 266, p. 454-481.

Snavely, P. D., Jr., Wagner, H. C., Lander, D. L., 1980, Geologic cross section of the central Oregon continental margin: GSA Map and Chart Series, MC-28J (scale 1:250,000).

Snavely, P. D., Jr., Wagner, H. C., and MacLeod, N. S., 1964, Rhythmically-bedded eugeosynclinal deposits of the Tyee Formation, Oregon Coast Range: Kansas State Geological Survey Bull. 169, p. 461-480.

Snyder, G. L. and Fraser, G. D., 1963, Pillowed lavas I: intrusive layered lava pods and pillowed lavas, Unalaska, Alaska: U.S. Geol. Survey Prof. Pap. 454B, 23 p.

Soper, E. G., 1974, Geology of a portion of the Timber quadrangle, Oregon: unpub. M.S. thesis, Univ. of Oregon, Eugene, 102 p.

Stanley, K. O. and Benson, L. V., 1979, Early diagenesis of high plains Tertiary vitric and arkosic sandstones, Wyoming and Nebraska, in Scholle, P. A. and Schluger, R. R., eds., Aspects if diagenesis: Soc. Econ. Paleon, Min. Spec. Pub. 26, p. 401-424.

Stone, D. B., and Packer, D. R., 1979, Paleomagnetic data from the Alaska Peninsula: Geol. Soc. Amer. Bull., v. 90, p. 545-560.

Summer, N. S., and Verosub, K. L., 1987, Extraordinary maturation profiles of the Pacific Northwest, Oregon Geology, v. 49, no. 11, p. 135-140.

Surdam, R. C. and Boles, J. R., 1979, Diagenesis of volcanic sandstones, in Scholle, P. A. and Schluger, R. R., eds., Aspects of diagenesis: Soc. Econ. Paleon. Min. Spec. Pub. 26, p. 307-318.

Swanson, D. A., 1967, Yakima Basalt of the Treton River area, southcentral Washington: Geol. Soc. Amer. Bull., v. 78, p. 1077-1110.

Swanson, D. A. and Wright, T. L., 1978, Bedrock geology of the northern Columbia Plateau and adjacent area: in Baker, V. R. and Nummedal, D., eds., The Channeled Scabland: N.A.S.A., Planetary Geology Program, p. 186.

Swanson, D. L., Wright, T. L., Hooper. P. R., and Bentley, R. D., 1979, Revisions in stratigraphic nomenclature of the Columbia River Basalt Group: U.S. Geol. Survey Bull. 1457-G, 59 p.

Taubeneck, W. H., 1970, Dikes of the Columbia River Basalt in northeastern Oregon, western Idaho, southeastern Washington, in Gilmour, E. H. and Stradling, D., eds., Proceeding of the second Columbia River Basalt Symposium: Cheney, Eastern Washington State College Press, p. 73-96.

Timmons, D. M., 1981, Stratigraphy, lithofacies and depositional environment of the Cowlitz Formation, T4 and 5N, R5W, northwest Oregon: unpub. M.S. thesis, Portland State Univ., Oregon, 89 p.

Tolan, T. L. and Beeson, M. H., 1984, Intracanyon flows of the Columbia River Basalt Group in the lower Columbia River Gorge and their relationship to the Troutdale Formation: Geol. Soc. Amer. Bull., v. 95, p. 463-477.

Tolson, P. M., 1976, Geology of the Seaside-Young's River Falls area, Clatsop County, Oregon: unpub. M.S. thesis, Oregon State Univ., Corvallis, 191 p.

U.S. Department of Interior, 1970, National Atlas.

U.S. Geol. Survey, 1984, Aeromagnetic map of southwest Washington and northwest Oregon: U.S. Geol. Survey Open-file rept. 84-205.

Vallier, T. L. and H. C. Brooks, 1987, eds., Geology of the Blue Mountains Region of Oregon, Idaho, and Washington: U. S. Geol. Survey Prof. Pap. 1436

Van Atta, R. O., 1971, Sedimentary petrology of some Tertiary formations, upper Nehalem River basin Oregon: Ph.D. dissertation, Oregon State Univ., Corvallis, 245 p.

Van Atta, R. O. and Kelty, K. B., 1985, Scappoose Formation, Columbia County, Oregon: new evidence of age and relation to Columbia River Basalt Group: Amer. Assoc. of Petrol. Geol. Bull., v. 69, p. 688-698.

Visher, G. S., 1969, Grain size distributions and depositional processes: Jour. Sed. Pet., v. 39, p. 1074-1106.

Vokes, H. E., Myers, D. A., and Hoover, L., 1954, Geology of the west central border area of the Willamette Valley, Oregon, U. S. Geol. Survey Oil and Gas invest. Map OM-150

Vokes, H. E., Snavely, P. D., Jr., and Myers, D. A., 1951, Geology of the southern and southwestern border areas, Willamette Valley, Oregon, U. S., Geol. Survey Oil and Gas Invest. Map OM-110

Walker, G. P. L., 1960, Zonal distribution of amygdule minerals: Jour. Geol., v. 68, p. 515-

Walker, R. G. and E. Mutti, 1973, Turbidite facies and facies asociations in G. V. Middleton, and A. H. Bouma, eds., Turbidites and deep-water sedimentation: SEPM Pacific Sec., p. 119-157.

Walton, M. S. and O'Sullivan, R. B., 1950, The intrusive mechanics of a clastic dike: Amer. Jour. Sci., v. 248, p. 1-21.

Warren, W. C. and Norbisrath, H., 1946, Stratigraphy of upper Nehalem River basin, northwestern Oregon: Amer. Assoc. Pet. Geol. Bull., v. 30, no. 2, p. 213-237.

Warren, W. C., Norbisrath, H., and Grivetti, R. M., 1945, Geology of northwestern Oregon west of the Willamette River and north of latitude 45° 15': U.S. Geol. Survey Oil and Gas Invest., Prelim. map 42, scale 1:143,000.

Washburne, C. W., 1914, Reconnaissance of the geology and oil prospects of northwestern Oregon: U.S. Geol. Survey Bull. 590.

Waters, A. C., 1961, Stratigraphic and lithologic variations in the Columbia River Basalt: Amer. Jour. Sci., v. 259, p. 583-611.

Watkins, N. D., and Baski, A. K., 1974, Magnetostratigrphy and oroclinal folding of the Columbia River, Steens and Owyhee Basalts in Oregon, Washington and Idaho: Amner. Jour. of Science, V. 274, pl. 148-189.

Weaver, C. E., 1912, A preliminary report on the Tertiary paleontology of western Washington: Washington State Geol. Sruvey Bull. 15, 80 p.

Weaver, C. E., 1937, Tertiary stratigraphy of western Washington and northwestern Oregon: Univ. of Washington Pub. in Geol., Seattle, v. 4, 266 p.

Weaver, C. E., 1942, Paleontology of the marine Tertiary formations of Oregon and Washington: Univ. of Washington Pub. in Geol., Seattle, v. 5, 790 p.

Wells, F. G. and Peck, D. L., 1961, Geologic map of Oregon west of the 121st Meridian: U.S. Geol. Survey Misc. Geol. Inv. Map I-325, scale 1:500,000.

Wells, R. E., 1981, Geologic map of the eastern Willapa Hills, Cowlitz, Lewis, Pacific, and Wahkiakum counties, Washington: U.S. Geol. Survey Open-file Rept. 81-674.

Wells, R. E., 1984, Paleomagnetic constraints on the interpretation of early Cenozoic Pacific Northwest paleogeography, in Nilsen, T. H., ed., 1984, Geology of the upper Cretaceous Hornbrook Formation, Oregon and California: Pacific Section S.E.P.M., v. 42, p. 231-237.

Wells, R. E., 1985, The Tillamook Volcanics of Oregon is not an accreted terrane: G.S.A. Abs. with Programs, Cordilleran Section, No. 70487.

Wells, R. E. and Coe, R. S., 1980, Tectonic rotations in southwest Washington (abstract): EOS Trans. Amer. Geophys. Union. v. 61, p. 949.

Wells, R. E. and Coe, R. S., 1985, Paleomagnetism and geology of Eocene volcanic rocks in southwest Washington, implication for mechanisms of tectonic rotation: Jour of Geophys. Res., v. 90, no. B2, p. 1925-1947.

Wells, R. E., Engebretson, D. C., Snavely, P. D., Jr., and Coe, R. S., 1984, Cenozoic plate motions and the volcano-tectonic evolution for western Oregon and Washington: Tectonics, v. 3, p. 275-294.

Wells, R. E., and Heller, P. L., 1988, The relative contribution of accretion, shear, and extension to Cenozoic tectonic rotation in the Pacific Northwest: Geol. Soc. Amer. Bull, v. 100, p. 325-338.

Wells, R. E. and Niem, A. R., 1987, Geology of the Columbia River Basalt Group in the Astoria Basin, Oregon and Washington: Evidence for Invasive flows, G.S.A. Abs. with Programs No. 134238.

Wells, R. E., Niem. A. R., MacLeod, N. S., Snavely, P. D., and Niem W. A., 1983, Preliminary geologic map of the west half of the Vancouver (WA-OR) 1° X 2° quadrangle, Oregon: U.S. Geol. Survey Open-file Rept. 83-591, scale 1:250,000.

Welton, J. E., 1984, SEM Petrology atlas: Amer. Assoc. of Petrol. Geol., Tulsa, 237 p.

Wermeil, D. E., 1987, Oil and gas exploration and development in Oregon, 1986: Oregon Geology, v. 49, no. 3, p. 31-36.

Wilcox, R. E., Harding, T. P., and Seely, D. R., 1973, Basic wrench tectonics: Amer. Assoc. of Petrol. Geol. Bull., v. 57, p. 74-96.

Wilkinson, W. D., Lowry, W. D., and Baldwin, E. M., 1946, Geology of the St. Helens quadrangle, Oregon: Oregon Dept. Geol. Min. Ind. Bull. 31, 39 p.

Williams, H. and McBirney, A. R., 1979, Volcanology: Freeman, Cooper, and Co., San Francisco, CA., 397p.

Williams, H, Turner, F. J., and Gilbert, C. M., 1954, Petrography: W. H. Freeman and Co., San Francisco. 460 p.

Wilson, J. T., 1973, Mantle plumes and plate motions: Tectonophysics, v. 19, p. 149-164.

Wolfe, E. W. and McKee, B. H., 1972, Sedimentary and igneous rocks of the Grays River quadrangle, Washington: U.S. Geol. Survey Bull. 1335, 70 p.

Wright, T. L., and R. Fiske, 1971, Origin of the differentiated and hybrid lavas of Kilaeua volcano, Hawaii: Jour. Petrology, v. 12, p. 1-65.

Wright, T. L., Grolier, M. J., and Swanson, D. A., 1973, Chemical variation related to the stratigraphy of the Columbia River Basalt: Geol. Soc. Amer. Bull., v. 84, p. 371-381.

Yett, J. R., 1979, Eocene foraminifera from the Olequa Creek Member of
    the Cowlitz Formation, southwestern Washington:
    unpub. M.S. thesis, Univ. of Washington, Seattle, 110 p.

Yoder, H. S. Jr. and Tilley, C. E., 1962, Origin of basalt magmas: an
    experimental study of natural and synthetic rock systems:
    Jour. Petrology, v. 3, p. 342-532

APPENDIX I: SAMPLE DATA

SEDIMENTARY ROCK DATA

SAMPLE	LOCATION	LITHOLOGY	UNIT	THIN SEC.	SIZE ANALYSIS	HEAVY MINERAL G.M.	POROSITY PERMEAB.	SOURCE ROCK GEOCHEM.	CLAYS	FORAMS	MOLLUSCS	COCCOLITHS
	T. R.											
43-1	4N, 7W NE 1/4 SW 1/4 sec. 16. Phil Rarey area.	basaltic sandstone	Thrc	-	-	-	-	-	-	-	X	-
625-1	4N, 7W NW 1/4 NE 1/4 sec. 6. U. S. 26 Rd. cut.	mudstone	Tkj	-	-	-	-	-		-2	-	-
627-2	4N, 7W NE 1/4 SE 1/4 sec. 4.	mudstone/ sandstone	Tshc		-18		-18	-		-11,14	X,10	-
629-6	4N, 7W SW 1/4 SE 1/4 sec. 4.	mudstone	Thsh?	-	-	-	-	-		-1	X	-
73-4	4N, 7W SW 1/4 NW 1/4 sec. 5 Rd. cut along lower Nehalem highway 3/4 S. of Elsie.	mudstone/ tuff beds/ clastic dikes	Tkj	-	-	-	-	-		-1,5,10	-	-13
74-1	4N, 7W NE 1/4 SW 1/4 sec. 7.	mudstone	Thshc	-	-	-	-	-	-	-1	-	-
74-4	4N, 7W SW 1/4 sec. 7. Rd. cut along lower Nehalem highway.	mudstone	Thshc	-	-	-	-	-	-	-1	-	-
75-4	4N, 7W NW 1/4 NW 1/4 sec. 18. Lower Nehalem highway Rd. cut 1/4 mi. N. of Lukarilla.	siltstone/ mudstone	Thshc	-	-	-	-	-	-	-1	-	-
77-11	4N, 7W NE 1/4 NE 1/4 sec. 17. Spur off Lost Lake Road.	mudstone	Tkj/ Thshc	-	-	-	-	-	-	X	-	-
79-5	4N, 7W NW 1/4 SW 1/4 sec. 15. AFR Rd. cut.	mudstone	Thshc	-	-	-	-	-	-	-1	-	-
715-2	4N, 7W NE 1/4 sec. 10. U. S. 26 Rd. cut. E. boundary.	arkosic sandstone	Thsh		-2,3	-2,3	-	-	-	-	-	-
715-4	4N, 7W NE 1/4 sec. 10. U. S. Rd. cut. New exposures.	basaltic sandstone	Thsh		-1	-1	-	-	-	-	-2	-
716-6 cf. 371-1	4N, 7W SE 1/4 SE 1/4 sec. 3. U. S. 26 Rd. cut	mudstone/ sandstone	Thshc	-	-	-	-	-	-	-2	-	-
716-9	4N, 7W SW 1/4 sec. 3. U. S. 26 Rd. cut 1 mi. E. of Jewell Junc.	mudstone/ siltstone	Thshc		-3	-3	-	-1		-2	-	-4
717-1	4N, 7W NE 1/4 SW 1/4 sec. 3. Osweg Cr. stream cut along U. S. 26.	mudstone/ siltstone	Thshc	-	-	-	-	-	-	-1	-	-2

APPENDIX I cont.

SAMPLE	LOCATION T. R.	LITHOLOGY	UNIT	THIN SEC.	SIZE ANALYSIS	HEAVY MINERAL G.M.	POROSITY PERMEAB.	SOURCE ROCK GEOCHEM.	CLAYS	PALEONTOLOGY FORAMS	MOLLUSCS	COCCOLITHS
719-4 = 3623-1	4N, 7W SW 1/4 NW 1/4 sec. 28. Spur off Quartz Creek Rd.	basaltic sandstone	Thrc	-	-	-	-	-	-	-	X	-
729-8	4N, 7W SE 1/4 SW 1/4 sec. 19	basaltic sandstone	Thrc	-	-	-	-	-	-	-	X	-
730-6	4N, 7W SE 1/4 sec. 5. Luukinen Rd. cut.	siltstone	Thsh	-	-	-	-	-	~	-2,5	-	-
829-1	4N, 7W NE 1/4 NW 1/4 sec. 9. Nehalem River cut.	siltstone/ mudstone	Thshc	-	-	-	-	-	~	-1,2	(X)	-2
3623-3 = 3812-1-6	4N, 7W SW 1/4 NW 1/4 sec. 15 AFR measured section.	f.g. arkosic sandstone	Thsh	X	X	-2	~	-	-	-	-	-
3624-5	4N, 7W Extreme SE 1/4 sec. 7.	same as 3623-3	Thsh	X	( )	-	-	~	-	-	~	-
371-1	4N, 7W SE 1/4 SE 1/4 sec. 3. U. S. 26 Rd. cut 1 mi. W. of Quartz Creek Bridge	mudstone/ sandstone	Thshc	( )	-4	-4	-1	-2	( )	-5	X	-6
3715-2 cf. 4220-1	4N, 7W SE 1/4 sec. 17.	mudstone	Tkj	-	-	-	-	-4	( )	-	-	-
4220-1	4N, 7W SE 1/4 sec. 17. Above Spruce Run Lake.	mudstone	Tkj	-	-	-	-	-	( )	-1,2,3	-	-3
4327-4	6S, 8W Rock Cr. stream cut S. of Grande Ronde.	mudstone	Ty	-	-	-	-	-	-	-1	-	-
4327-6	6S 6W sec 52. Mill Creek stream cut under U. S. 22.	mudstone	Ty	-	-	-	-	-	~	-1	-	-
N83-45 = 94-2	5N, 7W Center SE 1/4 sec. 31. Elsie garbage dump.	mudstone	Tkj	-	-	-	-	-	-	X	-	-
N84-213	5N, 7W D. Nelson area. Type Jewell Rt. 202.	mudstone	Tkj	-	-	-	-	-	-	X	-	-
N84-240 = 73-4	4N, 7W NW 1/4 sec. 5. Clastic dike locality.	mudstone/	Tkj	-	-	-	-	-	-	X	-	-
FM32-Tec	4N, 7W 0.2 mi. W. of Jewell Junction.	?	(Thsh?)	-	-	-	-	-	-	-	X	X
M33-Tec cf. 627-2	4N, 7W SE 1/4 sec. 4 or SW 1/4 sec. 3.	?	(Thsh?)	-	-	-	-	-	-	-	X	-
F34-Tec cf. 716-9, 717-1	4N, 7W S 1/2 sec. 3.	?	(Th/ Thsh?)	-	-	-	-	-	~	X	-	-

APPENDIX I cont.

SAMPLE	LOCATION	LITHOLOGY	UNIT	THIN SEC.	SIZE ANALYSIS	HEAVY MINERAL G.M.	POROSITY PERMEAB.	SOURCE ROCK GEOCHEM.	CLAYS		PALEONTOLOGY	
										FORAMS	MOLLUSCS	COCCOLITHS
	T. R.											
M35-Tec	4N, 7W NW 1/4 sec. 11/NE 1/4 sec. 10.	?	(Trc?)	-	-	-	-	-	-	X	-	
M36-Tec cf. 719-3/ 720-1	4N, 7W E. 1/2 sec. 29/W. 1/2 sec. 28.	?	(Trc?)	-	-	-	-	-	-	X	-	

APPENDIX I cont.

IGNEOUS ROCK DATA

UNIT	SAMPLE	LOCATION	THIN SEC.	GEOCHEM.	PALEOMAG
TILLAMOOK VOLCANICS					
	75-6	T4N, R7W. NW1/4 S/W1/4 sec. 15	-2	-1	-1 (R)
	76-1	T4N, R7W. SW 1/4 sec. 13	-1		
	76-3	T4N, R8W. SE 1/4 NE 1/4 sec. 24	-1		
	77-4	T4N, R7W. NW 1/4 sec. 19	-3	-2	-1 (N)
	77-7	T4N, R7W. NW 1/4 sec. 19. Lost Lake Rd.	-1	-2,3	
	719-9	T4N, R7W. NW 1/4 SW 1/4 sec. 28		-1	
	719-10	T4N, R7W. SW 1/4 sec. 28 Pig Trail.		-1	
	720-4	T4N, R7W. NE 1/4 SW 1/4 sec. 30. 47 Ridge Road.	-1		
	720-5	T4N, R7W. NE 1/4 SW 1/4 sec. 30. 47 Ridge Road.	-1	-2	
	731-9	T3N, R8W. Extreme NE 1/4 SE 1/4 sec. 12	-1		
	822-2	T4N, R7W. SW 1/4 SW 1/4 sec. 34. LR116		-2	-1 (R)
	824-7	T3N, R7W. SW 1/4 SW 1/4 sec. 8.		-2	-1 (N)
	825-2	T3N, R7W. NW 1/4 NE 1/4 SW 1/4 sec 6.		-1	-1 (N)
	826-1	T3N, R7W. SE 1/4 SE 1/4 NE 1/4 sec. 2.		-2	-1 (N)
	826-7	T3N, R7W. NE 1/4 SE 1/4 sec. 2. LR101		-2	-1 (N)
	919-3	T3N, R7W. NW 1/4 NW 1/4 sec. 12. LR101	-3	-2	
	919-6	T3N, R7W. SW 1/4 SW 1/4 sec. 2. LR101	-1	-2	-1 (N)
	3623-6	T4N, R7W. Central NE 1/4 sec. 16.		-1	
	3721-1	T3N, R7W. NE 1/4 SE 1/4 sec. 3.		-3	
	3721-2	Same as 3721-1.		-2	
	3721-4	Same as 3721-1.		-2,4	

APPENDIX I cont.

COLE MTN.
BASALT

Sample	Location				
629-3	T4N, R7W. SE 1/4 NE 1/4 sec. 4. Quarry N. of Elderberry Inn.	-2			-1 (N)
630-1	T5N, R7W. SW 1/4 sec. 33. Near sub-station.		-3		-1 (N)
630-3	T4N, R7W. NW 1/4 sec. 4.	-2			-1 (N)
630-4	T4N, R7W. NW 1/4 sec. 4.	-1			-1
630-7	T4N, R7W. SW 1/4 sec. 4.				-1 (R) weak
73-2	T4N, R7W. SE 1/4 SW 1/4 sec. 4.	-1	-1		
73-3	T4N, R7W. NW 1/4 sec. 9.		(cf. 73-2)		-1 (N)
73-7	T4N, R7W. NW 1/4 SW 1/4 sec. 5.		-3		-1 (R) weak
74-5	T4N, R7W. SW 1/4 sec. 7.	-5,6			
717-10	T4N, R7W. SW 1/4 NE 1/4 sec. 20	-1	-3		-2 (N)
730-1	T4N, R7W. SW 1/4 NE 1/4 sec. 4.	-5			-1 (N)
730-2	T4N, R7W. SW 1/4 NE 1/4 sec. 4.	-2			-1 (N)
730-3	T4N, R7W. NW 1/4 SE 1/4 sec. 4. Luukinen Rd.	-2	-4		-1 (N)
730-4	T4N, R7W. SW 1/4 NW 1/4 sec. 5.		-2		-3 (N) weak
99-6	T4N, R8W. NW 1/4 sec. 11. CCC Rd.		-1		
3624-1	T4N, R7W. NW 1/4 SE 1/4 sec. 7.		-1		

GRANDE RONDE
BASALT

Sample	Location				
77-13	T4N, R7W. SW 1/4 NW 1/4 sec. 16. Lost Lake Rd.	-2	-3		-1 (N)
78-4	T4N, R7W. SE 1/4 NW 1/4 sec. 16. Quarry, AFR.				-1 (N) weak
79-12	T4N, R7W. SW 1/4 SW 1/4 sec. 15. Quartz Creek Rd. Flat Iron Mtn.	-2			-1 (N)
718-1	T4N. R7W. SW 1/4 NW 1/4 sec. 21.		-3		-2 (?)

APPENDIX I cont.

97-7   T4N, R8W. NW 1/4 _____   _____ -1   _____ -1 (R) weak
         sec. 3.
3623-8   T4N, R7W. SW 1/4 _____ -1 _____   _____
         sec. 16.
3630-2   T4N, R7W. NE 1/4 _____   _____ -2   _____
         SW 1/4 sec. 17.
         Spruce Run Lake
         irregular intrusion.
3715-2   T4N, R7W. NW 1/4 _____   _____ -1   _____
         SE 1/4 sec. 17.
         Spruce Run Lake
         irregular intrusion.

ROY CREEK MEMBER

CS Tc1   U. S. 26, Quartz _____ X _____   _____
         Creek.
729-8   T4N, R7W. SE 1/4 _____ -1 _____   _____
         sec. 19. Spruce
         Run Rd.
3720-2   T4N, R7W. SW 1/4 _____   _____ -1,2,3 ___
         NE 1/4 sec. 10
3723-1   T4N, R7W. SE 1/4 _____   _ -1,2,3,4 _
         NE 1/4 sec. 29.
         Spruce Run Rd. spur.

APPENDIX II: GRAIN SIZE ANALYSIS

\Sample	----------------Sunset Highway member[1]-------------						-Sweet Home Cr. mem-	
	715-2-2	715-2-3	715-4-1	3812-1-6	3812-1-7	3624-5-1	371-1-4	716-9-3
Median ($\emptyset$)\	2.7	2.35	0.4	2.8	2.7	2.6	3.5	0.35
Mean ($\emptyset$)	2.5	2.28	0.47	2.4	2.58	2.6	3.5	1.5
Std. Dev. (sorting)	0.96	0.86	1.06	1.43	0.75	0.72	1.1	1.51
Simple Sorting	1.7	1.6	2.0	1.75	1.32	1.25	1.73	1.80
Inclusive Graphic Skewness	-0.39	-0.15	0.24	-0.25	-0.19	0.04	-0.29	0.1
Simple Skewness	-1.5	-0.5	1.6	-0.6	-0.45	0.30	-0.85	1.6
Kurtosis	1.16	1.25	1.36	0.25	1.81	1.14	1.09	1.02
Coarsest 1% (mm)	2.38	1.68	2.5	0.5	0.70	0.87	0.62	2.8
Percent smaller than 4.5$\emptyset$	0.9	2.8	2.8	18.3	1.0	7.1	12.5	3.75

[1]Calculated without the grain fractions smaller than 4.5$\emptyset$

APPENDIX III: HEAVY MINERAL ANALYSES

Mineral	715-2-2 3φ	715-2-2 4φ	715-2-3 3φ	715-2-3 4φ	715-4-1 3φ	715-4-1 4φ	3812-1-6 3φ	3812-1-6 4φ	3812-1-7 3φ	3812-1-7 4φ	3626-5-1 3φ	3626-5-1 4φ	371-1-4 3φ	371-1-4 4φ	716-9-3 3φ	716-9-3 4φ
Amphiboles																
Hornblende					R						VR?				VR	
Lamprobolite		VR		R												
Actinolite														VR		
Tremolite				R-O												
Pyroxene																
Hypersthene	VR	R						VR	VR							
Augite	VR	VC	A	C	R	R			C	C	A	R				R
Diopside									?							
Micas																
Biotite	A				R		A	C	O				VA	A	O	C
Muscovite	VC				R		A	C	O	O	O		VA	VA	C	C
"Chlorite"	O							C		VR	R		C	C	C	C
Epidote																
Undiff.	O	A	VA	A				R	A-C	C	VC		VR	R	C	C
Zoisite									R							
Zircon																
Colorless		VR	VR	O		VR		R	O	O	C	C				R
Pink		R										R				
Garnet																
colorless	VR	O	R-O						O	C	C	R-O		VR	R	VR
pink		R										R				
Tourmaline																
brwn-grn									R	R	R	R				
Rutile					VR				VR	R						
Staurolite								VR		VR						
Opaques																
Fe-Ti oxides	C	O	C	C	A	A	C	O	C	C	C	O	C	C	C	O
Hematite	C	C	O	C	A	VA	C	O	C	C	O	O	C	C	C	VC
Pyrite and pyritized mat.	O	O	VC		VA	VA	R	O	VC	VC	C	C	C	O	VA	VA

Header spans: 715-2-2 through 3626-5-1 = Sunset Highway member; 371-1-4 and 716-9-3 = Sweet Home Cr. mem.

VA (very abundant) >45%, A (abundant) 25-45%, VC (very common) 15-25%, C (common) 10-15%,
O (occasional) 5-10%, R (rare) 1-5%, VR (very rare) <5%.

APPENDIX IV

MICROFOSSIL RECOVERY METHOD

I. Drying (4-8 samples can be run at a time)

    A. Select approximately 100 g. of the freshest

        sample

    B. Place sample in 1000 ml beaker

    C. Place beaker in oven set at 90°C and dry overnight.

II. Kerosene soak

    A. Remove <u>hot</u> beakers from the oven and place

        under the fume hood.

    B. Cover rock with kerosene (filtered if previously

        used in the process) and let soak for a minimum

        of 5 hours.

        1. The rock will not disaggregate during this

            process.

        2. The beakers do not have to be covered, but

            covering will reduce evaporation of kerosene.

III. Disaggregation

    A. Pour off the kerosene into a separate 1000 ml

        recovery beaker.

        1. Do all of the samples of the run.

        2. During this process, the kerosene can be

            filtered through a coffee filter into a

            sealable metal or plastic (not glass) con-

            tainer.

    B. Fill the beakers ½ full with hot tap water.

C. Place the beakers on a large hot plate (temperature set at 300-400° F) under the fume hood.

D. Add ½ tablespoon of sodium carbonate (Na_2CO_3) which goes by the commercial name of Calgon, or similar water softener.

1. The Na_2CO_3 flocculates the clay particles.

E. Heat for a period up to 3 hours. Some samples may be completely disaggregated within a few minutes; other samples will not dissolve at all and are probably cemented.

1. Let the samples cook until the rock has completely disaggregated, but not more than 3 hours.

2. Do not dissolve samples with HCl if the intention is to recover calcareous forams!

IV. Wet Sieving

A. Stack the 1∅, 2∅ and 4∅ (or 3.75∅) wet sieves on the sieve funnel in the sink.

1. Be sure to place the sieves in proper order.

B. Remove a sample from the hot plate and add a small amount of detergent to help cut the kerosene.

C. Stir the sample throughly to suspend all the particles and pour the slurry into the stack of sieves.

1. Wash each fraction thoroughly being careful not to overfill the smallest sieve.

2. A sample that is well-disaggregated will
tend to clog the 4∅ sieve. Be patient.
if the other 2 sieves are removed from the
stack and the 4 sieve sits undisturbed for
a few minutes, the very fine sand will settle
and only silt and clay will be left in
suspension. The suspended sediment can be
poured off carefully over the edge of the
sieve.

D. Once each sieve separate has been thoroughly
washed, label 3 paper towels with the sample
number and sieve size.

1. Tamp the sieve upside-down on the towel.

2. Fold the towel over and place in drying oven.

E. Wash the sieves thoroughly before sieving the
next sample.

F. Follow the above procedure for each sample of
the run.

V. Drying, storing, and examination .

A. Dry samples overnight at 90°C.

B. Transfer to plastic bags (or small vials) with
sample number and sieve separate clearly labeled.
It is a good idea to include a paper label in
the bag in case the ink rubs off.

C. Examine each separate for foraminifers. Crush
the 1∅ separate for nannofossil smear mounts.

APPENDIX V: FORAMINIFERA DATA

LOCATIONS OF FORAMINIFERA SAMPLES

SAMPLE		LOCATION
625-1-2	T. 4 N., R. 7 W.	NW 1/4 of NE 1/4 sec. 6. Road cut on N. side of U. S. 26 about 1/4 mi. E. of Elsie.
627-2-11	T. 4 N., R. 7 W.	SE 1/4 sec. 4. Road cut on spur off Fishhawk Falls about 1/2 mi. S. of Jewell Junction.
627-2-14	T. 4 N., R. 7 W	Same as 627-2-11.
629-6-1	T. 4 N., R. 7 W.	SW 1/4 of SE 1/4 sec. 4. About 3/4 mi. S. of Jewell Junction on spur road off Fishhawk Falls Highway.
73-4-1	T. 4 N., R. 7 W.	SW 1/4 of NW 1/4 sec. 5. Road cut along Nehalem River Road about 3/4 mi. S. of Elsie.
74-1-1	T. 4 N., R. 7 W.	NE 1/4 of SW 1/4 sec. 7. Road cut along Nehalem River Road about 1/2 mi. S. of bridge over Nehalem River.
74-4-1	T. 4 N., R. 7 W.	SW 1/4 sec. 7. Road cut along Nehalem River Road.
75-4-1	T. 4 N., R. 7 W.	NW 1/4 of NW 1/4 sec. 18. Road cut along Nehalem River Road about 1/4 mi. N. of Lukarilla.
77-11	T. 4 N., R. 7 W.	NE 1/4 of NE 1/4 sec. 17. Road cut on spur road off Lost Lake Road.
79-5-1	T. 4 N., R. 7 W.	NW 1/4 of SW 1/4 sec. 15. Road cut along August Fire Road.
716-6-2	T. 4 N., R. 7 W.	SE 1/4 of SE 1/4 sec 3. Road cut along U. S. 26 about 3/4 mi. W. of Quartz Creek bridge.
730-6-2	T. 4 N., R. 7 W.	SE 1/4 sec 5. Road cut along Luukinen Road.
730-6-5	T. 4 N., R. 7 W.	Same as 730-6-2.
829-1-1	T. 4 N., R. 7 W.	NE 1/4 of NW 1/4 sec. 9. River cut along Nehalem River 1/4 mi. S. of Quartz Creek confluence.
4327-6-1	T. 6 S., R. 6 W.	Sec. 52. River cut along Mill Creek under U. S. 22 bridge over Mill Creek.
73-4-10	T. 4 N., R. 7 W.	SW 1/4 of NW 1/4 sec. 5. Road cut along Nehalem River Road about 3/4 mi. S. of Elsie
829-1-2	T. 4 N., R. 7 W.	NE 1/4 of NW 1/4 sec. 9. River cut along Nehalem River 1/4 mi. S. of Quartz Creek confluence.
371-1-5	T. 4 N., R. 7 W.	SE 1/4 of SE 1/4 sec. 3. Road cut on U. S. 26 about 1 mi. W. of Quartz Creek bridge.
4220-1-1	T. 4 N., R. 7 W.	SW 1/4 sec. 17. Stream cut along Spruce Run Creek about 0.1 mi. S. of Spruce Run Lake.
4220-1-2	T. 4 N., R. 7 W.	Same as 4220-1-1.
4220-1-3	T. 4 N., R. 7 W.	Same as 4220-1-1.
4327-4-1	T. 6 S., R. 8 W.	Stream cut in Rock Creek S. of Grand Ronde.
73-4-5	T. 4 N., R. 7 W.	SW 1/4 of NW 1/4 sec 5. Road cut along Nehalem River Road about 3/4 mi. S. of Elsie.
716-9-2	T. 4 N., R. 7 W.	SW 1/4 sec. 3. Road cut along U. S. 26 about 1 mi. E. of Jewell Junction.
717-1-1	T. 4 N., R. 7 W.	NE 1/4 of SW 1/4 sec. 3. Stream cut in Osweg Creek along U. S. 26 about 3/4 mi. E. of Jewell Junction.

United States Department of the Interior

GEOLOGICAL SURVEY

Branch of Paleontology and Stratigraphy - M/S 915
345 Middlefield Road
Menlo Park, California 94025

Shipment No. 0-84-22M

July 16, 1984

Mr. Daniel Mumford
Department of Geology
Oregon State University
Corvallis, Oregon 97331

Dear Dan:

Enclosed is the foram analysis of your thesis samples.

Samples 716-6-2, 371-1-5, 716-9-2, and 717-1-1 are from a section I called Wolf Creek (McDougall, 1980). I originally interpreted the Refugian, Keasey Formation in this section as being deposited in the outer neritic biofacies. I now favor a slightly deeper interpretation, i.e., upper bathyal (200-500 m) and consider the presence of abundant outer species to be the result of turbidites or downslope creep. The presence of Uvigerina garzaensis and U. rustica in your sample 716-9-2 suggests that deposition may have occurred at even greater depths, i.e., middle bathyal (500 to 1200 m). The dominance of shallower water species in your samples as well as mine suggests that this area was subjected to considerable downslope transport.

Samples 629-6-1 and 627-2-11, 14 are from the section I called Castor Creek (McDougall, 1980) and interpreted as upper bathyal (200 to 600 m). Unfortunately your samples have been strongly dissolved and thus provide no new information.

The Yamhill Formation samples are in the same age range as the Cowlitz and Keasey Formations. It is difficult to do a more precise comparison from spot samples.

Good luck with your thesis. Please send me a copy.

Sincerely,

Kristin McDougall

Attachment

APPENDIX V cont.

Hamlet formation

(COWLITZ FORMATION)

Field Number 74-1-1. T. 4 N., R. 7 W., NE 1/4 of SW 1/4 sec. 7. Road cut
along Nehalem River Road about 1/2 mi. S. of bridge over Nehalem River.

Sample is strongly weathered. "Specimens" present resemble benthic
foraminifers: Bathysiphon eocenica, Cyclammina pacifica, Globobulimina
pacifica, Lenticulina spp., and Praeglobobulimina pupoides, and planktic
foraminifers.

No age or environmental interpretation is made on this fauna.

Field Number 74-4-1. T. 4 N., R. 7 W. SW 1/4 sec. 7. Road cut along Nehalem
River Road.

Benthic foraminifers:
Bathysiphon eocenica Cushman and Hanna
Chilostomella oolina Schwager
Cyclammina pacifica Beck
Lenticulina rotulata Lamarck
Martinottiella communis (d'Orbigny)
Nodosaria longiscata d'Orbigny
Diatoms
Radiolarians

Age and Ecology: Eocene-Oligocene, probably late Eocene; bathyal or
deeper (200-2000 m).

Field Number 75-4-1. T. 4 N., R. 7 W. NW 1/4 of NW 1/4 sec. 18. Road cut
along Nehalem River Road about 1/4 mi. N. of Lukarilla.

Benthic foraminifers:
Globobulimina pacifica Cushman
Trochammina globigeriniformis (Parker and Jones)
Megafossil fragments

Age and Ecology: Probably late Eocene; ecology unknown.

Field Number 77-11. T. 4 N., R. 7 W. NE 1/4 of NE 1/4 sec. 17. Road cut on
spur road off Lost Lake Road.

Benthic foraminifers:
Cyclammina pacifica Beck

Age and Ecology: Probably late Eocene; ecology unknown.

APPENDIX V cont.

Field Number 79-5-1. T. 4 N., R. 7 W. NW 1/4 of SW 1/4 sec. 15. Road cut
    along August Fire Road.

    Benthic foraminifers:
        Bathysiphon eocenica Cushman and Hanna
        Cyclammina pacifica Beck

Age and Ecology: probably late Eocene; ecology unknown.

Field Number 371-1-5. T. 4 N., R. 7 W. SE 1/4 of SE 1/4 sec. 3. Road cut on
    U.S. 26 about 1 mi. W. of Quartz Creek bridge.

    Benthic foraminifers:
        Alabamina wilcoxensis californica Mallory
        Bathysiphon eocenica Cushman and Hanna
        Caucasina schencki (Beck)
        Cibicides fortunatus Martin
        Cyclammina pacifica Beck
        Globocassidulina globosa (Hantken)
        Lenticulina sp.
        Lenticulina welchi (Church)
        Marginulina subbullata Hantken
        Nodosaria longiscata d'Orbigny
        Plectofrondicularia packardi Cushman and Schenck
        Praeglobobulimina pupoides (d'Orbigny)
        Pseudonodosaria conica (Neugeboren)
        Quinqueloculina imperialis Hanna and Hanna
        Quinqueloculina weaveri Rau
        Stilostomella lepidula (Schwager)
        Trochammina globigeriniformis (Parker and Jones)
        Vaginulinopsis nudicostata (Cushman and Hanna)

Age and Ecology: Late Narizian to early Refugian, late Eocene; outer neritic
    depths (100 to 200 m) or deeper.

Field Number 627-2-11. T. 4 N., R. 7 W. SE 1/4 sec. 4. Road cut on spur off
    Fishhawk Falls about 1/2 mi. S. of Jewell Junction.

    Benthic foraminifers:
        Bathysiphon eocenica Cushman and Hanna
        Bifarina eleganta (Plummer)
        Cyclammina pacifica Beck

Age and Ecology: Narizian, late Eocene; ecology unknown.

Field Number 627-2-14. T. 4 N., R. 7 W. Same as 627-2-11.

    Benthic foraminifers:
        Ammodiscus incertus (d'Orbigny)

APPENDIX V cont.

Benthic foraminifers (continued):
     Bathysiphon eocenica Cushman and Hanna
Ostracodes

Age and Ecology: Probably late Eocene; ecology unknown.

Field Number 629-6-1. T. 4 N., R. 7 W. SW 1/4 of SE 1/4 sec. 4. About 3/4
    mi. S. of Jewell Junction on spur road off Fishhawk Falls Highway.

    Benthic foraminifers:
        Bathysiphon eocenica Cushman and Hanna
        Cyclammina pacifica Beck

Age and Ecology: Probably late Eocene; ecology unknown.

Field Number 716-6-2. T. 4 N., R. 7 W. SE 1/4 of SE 1/4 sec. 3. Road cut
    along U.S. 26 about 3/4 mi. W. of Quartz Creek Bridge.

    Benthic foraminifers:
        Bathysiphon eocenica Cushman and Hanna
        Cyclammina pacifica Beck
        Lenticulina inornata (d'Orbigny)
        Nodosaria longiscata d'Orbigny
        Quinqueloculina imperialis Hanna and Hanna
        Stilostomella advena (Cushman and Laiming)
        Trochammina globigeriniformis (Parker and Jones)
    Megafossil fragments

Age and Ecology: Late Narizian to early Refugian, late Eocene; outer neritic
    depths (100 to 200 m).

Field Number 716-9-2. T. 4. N., R. 7 W. SW 1/4 sec. 3. Road cut along U.S.
    26 about 1 mi. E. of Jewell Junction.

    Benthic foraminifers:
        Alabamina wilcoxensis californica Mallory
        Allomorphina trigona Reuss
        Caucasina schencki (Beck)
        Ceratobulimina washburnei Cushman and Schenck
        Chilostomella ovoidea Reuss
        Cibicidina walli (Bandy)
        Cyclammina pacifica Beck
        Dentalina cocoaensis (Cushman)
        Eponides mexicanus (Cushman)
        Globobulimina pacifica Cushman
        Globocassidulina globosa Hantken
        Guttulina irregularis (d'Orbigny)
        Hoeglundina eocenica (Cushman and Hanna)
        Karreriella chapapoensis monumentensis Mallory

APPENDIX V cont.

Benthic foraminifers (continued):
      Karreriella washingtonensis Rau
      Lenticulina chehalisenis (Rau)
      Lenticulina inornata (d'Orbigny)
      Lenticulina lincolnensis (Rau)
      Lenticulina cf. L. pseudorotulata (Asano)
      Lenticulina texana (Cushman and Applin)
      Lenticulina welchi (Church)
      Marginulina subbullata Hantken
      Nodosaria longiscata d'Orbigny
      Nodosaria pyrula d'Orbigny
      Nodosaria spp.
      Plectofrondicularia vaughani Cushman
      Pseudonodosaria inflata (Costa)
      Quinqueloculina imperialis Hanna and Hanna
      Saracenaria hantkeni (Cushman)
      Trifarina hannai (Beck)
      Trochammina globigeriniformis (Parker and Jones)
      Uvigerina garzaensis Cushman and Siegfus
      Uvigerina rustica Cushman and Edwards
      Vaginulinopsis nudicostata (Cushman and Hanna)
   Planktic foraminifers
   Radiolarians
   Megafossil fragments
   Fish debris

Age and Ecology: Late Narizian-early Refugian, late Eocene; middle bathyal depths (500 to 1200 m) with considerable amounts of transported outer shelf material.

Field Number: 717-1-1. T. 4 N., R. 7 W. NE 1/4 of SW 1/4 sec. 3. Stream cut in Osweg Creek along U.S. 26 about 3/4 mi. E. of Jewell Junction.

   Benthic foraminifers:
      Alabamina wilcoxensis Mallory
      Allomorphina trigona Reuss
      Bathysiphon eocenica Cushman and Hanna
      Boldia hodgei (Cushman and Schenck)
      Bulimina sculptilis lacinata Cushman and Parker
      Caucasina schencki (Beck)
      Ceratobulimina washburnei Cushman and Schenck
      Cyclammina pacifica Beck
      Cyclammina sp.
      Dentalina consobrina d'Orbigny
      Dorothia sp.
      Globobulimina pacifica Cushman
      Globocassidulina globosa (Hantken)
      Guttulina irregularis (d'Orbigny)
      Karreriella washingtonensis Rau
      Lenticulina budensis (Hantken)
      Lenticulina chehalisensis (Rau)

APPENDIX V cont.

Benthic foraminifers (continued):
        Lenticulina inornata (d'Orbigny)
        Lenticulina rotulata Lamarck
        Lenticulina texana (Cushman and Applin)
        Nodosaria longiscata d'Orbigny
        Plectofrondicularia packardi Cushman and Schenck
        Plectofrondicularia vaughani Cushman
        Quinqueloculina imperialis Hanna and Hanna
        Sigmoilina tenuis (Czyzek)
        Trifarina hannai (Beck)
        Vaginulinopsis nudicostata (Cushman and Hanna)
Echinoid Spines
Fish debris
Micromollusks

Age and Ecology: Late Narizian-early Refugian, late Eocene; species present indicate outer neritic to upper bathyal (100-500 m), however, the stratigraphic sequence including 716-6-2, 371-1-5, 716-9-2, and 717-1-1, was probably deposited at middle bathyal depths (500 to 1200 m) during the early Refugian.

Field Number 730-6-2. T. 4 N., R. 7 W. SE 1/4 sec. 5. Road cut along Luukinen Road.

    Benthic foraminifers:
        Bathysiphon eocenica Cushman and Hanna
        Cyclammina pacifica Beck

Age and Ecology: Unknown.

Field Number 730-6-5. T. 4 N., R. 7 W. Same as 730-6-2.

    Benthic foraminifers:
        Bathysiphon eocenica Cushman and Hanna
        Cyclammina pacifica Beck
        Dorothia sp.
        Textularia adalta Cushman

Age and Ecology: Late Eocene, latest Narizian to earliest Refugian; ecology unknown.

Field Number 829-1-1. T. 4 N., R. 7 W. NE 1/4 of NW 1/4 sec. 9. River cut along Nehalem River 1/4 mi. S. of Quartz Creek confluence.

    Benthic foraminifers:
        Bathysiphon eocenica Cushman and Hanna
        Cyclammina pacifica Beck

Age and Ecology: Probably late Eocene; ecology unknown.

APPENDIX V cont.

Field Number 829-1-2. T. 4 N., R. 7 W. NE 1/4 of NW 1/4 sec. 9. River cut
    along Nehalem River 1/4 mi. S. of Quartz Creek confluence.

    Benthic foraminifers:
        Bathysiphon sp.
        Boldia hodgei (Cushman and Schenck)
        Chilostomella oolina Schwager
        Chilostomella ovoidea Reuss
        Cyclammina pacifica Beck
        Dentalina communis (d'Orbigny)
        Fursenkoina bramletti (Galloway)
        Lenticulina rotulata Lamarck
        Marginulina subbullata Hantken
        Nodosaria longiscata d'Orbigny
        Oridorsalis umbonatus (Reuss)
        Planulina markleyana Church
        Praeglobobulimina pupoides (d'Orbigny)
        Stilostomella advena (Cushman and Laiming)
    Planktic foraminifers

Age and Ecology: Refugian, late Eocene; upper bathyal (200-500 m) or deeper.

Field Number 4220-1-1. T. 4 N., R. 7 W. SW 1/4 sec. 17. Stream cut along
    Spruce Run Creek about 0.1 mi. S. of Spruce Run Lake.

    Benthic foraminifers:
        Alabamina wilcoxensis californica Mallory
        Cibicides fortunatus Martin
        Gyroidina soldanii octocamerata Cushman and Hanna
        Lenticulina rotulata Lamarck
        Nodosaria longiscata d'Orbigny
        Plectofrondicularia packardi Cushman and Schenck
        Praeglobogulimina pupoides (d'Orbigny)
        Spiroloculina texana Cushman and Ellisor
        Uvigerina garzaensis Cushman and Siegfus
    Planktic foraminifers
    Ostracodes
    Diatoms

Age and Ecology: Refugian, late Eocene; middle bathyal (500 to 1200 m).

Field Number 4220-1-2. T. 4 N., R. 7 W. Same as 4220-1-1.

    Benthic foraminifers:
        Alabamina wilcoxensis californica Mallory
        Boldia hodgei (Cushman and Schenck)
        Caucasina schencki (Beck)
        Cycalammina pacifica Beck
        Fissurina marginata (Montagu)
        Globocassidulina globosa (Hantken)

APPENDIX V cont.

Benthic foraminifers (continued):
     Guttulina irregularis (d'Orbigny)
     Gyroidina soldanii octocamerata Cushman and Hanna
     Hoeglundina eocenica (Cushman and Hanna)
     Lagena costata (Williamson)
     Nodosaria longiscata d'Orbigny
     Nodosaria pyrula d'Orbigny
     Nonion halkyardi Cushman
     Plectofrondicularia packardi Cushman and Schenck
     Plectofrondicularia vaughani Cushman
     Praeglobobulimina ovata (d'Orbigny)
     Praeglobobulimina pupoides (d'Orbigny)
     Pseudonodosaria inflata (Costa)
     Spiroloculina texana Cushman and Ellisor
     Spiroplectammina richardi Martin
     Stilostomella adolphina (d'Orbigny)
     Uvigerina garzaensis Cushman and Siegfus
Planktic foraminifers
Ostracodes
Radiolarians

Age and Ecology: Refugian, late Eocene; middle bathyal (500 to 1200 m) or deeper.

Field Number 4220-1-3. T. 4 N., R. 7 W. Same as 4220-1-1.

Benthic foraminifers:
     Ammodiscus incertus (d'Orbigny)
     Allomorphina trigona (Reuss)
     Bolivina kleinpelli Beck
     Caucasina schencki (Beck)
     Globocassidulina globosa (Hantken)
     Lenticulina sp.
     Nodosaria longiscata d'Orbigny
     Plectofrondicularia packardi Cushman and Schenck
     Praeglobobulimina pupoides (d'Orbigny)
     Valvulineria jacksonensis welcomensis Mallory
Planktic foraminifers
Diatoms
Radiolarians
Megafossil fragments

Age and Ecology: Refugian, late Eocene; upper bathyal (200 to 500 m) or deeper.

APPENDIX V cont.

KEASEY FORMATION

Field Number 73-4-1. T. 4 N., R. 7 W. SW 1/4 of NW 1/4 sec. 5. Road cut
    along Nehalem River Road about 3/4 mi. S. of Elsie.

    Benthic foraminifers:
        Bathysiphon eocenica Cushman and Hanna
        Fursenkoina bramletti (Galloway and Morrey)
        Globobulimina pacifica Cushman
        Marginulina exima Neugeboren
        Nodosaria sp.
        Planulina sp.
        Uvigerina garzaensis Cushman and Siegfus

Age and Ecology: Eocene; middle bathyal (500 to 1200 m).

Field Number 73-4-5. T. 4 N., R. 7 W. SW 1/4 of NW 1/4 sec 5. Road cut
    along Nehalem River Road about 3/4 mi. S. of Elsie.

    Benthic foraminifers:
        Alabamina wilcoxensis californica Mallory
        Allomorphina trigona (Reuss)
        Bifarina eleganta (Plummer)
        Cyclammina pacifica Beck
        Dentalina cocoaensis (Cushman)
        Dentalina consobrina d'Orbigny
        Dentalina dusenburyi Beck
        Globocassidulina globosa (Hantken)
        Gyroidina condoni (Cushman and Schenck)
        Gyroidina soldanii octocamerata Cushman and Hanna
        Hoeglundina eocenica (Cushman and Hanna)
        Lenticulina budensis (Hantken)
        Lenticulina inornata (d'Orbigny)
        Lenticulina limbosa hockleyensis (Cushman and Applin)
        Lenticulina rotulata Lamarck
        Lenticulina terryi (Coryell and Embich)
        Marginlina exima Neugeboren
        Marginlina subbullata Hantken
        Nodosaria longiscata d'Orbigny
        Nodosaria pyrula d'Orbigny
        Orthomorphina rohri (Cushman and Stainsforth)
        Plectofrondicularia packardi Cushman and Schenck
        Plectofrondicularia packardi multilineata Cushman and Simonson
        Plectofrondicularia vaughani Cushman
        Praeglobobulimina pupoides (d'Orbigny)
        Pseudonodosaria inflata (Costa)
        Pullenia salisburyi Stewart and Stewart
        Spiroplectammina richardi Martin
        Stilostomella adolphina (d'Orbigny)
        Stilostomella lepidula (Schwager)

Benthic foraminifers (continued):
    Trochammina sp.
    Uvigerina garzaensis Cushman and Siegfus
    Valvulineria jacksonensis welcomensis Mallory
Planktic foraminifers
Radiolarians
Fish debris

Age and Ecology: Late Narizian to early Refugian, late Eocene; lower middle to lower bathyal (1200 to 2000 m) with considerable transported shelf and upper slope species.

Field Number 73-4-10. T. 4 N., R. 7 W. SW 1/4 of NW 1/4 sec. 5. Road cut along Nehalem River Road about 3/4 mi. S. of Elsie.

Benthic foraminifers:
    Alabamina wilcoxensis californica Mallory
    Caucasina schencki (Beck)
    Cibicides fortunatus Martin
    Cyclammina pacifica Beck
    Gyroidina soldanii octocamerata Cushman and Hanna
    Hoeglundina eocenica (Cushman and Hanna)
    Lenticulina inornata (d'Orbigny)
    Lenticulina rotulata Lamarck
    Nodosaria delicata Martin
    Nodosaria jacksonensis Cushman
    Nonion halkyardi Cushman
    Orthomorphina rohri (Cushman and Stainsforth)
    Praeglobobulimina pupoides (d'Orbigny)
    Spiroplectammina richardi Martin
    Stilostomella adolphina (d'Orbigny)
    Stilostomella lepidula (Schwager)
    Trochammina sp.
    Uvigerina garzaensis Cushman and Siegfus
    Valvulineria jacksonensis welcomensis Mallory
Planktic foraminifers
Radiolarians
Fish debris

Age and Ecology: Late Narizian to early Refugian, late Eocene; lower middle to lower bathyal (1200 to 2000 m) with considerable transported shelf and upper slope species.

Field Number 625-1-2. T. 4 N., R. 7 W. SW 1/4 of NE 1/4 sec. 6. Road cut on N. side of U.S. 26 about 1/4 mi. E of Elsie.

Benthic foraminifers:
    Budashevaella multicameratus (Voloshinova)
    Haplophragmoides sp.
    Martinottiella communis (d'Orbigny)

APPENDIX V cont.

Benthic foraminifers (continued):
    Nodosaria longiscata d'Orbigny
    Nodosaria sp. ·
    Pseudonodosaria inflata (Costa)
Radiolarians
Megafossil fragments

Age and Ecology: Probably late Eocene; ecology unknown.

YAMHILL FORMATION

Field Number 4325-4-1. T. 6 S., R. 8 W. Stream cut in Rock Creek S. of Grand
    Ronde.

Benthic foraminifers:
    Bathysiphon eocenica Cushman and Hanna
    Bulimina sculptilis lacinata Cushman and Parker
    Cyclammina pacifica Beck
    Gyroidina soldanii octocamerata Cushman and Hanna
    Lenticulina welchi (Church)
    Nodosaria longiscata d'Orbigny
    Nodosaria pyrula d'Orbigny
    Planulina markleyana Church
    Plectofrondicularia packardi Cushman and Schenck
    Praeglobobulimina pupoides (d'Orbigny)
    Stilostomella advena (Cushman and Laiming)
    Uvigerina garzaensis Cushman and Siegfus
Ostracodes
Radiolarians
Echinoid Spines

Age and Ecology: Late Narizian to early Refugian, late Eocene; middle bathyal
    (500 to 1200 m).

Field Number 4327-6-1. T. 6 S., R. 6 W. Sec. 52. River cut along Mill Creek
    under U.S. 22 bridge over Mill Creek.

Benthic foraminifers:
    Amphimorphina jenkinsi (Church)
    Bulimina sculptilis lacinata Cushman and Parker
    Dentalina consobrina d'Orbigny
    Lenticulina cf. L. pseudorotulata (Asano)
    Lenticulina welchi (Church)
    Nodosaria longiscata d'Orbigny

Age and Ecology: Narizian, late Eocene; upper bathyal (200 to 500 m)

APPENDIX V cont.

BIOSTRATIGRAPHIC AND PALEOECOLOGIC DETERMINATIONS
FOR DAN MUMFORD ASSEMBLAGES, OSU
BY W.W. RAU

Sample

#371-1-5   A good general Narizian fauna – is best referred to a
middle to upper part of the stage.

The fauna contains a mix of outer shelf and middle
bathyal taxa. I suggest a middle bathyal environment
for final deposition.

#627-2-11   Not diagnostic for age.
Possibly represent a general bathyal environment of
deposition.

#627-2-14   Non-diagnostic

#629-6-1   Non-diagnostic

#716-6-2   Probably a Narizian fauna but not greatly diagnostic,
generally a bathyal fauna.

#716-9-2   A diagnostic Narizian assemblage that usually occurs
in rocks referred to an upper part of the stage.

This is a fairly diagnostic upper bathyal fauna.
(150-500m)

#717-1-1   A diagnostic assemblage for a high position in the
Narizian stage.

The assemblage suggests mixed depth ranges from outer
shelf to lower middle bathyal conditions – I suggest
an upper middle bathyal depth of final deposition
based on abundance of taxa.

#730-6-2   Non-diagnostic

#730-6-5   Non-diagnostic

#829-1-1   Non-diagnostic

#829-1-2   A diagnostic Narizian assemblage – probably a middle
to lower part of the stage.

Water depths suggested by this assemblage were at
least as great as upper bathyal. Minor elements
suggest even greater depths, possibly to lower middle
bathyal conditions.

#74-1-1   Essentially non-diagnostic of age.
Probably generally a bathyal assemblage.

#74-4-1   Essential non-diagnostic of age, generally a bathyal
assemblage.

APPENDIX V cont.

Sample

#75-4-1   Non-diagnostic

#77-11   Non-diagnostic

#79-5-1   Non-diagnostic

#4220-1-1   A fairly diagnostic late Narizian assemblage
Diagnostic of upper to upper middle bathyal conditions.

#4220-1-2   A Narizian assemblage, probably from an upper part.
A bathyal assemblage, most likely upper to upper
middle bathyal.

#4220-1-3   A Narizian assemblage, probably upper.
A bathyal assemblage, probably an upper part.

#625-1-2   Non-diagnostic

#73-4-1   This sample is badly weathered. The forams are badly
altered and positive identification is not possible.
Thus, the fauna is not very diagnostic, it probably is
Narizian.

It is most likely a bathyal assemblage in general.

#73-4-10   This is a late Narizian assemblage. It may be as
young as the Refugian but it contains nothing to
confirm that young an age.

A bathyal assemblage, probably from well down, middle
to possible lower bathyal.

#73-4-5   Although this is a rather large assemblage, it is not
completely diagnostic of age. It is best referred to
a late part of the Narizian stage but could be as
young as the Refugian stage.

#73-4-5 (cont) The assemblage distinctly represents bathyal
conditions at least as deep as middle bathyal depths.

#4327-4-1   This assemblage is typical of the Narizian stage in
general, but is not particularly characteristic of a
specific part. It is likely from a middle or upper
part but not lower.

The assemblage indicates fairly deep water of
deposition - probably at least as deep as lower middle
bathyal depths.

#4327-6-1   This small assemblage indicates a middle or lower
Narizian age.

Water depths were at least as deep as lower middle
bathyal.

APPENDIX V cont.

General Remarks:

Regarding the two assemblages from the type Yamhill Fm. (#4327-4-1 and #4327-6-1) and other known Yamhill assemblages compared to the "Cowlitz" assemblage of this report.

Usually "Cowlitz" faunas can be distinguished from those of the Yamhill Fm., but not always. Of the two Yamhill faunas of this report, only one (#4337-6-1) is distinctive from Cowlitz fauna and can be recognized as a Yamhill, lower or middle Narizian fauna. Also, none of the assemblages of the report that are referred to the "Cowlitz" Fm. contain any found elements that are known only in Yamhill faunas, so this is no problem with them being Cowlitz rather than Yamhill. I should point out, however, that without certain found elements in an assemblage, Cowlitz assemblages can not be distinguished from Yamhill faunas.

Regarding the four assemblages from the Keasey formation - I am surprised to find essentially nothing in them that would place them in the Refugian Stage. They simply lack any taxa normally confined to Refugian and younger strata. Therefore, they are best compared to known late Narizian assemblage.

W. W. Rau

APPENDIX V cont.

AGREEMENT OF FORAM CALLS BY
KRISTIN McDOUGALL AND WELDON RAU
FOR DANIEL MUMFORD'S THESIS AREA.

SAMPLE	#IO's at least to Genus level		# agreements	# IO's to Genus cf. G. species level		# agreements	# IO's to Genus species level		# agreements	# IO's to Genus species subspecies level		# agreements
	UR	KM		UR	KM		UR	KM		UR	KM	
371-1-5	18	16	10	16	16	9	11	16	4	0	1	0
627-2-11	5	3	1	3	3	1	1	3	0	0	0	0
627-2-14	1	2	1	1	2	1	0	2	0	0	0	0
629-6-1	2	2	2	1	2	1	0	2	2	0	0	0
716-6-2	7	7	4	4	7	2	1	7	1	0	0	0
716-9-2	19	33	16	16	32	11	13	31	11	1	2	1
717-1-1	17	27	14	16	25	8	12	25	8	1	1	0
730-6-2	2	2	2	1	2	1	0	2	0	0	0	0
730-6-5	3	4	2	1	3	1	0	3	0	0	0	0
829-1-1	2	2	2	1	2	1	0	2	0	0	0	0
829-1-2	13	14	6	11	13	1	5	13	1	1	0	0
74-1-1	5	5	4	4	4	2	3	4	1	0	0	0
74-4-1	3	6	2	2	6	1	1	6	0	0	0	0
75-4-1	2	2	1	1	2	1	1	2	1	0	0	0
77-11	1	1	1	0	1	0	0	1	0	0	0	0
79-5-1	2	2	2	1	2	1	0	2	0	0	0	0
4220-1-1	11	9	7	9	9	2	6	9	1	0	2	0
4220-1-2	16	22	12	13	22	7	10	22	7	1	2	1
4220-1-3	8	10	5	6	9	1	4	9	1	0	1	0
625-1-2	4	6	1	0	4	0	0	4	0	0	0	0
73-4-1	6	7	3	3	5	2	2	5	2	0	0	0
73-4-10	11	19	10	10	18	5	8	18	4	2	3	1
73-4-5	22	33	15	18	32	11	13	32	9	3	5	2
4327-4-1	15	12	8	12	12	3	8	12	3	1	2	0
4327-6-1	6	6	5	6	6	2	4	5	2	0	1	0

APPENDIX VI: COCCOLITH DATA

LOCATIONS OF COCCOLITH SAMPLES

SAMPLE   LOCATION

716-9-4   T. 4 N., R. 7 W.   SW 1/4 sec. 3. Road cut along U. S. 26 about 1 mi. east of Jewell Junction.

717-1-1   T. 4 N., R. 7 W.   NE 1/4 of SW 1/4 sec 3. Stream cut in Osweg Creek along U. S. 26 about 3/4 mi. of Jewell Junction.

4220-1-3   T. 4 N., R. 7 W.   SW 1/4 sec. 17. Stream cut along Spruce Run Creek about 0.1 mi. south of Spruce Run Lake.

829-2-2   T. 4 N., R. 7 W.   NE 1/4 of NW 1/4 sec. 9. River cut along Nehalem River 1/4 mi. south of Quartz Creek confluence.

73-4-13   T. 4 N., R. 7 W.   SW 1/4 of NW 1/4 sec. 5. Road cut along Nehalem River Road about 3/4 mi. south of Elsie.

371-1-6   T. 4 N., R. 7 W.   SE 1/4 of SE 1/4 sec. 3. Road cut along U. S. 26 about 1 mi. west of Quartz Creek bridge.

APPENDIX VI cont.

**UNITED STATES
DEPARTMENT OF THE INTERIOR**
GEOLOGICAL SURVEY
La Jolla Marine Geology Laboratory (A-015)
Scripps Institution of Oceanography
La Jolla, California 92093

May 1, 1984

Daniel Mumford
Department of Geology
Oregon State University
Corvallis, Oregon 97331

Dear Mr. Mumford:

Three of the six samples from northwest Oregon contain coccoliths which are guides
to the late middle Eocene or late Eocene. All of the assemblages contain pentalith
taxa which indicate relatively shallow-water deposition. Key zonal taxa of
Chiasmolithus, Discoaster, and Helicosphaera are essentially absent. The three
best samples (716-9-4, 717-1-1, and 829-2-2) contain Pemma stradneri Chang which
is limited to late middle Eocene or early late Eocene and has previously been
reported from the Tillamook Volcanic Series. The sample results are summarized
below:

Sample	Age	Remarks
73-4-13	Late mid Eocene to earliest Oligocene	Sparse assemblage dated by the overlap of Dictyococcites bisectus (Hay et al.) and Reticulofenestra reticulata (Gartner et Smith).
371-1-6	Mid Eocene to early Oligocene	Sparse assemblage dated by the overlap of Dictyococcites scrippsae Bukry et Percival and Pemma sp.
716-9-4	Late mid Eocene or late Eocene	The presence of Reticulofenestra umbilica (Levin), with Lanternithus minutus Stradner, and Pemma stradneri Chang indicates the age for this moderately diverse shallow-water assemblage.
717-1(-1) -2	Late mid Eocene or late Eocene	Similar to 716-9-4 with L. minutus, P. stradneri, one eight-rayed Discoaster nodifer (Bramlette et Riedel).
829-2-2	Late mid Eocene or late Eocene	Contains Dictyococcites bisectus, Pemma papillatum Martini, P. stradneri, and Sphenolithus spiniger Bukry.
4220-1-3	Late mid Eocene to Oligocene	Low diversity assemblage with D. bisectus.

Sincerely yours,

David Bukry

APPENDIX VII: MACROFOSSIL DATA

memorandum

DATE: May 7, 1984

REPLY TO
ATTN OF: Ellen J. Moore

SUBJECT: Examination and Report
Shipment No. WRG-84-9M

TO: Alan Neim (WRG) and Daniel Mumford

All samples are supposedly from the Cowlitz Formation (Eocene), Clatsop County, Oregon, and have been returned.

· 627-2: Pelecypods: Unidentified nuculanid
LUCINOMA? sp.

Undeterminable and/or unidentified micromollusks and molluscan

fragments; possible fecal pellets also present.

· 627-2-1: Unidentified gastropod

· 627-1-1: Unidentified echinoid

· 627-2-3: Unidentified gastropod

·627-2-10: Coral: BALANOPHYLLIA? sp.

Age: Note that B. cf. VARIABILIS Nomland is found in the Gries Ranch

Formation and that coral has not been found in the Cowlitz Formation.

Habitat: Scleractinid corals are exclusively marine with little or no

tolerance for other than normal salinity and are commonest in warm,

clear, shallow water of the tropical zone (Wells, J. W., 1956, _in_ Moore,

R. C., Treatise). Echinoids are strictly marine.

. 629-6: Unidentified pelecypod
Echinoid spine?

· 79-10: Unidentified organic remains

· 715-4-2: Crab: RANOIDES sp.

RANINOIDES is a sand crab. Sand crabs live on the shore in wave-washed

sand. They burrow into the sand just below the surface with the eye

stalks extending into the water.

· 719-4: Pelecypod: BRACHIDONTES n. sp.?
CHLAMYS? sp.

APPENDIX VII cont.

·719-4-1: Unidentified

·719-4-2: Pelecypod: BRACHIDONTES n. sp. ?

·719-4-3: Unidentified

·719-4-4: Pelecypod: CHLAMYS? sp.
           Gastropod: Unidentified fissurellid

·719-4-5: Unidentified fragment of gastropod

    Age: This is not the BRACHIDONTES commonly found in the Cowlitz
    Formation. Are you certain of the stratigraphic position of these
    samples?

    Habitat: BRACHIDONTES is intertidal on rocks to 30 meters; some forms

    prefer slightly brackish water; both epifaunal and infaunal; some

    species with weak byssal attachment, partly or entirely buried in soft

    sediment.

·729-6: Unidentified trace fossil; burrow?

·729-8: Gastropod: CREPIDULA sp.
                     CALYPTRAEA? sp.
         Pelecypod: Unidentified oysters
                     CHLAMYS? sp

    Habitat: CREPIDULA lives intertidally to about 100 meters attached to

    rocks or shells.

·729-8-1: Unidentified

·371-1: Pelecypod: Nuculanid?
         Gastropod: Unidentified naticids

    Note: One large foram could be seen without magnification other than x10

    lens.

·730-6-1: Pelecypod: PITAR? (LAMELLICONCHA?) sp.

    Habitat: Living eastern Pacific series assigned to LAMELLICONCHA live in

    warm water (southern California and south) and depths of intertidal to

    110 meters, with more species in the intertidal to 50 meter range.

·829-1: Unidentified

APPENDIX VII cont.

· 829-2: Unidentified gastropod fragment
          Forams

.829-2-1: Probably a burrow, not bone

CS SE-8: Unidentified oyster?

43-1: Pelecypod: MARCIA (MERCIMONIA?) cf. BUNKERI M. A. Hanna

   Habitat: The subgenus is extinct.

716-9-2: Unidentified

627-2-11: Lost in transit. Always crimp metal ends of slides to keep glass

   cover in place. The preservation of most all of these samples is such

   that the age can neither be substantiated nor refuted.

          Ellen J. Moore

APPENDIX VII cont.

DAN MUMFORD'S RANINID CRAB COLLECTED S.W. OF PORTLAND AREA

The specimen is a large Raninid moult; the tips of all the anterior and antero-lateral teeth missing; chelipeds and periopods missing---only the coxae remain. The carapace is fractured; an approximation of its length is 51 m.m., and its width is 30 m.m.

CARAPACE

Typically raninid; L/W = 1.70

Convexity: Longitudinal direction--posterior slightly convex to nearly flat; anteriorly more convex.
Transverse direction--very convex.
Surface decoration; Most of original integument missing except for small patches along anterolateral & frontal margins. Smallareas along the R.H. anterolateral margin & L.H. anterior--immediately behind the orbital & outerorbital teeth--contain numerous punctae with heavy granulation between.
The branchiocardiac grooves not preserved; no evidence of a post-frontal ridge.
Rostrum: Tip missing; base very broad, with a shorter& sharply-tipped basal tooth on each side.   SLIGHTLY
Orbital teeth: Apparently broad and flat--broader at the base than the antero-lateral teeth. They appear to have been bispinous
Outerorbital teeth: Bispinous, with the inner spine circular in cross-section.
Anterolateral teeth: Although the tips of these teeth are missing, the re-maining stubs are broad at the base, elliptical in cross-section.
These teeth appear to have extended more forward than outward.
Sinuses: Of the two frontal sinuses, the outer (distal) extends father back than the inner (proximal); the posterior ends of both terminating in shallow gutters. The inner sinuses are parallel to the median--- the outer are slightly convergent anteriorly.
Posterior margin: Nearly straight.

STERNUM

Pterygostomial region: Inflated
Periopods: Missing; only the coxae remain. The first periopods are closer to chelipeds than to second periopods. Diameters of first & second per-iopods approximately equal at the coxa. Diameter of third periopod approx. half that of the first & second. Diameter of fourth indeter-minate.
Chelipeds: Missing. Diameter at coxae approx a third larger than for periopods #1 & #2
Sternites: Sternites #1 - #3 covered by matrix, but like #4 are probably flat and smooth. A deep groove that begins at the posterior end of stern-ite #4 extends along the sternal median through sternite #6.
Abdomen: Not preserved.

APPENDIX VII cont.

ANALYSIS

1. The transverse convexity of the carapace isnt sufficient to correspond to either <u>Raninoides</u> <u>vaderensis</u> or R. <u>lewisanus</u>, although the L/W relationship is in the range for both.

2. The backward extension of the two frontal sinuses differs from those for R. washburnei and R. eugenensis. Inthose two species the inner extends farther backward. Also, the L/W relationship for R. <u>washburnei</u> is 1.45, and for R. <u>eugenensis</u> is 1.65.

3. The anterolateral teeth of R. <u>asper</u> extend more outward than forward; for this specimen they appear to have extended more forward than outward.

4. The carapace surface of R. <u>asper</u> is smooth---with no punctae or gramula-tion

5. There is no indication of a post frontal ridge as for R. oregonensis.

In consideration of items #1 thru #5 above, I believe that this crab is most closely related to <u>Raninoides</u> <u>fulgidus</u>, and would refer to it as Raninoides cf. R. fulgidus.

Ross E. Baughman

11/2/86

APPENDIX VIII

MAJOR OXIDE ANALYSES

TILLAMOOK VOLCANICS

SAMPLE	SiO2	Al2O3	TiO2	Fe2O3	FeO	MnO	CaO	MgO	K2O	Na2O	P2O5
824-7-2	49.60	14.91	3.16	6.30	7.21	0.18	10.35.	4.24	0.64	2.99	0.41
826-7-2	50.66	14.27	3.56	6.20	7.11	0.21	9.40	3.99	0.82	3.27	0.51
720-5-2	49.60	18.33	2.98	5.13	5.88	0.19	10.46	3.16	0.76	3.07	0.45
719-10-1	51.57	15.10	3.21	5.74	6.58	0.22	8.36	3.86	1.07	3.68	0.61
77-7-3	49.51	14.20	3.88	6.59	7.55	0.23	9.03	4.26	0.94	3.23	0.58
3721-1-3	49.19	10.07	1.92	5.16	5.91	0.17	11.49	13.81	0.42	1.64	0.23
3721-2-2	48.70	14.16	3.64	6.33	7.25	0.28	10.07	5.09	0.86	3.08	0.51
3721-4-2	58.42	15.76	1.68	4.44	5.08	0.18	5.59	2.01	1.92	4.30	0.63
3721-4-4	58.18	15.89	1.67	4.36	4.99	0.17	5.58	2.11	1.93	4.50	0.64
3623-6-1	50.58	14.86	3.62	5.85	6.70	0.21	9.19	4.18	0.83	3.42	0.57
822-2-2	52.92	15.31	2.96	5.42	6.20	0.24	7.70	3.68	1.11	3.60	0.87
919-6-2	49.98	15.09	3.17	5.94	6.81	0.18	10.26	4.62	0.59	2.94	0.42
919-3-2	51.12	14.78	3.56	5.94	6.81	0.24	9.41	3.65	0.87	3.13	0.50
77-7-2	49.47	13.93	3.78	6.64	7.61	0.23	9.26	4.25	0.91	3.34	0.58
826-1-2	50.45	16.61	3.15	5.40	6.18	0.18	9.66	3.86	0.82	3.23	0.45
719-9-1	52.47	14.31	3.01	6.18	7.08	0.24	7.88	3.53	1.12	3.50	0.69
77-4-2	53.16	14.83	2.85	5.75	6.59	0.25	7.53	3.42	1.13	3.57	0.72
75-6	49.53	14.69	3.39	5.89	6.75	0.20	11.13	4.24	0.76	2.89	0.51

COLE MOUNTAIN BASALT

SAMPLE	SiO2	Al2O3	TiO2	Fe2O3	FeO	MnO	CaO	MgO	K2O	Na2O	P2O5
3/624-1-1	58.00	15.81	1.47	4.19	4.80	0.18	7.55	3.80	0.60	3.29	0.31
99-6-1	56.86	17.75	1.55	3.85	4.41	0.10	8.22	3.32	0.70	2.96	0.27
630-1-3	58.62	16.53	1.51	3.96	4.54	0.12	6.93	3.26	0.78	3.44	0.33
730-4-2	56.93	15.92	1.47	4.53	5.19	0.17	7.85	3.98	0.41	3.21	0.33
730-3-4	58.10	15.92	1.45	4.31	4.94	0.17	7.28	3.61	0.35	3.56	0.32
73-7-3	56.51	15.08	1.40	4.41	5.06	0.16	9.01	4.02	0.69	3.34	0.31
717-10-3	55.74	16.93	1.50	4.63	5.31	0.13	8.12	3.80	0.70	2.87	0.26

APPENDIX VIII cont.

GRANDE RONDE BASALT OF THE COLUMBIA RIVER BASALT GROUP

SAMPLE	SiO2	Al2O3	TiO2	Fe2O3	FeO	MnO	CaO	MgO	K2O	Na2O	P2O5
97-7-1	54.85	13.86	1.88	5.73	6.56	0.20	8.17	4.56	1.02	2.85	0.32
3630-2-2	56.53	13.37	2.12	6.05	6.93	0.19	6.92	3.31	1.40	2.83	0.36
718-1-3	55.47	13.64	2.13	5.97	6.84	0.21	7.24	3.57	1.50	3.07	0.37
3715-2-1	56.02	13.22	2.14	6.13	7.02	0.19	6.87	3.49	1.54	3.02	0.37
77-13-3	55.84	13.44	2.13	5.97	6.83	0.20	7.07	3.61	1.53	3.02	0.38
78-4-3	56.18	13.25	2.11	6.06	6.94	0.19	6.83	3.41	1.55	3.09	0.38
79-12-3	56.13	13.30	2.08	6.01	6.89	0.20	7.06	3.42	1.58	2.95	0.37

CLASTS FROM THE ROY CREEK MEMBER OF THE HAMLET FORMATION

SAMPLE	SiO2	Al2O3	TiO2	Fe2O3	FeO	MnO	CaO	MgO	K2O	Na2O	P2O5
3720-2-1	48.52	16.00	4.43	5.80	6.64	0.23	9.10	4.08	1.02	3.27	0.92
3720-2-2	51.08	17.65	3.41	5.28	6.05	0.16	7.06	3.21	1.24	3.57	1.29
3720-2-3	51.72	16.96	4.05	5.20	5.96	0.24	6.67	2.19	2.39	4.01	0.62
3723-1-1	53.30	15.59	2.56	5.35	6.13	0.27	7.59	2.85	1.44	3.83	1.08
3723-1-2	50.33	16.31	3.67	5.13	5.87	0.22	8.48	2.88	1.27	3.81	2.03
3723-1-3	52.21	16.06	2.73	5.45	6.24	0.23	7.55	2.95	1.52	3.93	1.14
3723-1-4	51.96	16.13	3.54	4.90	5.62	0.22	8.77	3.19	1.17	3.80	0.69

APPENDIX IX: NORMATIVE MINERALS

TILLAMOOK VOLCANICS

	824-7-2	826-7-2	720-5-2	719-10-1	77-7-3	3721-1-3	3721-2-2	3721-4-2	3721-4-4	3623-6-1
Ap	0.88	1.10	0.96	1.31	1.25	0.48	1.10	1.34	1.36	1.22
Il	4.53	5.11	4.24	4.58	5.58	2.67	5.21	2.38	2.36	5.17
Mt	6.78	6.68	5.48	6.14	7.11	5.38	6.80	4.71	4.62	6.27
Or	3.89	4.99	4.59	6.47	5.73	2.47	5.22	11.52	11.55	5.03
Ab	27.65	30.25	28.18	33.81	29.93	14.68	28.42	39.21	40.93	31.50
An	26.13	22.50	34.76	22.03	22.16	18.82	22.89	18.31	17.69	23.33
Di	19.19	17.70	12.24	13.07	16.13	29.22	20.02	4.54	4.90	15.70
Hy	5.20	4.63	4.52	6.49	6.20	25.42	6.68	6.13	6.12	5.62
Ol						0.85				
Q	5.74	7.04	5.02	6.12	5.90		3.66	11.86	10.49	6.15

	822-2-2	919-6-2	919-3-2	77-7-2	826-1-2	719-9-1	77-4-2	75-6
Ap	1.86	0.90	1.08	1.25	0.96	1.49	1.54	1.10
Il	4.22	4.53	5.11	5.43	4.49	4.32	4.07	4.86
Mt	5.80	6.38	6.40	7.16	5.77	6.65	6.17	6.34
Or	6.71	3.58	5.30	5.55	4.95	6.81	8.06	4.62
Ab	33.07	27.10	28.98	30.93	29.66	32.35	32.89	26.71
An	22.86	26.94	24.45	20.97	29.05	20.62	21.05	25.60
Di	8.33	18.01	16.26	18.01	13.57	11.99	9.97	22.25
Hy	8.36	6.43	4.15	5.43	5.86	6.97	7.40	2.93
Ol								
Q	8.79	6.12	8.27	5.27	5.68	8.80	8.85	5.59

COLE MOUNTAIN BASALT

	3624-1-1	73-2-1	99-6-1	630-1-3	730-4-2	730-3-4	73-7-3	717-10-3
AN	48.86	51.90	56.91	48.45	50.60	46.73	46.04	56.27
Q	14.64	11.72	14.38	15.55	13.37	14.52	10.66	12.10
or	3.55	3.55	4.14	4.61	2.42	2.07	4.08	4.14
ab	27.84	26.74	25.05	29.11	27.16	30.12	28.26	24.29
an	26.60	28.85	33.08	27.36	27.82	26.43	24.12	31.25
di	7.21	8.00	4.82	3.97	7.35	6.23	15.20	6.03
hy	12.22	13.44	10.45	11.33	13.85	12.74	9.94	14.23
mt	4.31	4.23	4.42	4.36	4.31	4.28	4.20	4.35
il	2.79	2.70	2.94	2.87	2.79	2.75	2.66	2.85
ap	0.72	0.63	0.63	0.76	0.76	0.74	0.72	0.60

GRANDE RONDE BASALT

	97-7-1	3630-2-2	718-1-3	3715-2-1	77-13-3	78-4-3	79-12-3
AN	47.72	45.07	42.25	41.29	42.12	40.38	42.41
Q	9.78	13.80	10.52	11.71	11.31	11.72	11.96
or	6.03	8.27	8.86	9.10	9.04	9.16	9.34
ab	24.12	23.95	25.98	25.55	25.55	26.15	24.96
an	22.01	19.65	19.01	17.97	18.60	17.71	18.38
di	13.55	10.29	12.05	11.42	11.63	11.42	11.86
hy	15.07	13.70	13.19	13.81	13.47	13.47	13.25
mt	4.90	5.25	5.26	5.28	5.26	5.23	5.19
il	3.57	4.03	4.05	4.06	4.05	4.01	3.95
ap	0.74	0.83	0.86	0.86	0.88	0.88	0.86

APPENDIX X

X-RAY ANALYSIS OF CLAY MINERALS IN SEDIMENTARY ROCKS (Methodology after M. Harward, 1976)

A. Segregation of clay size material (<2μ) in rock sample.

1. Disaggregate sample - boiling in water is often sufficient. Grind gently in mortar and pestle if necessary.
2. Wet sieve the sample using a 4∅ size sieve. Save the <4∅ size fraction in beaker. Air dry or dry at very low temperature in overn. Save sand-size material if desired.
3. Break up dry sample by gently grinding with rubber pestle.
4. Measure out approximately 15 grams of sample.
5. Add enough water to sample to disperse the clay and silt. Add Calgon to mixture if flocculation is a problem. Suspend the clay and silt by agitating in a rotary stirrer or by pouring the clay and silt mixture in plastic centrifuge tube and shaking by hand.
6. Centrifuge the clay-silt suspension for 5 minutes at 750 R.P.M. This will leave the 2μ and smaller clay in suspension. Pour the suspension in beaker and save.
7. Repeat step (6) four times using the silt residue left after each centrifugation. Save the clay suspension after each run.
8. Place the clay suspension in centrifuge tube and centrifuge a 6,000 R.P.M. for 10 minutes.
9. Discard the supernatant and save the clay residue.

B. Potassium and Magnesium saturation and x-ray slide preparation

1. Place 2/3 of the clay residue (from step 9) in a plastic centrifuge tube and the remainder in another tube.
2. Mg - saturation: Add a small portion of 1N $MgCl_2$ solution to the tube containing 2/3 of the clay residue. Place a rubber stopper on the tube and shake. Centrifuge at 6,000 R.P.M. for 10 minutes and discard supernatant. Repeat this twice, remove excess Mg by wasing 2-3 times with H_2O.
3. K-Saturation: Wash the clay in the tube containing 1/3 of the clay residue 2-3 times with 1N KCl solution according to the procedure in step (2). Then remove excess K by 2-3 washings with H_2O.
4. Prepare two slides or Mg-saturated clay and one slide of K-saturated clay. This is done by smearing an even coating of the clay paste on a petrographic slide. Label slides.
5. Allow the Mg-saturated samples to air dry. Dry the K-saturated sample in the oven at 105°C.

C. X-ray analysis of clay samples

1. Mg-saturated samples

   a. Allow the two Mg-saturated slides to equilibrate in the 54% R.H. dessicator. Run x-ray analysis on one of the slides (a range from 2° to 25° 2θ is usually sufficient). Be sure that the humidity control on the goniometer is set for 54% R.H. Return slide to 54% dessicator.

   b. Place one of the Mg-saturated slides in the Glycerol dessicator so that it lies flat. Draw a vacuum on the dessicator. Place dessicator in the Sed Pet. oven and heat at 105°C for 2-3 hours. Cool for 12 hours before opening. Run x-ray analysis. Humidity control at 54% R.H.

   c. Place the other Mg-saturated slide in the Ethylene Glycol dessicator (Flat-lying). Draw a vacuum and heat at 65°C for 2-3 hours. Cool for 12 hours. Run x-ray analysis. Humidity control at 54% R.H.

2. K-saturated samples

   a. Run x-ray analysis of the K-saturated slide (dried at 105°C) with the humidity control set at 0% R.H.

   b. Place the slide in the 54% R.H. dessicator and allow 12 hours to equilibrate. Run x-ray analysis with humidity control at 54%.

   c. Heat K-saturated slide at 300°C for 3 hours and analyze in dry air (0% R.H.).

   d. Heat the K-saturated slide at 550°C for 3 hours and analyze in dry air.

You should have a total of 7 diffractograms when done.

Identification of Major Clay Mineral Types Based
on Basal Spacings A° Unit and Treatments (after Harwood 1976)

				◄— SMECTITE —►				LC
Mineral Name:	Kaolinite	Halloysite	Illite or Mica	Mont.	Beide-[2] llite	Vermiculite	Chlorite	Chlorite intergrades
Treatment								
1. Mg 54% (relative Humidity)	7.15	10 wet– 7.3 dry	10–10.5	∿15	14.5–15	∿14.5	14–14.5	14–15
2. Mg Ethylene Glycol	7.15	10 wet– 7.3 dry	10–10.5	16.5–17	16.5–17	∿14.5	14–14.5	14–17
3. Mg glycerol	7.15	10 wet– 7.3 dry	10–10.5	17.5	14.5–15	∿14.5	14–14.5	14–17
4. K + 105°C	7.15	7.3–7.5	10–10.5	10–10.5	10	10–10.5	14–14.5	11–14
5. K 54% humidity	7.15	7.3–7.5	10–10.5	∿12	11.5	10–10.5	14–14.5	14
6. K + 300°C	7.15	7.3	10–10.5	10.1	10–10.5	10–10.2	14–14.5	11–14
7. K + 550°C	no peak [1]	no peak	10–10.5	10	10	∿10	14.145	10–13

*1 Serpentine (antigorite)
peak won't disappear?
(crysotille) will??

*1 Also check 060 spacings
Diocta(Kaolins) = 1.49A°
Triocta(serpe) = 1.54A°

*2 may also have something
with hydroxy interlayers
with these characteristics

other peaks:
Gibbsite   4.85, 4.37, 2.39A°
Qtz.   3.34A°
Zeolites 7, 8, 9 A°

A. Well crystallized kaolinite has a sharp peak at about 7.0 A° and higher orders are present; poorly crystallized mineral has broader peaks.

B. If hydrated halloysite is dried it does not re-expand to 10 A°.

C. A distinction between it and kaolinite using X-ray diffraction criteria is generally difficult. Electron photo micrographs are, however, useful to detect the tube structure generally characteristic of halloysite.

D. Montmorillonite peaks are generally broad and the higher orders are very weak. Some montmorillonites believed to be beidellite collapse to 10 A° upon K saturation.

E. The 10 A° mica (illite) peak becomes sharper and sometimes more intense upon heating.

F. First order vermiculite peaks are sharper than montmorillonite but not as sharp as those of illite; the higher orders are weak.

G. If 14 A° firstorder chlorite peak and a 7A° peak occur the 7A° peak may be a second order reflection of chlorite and/or a kaolinite peak.

H. The second order reflection of chlorite is generally strong and all the peaks are sharp.

APPENDIX XI

SOURCE ROCK GEOCHEMISTRY SUMMARY

Sample No.	% TOC	V.R. % RO	Visual Kerogen Type*	Kerogen Type Oil/Gas	Generation Rating	Stage of Diagenesis
371-1-2	1.2	0.50	S	Gas	Non-source	Pre-generation
3715-2-2	1.1	---	--	Gas	Non-source	Early peak gas
716-9-1	0.9	---	--	Gas	Non-source	Pre-generation

Meters

Sunset Highway member

105 —

100 —

COVER

95 — ?

Sweet Home Creek member

90 —

COVER

85 —
60 —

COVER

55 —

COVER

40 —

35 —

COVER

30 —

25 —

Roy Creek member

COVER

20 —

15 —

COVER

10 —

5 —

COVER

fault

Tillamook Volcanics

0 —

Moderately to poorly sorted basaltic sandstone and pebble-bearing basaltic sandstone. Weakly normal graded to very poorly sorted fine-grained micromicaceous basaltic sandstone with admixed basaltic grits. Disseminated Pyrite.

Dusky blue finely cross-laminated very fine-grained micaceous and carbonaceous arkosic sandstone with flasers and climbing ripples of olive gray micromicaceous siltstone and mudstone. Local burrows and ovoid to nodular calcite-cemented concretions. Ledge-former.

Thinly parallel and cross-laminated micaceous medium-grained arkosic sandstone with thin interbeds and pebbly lenses of massive coarse-grained basaltic sandstone and grits. Calcite-cemented discoidal concretions up to 10 cm. in diameter.

Probable fault

Olive-gray mudstone. Poorly exposed

Massive, dark olive gray micaceous and carbonaceous pyritic mudstone with pyrite-filled vertical to subvertical cylindrical burrows.

Mottled greasy mudstone. Spotted light and dark gray. Extensively burrowed (?). Low-angle shears (?). Fault?.

Massive poorly sorted conglomerate with subangular basaltic boulders, cobbles, and pebbles in a clay-rich matrix. Poorly indurated.

Olive gray micaceous mudstone. Poorly exposed

Probable fault

Massive dusky blue pebble-bearing very coarse-grained basaltic sandstone. One to three per cent disseminated fine-grained pyrite.

Massive pyritic pebbly very coarse-grained basaltic grits interbedded with pyritic pebble-bearing very coarse-grained basaltic sandstone with pebbly lenses. Undulose bedding planes. Moderately indurated. Ledge former. Sample 3810-2-1.

Thinly interbedded pebble-bearing micaceous medium-grained basaltic sandstone and pebble-bearing coarse- to very coarse-grained basaltic sandstone. Undulose bedding planes. Moderately indurated.

Sheared basaltic conglomerate with calcite-pyrite veins. Slickensided basaltic boulders, cobbles, and pebbles set in a greenish-gray chloritic matrix.

12 m waterfall in Cow Creek.

Fine-grained basalt with sparse labradorite (An₆₀) microphenocrysts and sparse two to four mm. chalcedony-filled amygdules. Sample 3810-1-1